Mariana Moreira da Silva Alves Barbosa

PhD Thesis

CLAMP – CLick chemistry as a tool to create **A**nti**M**icrobial **P**eptide-based materials

Dissertação submetida à Faculdade de Engenharia da Universidade do Porto para obtenção do grau de Doutor em Engenharia Biomédica

Universidade do Porto

2018

This thesis was supervised by:

Doctor Paula Alexandra de Carvalho Gomes

FCUP – Departamento de Química e Bioquímica da Faculdade de Ciências da Universidade do Porto
LAQV/REQUIMTE – Laboratório Associado para a Química Verde

Doctor M. Cristina L. Martins

INEB – Instituto de Engenharia Biomédica, Universidade do Porto
ICBAS – Instituto de Ciências Biomédicas Abel Salazar, Universidade do Porto
I3S – Instituto de Investigação e Inovação em Saúde, Universidade do Porto

The research described in this thesis was conducted at:

LAQV/REQUIMTE – Laboratório Associado para a Química Verde
FCUP – Departamento de Química e Bioquímica da Faculdade de Ciências da Universidade do Porto
INEB – Instituto de Engenharia Biomédica, Universidade do Porto
I3S – Instituto de Investigação e Inovação em Saúde, Universidade do Porto

The research described in this thesis was financially supported by:

- Fundação para a Ciência e Tecnologia, Portugal, through project UID/QUI/50006/2013 to LAQV-REQUIMTE and PhD Grant SFRH/BD/108966/2015 to MB;
- Comissão de Coordenação e Desenvolvimento Regional do Norte (CCDR-N) /NORTE2020/Portugal2020, through project DESignBIOtechHealth (ref. Norte-01-0 145-FEDER-000024);
- Project BIOENGINEERED THERAPIES FOR INFECTIOUS DISEASES AND TISSUE REGENERATION (ref. NORTE-01-0145-FEDER-000012).

Publications

The work performed in the frame of this thesis resulted in the following international scientific publications:

- Barbosa, M., Monteiro C., Costa, F. M. T. A., Martins, M. C. L., Gomes, P. Influence of chemical immobilization parameters on the antibacterial properties of antimicrobial peptide-based coatings. Manuscript in preparation.

- Barbosa, M., Monteiro C., Costa, F. M. T. A., Duarte, F., Martins, M. C. L., Gomes, P. Only a "click" away: development of novel antibacterial coatings. Manuscript submitted.

- Barbosa, M., Vale, N., Costa, F. M. T. A., Martins, M. C. L., Gomes, P. Tethering antimicrobial peptides onto chitosan: optimization of azide-alkyne "click" reaction conditions. Carbohydrate Polymers 2017, 165, 384-393.

DOI: 10.1016/j.carbpol.2017.02.050
URL: http://www.sciencedirect.com/science/article/pii/S0144861717301807

- Barbosa, M.; Martins, M.C.L.; Gomes, P. Grafting Techniques towards Production of Peptide-Tethered Hydrogels, a Novel Class of Materials with Biomedical Interest. Gels 2015, 1, 194-218.

DOI: 10.3390/gels1020194
URL: http://www.mdpi.com/2310-2861/1/2/194

Acknowledgements

Quando comecei a escrever os agradecimentos da tese mal podia acreditar que esta fase tinha finalmente chegado. Concluir este projeto de doutoramento significa o fim de uma longa jornada, a qual não seria possível levar a bom porto sem o apoio de um conjunto de pessoas e instituições. O meu percurso ao longo destes quatro anos foi por vezes sinuoso, com muitas incertezas e dificuldades, mas também repleto de alegrias e vitórias. E foram muitos os que me acompanharam e a quem quero deixar aqui a minha mais sincera gratidão.

À minha orientadora, Professora Paula Gomes, por toda a confiança em mim depositada, pela sua orientação e apoio, pela ajuda e suporte nas decisões tomadas. Pela sua disponibilidade em me acolher quando decidi iniciar este percurso e por ter continuado sempre presente. Vou sempre recordar o seu sorriso e palavras de encorajamento mesmo quando tudo parecia correr mal. Obrigada por ver sempre a luz ao fundo do túnel e me fazer acreditar que seria possível concretizar este trabalho. Expresso a minha gratidão por todos os conselhos, oportunidades de aprendizagem e pelas reflexões que me fizeram crescer e me ajudaram a tornar na pessoa que sou hoje. Principalmente, obrigada pela amizade! Desejo-lhe tudo de melhor! Que o futuro lhe recompense verdadeiramente por todo o trabalho e dedicação!

À Cristina Martins o meu sentido agradecimento. Obrigada por me fazer sentir tão benvinda no grupo, pela paciência e amabilidade com que tirou todas as minhas dúvidas, pela disponibilidade para discutir e corrigir resultados. Um obrigada sincero por todas as oportunidades de aprendizagem e de trabalho que me proporcionou e que enriqueceram este trabalho e sem as quais não o tinha conseguido terminar.

O meu agradecimento muito especial ao meu grupo Bioengineered Surfaces. Obrigada a todas por me fazerem sentir parte da equipa, pelo espírito de camaradagem, pelo bom ambiente no laboratório. Todas foram essenciais para que eu chegasse ao fim desta jornada por vezes tumultuosa que é a investigação. Um beijinho especial à Cláudia. Obrigada por me acolheres no laboratório e me ensinares tudo o que sei, pelo teu apoio e disponibilidade. À Fabíola por todas as dúvidas tiradas, por todos os conselhos e sugestões. Sem vocês eu não teria conseguido!

Às meninas do Lab 2.28. Muito, muito, muito obrigada Ana, Cátia, Luísa e membros honorários Cláudia e Filipa. Conhecer-vos foi sem dúvida um dos motivos pelos quais sorrio e sinto o coração cheio de alegria quando penso no tempo que passou. Obrigada por todas as gargalhadas, por quase fazermos do laboratório uma discoteca, por todos os almoços/jantares/sushis/lanches, pausas (por vezes longas) para o café. Às "bebés" do grupo Mélanie e Natália pela vossa constante boa disposição. Um beijinho especial também para o Ivo e para a Vânia. Obrigada pela vossa companhia e amizade!

Às amiguinhas do coração um sincero obrigada! À Graciosa, um beijinho cheio de saudades, obrigada por todos os momentos que passamos juntas, por todas as conversas, longos almoços e idas às compras. À Teresa, ainda me recordo do dia em que nos conhecemos, parece que foi ontem. Obrigada por tudo, principalmente por me acompanhares pelo mundo da Disney! À Raquel, querida Raquel, obrigada pela tua bondade e carinho e por me aturares todos estes anos, e já lá vão mais de 20. Susana obrigada pela tua amizade, por todas as conversas mais ou menos sérias, mas sempre acompanhadas por um bom copo de vinho! Nilma, obrigada pela tua energia contagiante e sorriso rasgado. Obrigada também pela viagem gastronómica até à India!
Obrigada a todas por estarem ao meu lado!

Agradeço a toda a minha família. Deixo um agradecimento especial aos meus pais, Teresa e Abílio, por me terem incentivado em prosseguir para o doutoramento, pelo apoio constante e incondicional ao longo de toda a minha vida. Pelo amor dedicado, pelo exemplo e por todos os sacrifícios feitos em nome da minha felicidade.

A ti Filipe não encontro palavras suficientes para te agradecer. Obrigada pelo teu apoio, pela tua paciência, pela tua presença constante desde que nos conhecemos. Fazes-me sentir segura e confiante, mesmo quando as forças pareciam querer abandonar-me, mesmo quando o caminho a percorrer se mostrava mais difícil. Obrigada por acreditares em mim e nas minhas capacidades, por não duvidares do futuro. Obrigada por todos os momentos que passamos juntos, por tudo que aprendi contigo, por me incluíres nos teus sonhos e na tua vida. Obrigada por fazeres de mim uma pessoa melhor!

Abstract

Implant-associated infections (IAI) and chronic wound infections (CWI) remain a considerable problem in medical care. IAI are amongst the most common problems of *in vivo* implantation of any material and involve bacterial colonization and biofilm formation on the implant surface. CWI occur in individuals with alterations in the complex process of wound healing such as patients with diabetes or poor vascular supply, whose incapacity to fight infection on its onset leads to bacterial growth and wound colonization with subsequent establishment of mixed-species biofilms. Biofilms are difficult to eradicate as they are resistant to host defenses and not affected by existing antibiotics. Also, the growing prevalence of antibiotic-resistant strains such as gentamicin- (GRSA) and methicillin-resistant *Staphylococcus aureus* (MRSA) compromises current antibiotherapy. Therefore, IAI and CWI require prevention or treatment on onset with efficient antimicrobials.

Antimicrobial peptides (AMP) are well-known components of the innate immune system that can be used to overcome IAI and CWI, as their relevance as alternatives to conventional antibiotics is increasing. AMP have valuable features, including wide activity spectrum, high efficacy at low concentrations, target specificity, synergistic action with classical antibiotics, and low propensity for eliciting resistant pathogens. However, therapeutic applications of have some challenges, namely short half-life due to proteolytic digestion or peptide aggregation, which requires use of high concentrations that may be raise toxicity issues. To overcome these drawbacks, covalent immobilization of AMP through different coupling strategies has been reported, and the overall results suggest that immobilized AMP may efficiently prevent biofilm formation by reduction of microorganism survival post-contact with coated material.

In the above connection, this project targeted novel antimicrobial materials for bone implants or adhesive patches, to prevent IAI and/or CWI. In this context, peptide tethering through the so-called "click chemistry" reactions is a highly promising, yet underexplored, approach. Amongst chemoselective reactions that fit the "click chemistry" concept, the azide-alkyne coupling (Huisgen's dipolar 1,3-cycloaddition) is one of the most attractive, given the (i) stability of the triazole link created between the building blocks that are joint together, and (ii) diversity of adequately functionalized (i.e., bearing either an azide or an alkyne functionality) building blocks that are commercially available.

Dhvar-5 (LLLFLLKKRKKRKY) is a short AMP with a head-to-tail amphipathicity and a broad spectrum of activity, including against MRSA, GRSA and *Pseudomonas aeruginosa* hospital isolates, which are major health concerns of our time. This AMP was immobilized onto chitosan, a natural polymer commonly explored for biomedical applications that was previously described to have antimicrobial and osteoconductive properties.

The selected AMP was synthesized using solid phase peptide synthesis (SPPS) and conveniently modified with a spacer and an alkyne moiety (alkyne-AMP). Additionally, chitosan was chemically functionalized by introduction of an azide moiety and reacted with the alkyne-AMP through the Cu(I)-catalyzed azide-alkyne cycloaddition (CuAAC) reaction, in the presence of Cu(II) sulfate and sodium ascorbate. Conversion of chitosan into azido-chitosan was confirmed by the observed increase in nitrogen content, according to X-ray photoelectron spectroscopy (XPS) analysis and the appearance of a new peak in the infra-red (FT-IR) spectrum, at ca. 2200 cm^{-1}, typical of azide groups. Subsequent coupling of azido-chitosan to alkyne-AMP yielded a polymer whose XPS and FT-IR data were both in agreement with the formation of the expected triazole ring, indicating that the desired "click" reaction took place, producing the target conjugate.

The immobilization strategy could affect AMP antimicrobial activity, therefore different parameters were investigated namely, AMP orientation (coupled through the *N*- versus the *C*-terminus) and AMP immobilization process (immobilization before or after films formation).

The synthetic AMP-chitosan conjugates obtained after CuAAC-mediated immobilization of Dhvar-5 in both possible orientations were used to produce thin films. Antimicrobial activity assays were carried out using a combination dye of the LIVE/DEAD® Bacterial Viability Kit (Baclight™) for quantifying the viability of adherent bacteria. The bacterial adhesion studies demonstrated that the AMP-chitosan thin films had bactericidal effects whose potency depended on which region of the peptide was exposed; as such, higher antimicrobial activity was observed when Dhvar-5 was immobilized through its cationic *C*-terminus, i.e., exposing its hydrophobic domain.

CuAAC was also used to immobilize the modified Dhvar-5 directly onto previously prepared chitosan ultrathin films. Again, antimicrobial studies demonstrated that when immobilized through the *C*-terminus (exposing its hydrophobic end), Dhvar-5 was able to improve chitosan antimicrobial effect by decreasing bacterial colonization.

Altogether, the specific research goals of this work provided proof-of-concept on the project's working hypothesis, i.e., that "click" chemistry is a valuable tool to create AMP-based materials which may find application in the development of effective antimicrobial coatings with potential biomedical interest.

Resumo

As infeções associadas quer a implantes (IAI), quer a feridas crónicas (CWI), continuam a ser um problema considerável nos cuidados médicos. As IAI encontram-se entre os problemas mais comuns relacionados com a implantação de qualquer material e envolvem colonização bacteriana e formação de biofilmes na superfície do implante. As CWI ocorrem em indivíduos com alterações no complexo processo de cicatrização de feridas, tais como pacientes com diabetes ou com insuficiência venosa, cuja incapacidade de combater estados iniciais de infeção leva ao desenvolvimento bacteriano e à colonização das feridas com consequente formação de biofilmes. Os biofilmes são difíceis de erradicar, pois são resistentes às defesas do hospedeiro e aos antibióticos mais comuns. Além disso, a prevalência crescente de estirpes resistentes aos antibióticos, como *Staphylococcus aureus* resistentes à meticilina (MRSA) ou à gentamicina (GRSA), comprometem o sucesso das terapias atuais. Portanto, as IAI e as CWI exigem o desenvolvimento de novos agentes antibacterianos eficazes, quer para uma ação preventiva, quer para tratamento numa fase mais precoce do processo infecioso.

Os péptidos antimicrobianos (AMP) são componentes bem conhecidos do sistema imune inato que podem ser usados no tratamento de IAI e CWI, pois a sua relevância como alternativas aos antibióticos convencionais tem vindo a tornar-se cada vez mais evidente. Os AMP têm características valiosas, incluindo amplo espectro de atividade, alta eficácia a baixas concentrações, ação específica, ação sinérgica com antibióticos clássicos e baixa propensão para induzir resistência. No entanto, a aplicação terapêutica dos AMP apresenta alguns desafios, como curto tempo de semi-vida devido à ação de protéases ou à agregação dos próprios péptidos, o que leva à administração de concentrações mais elevadas que podem estar subjacentes a problemas de toxicidade. Para ultrapassar estas desvantagens, foi descrita a imobilização covalente de AMP através de diferentes estratégias, com resultados que sugerem que a imobilização pode prevenir eficazmente a formação de biofilmes, por redução da sobrevivência dos microrganismos após o contacto com o material revestido.

Considerando o acima referido, este projeto visou o desenvolvimento de novos materiais antimicrobianos para utilização em implantes ósseos ou pensos hidrocolóides, para prevenir IAI ou CWI, respetivamente. Neste contexto, a imobilização de péptidos através das chamadas reações "click" é uma abordagem altamente promissora, porém ainda pouco explorada. Entre as reações mais seletivas que se enquadram no conceito de

química "click", o acoplamento azida-alcino (cicloadição 1,3-dipolar por Huisgen) é uma das mais atrativas, dada a (i) estabilidade do anel triazole criado entre os dois grupos funcionais e (ii) diversidade de grupos químicos adequadamente funcionalizados (ou seja, com uma azida ou um alcino) que se encontram comercialmente disponíveis.

O péptido Dhvar-5 (LLLFLLKKRKKRKY) é um AMP curto, catiónico e anfipático, com um amplo espectro de ação antimicrobiana, incluindo contra MRSA, GRSA e isolados hospitalares de *Pseudomonas aeruginosa*, todos estes sendo agentes patogénicos preocupantes no contexto das infeções nosocomiais. Este AMP foi imobilizado em quitosano, um polímero natural frequentemente explorado para aplicações biomédicas e já amplamente descrito como possuindo propriedades antimicrobianas e osteocondutoras. O AMP selecionado foi sintetizado usando síntese peptídica em fase sólida (SPPS) e convenientemente modificado com um espaçador e um grupo alcino (alcino-AMP). Posteriormente, o quitosano, previamente funcionalizado pela introdução de um grupo azida, reagiu com o alcino-AMP através da reação de cicloadição de azida-alcino catalisada por Cu(I) (CuAAC), na presença de sulfato de Cu(II) e ascorbato de sódio. A conversão de quitosano em azida-quitosano foi confirmada pelo aumento observado no teor de azoto, de acordo com análises da espectroscopia de fotoeletrões de raio-X (XPS), e pelo aparecimento de um novo pico no espectro de infra-vermelhos (FT-IR), aproximadamente a 2200 cm^{-1}, típico dos grupos azida. O acoplamento subsequente de azida-quitosano ao alcino-AMP produziu um polímero cujos dados de XPS e FT-IR estavam de acordo com a formação do anel de triazole esperado, confirmando a ocorrência da reação "click" desejada, produzindo o conjugado alvo.

A estratégia de imobilização pode afetar a atividade antimicrobiana do AMP, portanto, diferentes parâmetros foram investigados, nomeadamente, a orientação do AMP (imobilização através do extremo *N*- *versus C*-terminal) e o processo de imobilização de AMP (imobilização antes ou depois da formação dos filmes).

Os conjugados de AMP-quitosano obtidos por imobilização do Dhvar-5 via CuAAC, em ambas as orientações possíveis, foram depois utilizados para produzir filmes finos. Estes filmes foram submetidos a ensaios de atividade antimicrobiana, realizados usando o corante específico LIVE/DEAD® (Baclight™) para quantificar a viabilidade das bactérias aderentes. Os estudos de adesão bacteriana demonstraram que os filmes finos de AMP-quitosano apresentaram efeitos bactericidas, cuja potência dependeu da orientação dos péptidos, ou seja, da região deste que ficou mais exposta; como tal, observou-se maior

atividade antimicrobiana quando o Dhvar-5 foi imobilizado através do extremo *C*-terminal, isto é, expondo o seu domínio hidrofóbico.

O péptido Dhvar-5 modificado foi diretamente imobilizado, também via CuAAC, sobre filmes ultrafinos de quitosano previamente preparados. Novamente, os estudos antimicrobianos demonstraram que, quando imobilizado através do extremo *C*-terminal (expondo a sua extremidade hidrofóbica), o Dhvar-5 melhora o efeito antimicrobiano do quitosano, diminuindo a colonização bacteriana.

Globalmente, os resultados obtidos constituem prova de conceito quanto à hipótese de trabalho do projeto doutoral desenvolvido, ou seja, que a química "click" é uma ferramenta valiosa para o desenvolvimento de materiais modificados com AMP, os quais poderão revelar-se úteis na conceção futura de revestimentos antimicrobianos eficazes com potencial interesse biomédico.

Table of contents

List of figures

Chapter I

Chapter II

Chapter III

Chapter IV

Chapter V

Chapter VI

List of tables

Chapter IV

Chapter V

Chapter VI

List of abbreviations

A

AAA Amino acid analysis
AHL *N*-acyl homoserine lactone
Alkyne-AMP AMP conveniently modified with a spacer and an alkyne moiety
AMP Antimicrobial peptides
a.m.u. Atomic mass units
AQC 6-aminoquinolyl-*N*-hydroxysuccinimidyl carbamate
Arg Arginine
Asp Aspartic acid

B

BB Building blocks
bFGF Basic fibroblast growth factor
Boc *tert*-butoxycarbonyl group
BSE backscattered electrons
BSTFA *N*,*O*-bis-(trimethylsilyl)trifluoroacetamide
Bzl Benzyl group

C

C Cysteine
CHIT Unmodified chitosan
Cu(I) Copper(I)
Cu(II) Copper(II)
CuAAC Copper-catalysed azide-alkyne cycloaddition
$CuSO_4$ Copper(II) sulfate
$CuSO_4 \cdot H_2O$ Copper(II) sulfate hydrate
CWI Chronic wound infection
Cys Cysteine

D

3D Three-dimensional
D Aspartic acid
DA Diels–Alder reaction
DAD Diode Array Detector
DCM Dichloromethane
DD Degree of deacetylation
DIFO Difluorinated cyclooctyne
DIPCDI or DIC *N*,*N*'-diisopropylcarbodiimide
DIPEA *N*-ethyl-*N*,*N*-diisopropylamine
DIU *N*,*N*'-diisopropylurea
DMF *N*,*N*-dimethylformamide
DNA Deoxyribonucleic acid
DTGS Deuterated triglycine sulfate

E

E Glutamic acid
EBSD Electron backscatter diffraction
ECM Extracellular matrix
EDC 1-ethyl-3-(3-dimethylaminopropyl)carbodiimide
eDNA Extracellular deoxyribonucleic acid
EDS Energy-dispersive X-ray spectroscopy
EDT Ethane-1,2-dithiol
EEDQ 2-ethoxy-1-ethoxycarbonyl-1,2-dihydroquinoline
Escherichia coli *E. coli*
ESI Electrospray ionization
ESI/IT Electrospray ionization/ion trap

F

Fmoc 9-fluorenylmethoxycarbonyl group
Fmoc-AA-OH N^{α}-Fmoc-protected amino acid
FT-IR Fourier-transform infrared spectroscopy

G

G Glycine
GC Gas chromatography
GC-MS Gas chromatography mass spectrometry
GAG glycosaminoglycans
Glu Glutamic acid
Gly Glycine
GRSA Gentamicin-resistant *Staphylococcus aureus*

H

H Histidine
HBTU *O*-(benzotriazol-1-yl)-1,1,3,3-tetramethyluronium hexafluorophosphate
His Histidine
HMPB 4-(4-hydroxymethyl-3-methoxyphenoxy)butyric acid
HOBt 1-hydroxybenzotriazole
HPLC High performance liquid chromatography

I

IAI Implant-associated infection
IRRAS Infrared reflection absorption spectroscopy
ISA·HCl Imidazole-1-sulfonyl azide hydrochloride

K

K Lysine

L

L Leucine
LC Liquid chromatography
LC-MS Liquid chromatography mass spectroscopy
LC-ESI/IT MS Liquid chromatography-electrospray ionization/ion trap mass spectrometry
Leu Leucine
Lys Lysine

M

M Methionine
MBC Minimal bactericidal concentration
MBHA 4-methylbenzhydrylamine
Met Methionine
MHB Mueller Hinton Broth
MIC Minimal inhibitory concentration
MRSA Methicillin-resistant *Staphylococcus aureus*
MS/MS Tandem mass spectroscopy
MS^n Multiple MS
M_w Molecular weight
MW Microwave
MTBSTFA *N*-tertbutyldimethylsilyl-*N*-methyl trifluoroacetamide

N

N_3-CHIT Azido-chitosan
NAC *N*-acetyl cysteine
NHS *N*-hydroxysuccinimide
NMM *N*-methylmorpholine
NMP *N*-methylpyrrolidone

P

P Proline
P. aeruginosa *Pseudomonas aeruginosa*
PAA Poly(acrylic acid)
PAAm Polyacrylamide
PAL Peptide Amide Linker
Pbf Pentamethyl-2,3-dihydrobenzofuran-5-sulfonyl group
PBS Phosphate-buffered saline
PCSA Polarizer-compensator-sample-analyzer
PDITC *p*-phenylene diisothiocyanate
PEG Poly(ethylene glycol)
PHEMA Poly(hydroxyethyl-methacrylate)
PI Propidium iodide
Pmc 2,2,5,7,8-pentamethylchroman group
Pro Proline
PVA Poly(vinyl alcohol)
PyBOP Benzotriazol-1-yloxytri(pyrrolidino)-phosphonium hexafluorophosphate

Q

QS Quorum sensing

R

R Arginine
RP-HPLC Reverse-phase preparative HPLC

S

S Serine
S. aureus *Staphylococcus aureus*
S. epidermidis *Staphylococcus epidermidis*
SEM Scanning electron microscope
Ser Serine
siRNA Small interfering ribonucleic acid
SPAAC Strain-promoted alkyne-azide cycloaddition
SPOS Solid-phase organic synthesis
SPPS Solid-phase peptide synthesis
sulfo-NHS sulfo-*N*-hydroxysuccinimide

T

T Threonine
TBDMS Tertbutyldimethylsilyl
^{t}Bu *tert*-butyl group
TFA Trifluoroacetic acid
THPTA Tris(3-hydroxypropyltriazolylmethyl)amine
Thr Threonine
TIS Triisopropilsilane
Trp Tryptophan
Trt Trityl group
TSA Tryptic Soy Agar
Tyr Tyrosine

W

W Tryptophan
WCA Water contact angle

X

XPS X-ray photoelectron spectroscopy

Y

Y Tyrosine

Aim and structure of the thesis

Implant-associated infection (IAI) and chronic wound infection (CWI) remain a considerable burden in medical care. IAI are amongst the most common problems of *in vivo* implantation of any material and involve bacterial colonization and biofilm formation on the implant surface [1]. CWI occur in individuals with alterations in the complex process of wound healing such as patients with diabetes or poor vascular supply, whose incapacity to fight infection at its onset leads to bacterial growth and wound colonization with subsequent establishment of mixed-species biofilms [2, 3]. Biofilms are difficult to eradicate as they are resistant to host defenses and not affected by existing antibiotics. Also, the growing prevalence of antibiotic-resistant strains such as gentamicin- and methicillin-resistant *Staphylococcus aureus* (GRSA and MRSA, respectively) compromises current antibiotherapy [4]. Therefore, IAI and CWI require prevention or treatment at onset with efficient antimicrobials.

Antimicrobial peptides (AMP) are well-known components of the innate immune system that can be used to overcome IAI and CWI, as their relevance as alternatives to conventional antibiotics is increasing. AMP have valuable features, including wide activity spectrum, high efficacy at low concentrations, target specificity, synergistic action with classical antibiotics, and low propensity for eliciting resistant pathogens [5-7]. Hence, development of orthopedic implants or adhesive patches with coatings having such features seems worthwhile. AMP immobilization onto material surfaces has the further advantage of also helping to circumvent AMP's limitations, as short half-life and cytotoxicity associated with high concentrations [7]. Peptides MSI-78 [8-11], hLF(1-11) [12, 13] or Dhvar-5 [14-16] are particularly interesting AMP in this scenario, given their well-documented efficacy against a wide panel of microbes, including MRSA, GRSA and *Pseudomonas aeruginosa* (*P. aeruginosa*) hospital isolates, which are major health concerns of our time [17, 18].

Covalent immobilization of AMP onto surfaces through different coupling strategies has been reported, and the overall results suggest that immobilized AMP may efficiently prevent biofilm formation by reduction of microorganism survival post-contact with coated material. Minimal cytotoxicity and long-term stability were obtained by optimizing immobilization parameters, indicating a promising potential for immobilized AMP in clinical applications [7]. In this context, peptide tethering through the so-called "click chemistry" reactions [19] is a highly promising, yet underexplored, approach.

Amongst chemoselective reactions that fit the "click chemistry" concept, the azide-alkyne coupling (Huisgen's dipolar 1,3-cycloaddition) [20, 21] is one of the most attractive, given the (i) stability of the triazole link created between the building blocks that are joint together, and (ii) diversity of adequately functionalized (i.e., bearing either an azide or an alkyne functionality) building blocks that are commercially available.

Most literature reports where azide-alkyne coupling was combined with peptides did not aim to produce antimicrobial coatings for prevention/treatment of bone or skin infections [22]. This shows there is a void to be filled towards the advance of scientific knowledge in this area. Moreover, the relevance of future research work in this field is obvious, given not only the global impact of drug-resistant mono- and poly-microbial infections, but also specific delicate cases as infected skin ulcers of the diabetic foot [23] or severe osteomyelitis following orthopedic surgery [24].

The ultimate purpose of this project is development of antimicrobial coatings with potential biomedical interest, namely, for prevention/treatment of IAI, like osteomyelitis, or of CWI, like diabetic foot ulcers. To this end, copper(I)-catalyzed azide-alkyne couplings (CuAAC), which are amongst the preferred "click" reactions, were explored for covalent immobilization of AMP onto chitosan, used as biocompatible polymer carrier. Azide-alkyne "click" tethering of AMP was carried out either on (i) ground chitosan powder, or (ii) pre-formed chitosan films, in both cases producing thin films potentially suitable for future use as coatings for either skin patches or bone implants.

The specific research goals set for this thesis defined the experimental tasks carried out, which were as follows:

1 – solid phase synthesis (SPPS) of AMP, both parent sequences and derivatives modified to include an alkyne (–C≡CH) functional group and a spacer between this group and the bioactive sequence (alkyne-AMP);

2 – convenient chemical functionalization of chitosan, chosen as carrier biopolymer, by introduction of an azide moiety to be reacted with the alkyne-AMP;

3 – synthesis of two different AMP-chitosan conjugates *via* CuAAC, in order to provide information regarding influence of AMP orientation and exposure on conjugates' antimicrobial performance;

4 – production of thin films of the AMP-chitosan conjugates prepared (type 1 thin films), and their characterization by a toolbox of structural analysis techniques;

5 – *in vitro* evaluation of the thin films produced regarding their antimicrobial properties;

6 – production of chitosan thin films and subsequent on-film chemical reactions to promote AMP grafting *via* CuAAC (type 2 thin films);

7 – *in vitro* evaluation of type 2 AMP-chitosan thin films, for assessment of the implication of the different immobilization parameters on the antimicrobial activity of the coatings.

Altogether, the specific research goals above were set to provide proof-of-concept on the project's working hypothesis, i.e., that "click" chemistry is a valuable tool to create AMP-based antimicrobial coatings of interest for clinical applications.

This thesis is divided in seven chapters, where **Chapters I-III** provide background information that supports and puts into context the original research work undertaken, which is described in **Chapters IV-VI**. Finally, an integrated discussion of results obtained, major conclusions, and possible future directions are presented in **Chapter VII**. A more detailed view of the contents within each chapter follows.

Chapter I reviews the pathology, current treatment protocols as well as the different research lines involved in IAI and CWI. Moreover, considering the relevance of chitosan within scope both of this Thesis and of antibacterial dressings for wound care, this chapter also summarizes the implication of different chitosan characteristics on its biological activity and clinical applications. Likewise, given their potential as an emerging new class of antimicrobials, AMP are equally addressed in this chapter, regarding both their properties, and synthesis methods.

Chapter II presents a brief overview of characterization techniques that were relevant to the doctoral research project herein reported, and which are referred to in next chapters.

Chapter III is a critical review of some of the most popular approaches currently used to covalently immobilize peptides onto hydrogels (also applicable to other materials), highlighting advantages and limitations of each strategy, with particular emphasis on "click" chemistry techniques throughout the last decade. This literature review was published as a paper titled "Grafting Techniques towards Production of Peptide-Tethered Hydrogels, a Novel Class of Materials with Biomedical Interest" (*Gels* **2015**, *1*, 194-218).

Chapter IV addresses *Tasks 1-3* of the doctoral research plan, where Dhvar-5, a short AMP with broad antimicrobial activity already shown as promising on an *in vivo* chronic osteomyelitis model, was chosen as model peptide. Therefore, this chapter focuses on optimization of peptide immobilization parameters by means of "click" chemistry, namely, *via* the CuAAC reaction. As such, it also covers solid-phase synthesis of the convenient Dhvar-5 derivatives bearing an alkyne function (*Task 1*), and the conversion of chitosan's amines into azides (*Task 2*), which were next coupled to each other in the final CuAAC step (*Task 3*). This part of the doctoral project has been published in 2017, as an original research paper titled "Tethering antimicrobial peptides onto chitosan: optimization of azide-alkyne «click» reaction conditions" (*Carbohydrate Polymers* **2017**, *165*, 384-393).

Chapter V focuses on *Tasks 4-5* of the doctoral research project, where ultra-thin films prepared with the previously synthesized Dhvar-5-chitosan conjugates (type 1 thin films) were obtained and analyzed by different surface characterization techniques (*Task 4*); the antimicrobial properties of such thin films were equally assessed, allowing to infer not only about their potential as antimicrobial coatings, but also about the influence of peptide orientation/exposure on their anti-fouling properties (*Task 5*). Results obtained in this part of the research work have been compiled and submitted for publication in early 2018, as an original research paper titled "Only a «click» away: development of novel antibacterial coatings" (submitted, **2018**).

Chapter VI reports findings made in *Tasks 6-7*, where the CuAAC conditions optimized as described in Chapter III were applied to pre-formed chitosan ultra-thin films, to infer whether this alternate procedure leads or not to improved antibacterial coatings. In other words, this chapter addresses the most current approach for peptide tethering onto materials, where peptide is grafted onto pre-formed films, particles or scaffolds. As such,

chitosan ultra-thin films were first prepared and only next submitted to the sequential chemical transformations required for AMP tethering *via* CuAAC, whose success was confirmed by the convenient surface characterization techniques (*Task 6*). Finally, the ultra-thin films thus produced (type 2 thin films) where evaluated *in vitro* for their antibacterial properties, as previously done for their type 1 counterparts. Results obtained are being compiled into a manuscript, to be submitted for publication in due course, which focuses on the critical analysis of the influence of peptide immobilization procedure on the antimicrobial activity of the resulting coatings.

Chapter VII presents a critical analysis of the overall work reported in this thesis, with an integrated discussion of all results, highlighting the most striking findings and major conclusions. Finally, concluding remarks on prospects regarding translation for *in vivo* assays, and future directions in this field of research, are also included in this chapter.

Chapter I

Biopolymers-based materials as promising alternatives to current state-of-the-art antibiotherapy

1. Bacterial infections

Most living organisms are under continuous exposure to invasive bacteria with potential pathogenicity, which may be associated with appearance of severe infections [25, 26]. These bacteria survive in nature primarily by adherence to and growth on surfaces, of either nonliving materials or living tissues, developing the so-called biofilms [27, 28]. It is, therefore, no surprise that bacterial biofilms are commonly appointed as significant contributors to most of human infectious diseases, including infections both derived from medical devices and related to chronic wounds [29, 30].

Initial states of biofilm formation are characterized by bacteria attachment to a surface forming a structured consortium of bacteria which are able to communicate using quorum sensing (QS) molecules, such as, e.g., *N*-acyl homoserine lactone (AHL), and are then responsible for the production of a plethora of biochemical cues that facilitate adhesion and provide a structural matrix [28, 31]. The exact composition of this self-produced biofilm matrix depends on bacterial species, strain and environmental conditions, but usually consists of substances of diverse chemical nature such as exopolysaccharides, proteins, teichoic acids and extracellular deoxyribonucleic acid (eDNA) [30, 32]. Bacterial cells within the biofilm matrix are characterized by transition from a free-moving microorganism (Brownian motion) to an immobile one (latent state) [33, 34], which can significantly compromise the efficacy the currently available antibiotics, since their mechanisms of action interfere with bacterial metabolism or proliferation [32, 33, 35]. In addition, bacterial biofilms are elusive to attack by the host immune system [32, 36]. Therefore, the formation of bacterial biofilms is a major cause for the emergence of infectious diseases resistant to both state-of-the-art antibiotherapies and the components of the host's both innate and adaptive immunity and anti-inflammatory defense [30, 32].

In connection with the above, chronic (non-healing) wounds, including diabetic foot ulcers, pressure ulcers, and venous leg ulcers, are defined as cutaneous injury of long duration or frequent occurrence associated with persistent inflammation due to bacterial infections. Infection is caused by pathophysiologic effects resultant of the entrance, growth, and metabolic activities of microorganisms in wounded tissues. It represents a major health care problem associated with serious morbidity, impaired quality of life and significant economic costs [3, 17, 37-40]. Understanding the fundamental pathophysiology is an essential asset for the selection of appropriate wound management protocols [9, 40, 41].

The normal wound healing process (Figure 1A) requires proper circulation, nutrition, immune status, and avoidance of negative mechanical forces. This is a very complex physiological process, which depends on interactions between cells, extracellular matrix components and signaling compounds. The process comprises three phases: initial haemostatis and clot formation followed by inflammation, proliferation and closure, and scar maturation and remodeling with wound contraction [38, 42-44].

The first phase occurs in response to tissue injury and is a tightly regulated and intricate process. During the inflammatory phase, a fibrin plug is formed in order to re-establish homeostasis and local signals are released by cells near damage tissue that trigger an inflammatory cascade, which involves the recruitment of neutrophils that transmigrate across endothelia from local blood vessels, and monocytes that migrate from blood into the wounded area and differentiate into macrophages to phagocytize bacteria and debris. Additionally, cells are activated to release pro-inflammatory cytokines and chemotactic factors that further amplify the inflammatory response. A functioning immune system and adequate supply of growth factors are necessary in this phase of wound healing [38, 43-45].

In the proliferative phase, fibroblasts produce a collagen matrix, new blood vessels invade the forming granulation tissue, and epidermal cells migrate across the wound surface to close the breach. Fibroblasts and myofibroblasts lay down collagen-rich connective tissues comprising this composite and myofibroblasts, which contributes to wound contraction. Simultaneously, in a process termed re-epithelialization, keratinocytes at the wound edge migrate over the granulation tissue to differentiate the new outer layer of epidermis. Protein or vitamin deficiencies may impair collagen production, and necrotic tissue in the wound bed may impede re-epithelialization [38, 43-45].

The last phase of the wound healing process is characterized by the remodeling of the previously formed granulation tissue and by dermis regeneration. During the remodeling phase, fibroblasts reorganize the collagen matrix and ultimately assume a myofibroblast phenotype to effect connective tissue compaction and wound contraction [38, 43, 45].

The chronic wounds (Figure 1B) can be conceived when any of the components of the wound healing process is compromised due to the excessive amounts of bacteria in the tissue leading to prolonged inflammation, a defective wound matrix, and failure of re-epithelialization [3, 9, 38]. The invasion by aerobic pathogens, such as *Staphylococcus aureus* (*S. aureus*) and *Pseudomonas aeruginosa* (*P. aeruginosa*), is the main cause of wound infection. Chronic wounds often occur in individuals and tissues that are at

increased risk of bacterial invasion due to poor vascular supply and systemic factors [3, 23, 37]. Chronic wound infections (CWI) are characteristically associated with biofilms where the infecting bacteria are physically aggregated in clusters and surrounded by a self-produced polymer matrix, composed of exopolysaccharides, large surface proteins, fatty acids, and DNA [23, 46-49]. The action of enzymes and toxins produced by bacteria degrades the host tissue and consequently delays the healing process and establish as persistent infections that tolerate the host immune defenses [9, 46, 48-50]. Currently, most widespread practice against such persistent infections involve the administration of systemic antibiotics. However, even high concentrations of antibiotics may not be sufficient to combat such infections [9].

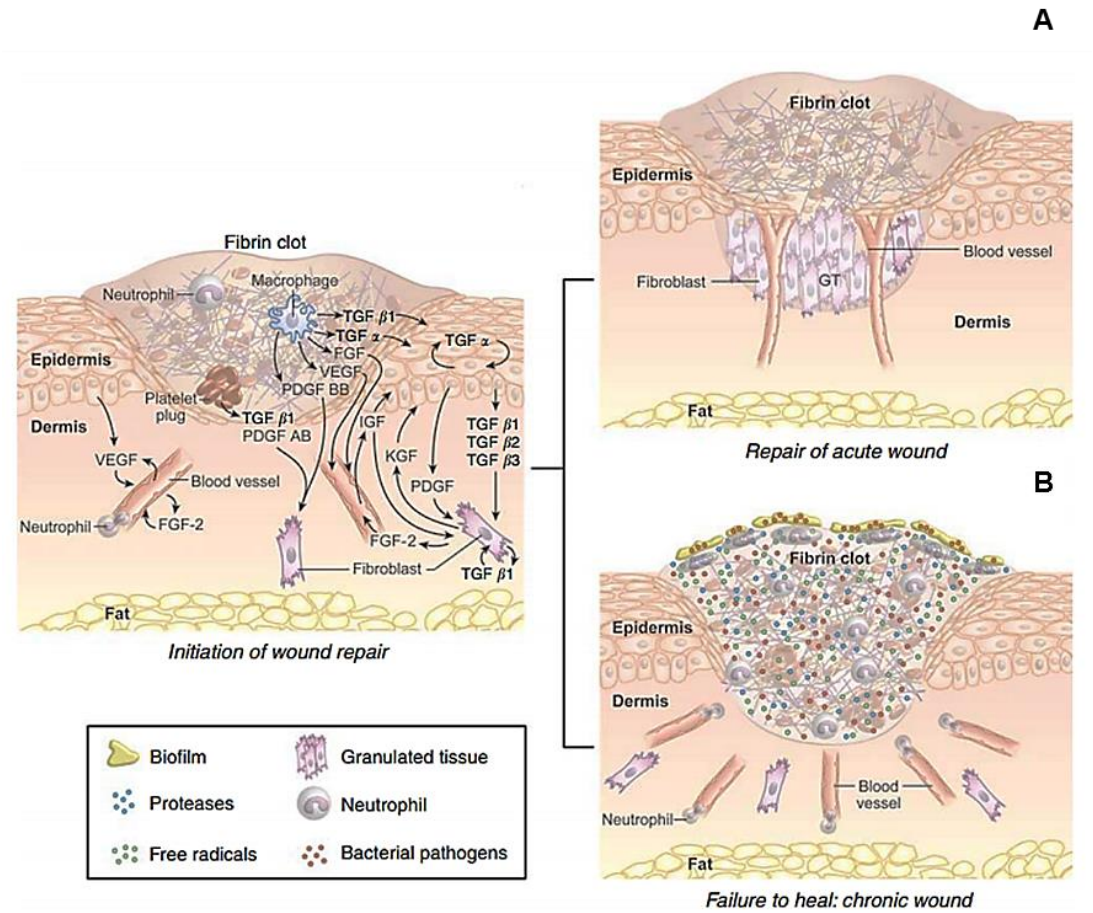

Figure 1 Wound healing process under **(A)** normal physiologic conditions and **(B)** after microbial invasion: tissue injury precipitates blood clotting, platelet aggregation, and migration of leukocytes, to the site of injury; the blood clot provides a scaffold for cell migration and aggregated platelets, which release growth factors into the surrounding tissue [51].

Another healthcare context where bacterial biofilms can lead to severe and/or chronic infections regards implant devices. The properties of synthetic implant devices

significantly influence the interactions with invading bacteria and potentially trigger device-associated infections [52]. Depending on the material and its properties (such as hydrophobicity and charge) the device surface can adsorb proteins or other organic compounds that are known to induce bacterial attachment and proliferation [31, 52]. In this connection, infections arising from implantation of orthopedic devices, as osteomyelitis, cause major morbidity and remain a difficult complication to treat after orthopedic surgery [53]. Implanted synthetic medical devices are associated with a considerable number of infections, involving bacterial colonization and the formation of a bacterial biofilm on the surface of the implant. Implant failure associated with compromised immunity at the implant/tissue interface may lead to persistent infections with consequent implant removal or replacement causing patient suffering and prolonged hospitalization [7, 24, 46, 54].

Pathogens such as *S. aureus*, *Staphylococcus epidermidis* (*S. epidermidis*) and *P. aeruginosa* can be acquired shortly after the surgical installation of implants or at a later stage (e.g. *via* a haematogenous route). Hence, implant-associated infections (IAI) are classified in three ways: superficial immediate infections, deep immediate infections and deep late infections. Superficial immediate infections are caused by bacteria that normally populate the skin and start to colonize the medical device (e.g. infected sutures). On the other hand, deep immediate infections may be due to inadvertent relocation of skin bacteria into the body, i.e. non-sterile implantation procedures, and become apparent shortly after invasive surgeries. Finally, deep late infections appear months or years after surgery and can be associated with a delayed display of contamination that was seeded during surgery or resulted from bacteria that migrated from another anatomic site [7, 55]. Upon implantation of the device, proteins from the blood or tissue directly adsorb onto the surface. This process of protein adsorption is influenced by surface hydrophobicity, roughness, potential, porosity, chemical composition, as well as composition and concentration of the protein solution, salt concentrations, pH, among others [7, 54, 56]. The layer of adsorbed proteins has been shown to be important for the adhesion of bacteria. The adhered bacteria will increase in numbers by proliferation and recruitment of other bacteria from the immediate environment forming the biofilm. The extracellular matrix surrounding the biofilm protects bacteria from stressful environmental conditions (UV radiation, pH variation, osmotic shock, desiccation and flow conditions), attack by the host's immune system and action of antibiotic substances, due to poor antibiotic penetration into the biofilm and the stationary phase of growth of bacteria underlying the

surface layer. Furthermore, the biofilm structure facilitates horizontal gene transfer between resistant and non-resistant microbial strains [7, 54, 55].

The emergence of multi-drug resistant bacteria like methicillin-resistant *S. aureus* (MRSA) and gentamicin-resistant *S. aureus* (GRSA) has critically challenged the use of conventional antibiotics [8, 24, 53]. The systemic administration of these agents is associated with several drawbacks such as the relatively low drug concentration at the target site and potential toxicity. In order to overcome these problems, conventional antibiotics like vancomycin, tobramycin, and gentamicin have been incorporated into controlled release devices. However, the release at levels below the minimal inhibitory concentration (MIC) is likely to evoke bacterial resistance by inducing specific gene expression, whereas high doses of antibiotics often generate cell toxicity [7, 24].

Several approaches concerning non-fouling surfaces were reported in order to prevent IAI such as (i) UV radiation of titanium surfaces to augment wettability, (ii) surfaces with covalently bound antimicrobial agents, (iii) surfaces covered with bacterium-repellent or anti-adhesive agents that use highly hydrated and close-packed chain-like molecules, such as poly(ethylene glycol) (PEG), poly(hydroxyethyl-methacrylate) (PHEMA), poly(methacrylic acid) polyurethanes, or bearing negative charges, and (iv) bioactive polymers which are synthesized by polymerization of constitutive monomers with therapeutic moieties [7, 56, 57]. However, the effectiveness of non-fouling coatings for reducing bacterial adhesion is limited and varies greatly depending on bacterial species. Even ultra-low fouling surfaces might eventually form substrates for the formation of biofilms – for example, due to degradation or inhomogeneity that might also be the result of damage caused during handling. Moreover, both the affinity of biomaterials with antibiotics and the available spectrum of therapeutics and active monomers with polymerization-compatible chemistry are quite limited. Another major obstacle is hemolytic activity, in particular, the toxicity of surfaces modified with quaternary ammonium or pyridinium salts and related compounds to human cells [7, 57, 58].

The decline in effectiveness of most clinically explored antibiotics has provided the stimulus to develop novel antimicrobial compounds and approaches. Additionally, there is also a need for strategies displaying long-term stability of antimicrobial action, even during the sterilization process, along with low cytotoxic profiles [7, 8].

2. Antimicrobial peptides - small biopolymers with big prospects

2.1 Brief overview

The discovery and use of antimicrobial agents has greatly contributed for treatment and reduction of the incidence of infectious diseases worldwide, and consequently became a key factor in the huge increase of the average life expectancy from the beginning of the 20th century to the current date. However, in recent decades a progressive decrease in the effectiveness of a large number of antibiotics, which were previously used with great success against several types of bacterial infections, has been observed. The rapid accumulation of mutations by bacteria and the continuous and sometimes inadequate use of antibiotics have resulted in the worldwide emergence of multidrug-resistant bacterial strains. Thus, the development of new classes of antimicrobial agents has become imperative [8, 9, 59].

A promising alternative to conventional antibiotics are antimicrobial peptides (AMP), peptides of natural origin that have intrinsic antimicrobial activity [24, 59, 60]. Most naturally-occurring AMP are small, basic, single gene-encoded peptides that are generally synthesized as pre-pro-proteins. These AMP are expressed during infection, inflammatory events and even in the wound repair phase in epithelial surfaces, in secretion fluids and in neutrophils, being widely distributed throughout nature either as the primary antimicrobial defense mechanism, or as an adjunct to existing innate and adaptive immune systems [53, 57, 60-62]. Thus, they play an important protective role against pathogens, and the induction of such peptides can allow a rapid and effective response against infectious organisms. In general, AMP possess broad-spectrum activity that includes efficient antimicrobial action against Gram-negative and Gram-positive bacteria, filamentous fungi and parasitic protozoans and metazoans. Furthermore, it has been suggested that these peptides may be potentially beneficial in the treatment of cancer and viral infections, including those caused by some enveloped viruses. As such, these natural compounds, as well as synthetic derivatives and analogues, are attractive candidates to treat microbial infections, particularly those caused by antibiotic-resistant bacteria due to their high efficacy at low concentrations, target specificity, anti-endotoxin activity and also synergism with classical antibiotics [8, 59, 60, 63, 64].

AMP are quite diverse in terms of charge and tridimensional structure, which is specified by the amino acid sequence (primary structure), and by disulfide bonds between cysteine

(Cys, C) residues, if present. Moreover, there is a diversity of equally effective derivatives of the native sequence that can be designed and easily synthesized [60, 61, 65].

Almost all AMP share the property of being highly amphipathic, with one face of the peptide being hydrophobic and the other face presenting a cluster of hydrophilic residues, a design that is consistent with membrane-specific interaction residues [8, 61]. Cationic peptides constitute the largest group of AMP and are widely distributed in animals and plants. The positive net charge of cationic AMP facilitates their binding to negatively charged membranes, as those in bacteria, on which they aggregate and subsequently act as destabilizers or disruptors, ultimately leading to cell death [61]. With respect to their structural characteristics, cationic AMP can be divided into three main classes: linear peptides forming α-helical structures, peptides rich in specific amino acids such as proline (Pro, P), glycine (Gly, G), histidine (His, H), arginine (Arg, R) and tryptophan (Trp, W), or Cys-rich peptides containing one or more disulfide bonds. The number of disulfide bonds ranges from 1 to 4 and results in β-hairpin-like structures [8, 59, 66].

Naturally occurring AMP with α-helical structures include, among others, cecropins from insects and mammals, magainins from frogs, and cathelicidins from mammals. AMP rich in specific amino acids include, e.g., indolicidin, a Trp-rich peptide from bovines and PR-39, a Pro/Arg-rich peptide from pigs. Examples of Cys-rich AMP are polyphemusin and tachyplesin from horseshoe crabs, protegrin-1 from pigs, and β-defensin-3 and α-defensin (HNP3) from humans [8, 59].

The release of AMP from storage sites can be induced extremely rapidly, making them particularly important in the initial phases of resistance to microbial invasion. On the other hand, there has been a wide and rather speedy development of *de novo* AMP, fully synthetic peptides inspired in the properties of natural AMP. These synthetic peptides are distinct from those in nature, with generally simpler but rationally engineered composition, obtained by varying the amino acid content and sequence and overall peptide length to achieve enhanced activity and very low cytotoxic properties [7].

AMP like MSI-78 (Pexiganan) [8-10], hLF(1-11) [12, 13] or Dhvar-5 [14, 53] are particularly interesting, given their well-documented efficacy against a wide panel of microbes, including MRSA, GRSA and *P. aeruginosa* hospital isolates, which constitute one of the major health concerns of our time [17, 18].

Pexiganan, a synthetic 22-amino acid peptide inspired in magainins (natural AMP isolated from skin secretions of *Xenopus laevis* frogs) has been proposed for topical treatment of diabetic foot ulcers (DFU), as its delivery to the wound-healing site showed

it to be effective against bacterial strains *P. aeruginosa* and *S. aureus*, whose growth was diminished [9, 25].

Human lactoferrin 1-11 (hLF1-11) is an AMP derived from the active domain of human lactoferrin, corresponding to the *N*-terminal segment of this protein, which comprises amino acids 1 to 11. hLF1-11 has a broad antimicrobial spectrum *in vitro* against both bacteria and fungi. Furthermore, studies demonstrated the efficacy of hLF1-11 *in vivo*, reducing the number of MRSA bacteria after systemic administration in the mouse thigh infection model [12, 67].

Dhvar-5 is a synthetic 14-residue peptide analogue of histatin-5, an antifungal peptide found in human saliva. Given that the bacterial cell membrane is negatively charged, Dhvar-5 was designed so as to have a net positive charge at the *C*-terminus and a hydrophobic *N*-terminus. The positive charge is presumed to play a crucial part in its antimicrobial activity since it promotes peptide penetration into the bacterial cell, enabling its targeting towards intracellular organelles. Dhvar-5 showed fungicidal and bactericidal properties, including against MRSA *in vitro* [14, 53].

2.2 Mechanisms of peptide antimicrobial action

Current scientific evidence demonstrates that most AMP are membrane-lytic molecules that, through mechanisms of pore formation, act as membrane-permeabilizing/destabilizing agents, ultimately leading to the disruption of the target cells. In other words, most AMP, often in aggregate form, infiltrate into cell membranes, making the target cells leaky and finally killing them [57, 61, 62, 68].

Though different specific molecular mechanisms of AMP-membrane interactions have been proposed, and remain an open topic, there is a consensual first step where the AMP adhere to the surface of bacteria by electrostatic interactions, after which different types of structural reorganization take place and lead to pore formation. It is established that such initial stages of AMP-membrane interaction require the peptide to possess both cationic and hydrophobic amino acids, which means that amino acid residues like (i) Arg, Lysine (Lys, K), and His, with positively charged side chains at physiological pH, favor AMP binding to the negatively charged membrane surfaces of target bacterial cells via electrostatic attraction, whereas (ii) Trp, Leucine (Leu, L) and Pro, with bulky, nonpolar side chains, occur frequently in AMP presumably to provide lipophilic anchors that promote subsequent steps in destabilization of the phospholipid bilayer [62, 68].

The specific mechanisms of bacterial cell wall/membrane binding and pore formation by AMP differ among various peptides and, as said, remain an open subject of research. Most AMP appear to be electrostatically attracted to Gram-negative bacteria by binding to the outer lipopolysaccharide membrane, and to teichoic and teichuronic acids in Gram-positive bacteria. When the inner membrane is encountered, the cationic peptides form channels, altering that membrane. On the other hand, eukaryotic membranes, which contain predominantly neutral phospholipids, are usually less susceptible to disruption by AMP. In addition, the presence of cholesterol in eukaryotic membranes increases their resistance to membrane disruption by AMP [8, 53, 57, 59, 61, 68-70].

Binding of AMP to cell membranes is generally not directly implicated as solely responsible for bacterial death. On contrary, this binding affinity maybe required for preferential accumulation of AMP in bacteria. Upon association with the membrane, unstructured peptides become structured and begin thinning the bacterial membrane and proceed to disrupt the membrane reaching inner layers and the cytoplasmic membrane. Once the cytoplasmic membrane is reached, the AMP interact with negatively charged groups of the external leaflet. At this stage, linear AMP re-organize and assume an optimal amphipathic conformation where the hydrophilic face interacts with the phospholipid head groups whereas their hydrophobic face is inserted into the bilayer core. Such interactions can lead to a wide variety of structural distortions/damages to the membrane architecture and can result from various possible mechanisms [8, 68].

In the carpet mechanism (Figure 2A), peptide molecules accumulate parallel to the surface and destabilize the membrane structure. When a saturation point is reached, extensive wormhole formation occurs, causing the abrupt lysis of the microbial cell. Cell lysis is believed to result from the lipid layer bending back on itself, with lateral expansions in the polar head-group region, providing the gaps that will be filled up by individual peptide molecules [7, 8, 14, 58, 68].

The toroidal pore model (Figure 2B) considers bending of the lipid bilayer resulting in pores in the membrane where lipids tilt in such a way that the lipid head groups define the surface of the pore until a water core is formed. These channels are responsible for the leakage of ions and possibly larger molecules throughout the membrane and also allows the peptides to cross the membrane without causing significant membrane depolarization. Once inside, the peptides eventually head to intracellular targets and exert their killing activities [7, 8, 58, 68].

Finally, the barrel stave model mechanism (Figure 2C) consists in the self-association of peptide molecules into barrel-like bundles that line amphipathic transmembrane pores followed by peptide insertion into the membrane parallel to the lipid bilayer normal. The non-polar side chains associate with the hydrophobic fatty acid tails at the inside of the phospholipid bilayer, and the hydrophilic side-chains are oriented inward into the water-filled pore [7, 8, 58, 68].

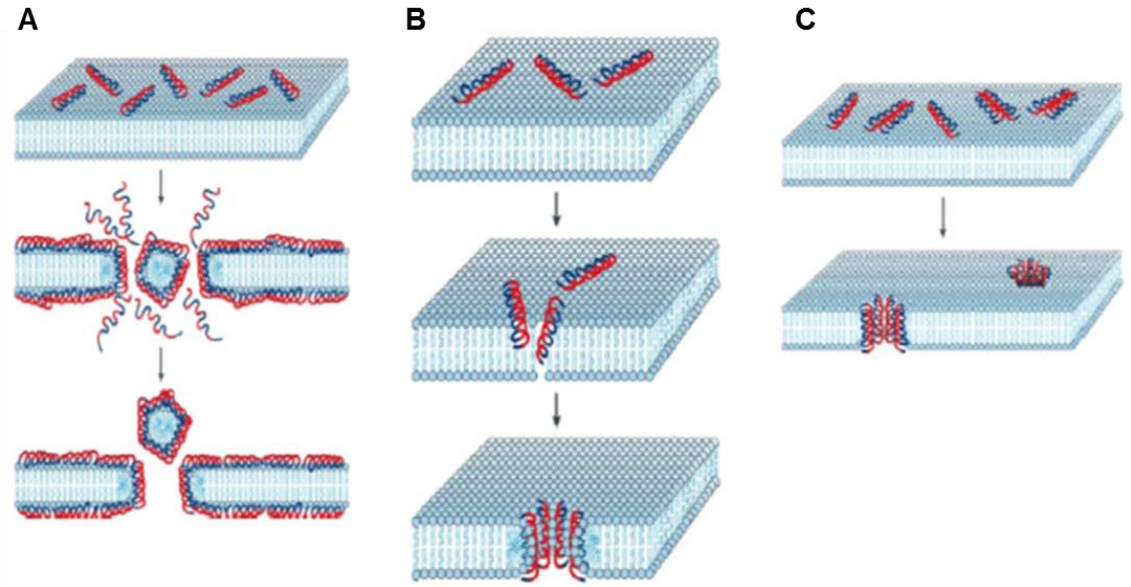

Figure 2 Current models of the mechanism of action of membrane-active antimicrobial peptides (AMP): **(A)** carpet model; **(B)** toroidal pore model; **(C)** barrel-stave model [7].

Bacterial resistance to AMP is expected to be reduced since the latter act by altering the permeability properties of the cell plasma membrane and because evolutionary changes in the bacterial membrane are improbable [8, 53, 57-59, 61].

2.3 Principles of peptide synthesis

The fight against severe bacterial infection has attracted much attention from the medical and scientific communities. As previously mentioned, there is a growing number of antibiotic-resistant bacteria associated with the absence of long-lasting and effective antibiotherapies. Therefore, there is an urgent need for new and more active antibiotics exploring novel antimicrobial mechanisms of action [71].

The promising properties of AMP has boosted the remarkable progress toward development of AMP-based therapeutics [72]. However, their limitations (e.g.,

cytotoxicity, short half-life) can restrain the applicability of AMP as therapeutic agents [72]. In order to overcome these issues, chemical modifications on the native AMP sequence have contributed significantly to enhance AMP therapeutic potential by tailoring its chemical properties according to the desired application [72]. This *de novo* design of AMP allows to carry out a tailor-made synthesis of a peptide combining unnatural amino acids and simultaneously maintaining the structural features of the natural sequences, while exhibiting comparable or even improved biological profiles.

The improvement of productions methods and peptide chemistry have made prompted the development of effective and high-yielding peptide synthesis strategies ideal for the development of novel AMP-based pharmaceuticals [72, 73].

2.3.1. Peptide bond formation

The so-called peptide bond corresponds to an amide group. The amide functionality is a crucial intervenient in the organization and structure of biological systems. This functional group is also a common feature, whether a synthetic molecule is small and simple or large and complex, due to its promising properties, such as high polarity and stability and conformational diversity [74-78]. The amide group is also the basis for some of the most versatile and broadly spread drugs since it is neutral and has both hydrogen-bond accepting and donating properties. These are the cases, for example, of Atorvastatin® (cholesterol-lowering medication), Diltiazem® (medication for hypertension and angina), Fuzeon® (anti-retroviral), Valsartan® (anti-hypertensive), Victoza® (medication for type 2 diabetes), and conventional antibiotics, from current β-lactams like penicillin or amoxicillin, to those reserved for more complicated cases, like vancomycin or daptomycin, all of which contain amide bonds [75, 76, 78-80].

Protein synthesis comprises a series of peptide coupling reactions, that is to say, is based on sequential amide bond formation between α-amino acid residues or peptide fractions. The synthesis has to be highly regulated in order to ensure chemoselective formation of the target amino acid sequence of each peptide sequence [75].

Amide or ester bond formation between an acid and an amine or an alcohol, respectively, is officially a condensation reaction. Reaction of a carboxylic acid with an alcohol is an equilibrium process that gives the ester as condensation product (Figure 3A); in turn, on mixing an amine with a carboxylic acid at room temperature, the kinetically favored acid-base reaction, rather than the condensation, occurs yielding the stable ammonium carboxylate salt depicted in Figure 3B.

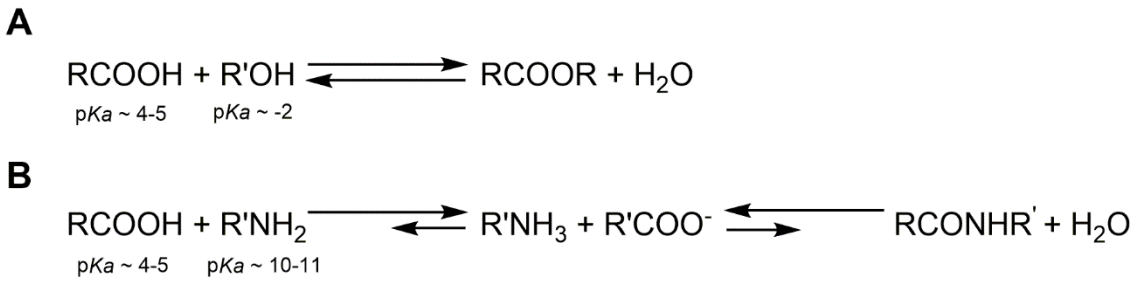

Figure 3 The standard method for formation of an **(A)** ester bond and an **(B)** amide bond [75].

Nevertheless, at high temperatures (> 200 ºC) or in the presence of appropriate carboxyl-activating agents, a reaction of a primary or secondary amine with the carboxylic acid occurs through the condensation process, leading to the formation of a thermodynamically stable amide. On that account, peptide bond formation at low temperature requires the activation of the carboxylic acid (Figure 4) [74, 75, 78].

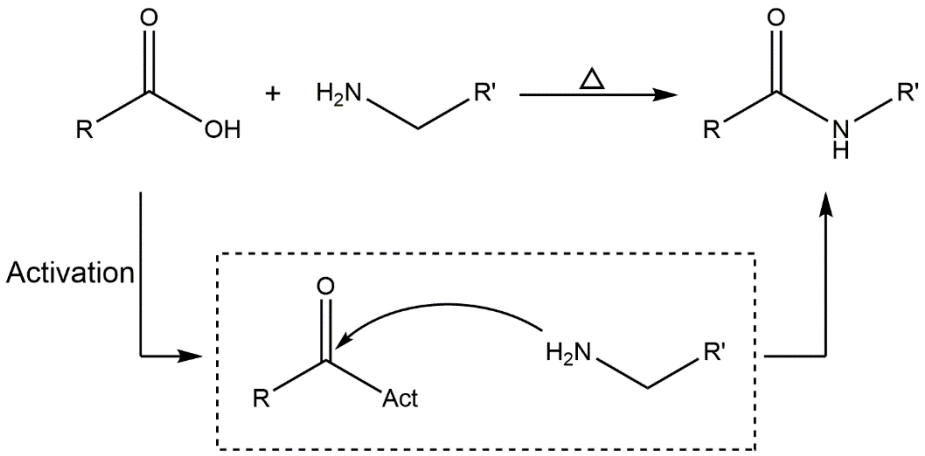

Figure 4 Activation process for amide-bond formation: The direct condensation of the salt can be achieved at high temperature, which is usually incompatible with other functionalities, or with the presence of chiral centers. Therefore, activation of the carboxylic acid, by an activating group (Act), is essential, in order to increase the reactivity of the carboxyl component towards nucleophilic attack by the amino group [78].

Usually, in the presence of *in situ* condensation agents the carboxylic acid moiety is activated. During this stage, the hydroxyl group of the carboxylic acid is substituted with a better leaving group, as the acid would otherwise simply form salts with the amine. The activators or condensation agents are also named as coupling reagents, while the reaction of the activated intermediate and the amine is known as the coupling reaction [77, 78].

2.3.2. Basic principles of solid-phase peptide synthesis (SPPS)

The concept of solid-phase peptide synthesis (SPPS) was developed in 1963 by Merrifield, in which peptide chain assembly occurs on a solid support [81-83]. This efficient and straightforward technique does not require isolation or purification of synthesis intermediates [83, 84]. Although, solid-supported strategies were initially developed to facilitate the synthesis of peptides, they were rapidly transposed to the synthesis of other organic compounds, receiving the general designation of solid-phase organic synthesis (SPOS) [75, 85, 86]. SPPS affords much higher yields of pure products and runs more rapidly than classical synthesis solutions. All amino acids are sequentially added and any unreacted materials or by-products are easily washed away [75]. The polymeric support, also known as resin, must be insoluble under the conditions of the synthesis, thus allowing filtration and washing of reagents and any by-products, as unreacted materials and impurities are dissolved and filtered. Moreover, resins must have a functional group where the first amino acid is linked through a suitable covalent bond, to guarantee that the elongating peptide is not washed away throughout peptide chain growing [75, 81, 87].

Synthetic organic chemistry is based on the concourse of reagents and catalysis to achieve the clean formation of new bonds. To ensure that only the desired peptide bond is formed between two amino acids, the basic (amine) group of the *N*-terminal amino acid and the acidic (carboxyl) group of the *C*-terminal amino acid must both be made unable to react. Hence, it is necessary to use appropriate protecting groups to prevent the formation of unwanted bonds and side reactions [88, 89]. This deactivation is known as the protection of reactive groups, and a group that is thus made unable to react is called protected group. A protecting group must be (i) easy to introduce into the functional group, (ii) stable to a broad range of reaction conditions and (iii) safely removable at the end of the synthetic process or when the functional group requires manipulation [88].

In the chemical synthesis of peptides, these are assembled in the C→N direction, i.e., the reverse to that of protein biosynthesis in ribosomes; this means that the *C*-terminal amino acid must have its carboxyl group protected throughout the whole chain elongation process. Also, each amino acid subsequently added to the growing chain must have its amino group protected during the condensation reaction, after which the amino-protecting group must be removed to allow for following coupling of the following *N*-protected amino acid [74, 82, 84, 88]. As such, in SPPS, the first *N*-protected amino acid of the sequence (i.e., the peptide's *C*-terminal amino acid) is typically loaded onto the resin by

a covalent bond using standard *in situ* coupling reagents; thereby, the resin will act as the *C*-terminal carboxyl-protecting group during peptide chain elongation (Figure 5) [82-84]. The resin can be retained in a syringe with a filter that is made either of polypropylene or of a sintered glass material [87].

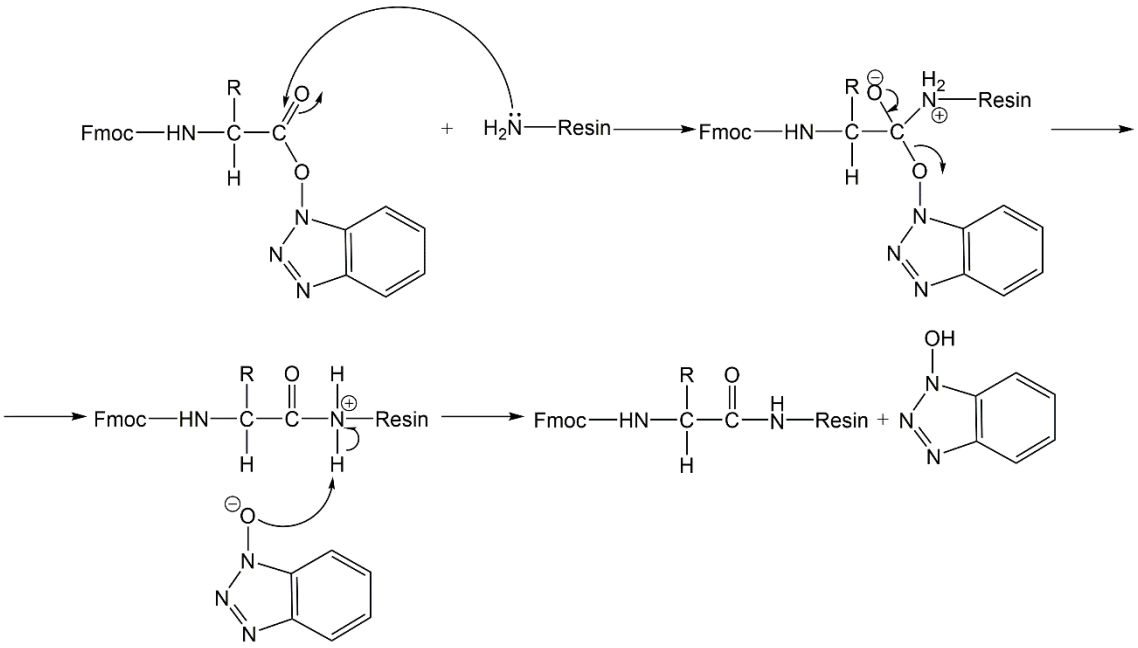

Figure 5 Coupling reaction of the 9-fluorenylmethoxycarbonyl (Fmoc)-amino acid, activated as, e.g., an 1-hydroxybenzotriazolyl ester, to an amine-functionalized resin. R_1 is the amino acid side chain [87].

After removal of the *N*-protecting group (deprotection) and washing of the resin, the second *N*-protected amino acid is activated *in situ* and coupled to the free amine of the first [82-84]; afterwards, the second amino acid's temporary *N*-protecting group will be removed in order to allow for coupling of the third *N*-protected amino acid, and so on. This deprotection/coupling procedure is repeated until all the amino acids of the sequence have been orderly coupled, i.e., on-resin assembly of the entire target peptide has been completed [82, 84, 88]. Once this has been achieved, suitable chemical treatment of the peptidyl-resin leads to release of the peptide chain from the resin, usually with concomitant removal of amino acid side-chain protecting groups ("permanent" protecting groups). A general scheme of SPPS is presented in Figure 6 [82, 84, 88].

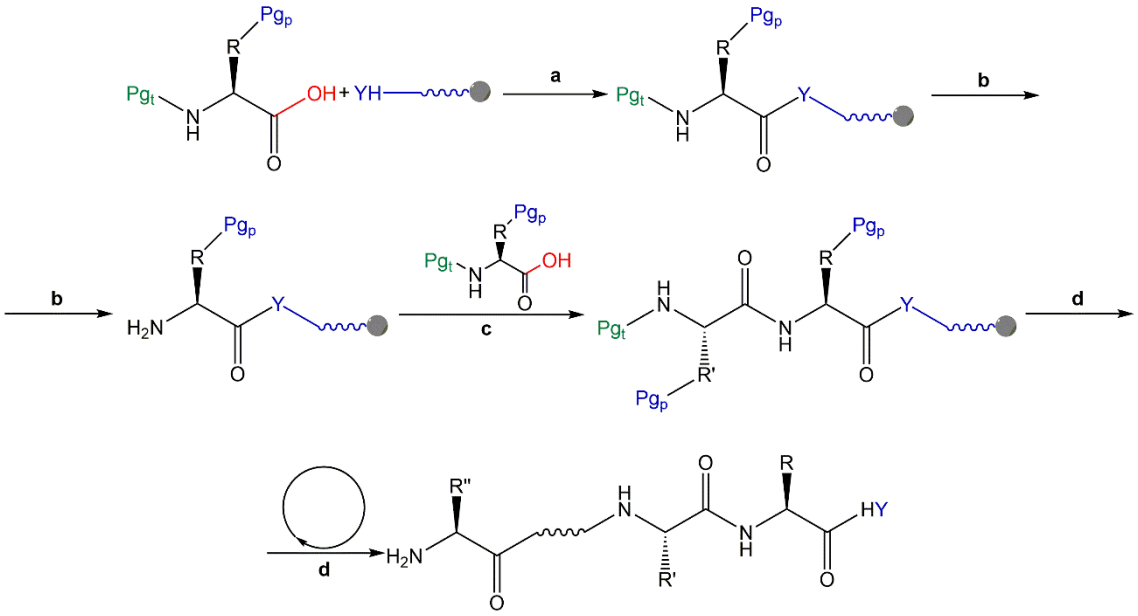

Figure 6 Schematic overview of SPPS: chemical synthesis proceeds from the carboxyl terminus to the amino terminus, i.e., in the opposite direction of protein synthesis *in vivo* [90]; Y is generally NH (synthesis of peptide carboxamides); **(Pg_t)** is the *N*-protecting group of the first amino acid; and **(Pg_p)** is the amino acid side-chain protecting groups.

There are two main α-amino protection schemes in SPPS: the selective protection scheme known as Boc/Bzl and the orthogonal protection scheme known as Fmoc/^{t}Bu. The first uses *tert*-butoxycarbonyl (Boc) as the α-amino temporary protecting group (labile to trifluoroacetic acid) and benzyl (Bzl) or alike (i.e., stable to trifluoroacetic acid used to remove Boc, but removable with stronger acidolytic agents such as hydrogen fluoride) as the permanent protecting group for amino acid side chains. On the other hand, the second method uses 9-fluorenylmethoxycarbonyl (Fmoc) as the α-amino temporary protecting group (labile to secondary amines such as piperidine) and *tert*-butyl (^{t}Bu) or alike (i.e., stable to secondary amines used to remove Fmoc, but removable with trifluoroacetic acid) to protect amino acid side chains throughout peptide chain assembly [82, 84].

The orthogonal Fmoc/^{t}Bu chemistry is the most popular protection scheme in SPPS, mainly due to the mild conditions used to remove the temporary protecting group, i.e., short treatment with 5 to 20% solutions of suitable secondary amines, such as piperidine, in *N*,*N*-dimethylformamide (DMF) or *N*-methylpyrrolidone (NMP) [82, 84, 87-89, 91]. In turn, although the Boc/Bzl protection scheme is cheaper than the Fmoc/^{t}Bu one, it requires repeated use of moderately concentrated (≥ 30%) solutions of trifluoroacetic acid (TFA) in dichloromethane (DCM), and these harsh conditions may result in peptide modification or even leaching (cleavage from resin) during the process of chain

elongation. Hence, both peptide linkage to the resin and permanent protecting groups must be stable to TFA, which means that even harsher conditions are required for final side-chain deprotection and cleavage of peptide from the resin [84, 88].

The most usual side chain protecting groups in Fmoc/^{t}Bu scheme are ^{t}Bu, used to protect carboxylated and hydroxylated side chains, as in aspartic acid (Asp, D), glutamic acid (Glu, E), serine (Ser, S), threonine (Thr, T), tyrosine (Tyr, Y); while triphenylmethyl or trityl (Trt) is commonly used to protect nucleophilic side-chain groups, as in His, Cys or Lys; Boc (also used in His or Lys) and 2,2,5,7,8-pentamethylchroman (Pmc) or pentamethyl-2,3-dihydrobenzofuran-5-sulfonyl (Pbf) are mostly used to protect the guanidine group of the Arg side chain. These are "permanent" protecting groups which remain linked throughout all steps of the synthesis, being removed only in the last step. Consequently, they need to be stable to the secondary amines used to remove Fmoc, and easily removable with TFA during the cleavage of the peptidyl-resin linkage [84, 87, 88].

2.3.3. General procedures in SPPS

In any SPPS, the first step to be considered is the choice of resin, taking into account two important factors: (i) form of the *C*-terminal of the peptide (native, i.e., carboxyl; carboxamide; other), and (ii) appropriate conditions for peptide-resin bond cleavage. In most Fmoc/^{t}Bu SPPS applications, peptide acids (*C*-terminal carboxyl) or amides (*C*-terminal carboxamide) are obtained after acidolytic cleavage of the peptide-resin bond, usually with TFA-based cleavage cocktails [75, 81, 84, 88, 92]. Currently, commercially available resins are modified by appropriate linkers which enable anchoring of the protected *C*-terminal amino acid residue by the creation of ester or amide bonds, thus forming peptide acids or peptide amides, respectively [87, 89]. The most popular linkers in such cases are Sasrin, Wang and 4-(4-hydroxymethyl-3-methoxyphenoxy)butyric acid (HMPB) with free hydroxyl groups, for the synthesis of peptide acids, or Rink amide linker as well as Peptide Amide Linker (PAL) or Sieber linkers with free amine groups, for the synthesis of peptide carboxamides. Most commonly, the *C*-terminal amino acid establishes an ester or an amide bond with, respectively, a Wang or a Rink resin, which are the two most popular resin types in Fmoc/^{t}Bu SPPS. These resins are available with different functionalizations, or loadings, i.e., mmol of reactive sites per gram of resin; also, particularly in the case of the Wang type, resins with pre-loaded *C*-terminal amino acid can be purchased to most suppliers [75, 81, 84, 87, 88, 92].

The Rink amide MBHA (4-methylbenzhydrylamine) resin (Figure 7) is extensively used since many peptides, including most AMP, are naturally found in the amidated form and *C*-terminal amides are more stable to degradation than *C*-terminal acids.

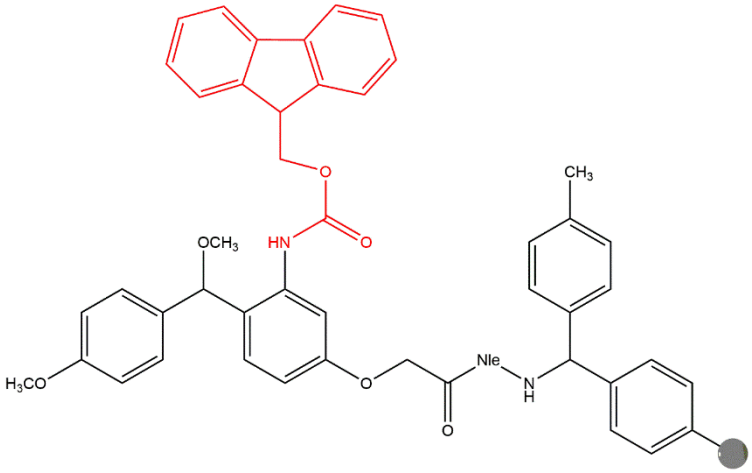

Figure 7 Structure of the Rink amide MBHA resin. The Fmoc-protected amino group is shown in **red** and in **grey** is the polymer chain from the resin [87].

Removal of the temporary N^{α}-protecting group, Fmoc, occurs under mild basic conditions using piperidine or similar secondary amines, as these are better at trapping the dibenzofulvene generated during the removal (Figure 8). As already mentioned, typically, a solution of 20% piperidine in DMF is employed to remove the Fmoc group in a few minutes, without peptide cleavage from the resin [75, 81, 84, 87, 88, 92].

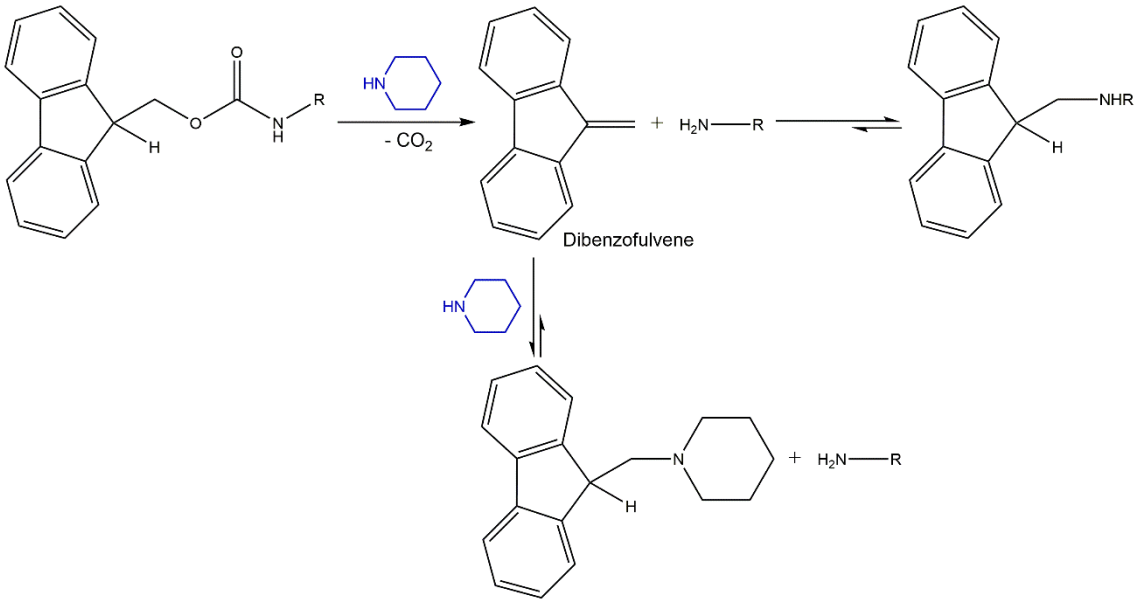

Figure 8 Removal of the Fmoc group by piperidine **(in blue)** for the formation of a free $-NH_2$ [93].

After removal of Fmoc the resin is carefully washed with suitable solvents like DMF and/or DCM and coupling of the subsequent N^{α}-Fmoc-protected amino acid (Fmoc-AA-OH) is carried out. To that extent, the Fmoc-AA-OH is pre-mixed with the chosen carboxyl activating agent in a minimal volume of DMF and/or DCM, and the slurry is immediately added to the resin [87].

Most common coupling agents are dialkylcarbodiimides, due to their low cost and general efficiency; carbodiimides can be regarded as dehydrating agents, which extract a molecule of water from the carboxyl and amino groups of both reactants, with the oxygen atom going to the carbon atom of the carbodiimide, and the hydrogen atoms to the nitrogen atoms, giving an *N*,*N*′-disubstituted urea, whose thermodynamic stability is regarded as the driving force towards formation of the desired peptide product [78, 94]. In the particular case of Fmoc/^{t}Bu SPPS, *N*,*N* -diisopropylcarbodiimide (DIPCDI or DIC) is the carbodiimide of choice, as it origins the *N*,*N'*-diisopropylurea (DIU) by-product, which is soluble in both DMF and DCM and can be easily washed out from the resin.

Whenever a given coupling step is not achieved using the aforementioned coupling reagents, especially with hindered substrates, alternative *in situ* coupling agents may be employed, as uronium or phosphonium salts like HBTU (*O*-(benzotriazol-1-yl)-1,1,3,3-tetramethyluronium hexafluorophosphate) or PyBOP (benzotriazol-1-yloxytri(pyrrolidino)-phosphonium hexafluorophosphate), among many others, which are usually more expensive, but also more effective, than carbodiimides [75, 78, 95, 96].

In the anchorage of Fmoc-amino acids to linkers like the Rink amide resin and for performing the peptide coupling reaction throughout the synthesis, basic tertiary amines like *N*-ethyl-*N*,*N*-diisopropylamine (DIPEA) or *N*-methylmorpholine (NMM) are also added. These tertiary amines are required to deprotonate the acid group of the Fmoc-amino acid, yielding the carboxylate anion that is more reactive towards uronium or phosphonium-based coupling agents (Figure 9) [75, 87, 95, 97].

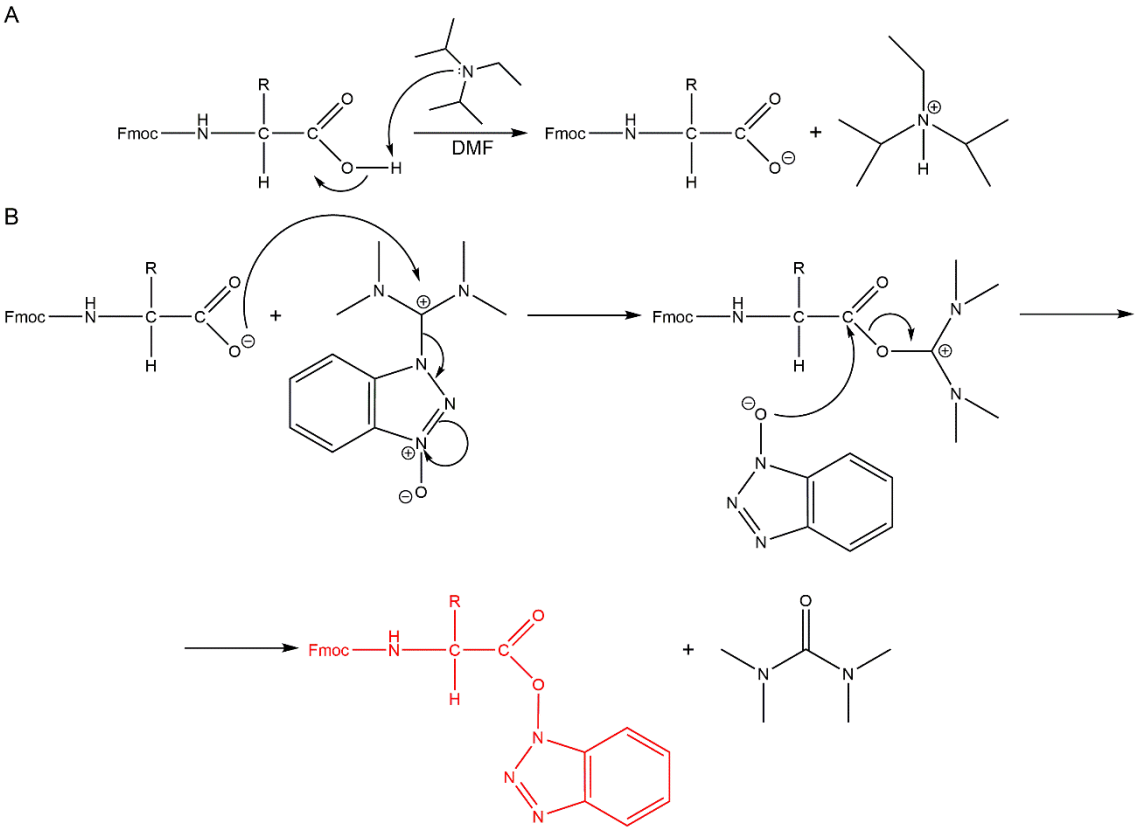

Figure 9 Mechanism for the activation reaction of the Fmoc-amino acid with HBTU, wherein R is the side chain of an amino acid: **(A)** Initially, the acidic proton of the Fmoc-amino acid is removed by DIPEA or another organic base. **(B)** Then, the deprotonated Fmoc-amino acid is added to HBTU, generating the elimination of a triazole derivative. Finally, this hydroxybenzotriazole derivative is added to the carbonyl group of the Fmoc-amino acid, leading to the formation of the activated Fmoc-amino acid (in **red**), by nucleophilic substitution [87].

Other coupling reagents, such as ethylchloroformate or 2-ethoxy-1-ethoxycarbonyl-1,2-dihydroquinoline (EEDQ), can be used to form anhydrides by reacting with acids. Anhydrides are formed slowly but react promptly with amines that are consequently rapidly consumed, avoiding amine accumulation and occurrence of side-reactions [75, 78].

Finally, it should be highlighted that, usually, both Fmoc-AA-OH and coupling agents are added in excess to the resin, usually 3 to 10 molar equivalents with respect to the resin reactive sites, to ensure that coupling reactions are quantitative [75, 83]. SPPS is currently completed with long reactions times and many washing steps between each step to avoid deletion, substitutions or addition of sequences [91]. Therefore, it is possible to obtain higher reaction yields by means of a clean synthesis procedure [87].

The efficiency of both the deprotection and coupling steps can be qualitatively monitored by colorimetric assays such as, among others, the Kaiser, or ninhydrin, test. This test

allows for the detection of free primary amine groups, as these readily react with ninhydrin (yellow) to give a deep blue-purple adduct known as Ruhemann's blue (Figure 10) [87, 98].

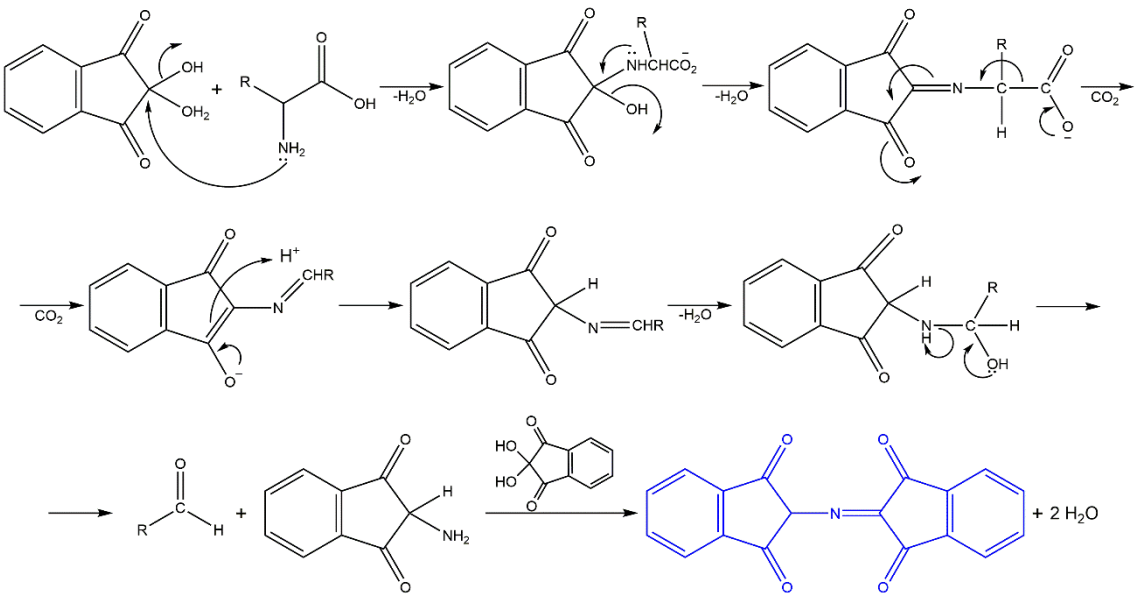

Figure 10 Ninhydrin reaction with α-amino acid with a primary amino group forming the Ruhemann s blue (in **blue**) [87].

The test is extremely sensitive and can be done efficiently on a few beads of the peptidyl-resin: successful deprotection steps confer a deep blue color to the beads, whereas beads after a successful coupling step remain light-yellow [87, 99].

Once the peptide is assembled through Fmoc/^{t}Bu SPPS, its cleavage from the resin is generally done by acidolysis with concentrated TFA, as above referred [75, 87]. The permanent protecting groups must, also, be removed in this final process of cleavage. During this acidolytic procedure, highly reactive cationic species are generated which may irreversibly modify amino acid side-chains containing nucleophilic functional groups, like, Trp, Tyr, methionine (Met, M), or Cys. These side reactions can be suppressed by adding to TFA minute amounts of small hydrophobic nucleophiles, which act as scavengers capable to capture the highly reactive cations generated during this acidolysis process. Amongst the most popular TFA-based cleavage cocktails, reagent K (TFA, phenol, triisopropylsilane (TIS), 1,2-ethanedithiol (EDT) in the 82.5 : 5 : 5 : 2.5 volumetric ratio) and reagent R (TFA, thioanisole, EDT, anisole (90 : 5 : 3 : 2) are seen as the most appropriate to promote peptide cleavage and full deprotection without significant occurrence of side reactions [87, 100-103]. For cleavage of complex peptides

that comprise several sensitive side-chains functionalities, or that include arginine residues, reagent R is usually applied [101, 102]. Whenever peptide sequences do not contain significantly susceptible amino acids, a thiol-free odorless reagent containing TFA, water and TIS in the 95 : 2.5 : 2.5 volumetric ratio is selected.

Finally, the purity of the crude peptide product is usually determined by high performance liquid chromatography (HPLC) and, when necessary, the peptide is purified by preparative reverse-phase HPLC (RP-HPLC). Peptide identification is usually achieved by mass spectrometry techniques and, if additionally required, amino acid analysis (AAA) [104].

3. Chitosan, a large biopolymer with wide biomedical relevance

Chitosan is a linear, polycationic copolymer of β-(1→4)-linked 2-acetamido-2-deoxy-D-glucopyranose and 2-amino-2-deoxy-D-glucopyranose units (Figure 11) derived from chitin, which is the main component of the exoskeleton of crustaceans as well as of the cell walls of some bacteria and fungi, widely available in nature [105-109]. The main parameters influencing the characteristics of chitosan are its biological origin, molecular weight (M_w) and degree of deacetylation (DD), representing the proportion of deacetylated units. These parameters are determined by the conditions set during alkaline deacetylation of chitin [107, 108, 110].

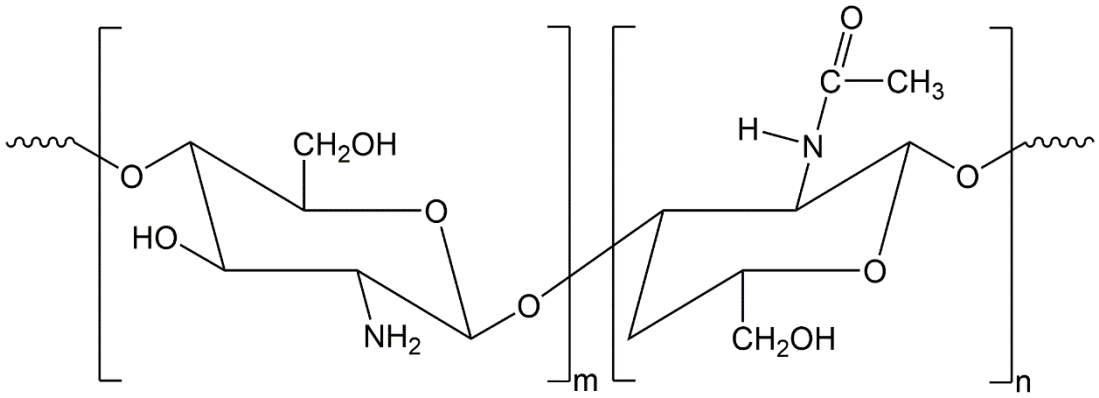

Figure 11 Chemical structure of chitosan: schematic representation of the conformation of a polymer chain of β-(1→4)-linked 2-acetamido-2-deoxy-D-glucopyranose and 2-amino-2-deoxy-D-glucopyranose units (adapted from [111]).

Chitosan is a weak base and is insoluble in water, but soluble in dilute aqueous acidic solutions below its pKa (~6.3), in which it can convert glucosamine units due to the presence of amino groups ($-NH_2$) into the soluble protonated form ($-NH_3^+$) [111, 112].

Currently, much attention is being paid to chitosan for its potential medical and pharmaceutical applications. A critical advantage of chitosan is its biocompatibility, which allows its use in various medical applications such as topical ocular application, implantation or injection. In addition, chitosan is considered as biodegradable since is metabolized by certain human enzymes, especially lysozyme. Due to its positive charge at physiological pH, chitosan is also bioadhesive, which increases retention at the site of application. It has been also reported that chitosan acts as a penetration enhancer by opening epithelial tight-junctions [107, 110, 113].

Chitosan is also particularly suitable as a biomaterial for tissue repair and regeneration (Figure 12), due to its ability to promote cell proliferation, naturally hydrophilic character, pH-dependent cationic nature and tendency to interact with anionic glycosaminoglycans (GAG), heparin, proteoglycans, and polynucleotides like DNA or small interfering ribonucleic acid (siRNA). In this context, chitosan has been widely used as implants for controlled drug release and in scaffolds to deliver growth factors [105, 106, 114]. Chitosan has also been found to possess a growth-inhibitory effect on tumor cells, suggesting that it may have potential value in cancer therapy [105]. Furthermore, chitosan assembles many important requirements for biomedical applications, in that it promotes wound-healing, due to its ability to foster adequate granulation tissue formation accompanied by angiogenesis and regular deposition of thin collagen fibers. Finally, chitosan has both antimicrobial activity and bacteriostatic effects *per se* [44, 105, 107]. The antimicrobial activity of chitosan was observed against a wide variety of microorganisms including fungi, algae and bacteria, being more active against Gram-positive than against Gram-negative bacteria, in particular if it has high M_w [109].

Moreover, the reactive functional groups present in chitosan (amino group at the C2 position of each deacetylated unit and hydroxyl groups at the C6 and C3 positions) can be readily subjected to chemical modification, allowing manipulation of mechanical and solubility properties, enlarging its biocompatibility, and tailoring its properties [111, 112].

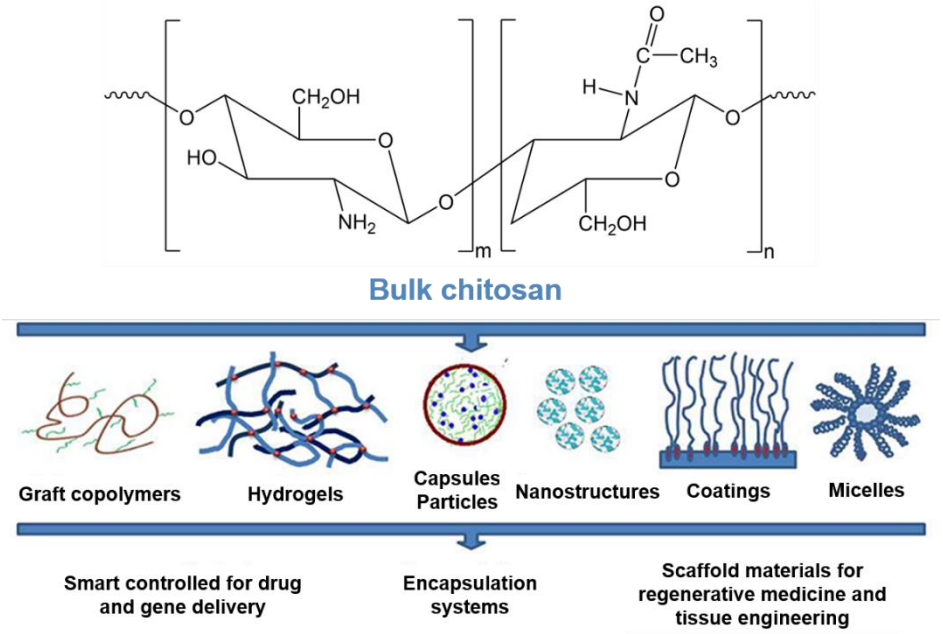

Figure 12 Chemical structure of chitosan and some of its key applications.

On top of all its aforementioned attributes, chitosan has the ability to be shaped in various forms such as films, microparticles, fibers and porous scaffolds, all of them being largely used in different biomedical applications [106, 113, 115]. For instance, chitosan films can be readily prepared by casting or dipping, resulting in dense and porous structures that are regarded as a biofunctional material, well tolerated by living tissues, particularly in applications as edible coatings, wound dressings, and as scaffolds for tissue and bone engineering, with promising results [67, 116-118].

4. "Click" chemistry as a tool to create AMP-based biomaterials

4.1 The relevance of AMP-based coatings

Peptide-based drugs are associated with short serum half-life, therefore systemic applications of AMP would require high dosages to achieve the desired therapeutic effect, and their inherent hydrophobicity combined with this high dosage correlates with haemolytic activity. Broad-spectrum antimicrobials also carry the risk of eradicating the natural flora, thereby providing a niche for opportunistic pathogens, such as fungi, to invade [58]. In view of this, a slow biodegradable delivery matrix capable of maintaining a nontoxic concentration throughout the healing process is highly desired for clinical applications of AMP [9]. Covalent immobilization of AMP onto surfaces through

different chemical coupling strategies has been reported, and the overall results suggest that immobilized AMP may be effective in the prevention of biofilm formation by reducing microorganism survival post-contact with the coated material. Minimal cytotoxicity and long-term stability profiles were obtained by optimizing immobilization parameters when compared to sole incorporation into release-based systems, indicating a promising potential for the use of immobilized AMP in clinical applications [7, 57, 58, 67]. However, many of such methods are inadequate, because either (i) the encapsulation process may need severe chemical conditions, for which peptides are incompatible [9], (ii) tethering reactions are not chemoselective, and may eventually modify amino acids that are crucial for antimicrobial action [119], or (iii) bonds established are chemo/bioreversible, possibly underlying undesirable fast release of the AMP [120, 121]. The effect of chemical immobilization of AMP on their antimicrobial activity has been studied by several investigators. The presence of a well-established secondary structure was found to be critical for the biocidal activity of immobilized AMP. Studies by Haynie *et al.* [122] and Cho *et al.* [123] clearly demonstrated that only the immobilized peptides still preserving the ability to form bioactive amphipathic α-helices or β-sheet structures retained antibacterial activity [7]. Parameters such as AMP orientation, concentration, surface density and exposure after immobilization can have influence on the antimicrobial performance of the conjugates. The length, flexibility and type of spacer between the active sequences and the solid matrices are also important activity-modulating parameters. Thus, the design of an optimal infection-resistant coating is very challenging as it must satisfy diverse requirements including optimal broad spectrum antimicrobial activity, protection against biofilm formation and biocompatibility [7, 52, 56, 57].

4.2 “Click” chemistry as a chemoselective peptide tethering tool

Peptide tethering through the so-called “click” chemistry reactions [19] is a highly promising, yet underexplored, approach. “Click” chemistry is a global term that refers to highly chemoselective reactions where two functional groups exclusively react with each other, even in the presence of other reactive functionalities. This highly selective and specific chemistry has the ability to promote, under mild conditions, covalent conjugation of two chemically dissimilar molecules, such as, e.g., complex carbohydrates with peptides, or chemoreporters, such as fluorescent dyes, with biopolymers. The reaction occurs in a manner that is high-yielding, rapid, modular, stereospecific, compatible with

aqueous environments and orthogonal to other functional groups. So, there are growing numbers of applications of "click" chemistry in diverse research areas, such as organic chemistry, bioconjugation, drug discovery, polymers and radiochemistry [124-126].
The Huisgen's 1,3-dipolar cycloaddition reaction between alkynes and azides, to yield triazoles, is the principal example of a "click" reaction and one of the most attractive chemoselective "click" reactions (Figure 13). The potential of this reaction is very high, since alkyne and azide components react selectively with each other and can be incorporated into a wide range of substituents [20, 127-129].

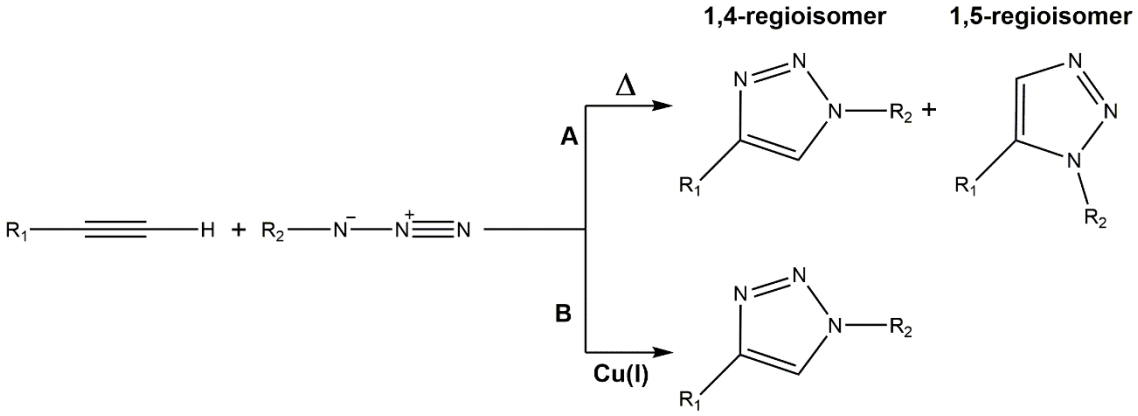

Figure 13 The 1,3-dipolar cycloaddition between azides and alkynes: (A) unactivated azide-alkyne cycloaddition yielding a mixture of the 1,5- and the 1,4-triazole regioisomers and (B) Cu(I) catalysis in alkyne-azide coupling reactions favouring exclusive formation of the 1,4-regioisomer (adapted from [128]).

The unactivated azide-alkyne cycloaddition was first discovered by Huisgen in 1963 and required high temperatures and pressures, since azides and alkynes have low reactivity towards each other at atmospheric pressure and room temperature. This stability, being essentially kinetic in basis, is responsible for the slow nature of the cycloaddition reaction and the inertness of these functional groups towards biological molecules and towards the reaction conditions inside living systems (i.e. aqueous, and mild reducing environments). Furthermore, as the directing effect of the substituents is usually weak, this reaction suffers from lack of regioselectivity, yielding a mixture of the 1,4- and the 1,5-triazole regioisomers, which may be laborious to separate using classical chromatographic procedures. These issues were overcome by Tornøe and Meldal, who introduced copper(I) catalysis in such reactions, leading to a major improvement in both rate and regioselectivity, as the copper catalyst favors formation of only the 1,4-regioisomer [20, 124, 126-128]. The formation of triazoles from azides and terminal alkynes catalyzed by

Cu(I) is an extraordinarily robust reaction, which can be performed under a wide variety of conditions and with almost any source of solvated Cu(I). The most common conditions are use of copper(II) sulfate ($CuSO_4$) in aqueous media containing a reducing agent for *in situ* generation of Cu(I), which may be eventually stabilized by addition of a suitable chelating agent [20]. Hence, the standard catalytic system uses Cu(II) salts (e.g., copper sulfate pentahydrate or copper acetate) in the presence of a reducing agent, such as sodium ascorbate or metallic copper [128, 130].

The triazole link created between the two building blocks (BB) that are coupled together is very stable and chemically inert to most reactive conditions. In contrast to amides, and due to their high aromatic stabilization, triazoles cannot be cleaved hydrolytically or otherwise, and unlike benzenoids and related aromatic heterocycles, they are almost impossible to oxidize or reduce [127]. These heterocycles have also an intermediate polarity with a high dipolar moment of ~5 D and are able to participate actively in hydrogen bond formation as well as in dipole–dipole and π stacking interactions [20]. Finally, triazoles are also considered as biocompatible and relatively resistant to metabolic degradation [128]; interestingly, they have been further found to display diverse biological activities, including anti-HIV activity and antimicrobial activity against Gram positive bacteria [131].

Most reports where the azide-alkyne coupling has been combined with peptides did not target antimicrobial coatings for local antibiotherapy [22]. This fact alone shows there is a void to be filled in this area. Moreover, the relevance of future research work in this field is obvious, given not only the global impact of drug-resistant mono- and poly-microbial infections, but also specific delicate cases as CWI [23] or severe IAI [24].

References

[1] T.F. Moriarty, S.A. Zaat, H.J. Busscher, Biomaterials associated infection: immunological aspects and antimicrobial strategies, Springer Science & Business Media2012.

[2] G.A. James, E. Swogger, R. Wolcott, P. Secor, J. Sestrich, J.W. Costerton, P.S. Stewart, Biofilms in chronic wounds, Wound Repair and regeneration 16(1) (2008) 37-44.

[3] K. Gjødsbøl, J.J. Christensen, T. Karlsmark, B. Jørgensen, B.M. Klein, K.A. Krogfelt, Multiple bacterial species reside in chronic wounds: a longitudinal study, International wound journal 3(3) (2006) 225-231.

[4] <http://www.who.int/mediacentre/factsheets/fs194/en/>, (accessed June.2017).

[5] H. Jenssen, P. Hamill, R.E. Hancock, Peptide antimicrobial agents, Clinical microbiology reviews 19(3) (2006) 491-511.

[6] N. van der Weerden, M. Bleackley, M. Anderson, Properties and mechanisms of action of naturally occurring antifungal peptides, Cellular and Molecular Life Sciences 70(19) (2013) 3545-3570.

[7] F. Costa, I.F. Carvalho, R.C. Montelaro, P. Gomes, M.C.L. Martins, Covalent immobilization of antimicrobial peptides (AMPs) onto biomaterial surfaces, Acta Biomaterialia 7(4) (2011) 1431-1440.

[8] L.M. Gottler, A. Ramamoorthy, Structure, membrane orientation, mechanism, and function of pexiganan — A highly potent antimicrobial peptide designed from magainin, Biochimica et Biophysica Acta (BBA) - Biomembranes 1788(8) (2009) 1680-1686.

[9] D. Gopinath, M.S. Kumar, D. Selvaraj, R. Jayakumar, Pexiganan-incorporated collagen matrices for infected wound-healing processes in rat, Journal of Biomedical Materials Research Part A 73A(3) (2005) 320-331.

[10] M.K.S. Batista, M. Gallemí, A. Adeva, C.A.R. Gomes, P. Gomes, Facile Regioselective Synthesis of a Novel Chitosan–Pexiganan Conjugate with Potential Interest for the Treatment of Infected Skin Lesions, Synthetic Communications 39(7) (2009) 1228-1240.

[11] C. Monteiro, M. Fernandes, M. Pinheiro, S. Maia, C.L. Seabra, F. Ferreira-da-Silva, F. Costa, S. Reis, P. Gomes, M.C.L. Martins, Antimicrobial properties of membrane-active dodecapeptides derived from MSI-78, Biochimica et Biophysica Acta (BBA) - Biomembranes 1848(5) (2015) 1139-1146.

[12] C. Faber, H.P. Stallmann, D.M. Lyaruu, U. Joosten, C. von Eiff, A. van Nieuw Amerongen, P.I. Wuisman, Comparable efficacies of the antimicrobial peptide human lactoferrin 1-11 and gentamicin in a chronic methicillin-resistant Staphylococcus aureus osteomyelitis model, Antimicrobial Agents and Chemotherapy 49(6) (2005) 2438-44.

[13] H.P. Stallmann, R. de Roo, C. Faber, A.V. Amerongen, P.I. Wuisman, *In vivo* release of the antimicrobial peptide hLF1-11 from calcium phosphate cement, Journal of orthopaedic research : official publication of the Orthopaedic Research Society 26(4) (2008) 531-8.

[14] C. Faber, H.P. Stallmann, D.M. Lyaruu, J.M.A. de Blieck, T.J.M. Bervoets, A. van Nieuw Amerongen, P.I.J.M. Wuisman, Release of antimicrobial peptide Dhvar-5 from polymethylmethacrylate beads, Journal of Antimicrobial Chemotherapy 51(6) (2003) 1359-1364.

[15] C. Faber, R.J.W. Hoogendoorn, H.P. Stallmann, D.M. Lyaruu, A. van Nieuw Amerongen, P.I.J.M. Wuisman, *In vivo* comparison of Dhvar-5 and gentamicin in an MRSA osteomyelitis prevention model, Journal of Antimicrobial Chemotherapy 54(6) (2004) 1078-1084.

[16] F.M.T.A. Costa, S.R. Maia, P.A.C. Gomes, M.C.L. Martins, Dhvar-5 antimicrobial peptide (AMP) chemoselective covalent immobilization results on higher antiadherence effect than simple physical adsorption, Biomaterials 52(0) (2015) 531-538.

[17] I. Pastar, A.G. Nusbaum, J. Gil, S.B. Patel, J. Chen, J. Valdes, O. Stojadinovic, L.R. Plano, M. Tomic-Canic, S.C. Davis, Interactions of Methicillin Resistant Staphylococcus aureus and Pseudomonas aeruginosa in Polymicrobial Wound Infection, PLoS ONE 8(2) (2013) e56846.

[18] G.W. Coombs, J.C. Pearson, G.R. Nimmo, P.J. Collignon, J.M. Bell, M.-L. McLaws, K.J. Christiansen, J.D. Turnidge, Antimicrobial susceptibility of Staphylococcus aureus and molecular epidemiology of meticillin-resistant S. aureus isolated from Australian hospital inpatients: Report from the Australian Group on Antimicrobial Resistance 2011 Staphylococcus aureus Surveillance Programme, Journal of Global Antimicrobial Resistance 1(3) 149-156.

[19] R.K. Iha, K.L. Wooley, A.M. Nyström, D.J. Burke, M.J. Kade, C.J. Hawker, Applications of Orthogonal "Click" Chemistries in the Synthesis of Functional Soft Materials, Chemical Reviews 109(11) (2009) 5620-5686.

[20] M. Meldal, C.W. Tornøe, Cu-catalyzed azide− alkyne cycloaddition, Chemical reviews 108(8) (2008) 2952-3015.

[21] L. Liang, D. Astruc, The copper(I)-catalyzed alkyne-azide cycloaddition (CuAAC) "click" reaction and its applications. An overview, Coordination Chemistry Reviews 255(23–24) (2011) 2933-2945.

[22] J. Thundimadathil, Click chemistry in peptide science: a mini-review Synthesis of clickable peptides and applications, Chimica Oggi-Chemistry Today 31(2) (2013) 34-37.

[23] R. Mohammadzadeh, N. Ahmadiyan, Skin Infection Management Using Novel Antibacterial Agents, Advanced pharmaceutical bulletin 3(1) (2013) 247.

[24] M. Kazemzadeh-Narbat, B.F.L. Lai, C. Ding, J.N. Kizhakkedathu, R.E.W. Hancock, R. Wang, Multilayered coating on titanium for controlled release of antimicrobial peptides for the prevention of implant-associated infections, Biomaterials 34(24) (2013) 5969-5977.

[25] K.V.R. Reddy, R.D. Yedery, C. Aranha, Antimicrobial peptides: premises and promises, International Journal of Antimicrobial Agents 24(6) (2004) 536-547.

[26] G.W. Coombs, J.C. Pearson, G.R. Nimmo, P.J. Collignon, J.M. Bell, M.-L. McLaws, K.J. Christiansen, J.D. Turnidge, Antimicrobial susceptibility of Staphylococcus aureus and molecular epidemiology of meticillin-resistant S. aureus isolated from Australian hospital inpatients: Report from the Australian Group on Antimicrobial Resistance 2011 Staphylococcus aureus Surveillance Programme, Journal of Global Antimicrobial Resistance 1(3) (2013) 149-156.

[27] R.M. Donlan, Biofilm formation: a clinically relevant microbiological process, Clinical infectious diseases : an official publication of the Infectious Diseases Society of America 33(8) (2001) 1387-92.

[28] R.M. Donlan, Biofilms and device-associated infections, Emerging infectious diseases 7(2) (2001) 277.

[29] D.F. Bayramov, J.A. Neff, Beyond conventional antibiotics — New directions for combination products to combat biofilm, Advanced Drug Delivery Reviews.

[30] A.W. Smith, Biofilms and antibiotic therapy: Is there a role for combating bacterial resistance by the use of novel drug delivery systems?, Advanced Drug Delivery Reviews 57(10) (2005) 1539-1550.

[31] R. Murga, J.M. Miller, R.M. Donlan, Biofilm formation by gram-negative bacteria on central venous catheter connectors: effect of conditioning films in a laboratory model, Journal of clinical microbiology 39(6) (2001) 2294-7.

[32] C.R. Arciola, D. Campoccia, P. Speziale, L. Montanaro, J.W. Costerton, Biofilm formation in Staphylococcus implant infections. A review of molecular mechanisms and implications for biofilm-resistant materials, Biomaterials 33(26) (2012) 5967-5982.

[33] J.A. Inzana, E.M. Schwarz, S.L. Kates, H.A. Awad, Biomaterials approaches to treating implant-associated osteomyelitis, Biomaterials 81 (2016) 58-71.

[34] J.W. Costerton, Introduction to biofilm, International Journal of Antimicrobial Agents 11(3) (1999) 217-221.

[35] C. de la Fuente-Núñez, F. Reffuveille, L. Fernández, R.E.W. Hancock, Bacterial biofilm development as a multicellular adaptation: antibiotic resistance and new therapeutic strategies, Current Opinion in Microbiology 16(5) (2013) 580-589.

[36] R. Serra, R. Grande, L. Butrico, A. Rossi, U.F. Settimio, B. Caroleo, B. Amato, L. Gallelli, S. de Franciscis, Chronic wound infections: the role of Pseudomonas aeruginosa and Staphylococcus aureus, Expert Review of Anti-infective Therapy 13(5) (2015) 605-613.

[37] G.A. James, E. Swogger, R. Wolcott, E.d. Pulcini, P. Secor, J. Sestrich, J.W. Costerton, P.S. Stewart, Biofilms in chronic wounds, Wound Repair and Regeneration 16(1) (2008) 37-44.

[38] M.A. Fonder, G.S. Lazarus, D.A. Cowan, B. Aronson-Cook, A.R. Kohli, A.J. Mamelak, Treating the chronic wound: A practical approach to the care of nonhealing wounds and wound care dressings, Journal of the American Academy of Dermatology 58(2) (2008) 185-206.

[39] A. Francesko, D. Soares da Costa, R.L. Reis, I. Pashkuleva, T. Tzanov, Functional biopolymer-based matrices for modulation of chronic wound enzyme activities, Acta Biomaterialia 9(2) (2013) 5216-5225.

[40] T. Abdelrahman, H. Newton, Wound dressings: principles and practice, Surgery (Oxford) 29(10) (2011) 491-495.

[41] K. Skórkowska-Telichowska, M. Czemplik, A. Kulma, J. Szopa, The local treatment and available dressings designed for chronic wounds, Journal of the American Academy of Dermatology 68(4) (2013) e117-e126.

[42] Y. Xu, J. Sun, R.R. Carter, K.M. Bogie, Personalized prediction of chronic wound healing: An exponential mixed effects model using stereophotogrammetric measurement, Journal of Tissue Viability 23(2) (2014) 48-59.

[43] L.I.F. Moura, A.M.A. Dias, E. Carvalho, H.C. de Sousa, Recent advances on the development of wound dressings for diabetic foot ulcer treatment—A review, Acta Biomaterialia 9(7) (2013) 7093-7114.

[44] R.A.A. Muzzarelli, Chitins and chitosans for the repair of wounded skin, nerve, cartilage and bone, Carbohydrate Polymers 76(2) (2009) 167-182.

[45] K. Wicks, T. Torbica, K.A. Mace, Myeloid cell dysfunction and the pathogenesis of the diabetic chronic wound, Seminars in Immunology (0).

[46] T. Bjarnsholt, M. Alhede, M. Alhede, S.R. Eickhardt-Sørensen, C. Moser, M. Kühl, P.Ø. Jensen, N. Høiby, The *in vivo* biofilm, Trends in Microbiology 21(9) (2013) 466-474.

[47] L. Hall-Stoodley, P. Stoodley, S. Kathju, N. Høiby, C. Moser, J.W. Costerton, A. Moter, T. Bjarnsholt, Towards diagnostic guidelines for biofilm-associated infections, FEMS Immunology And Medical Microbiology 65(2) (2012) 127-145.

[48] J. Valle, C. Solano, B. García, A. Toledo-Arana, I. Lasa, Biofilm switch and immune response determinants at early stages of infection, Trends in Microbiology 21(8) (2013) 364-371.

[49] C.J. Sánchez, K. Mende, M.L. Beckius, K.S. Akers, D.R. Romano, J.C. Wenke, C.K. Murray, Biofilm formation by clinical isolates and the implications in chronic infections, BMC infectious diseases 13(1) (2013) 47.

[50] M. Burmølle, T.R. Thomsen, M. Fazli, I. Dige, L. Christensen, P. Homøe, M. Tvede, B. Nyvad, T. Tolker-Nielsen, M. Givskov, C. Moser, K. Kirketerp-Møller, H.K. Johansen, N. Høiby, P.Ø. Jensen, S.J. Sørensen, T. Bjarnsholt, Biofilms in chronic infections – a matter of opportunity – monospecies biofilms in multispecies infections, FEMS Immunology & Medical Microbiology 59(3) (2010) 324-336.

[51] R.A. Clark, K. Ghosh, M.G. Tonnesen, Tissue engineering for cutaneous wounds, Journal of Investigative Dermatology 127(5) (2007) 1018-1029.

[52] G. Gao, D. Lange, K. Hilpert, J. Kindrachuk, Y. Zou, J.T.J. Cheng, M. Kazemzadeh-Narbat, K. Yu, R. Wang, S.K. Straus, D.E. Brooks, B.H. Chew, R.E.W. Hancock, J.N. Kizhakkedathu, The biocompatibility and biofilm resistance of implant coatings based on hydrophilic polymer brushes conjugated with antimicrobial peptides, Biomaterials 32(16) (2011) 3899-3909.

[53] C. Faber, R.J.W. Hoogendoorn, H.P. Stallmann, D.M. Lyaruu, A. van Nieuw Amerongen, P.I.J.M. Wuisman, o.b.o. STEGA, *In vivo* comparison of Dhvar-5 and gentamicin in an MRSA osteomyelitis prevention model, Journal of Antimicrobial Chemotherapy 54(6) (2004) 1078-1084.

[54] M.L. Knetsch, L.H. Koole, New strategies in the development of antimicrobial coatings: the example of increasing usage of silver and silver nanoparticles, Polymers 3(1) (2011) 340-366.

[55] M. Kazemzadeh-Narbat, J. Kindrachuk, K. Duan, H. Jenssen, R.E.W. Hancock, R. Wang, Antimicrobial peptides on calcium phosphate-coated titanium for the prevention of implant-associated infections, Biomaterials 31(36) (2010) 9519-9526.

[56] I. Banerjee, R.C. Pangule, R.S. Kane, Antifouling Coatings: Recent Developments in the Design of Surfaces That Prevent Fouling by Proteins, Bacteria, and Marine Organisms, Advanced Materials 23(6) (2011) 690-718.

[57] M. Bagheri, M. Beyermann, M. Dathe, Immobilization Reduces the Activity of Surface-Bound Cationic Antimicrobial Peptides with No Influence upon the Activity Spectrum, Antimicrobial Agents and Chemotherapy 53(3) (2009) 1132-1141.

[58] M. Salwiczek, Y. Qu, J. Gardiner, R.A. Strugnell, T. Lithgow, K.M. McLean, H. Thissen, Emerging rules for effective antimicrobial coatings, Trends in Biotechnology 32(2) (2014) 82-90.

[59] N.C. Silva, B. Sarmento, M. Pintado, The importance of antimicrobial peptides and their potential for therapeutic use in ophthalmology, International Journal of Antimicrobial Agents 41(1) (2013) 5-10.

[60] N.K. Brogden, K.A. Brogden, Will new generations of modified antimicrobial peptides improve their potential as pharmaceuticals?, International Journal of Antimicrobial Agents 38(3) (2011) 217-225.

[61] M.J. Mannis, The use of antimicrobial peptides in ophthalmology: an experimental study in corneal preservation and the management of bacterial keratitis, Transactions of the American Ophthalmological Society 100 (2002) 243.

[62] N. Dong, X. Zhu, Y.F. Lv, Q.Q. Ma, J.G. Jiang, A.S. Shan, Cell specificity and molecular mechanism of antibacterial and antitumor activities of carboxyl-terminal RWL-tagged antimicrobial peptides, Amino Acids (2014) 1-18.

[63] M. Gough, R.E. Hancock, N.M. Kelly, Antiendotoxin activity of cationic peptide antimicrobial agents, Infection and immunity 64(12) (1996) 4922-7.

[64] R. Hancock, A. Patrzykat, Clinical development of cationic antimicrobial peptides: from natural to novel antibiotics, Current drug targets-Infectious disorders 2(1) (2002) 79-83.

[65] C. Monteiro, M. Pinheiro, M. Fernandes, S. Maia, C.L. Seabra, F. Ferreira-da-Silva, S. Reis, P. Gomes, M.C.L. Martins, A 17-mer Membrane-Active MSI-78 Derivative with Improved Selectivity toward Bacterial Cells, Molecular Pharmaceutics 12(8) (2015) 2904-2911.

[66] J. Vizioli, M. Salzet, Antimicrobial peptides from animals: focus on invertebrates, Trends in pharmacological Sciences 23(11) (2002) 494-496.

[67] F. Costa, S. Maia, J. Gomes, P. Gomes, M.C.L. Martins, Characterization of hLF1–11 immobilization onto chitosan ultrathin films, and its effects on antimicrobial activity, Acta Biomaterialia 10(8) (2014) 3513-3521.

[68] S. Rotem, A. Mor, Antimicrobial peptide mimics for improved therapeutic properties, Biochimica et Biophysica Acta (BBA) - Biomembranes 1788(8) (2009) 1582-1592.

[69] K. Matsuzaki, Control of cell selectivity of antimicrobial peptides, Biochimica et Biophysica Acta (BBA) - Biomembranes 1788(8) (2009) 1687-1692.

[70] Y. Li, Q. Xiang, Q. Zhang, Y. Huang, Z. Su, Overview on the recent study of antimicrobial peptides: Origins, functions, relative mechanisms and application, Peptides 37(2) (2012) 207-215.

[71] V. Frecer, B. Ho, J.L. Ding, De Novo Design of Potent Antimicrobial Peptides, Antimicrobial Agents and Chemotherapy 48(9) (2004) 3349-3357.

[72] V. Mäde, S. Els-Heindl, A.G. Beck-Sickinger, Automated solid-phase peptide synthesis to obtain therapeutic peptides, Beilstein Journal of Organic Chemistry 10 (2014) 1197-1212.

[73] J.M. Palomo, Solid-phase peptide synthesis: an overview focused on the preparation of biologically relevant peptides, RSC Advances 4(62) (2014) 32658-32672.

[74] F. Albericio, Developments in peptide and amide synthesis, Current Opinion in Chemical Biology 8(3) (2004) 211-221.

[75] C.A.G.N. Montalbetti, V. Falque, Amide bond formation and peptide coupling, Tetrahedron 61(46) (2005) 10827-10852.

[76] V.R. Pattabiraman, J.W. Bode, Rethinking amide bond synthesis, Nature 480(7378) (2011) 471-9.

[77] M.M. Joullié, K.M. Lassen, Evolution of amide bond formation, Arkivoc: Online Journal of Organic Chemistry (2010) 189-250.

[78] E. Valeur, M. Bradley, Amide bond formation: beyond the myth of coupling reagents, Chemical Society Reviews 38(2) (2009) 606-631.

[79] B. Shen, D.M. Makley, J.N. Johnston, Umpolung reactivity in amide and peptide synthesis, Nature 465(7301) (2010) 1027-1032.

[80] P. Vlieghe, V. Lisowski, J. Martinez, M. Khrestchatisky, Synthetic therapeutic peptides: science and market, Drug Discovery Today 15(1–2) (2010) 40-56.

[81] R.B. Merrifield, Solid Phase Peptide Synthesis. I. The Synthesis of a Tetrapeptide, Journal of the American Chemical Society 85(14) (1963) 2149-2154.

[82] S. Chandrudu, P. Simerska, I. Toth, Chemical Methods for Peptide and Protein Production, Molecules 18(4) (2013) 4373-4388.

[83] G.A. Acosta, M. del Fresno, M. Paradis-Bas, M. Rigau-DeLlobet, S. Côté, M. Royo, F. Albericio, Solid-phase peptide synthesis using acetonitrile as a solvent in combination with PEG-based resins, Journal of Peptide Science 15(10) (2009) 629-633.

[84] K. Hojo, A. Hara, H. Kitai, M. Onishi, H. Ichikawa, Y. Fukumori, K. Kawasaki, Development of a method for environmentally friendly chemical peptide synthesis in water using water-dispersible amino acid nanoparticles, Chemistry Central Journal 5(1) (2011) 49.

[85] P. Cironi, M. Alvarez, F. Albericio, Solid-phase chemistry in the total synthesis of non-peptidic natural products, Mini reviews in medicinal chemistry 6(1) (2006) 11-25.

[86] Lundquist, J.C. Pelletier, Improved Solid-Phase Peptide Synthesis Method Utilizing α-Azide-Protected Amino Acids, Organic Letters 3(5) (2001) 781-783.

[87] D. Pires, M. Bemquerer, C. Nascimento, Some Mechanistic Aspects on Fmoc Solid Phase Peptide Synthesis, International Journal of Peptide Research and Therapeutics 20(1) (2014) 53-69.

[88] A. Isidro-Llobet, M. Álvarez, F. Albericio, Amino Acid-Protecting Groups, Chemical Reviews 109(6) (2009) 2455-2504.

[89] M. Góngora-Benítez, J. Tulla-Puche, F. Albericio, Handles for Fmoc Solid-Phase Synthesis of Protected Peptides, ACS Combinatorial Science 15(5) (2013) 217-228.

[90] M. Amblard, J.-A. Fehrentz, J. Martinez, G. Subra, Methods and protocols of modern solid phase peptide synthesis, Molecular Biotechnology 33(3) (2006) 239-254.

[91] J.M. Collins, K.A. Porter, S.K. Singh, G.S. Vanier, High-Efficiency Solid Phase Peptide Synthesis (HE-SPPS), Organic Letters 16(3) (2014) 940-943.

[92] C.M.B. Edwards, M.A. Cohen, S.R. Bloom, Peptides as drugs, QJM 92(1) (1999) 1-4.

[93] J.E. Sheppeck Ii, H. Kar, H. Hong, A convenient and scaleable procedure for removing the Fmoc group in solution, Tetrahedron Letters 41(28) (2000) 5329-5333.

[94] S. Drotleff, U. Lungwitz, M. Breunig, A. Dennis, T. Blunk, J. Tessmar, A. Göpferich, Biomimetic polymers in pharmaceutical and biomedical sciences, European Journal of Pharmaceutics and Biopharmaceutics 58(2) (2004) 385-407.

[95] T.I. Al-Warhi, H.M.A. Al-Hazimi, A. El-Faham, Recent development in peptide coupling reagents, Journal of Saudi Chemical Society 16(2) (2012) 97-116.

[96] F. Albeiicio, R. Chinchilla, D.J. Dodsworth, C. Nájera, NEW TRENDS IN PEPTIDE COUPLING REAGENTS, Organic Preparations and Procedures International 33(3) (2001) 203-303.

[97] S.-Y. Han, Y.-A. Kim, Recent development of peptide coupling reagents in organic synthesis, Tetrahedron 60(11) (2004) 2447-2467.

[98] M. Friedman, Applications of the Ninhydrin Reaction for Analysis of Amino Acids, Peptides, and Proteins to Agricultural and Biomedical Sciences, Journal of Agricultural and Food Chemistry 52(3) (2004) 385-406.

[99] C.B. Bottom, S.S. Hanna, D.J. Siehr, Mechanism of the ninhydrin reaction, Biochemical Education 6(1) (1978) 4-5.

[100] J. Alsina, T.S. Yokum, F. Albericio, G. Barany, Backbone Amide Linker (BAL) Strategy for Nα-9-Fluorenylmethoxycarbonyl (Fmoc) Solid-Phase Synthesis of Unprotected Peptide p-Nitroanilides and Thioesters1, The Journal of Organic Chemistry 64(24) (1999) 8761-8769.

[101] H. Choi, J.V. Aldrich, Comparison of methods for the Fmoc solid-phase synthesis and cleavage of a peptide containing both tryptophan and arginine, International journal of peptide and protein research 42(1) (1993) 58-63.

[102] F. Albericio, N. Kneib-Cordonier, S. Biancalana, L. Gera, R.I. Masada, D. Hudson, G. Barany, Preparation and application of the 5-(4-(9-fluorenylmethyloxycarbonyl)aminomethyl-3,5-dimethoxyphenoxy)-valeric acid (PAL) handle for the solid-phase synthesis of C-terminal peptide amides under mild conditions, The Journal of Organic Chemistry 55(12) (1990) 3730-3743.

[103] C.M. Gross, D. Lelièvre, C.K. Woodward, G. Barany, Preparation of protected peptidyl thioester intermediates for native chemical ligation by Nalpha-9-fluorenylmethoxycarbonyl (Fmoc) chemistry: considerations of side-chain and backbone anchoring strategies, and compatible protection for N-terminal cysteine, The Journal Of Peptide Research: Official Journal Of The American Peptide Society 65(3) (2005) 395-410.

[104] M. Danielsson, K. Wahlström, A. Undén, Protection of the indole nucleus of tryptophan in solid-phase peptide synthesis with a dipeptide that can be cleaved rapidly at physiological pH, Tetrahedron Letters 52(44) (2011) 5876-5879.

[105] M.L. Tan, P. Shao, A.M. Friedhuber, M. van Moorst, M. Elahy, S. Indumathy, D.E. Dunstan, Y. Wei, C.R. Dass, The potential role of free chitosan in bone trauma and bone cancer management, Biomaterials 35(27) (2014) 7828-7838.

[106] C. Pandis, S. Madeira, J. Matos, A. Kyritsis, J.F. Mano, J.L.G. Ribelles, Chitosan–silica hybrid porous membranes, Materials Science and Engineering: C 42(0) (2014) 553-561.

[107] J. Berger, M. Reist, J.M. Mayer, O. Felt, N.A. Peppas, R. Gurny, Structure and interactions in covalently and ionically crosslinked chitosan hydrogels for biomedical applications, European Journal of Pharmaceutics and Biopharmaceutics 57(1) (2004) 19-34.

[108] M.Z. Elsabee, E.S. Abdou, Chitosan based edible films and coatings: A review, Materials Science and Engineering: C 33(4) (2013) 1819-1841.

[109] E.M. Costa, S. Silva, C. Pina, F.K. Tavaria, M.M. Pintado, Evaluation and insights into chitosan antimicrobial activity against anaerobic oral pathogens, Anaerobe 18(3) (2012) 305-309.

[110] J. Berger, M. Reist, J.M. Mayer, O. Felt, R. Gurny, Structure and interactions in chitosan hydrogels formed by complexation or aggregation for biomedical applications, European Journal of Pharmaceutics and Biopharmaceutics 57(1) (2004) 35-52.

[111] R.C. Goy, D. De Britto, O.B.G. Assis, A review of the antimicrobial activity of chitosan, Polimeros 19(3) (2009) 241-247.

[112] I. Leceta, P. Guerrero, K. de la Caba, Functional properties of chitosan-based films, Carbohydrate polymers 93(1) (2013) 339-346.

[113] M.N.V. Ravi Kumar, A review of chitin and chitosan applications, Reactive and Functional Polymers 46(1) (2000) 1-27.

[114] J.R. Oliveira, M.C.L. Martins, L. Mafra, P. Gomes, Synthesis of an O-alkynyl-chitosan and its chemoselective conjugation with a PEG-like amino-azide through click chemistry, Carbohydrate Polymers 87(1) (2012) 240-249.

[115] M. Rinaudo, Chitin and chitosan: Properties and applications, Progress in Polymer Science 31(7) (2006) 603-632.

[116] F. Croisier, C. Jérôme, Chitosan-based biomaterials for tissue engineering, European Polymer Journal 49(4) (2013) 780-792.

[117] R.P. Carlson, R. Taffs, W.M. Davison, P.S. Stewart, Anti-biofilm properties of chitosan-coated surfaces, Journal of Biomaterials Science, Polymer Edition 19(8) (2008) 1035-1046.

[118] R. Lieder, M. Darai, M.B. Thor, C.H. Ng, J.M. Einarsson, S. Gudmundsson, B. Helgason, V.S. Gaware, M. Másson, J. Gíslason, G. Örlygsson, Ó.E. Sigurjónsson, *In vitro* bioactivity of different degree of deacetylation chitosan, a potential coating material for titanium implants, Journal of Biomedical Materials Research Part A 100A(12) (2012) 3392-3399.

[119] J.M. Langenhan, J.S. Thorson, Recent carbohydrate-based chemoselective ligation applications, Current Organic Synthesis 2(1) (2005) 59-81.

[120] S.A. Onaizi, S.S.J. Leong, Tethering antimicrobial peptides: Current status and potential challenges, Biotechnology Advances 29(1) (2011) 67-74.

[121] M.J. Roberts, M.D. Bentley, J.M. Harris, Chemistry for peptide and protein PEGylation, Advanced Drug Delivery Reviews 64 (2012) 116-127.

[122] S.L. Haynie, G.A. Crum, B.A. Doele, Antimicrobial activities of amphiphilic peptides covalently bonded to a water-insoluble resin, Antimicrobial agents and chemotherapy 39(2) (1995) 301-307.

[123] W.-M. Cho, B.P. Joshi, H. Cho, K.-H. Lee, Design and synthesis of novel antibacterial peptide-resin conjugates, Bioorganic & medicinal chemistry letters 17(21) (2007) 5772-5776.

[124] K. Nwe, M.W. Brechbiel, Growing applications of "click chemistry" for bioconjugation in contemporary biomedical research, Cancer Biotherapy and Radiopharmaceuticals 24(3) (2009) 289-302.

[125] D. Zeng, B.M. Zeglis, J.S. Lewis, C.J. Anderson, The growing impact of bioorthogonal click chemistry on the development of radiopharmaceuticals, Journal of Nuclear Medicine 54(6) (2013) 829-832.

[126] F. Amblard, J.H. Cho, R.F. Schinazi, Cu (I)-catalyzed Huisgen azide− alkyne 1, 3-dipolar cycloaddition reaction in nucleoside, nucleotide, and oligonucleotide chemistry, Chemical reviews 109(9) (2009) 4207-4220.

[127] H.C. Kolb, K.B. Sharpless, The growing impact of click chemistry on drug discovery, Drug discovery today 8(24) (2003) 1128-1137.

[128] G.C. Tron, T. Pirali, R.A. Billington, P.L. Canonico, G. Sorba, A.A. Genazzani, Click chemistry reactions in medicinal chemistry: Applications of the 1, 3-dipolar cycloaddition between azides and alkynes, Medicinal research reviews 28(2) (2008) 278-308.

[129] R. Jagasia, J.M. Holub, M. Bollinger, K. Kirshenbaum, M. Finn, Peptide Cyclization and Cyclodimerization by CuI-Mediated Azide− Alkyne Cycloaddition, The Journal of organic chemistry 74(8) (2009) 2964-2974.

[130] V. Castro, H. Rodriguez, F. Albericio, Wang Linker Free of Side Reactions, Organic Letters 15(2) (2012) 246-249.

[131] C.W. Tornøe, C. Christensen, M. Meldal, Peptidotriazoles on solid phase:[1, 2, 3]-triazoles by regiospecific copper (I)-catalyzed 1, 3-dipolar cycloadditions of terminal alkynes to azides, The Journal of organic chemistry 67(9) (2002) 3057-3064.

Chapter II

Characterization Techniques

Throughout this work, a plethora of characterization techniques were exploited, for analysis of synthetic peptides produced, monitorization of AMP-chitosan conjugates synthesis and characterization of final AMP-tethered materials. Regarding peptide synthesis, liquid chromatography–mass spectrometry (LC-MS) and high-performance liquid chromatography (HPLC) were used to identify and quantify each component in the crude peptide product, respectively.

The success of AMP-chitosan conjugates synthesis was evaluated by Fourier-transform infrared spectroscopy (FT-IR), X-ray photoelectron spectroscopy (XPS), Amino Acid Analysis (AAA) and scanning electron microscopy (SEM). Moreover, ultra-thin films produced where subject to analysis by surface characterization techniques, such as: contact angle goniometry, ellipsometry and Infrared Reflection-Absorption Spectroscopy (IRRAS). This section explains concisely their basic principles and applications within the aim and scope of the doctoral project herein reported.

1. Liquid chromatography–mass spectrometry (LC-MS)

In this work, LC-MS was applied for the determination of the molecular weight of the synthetic peptides produced. Briefly, samples were prepared in methanol (LC-MS grade) and all data were collected in positive ion mode, in a LCQ-Deca XP LC-MS system from ThermoFinnigan, equipped with both an electrospray ionization-ion trap mass spectrometer (ESI/IT MS) and a diode-array detector (DAD).

LC-MS (Figure 1) is an analytical chemistry technique that combines the physical separation properties of liquid chromatography (LC) with the mass analysis capabilities of mass spectrometry (MS). Hence, LC-MS is a highly sensitive and selective technique capable to separate, detect and identify peptides, even when they are embedded in complex matrices [1, 2].

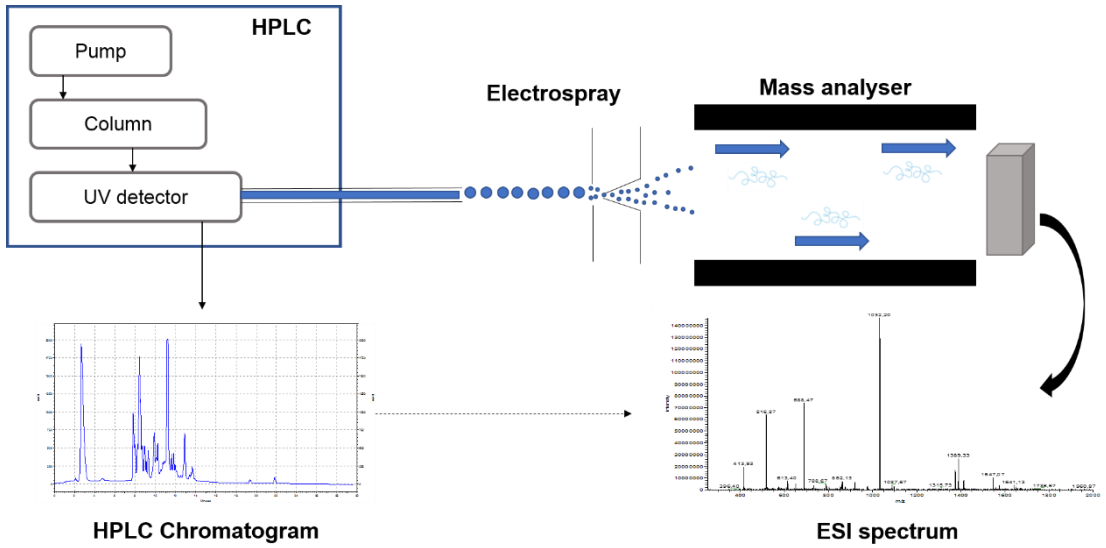

Figure 1 Scheme of a LC-MS system.

As MS detection is only possible when the peptides exist as ions in the gaseous state, coupling of LC to MS necessitates the volatilization of these bio-molecules from the LC-eluent. The analysis of peptides is usually performed by electrospray ionization (ESI). In ESI gas-phase ions are directly generated from the liquid phase by spraying the sample solution through a high voltage capillary in the presence of a strong electric field [1]. ESI is a highly sensitive and reproducible method with the further advantage of analyzing a wide range of different molecular weight compounds. Thus, ESI is a convenient mass-analysis platform for LC, especially when combined with tandem MS (MS/MS) [3]. However, during ionization, a part of the sensitivity of the MS detection can be lost as the signal is deviated over multiple charges, isotopes or adduct ions. To improve sensitivity, the ionization must be sufficiently optimized. MS/MS can improve the selectivity by selecting a specific product of the peptide after dissociation [1].

MS/MS are made of two successive mass analyzers with a collision cell in between that can select specific ions, induce their fragmentation in the collision cell, and measure the m/z of the fragment ions. In general, for peptides, the ion-trap mass spectrometer is the most employed mass analyzer. The ion-trap mass spectrometers trap the ions in an electric field, where specific ions can be activated and ejected by manipulation of this electric field. Ion traps can also perform multiple MS (MS^n) as the trapped ions can be fragmented inside the trap [1].

Regarding the LC elements, for the chromatography of peptides a hydrophobic stationary phase and aqueous mobile phase is usually used. This type of reversed-phase LC (RP-

LC) often uses a silica-based C_{18} stationary phase which consists of a silica support where the hydrophobic octadecyl group is attached [1]. The choice of the correct mobile phase and its additives in the RP-LC of peptides is very important to achieve good chromatographic separation as well as mass spectrometric performance. When LC is coupled to MS with ESI, the mobile phase needs to be compatible with the ESI source and, furthermore, the additives have to enhance or at least not to suppress ionization of the analyte. A suitable mobile phase for ESI-MS contains an organic modifier and should not contain non-volatile buffers or other mobile phase additives. The addition of ion-pairing reagents to the mobile phase improves the chromatographic separation of peptides, by forming ion pairs with charged groups and thereby increasing the hydrophobicity of the peptides and effecting interaction with the stationary phase. Most LC-MS applications for peptides use a water–acetonitrile or water-methanol mobile phase, mostly acidified with TFA, formic acid or acetic acid [1].

2. High Performance Liquid Chromatography (HPLC)

HPLC is the most frequently used LC technique (Figure 2) and is an extremely useful technique for assessment of peptides purity degree after solid-phase synthesis. Separation is carried out using a liquid mobile phase and a solid stationary phase packed in columns of convenient size. For peptide characterization, a reversed-phase (RP) separation mode is employed. The RP mode requires the combination of a polar mobile phase and a nonpolar stationary phase. The stationary phase comprises a silica-based packing material, previously modified with a derivatized silane bearing an n-alkyl hydrophobic ligand, typically octadecyl-(C18) ligand. This is relatively stable, with most aqueous eluents having a pH value below 8 [4-6].

As in LC-MS, RP-HPLC uses water and an organic modifier miscible with water, typically methanol or acetonitrile, as mobile phase. These organic solvents exhibit high optical transparency in the detection wavelengths used for peptide analysis. Moreover, analysis of peptides requires an acidic mobile phase. In this context, trifluoroacetic acid (TFA), due to its volatility, is usually added to water and used as ionic modifier [4-6].

A pump delivers the mobile phase into the separation system (column-packed stationary phase) with a stable, specific, and reproducible flow rate. The standard analysis with an analytical scale column run at a flow rate ranging between 0.5–2.0 mL/min. Two distinct types of elution modes are used in HPLC: isocratic and gradient elution. The isocratic

elution mode uses a mobile phase of constant composition, whereas the composition of the mobile phase is changed according to a previously set program in a gradient elution. Since high resolution isocratic elution of peptides can rarely be achieved as the experimental window of solvent concentration required for their elution is very narrow mixtures of peptides are therefore routinely eluted by the application of a gradient of increasing organic solvent concentration. Slight variations on the composition of the mobile phase can be used to control solute retention and resolution [4, 5].

As soon as the sample reaches the detector, a signal proportional to the amount of each component emerging from the column is generated. Detection of peptides in RP-HPLC, generally involves setting the detector between 210 and 220 nm, specific wavelength for the peptide bond, or at 280 nm, which corresponds to the aromatic amino acids tryptophan and tyrosine. The resulting spectra can then be applied for the identification of peaks specifically based on spectral characteristics and for the assessment of peak purity [4-6].

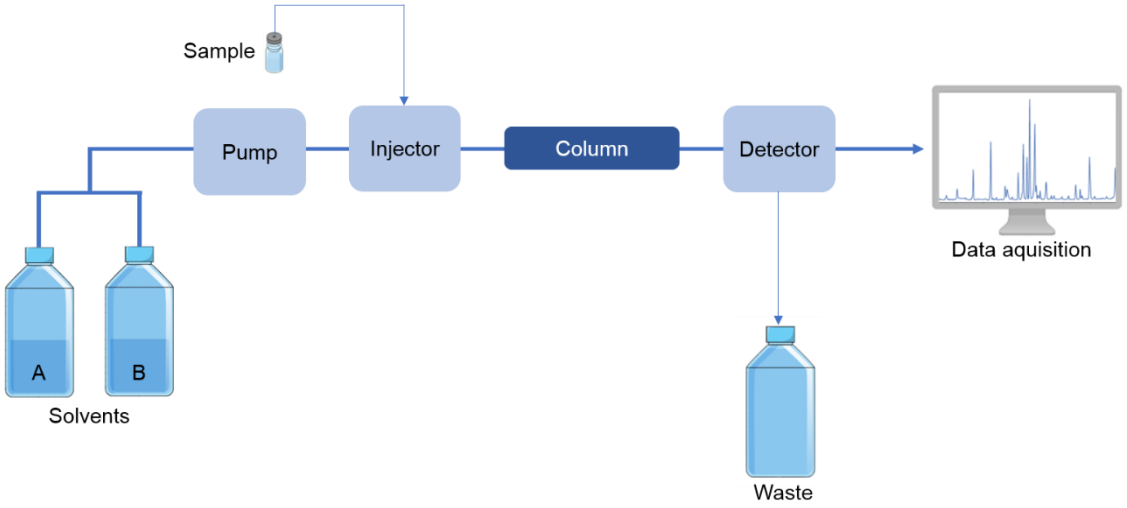

Figure 2 Representation of an HPLC system.

3. Fourier-transform infrared spectroscopy (FT-IR)

Fourier-transform infrared spectroscopy (FT-IR) is typically performed in the mid-IR wavelength range and examines the wavelengths of infrared radiation that are absorbed or transmitted by the sample. As depicted in Figure 3, radiation emitted from IR source is collimated and focused into the interferometer. The most usually employed interferometer is a Michelson interferometer. It consists of three active components: a moving mirror and a stationary mirror, perpendicular to each other, and a beam splitter.

Once in the interferometer radiant beams collide with the beam splitter, a semi-reflecting device, they are divided in two. Part of the IR beam is transmitted to the fixed mirror and the remaining half is reflected to the moving mirror, generating an optical path difference between the beams. After the divided beams are reflected from the mirrors, they return to the beam splitter where they are recombined producing repetitive interference signals. As a result of variations in the relative position between the mirrors, an interference pattern is generated. The resulting beam, the so-called interferogram, goes through the sample and is eventually focused on the detector. There, by means of Fourier transformation, a mathematical operation, the interferogram (a spectrum displaying intensity as a function of time within the mirror scan) is converted to the final IR spectrum, which is the known frequency domain spectrum presenting intensity versus frequency [7].

As the signal reaches the detector, a spectrum representative of each chemical structure present in the sample is formed. The different patterns displayed in the spectrum permits to identify the sample, since molecules exhibit a specific IR fingerprint. The absorption of infrared radiation generates characteristic vibrational movements in molecules, most of them defined as stretching and bending modes that are detected if causing change in electric dipole; in other words, the molecule changes its vibrational state as it passes from fundamental vibrational state to excited vibrational state [8, 9].

Each compound has a characteristic set of absorption bands; for biological materials, the most important spectral regions are typically the fingerprint region ranging between 600 and 1450 cm^{-1} and the amide I and amide II bands (~1650 and 1550 cm^{-1}, respectively), which are especially important for peptides and proteins, due to the peptide bonds that bind the amino acids to each other. The lower-wavenumber regions, reflect C–X vibrational frequencies of carbohydrates or nucleic acid bonds, whereas the higher-wavenumber region (2550–3500 cm^{-1}) is associated with stretching vibrations such as S-H, C–H, N–H and O–H. A major limitation of FT-IR is the presence of water in either instrumentation or sample, which may overlap with important spectral bands, due to the strong absorption bands at 1350-1950 cm^{-1} and 3600-3900 cm^{-1}. However, this problem can be overcome with complete dehydration of the samples and purge of the instrumentation with dry air or nitrogen and/or desiccants. This procedure has the further advantage of reducing the contribution of ambient CO_2 to the spectra [8-10].

IR spectroscopy is extremely useful for real time monitoring of various chemical process, among them, the CuAAC reaction herein applied for conjugation of peptides to chitosan. Actually, the three reacting groups directly involved in this reaction (azide and alkyne

from the starting materials, and 1,2,3-triazole, from the product) are all IR-responsive and can be straightforwardly traced [11], as given in more detail in Chapter IV.

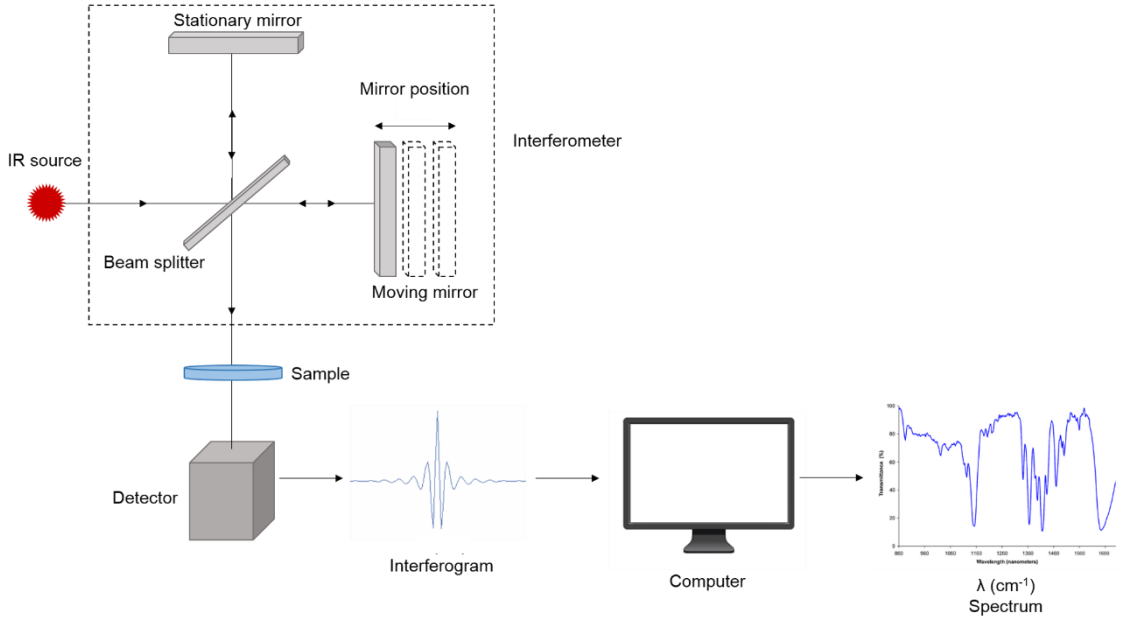

Figure 3 Representative scheme of the main components that composes a FT-IR system.

4. X-ray photoelectron spectroscopy (XPS)

X-ray photoelectron spectroscopy (XPS) is a non-destructive spectroscopic technique based on the photoelectric effect which is used for the semi-quantitative analysis of surfaces [12, 13]. Briefly, XPS quantifies the number and kinetic energy (E_k) of ejected electrons following irradiation of the surface's material with an X-ray beam. As a result of that it is possible to obtain information concerning elemental composition and respective chemical and electronic state of each element found within the uppermost 10 nm of the analyzed sample. Throughout the XPS analysis the sample is kept under ultra-high vacuum to guarantee that no other specimens are present in the compartment [12, 14, 15].

A scheme of an XPS system is depicted in Figure 4.

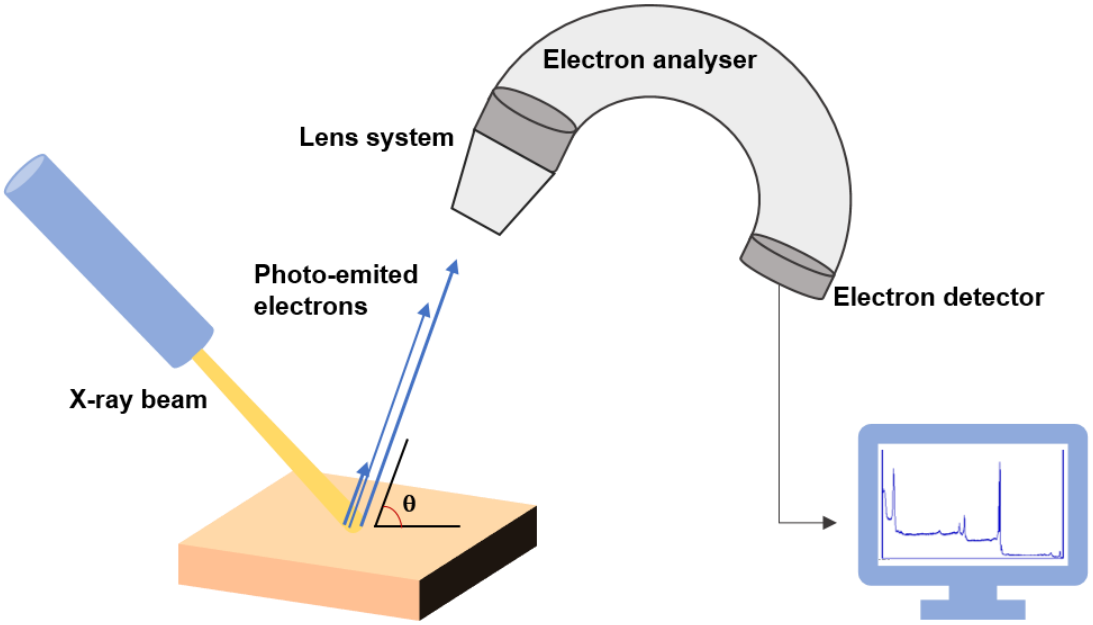

Figure 4 Scheme of an X-ray photoelectron spectroscopy system: x-ray source, sample, electrostatic analyzer and electron detector.

The binding energy of an electron to an atom (B_e) is determined from the photoelectric relationship displayed in Equation 1:

$$B_e = h\nu - E_k, \qquad \text{(Equation 1)}$$

where hν is the known energy of the incident X-ray beam and E_k is the kinetic energy of the emitted electron measured by the X-ray spectrometer. Since B_e is specific of each chemical element, XPS provides identification of all elements (with the exceptions of H and He) that exist in or on the surface of the material. Furthermore, since B_e is determined by the local chemical environment and type of atom, peak shifts can be used to obtain information about the chemical bond state of atom, e.g. if it is bond to other more electronegative atom [12, 13]. Therefore, this technique can be extremely valorous in detecting surface chemical modifications, as it can detect the introduction of new elements to the surface, as well as, clarifying changes on the chemical bonds established by specific elements. As FT-IR analysis, XPS is a useful tool for the analysis of "click" chemistry reactions, namely, the CuAAC reation. As previously mentioned, XPS is a highly sensitive surface analysis technique for determining the surface chemical properties such as quantitative surface elemental composition (survey scan) and chemical environment of different elements (high-resolution scans). The chemical shifts identified

in XPS analysis can be used to evaluate the integrity of the starting material and the success of the reaction [16]. Regarding the studies reported throughout this thesis, XPS was used to provide additional confirmation of the successive modifications of chitosan, used as a base biomaterial for peptide tethering by CuAAC. Initial functionalization of chitosan and insertion of an azide group can be confirmed by studying the azide and the chemical environment around the nitrogen atoms, namely, the characteristic band corresponding to nitrogen in the azide group at ~404.5 eV. The success of subsequent "click" reaction would originate the disappearance of the aforementioned band and formation of a new peak at ~400.0 eV, associated with nitrogen in the triazole ring. Carbon high-resolution spectra is also valuable to prove insertion of peptide as the 285.0 eV peak is associated with C–C and C–H type carbons present in the peptide chain [17].

5. Amino Acid Analysis (AAA)

Amino Acid Analysis (AAA) has been widely used for the characterization of peptides and peptide-based materials, since it provides information on the amino acid composition, confirming sample identity, and peptide concentration which gives a measure of sample purity [17-19]. AAA includes two steps, hydrolysis of the substrate, followed by chromatographic separation and detection of the amino acid residues. The hydrolysis consists in the quantitative release of all amino acids of the substrate followed by their recovery in the hydrolysate. The conventional acidic hydrolysis uses 6 M HCl for 24 h at 110 °C. This method requires minor amounts of the substrate, a crucial factor to consider when only limited amounts of the peptide sample are available [20].

Amino acids are highly polar analytes and, therefore, not suitable for conventional RP-HPLC or gas chromatographic (GC) analysis. Therefore, a derivatization step is often employed. Derivatization reagents react with the amino groups (both primary amines and secondary amines, such as proline and hydroxyproline) or with the carboxyl function [21]. The AAA methods are divided into two groups relatively to the chromatographic separation: (i) post-column, and (ii) pre-column amino acid derivatization. The post-column technique, first developed by Moore and Stein, comprises the separation of the residues from the hydrolysate on a cation-exchange LC column, followed by post-column UV-Vis detection after ninhydrin derivatization [20-22].

In a pre-column system, the amino acid residues are first derivatized, then separated by chromatography [20, 22]. LC coupled with optical detection, namely the pre-column derivatization previous to RP-HPLC, has been widely used for AAA. Waters (Milford, MA, USA) introduced AccQ·Tag technique which consists in the derivatization of amino acids with 6-aminoquinolyl-*N*-hydroxysuccinimidyl carbamate (AQC). AQC is responsible for converting both primary and secondary amino acids into stable fluorescent derivatives that are amenable to UV-absorbance, fluorescence, electrochemical, and mass spectrometric detection (Figure 5A) [21]. The derivatized amino acids are later separated by HPLC and detected by UV absorption at 254 nm.

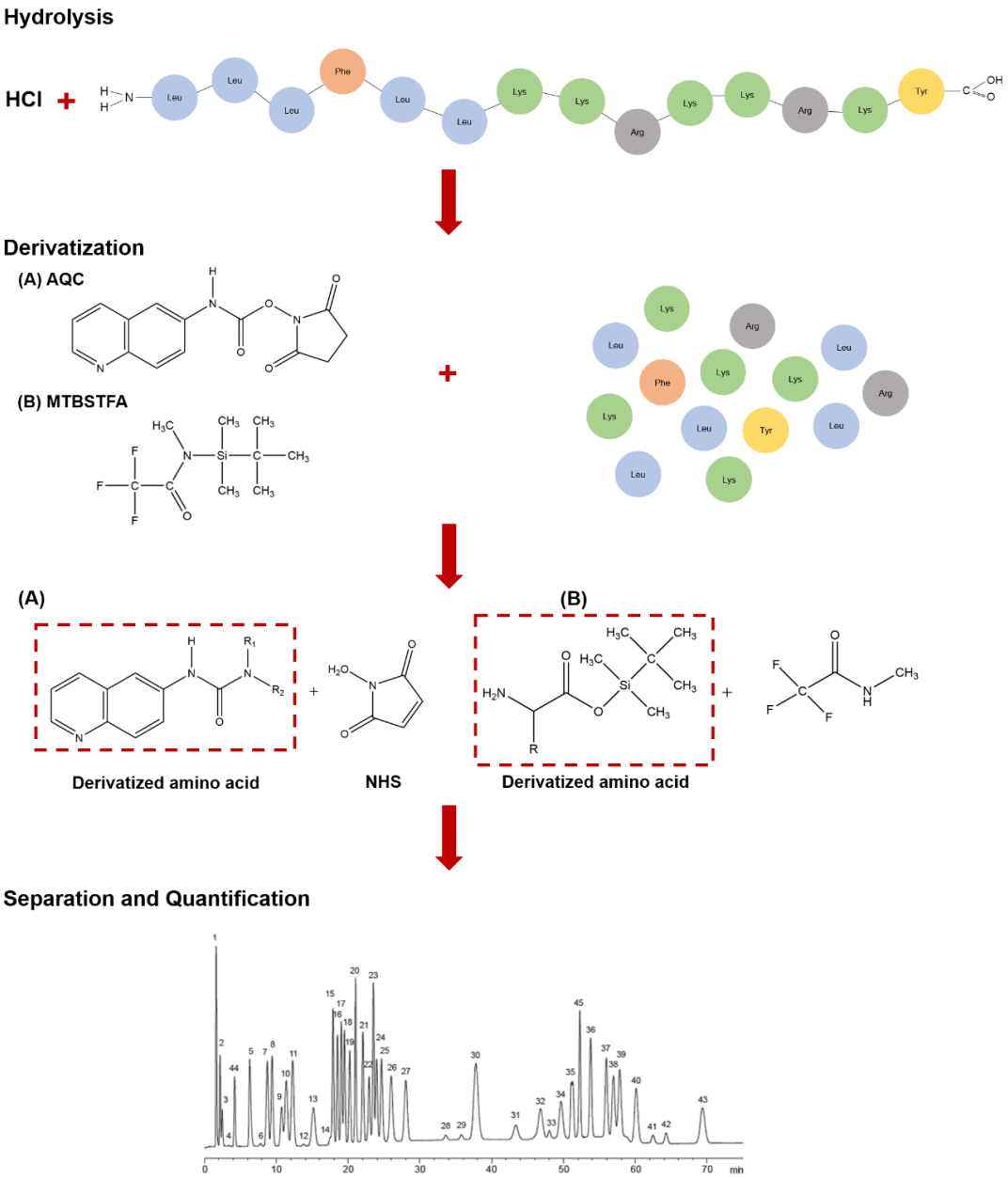

Figure 5 Scheme of AAA using (A) AQC and (B) MTBSTFA as derivatizing agents.

GC analysis coupled to MS (GC-MS) is another method to perform an AAA. In this case, the most common pre-column derivatization procedure is silylation, and involves replacing an active hydrogen by an alkylsilyl group, such as *N*,*O*-bis-(trimethylsilyl)trifluoroacetamide (BSTFA) or *N*-tertbutyldimethylsilyl-*N*-methyl trifluoroacetamide (MTBSTFA) [21, 23]. However, the BSTFA method can be sensitive to moisture, resulting in low reaction yields and unstable derivatized analytes. In this context, MTBSTFA, originates tertbutyldimethylsilyl (TBDMS) derivatives which are more stable and less moisture sensitive than those formed using lower molecular weight reagents such as BSTFA (Figure 5B) [23].

6. Scanning electron microscopy (SEM)

The scanning electron microscope (SEM) scans a sample with a focused beam of high-energy electrons to generate a range of signals at the surface of solid specimens. This high-energy electron beam scans across the surface, which is usually coated with a thin film of gold or platinum to improve contrast and the signal-to-noise ratio. The signals that derive from electron-sample interactions reveal detailed information about the sample including surface morphology, chemical composition, and crystalline structure and orientation of materials that compose the sample. In most applications, data are collected over a selected area of the surface of the sample, and a two-dimensional image is generated that displays spatial variations in these properties. The SEM is also capable of performing analyses of selected point locations on the sample; this approach is especially useful in qualitatively or semi-quantitatively determining chemical compositions using Energy Dispersive Spectroscopy (EDS) [4, 24].

As the beam scans across the sample's surface, interactions between the sample and the electron beam result in different types of electron signals emitted at or near the specimen surface. These signals, represented in Figure 6A, include low-energy secondary electrons (responsible for producing SEM images), high-energy backscattered electrons (BSE), photons (characteristic X-rays used for elemental analysis and continuum X-rays) and visible light (cathodoluminescence). Secondary electrons and BSE are commonly used for imaging samples: secondary electrons are most valuable for showing morphology and topography on samples and BSE are most valuable for illustrating contrasts in composition in multiphase samples (i.e. for rapid phase discrimination) [4, 24]. Diffracted backscattered electrons (EBSD), which are used to determine crystal structures

and orientations of minerals), are also generated. In an EBSD procedure, the sample is tilted to 70° towards the EBSD detector whereas the electron beam converges vertically with sample surface, originating diffracted electrons (Figure 6B). As previously mentioned, this technique provides information on regarding microstructural and crystallographic parameters, such as, phase detection and crystallographic orientation [25].

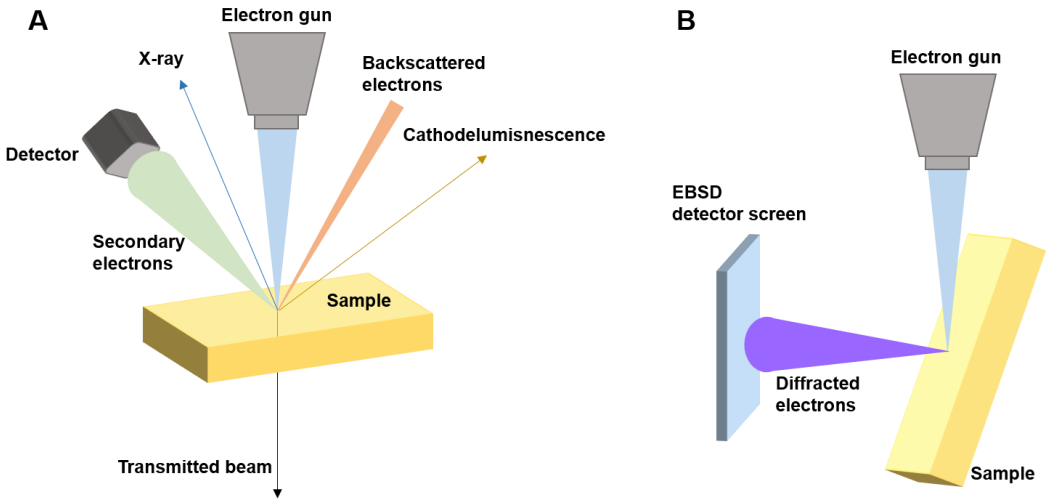

Figure 6 Scheme representing the different types of electron signals emitted after interaction between the electron beam and the sample.

X-ray generation is produced by inelastic collisions of the incident electrons with electrons in discrete orbitals of atoms in the sample. As the excited electrons return to lower energy states, they yield X-rays that are of a fixed wavelength (that is related to the difference in energy levels of electrons in different shells for a given element). Thus, characteristic X-rays are produced for each element in a mineral that is excited by the electron beam [4, 24].

SEM analysis is considered to be "non-destructive", since X-rays generated by electron interactions do not lead to volume loss of the sample, so it is possible to analyze the same materials repeatedly.

7. Contact angle goniometry

Contact angle measurements provide information about the wettability of a surface and allow the determination of the surface free energy that is directly proportional to the tendency of molecules to adsorb onto a material surface. This technique is very useful to

detect surface modifications (such as AMP immobilization), surface contamination and to predict future biological interactions with the material's surface [12, 26-28]. It measures the contact angle between the liquid/vapor interface and the liquid/solid interface (solid surface).

The phenomenon of the contact angle between a liquid and a solid surface can be explained as a balance between the force of attraction of the liquid molecules to each other (the cohesive force) and the attraction of the liquid molecules to the molecules of the surface (the adhesive force) [29, 30]. When a drop of liquid is placed on a surface, it spreads to reach equilibrium between cohesive and adhesive forces with minimum energy. This equilibrium between forces is described by the Young equation (Equation 2) [31]:

$$\gamma_{lv}.\cos\theta = \gamma_{sv} - \gamma_{sl}, \qquad \text{(Equation 2)}$$

where γ_{lv}, γ_{sv}, γ_{sl} and represent the liquid/vapor, solid/vapor and solid/liquid surface tension, respectively, and θ is the contact angle [29, 30].

The static sessile drop technique (Figure 7A) is the simplest method to measure the contact angle. It is usually established that a contact angle less than 90° (low contact angle) indicates that the liquid spreads over a large area of the surface, enabling the wetting of the surface. A contact angle higher than 90° (high contact angle) means that the liquid minimizes the contact with the surface, which is unfavorable for the wetting of the surface [30].

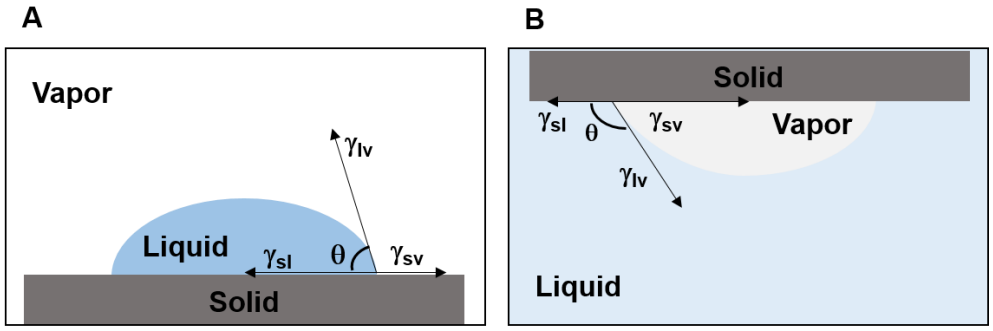

Figure 7 Scheme of contact angle measurements: (A) sessile drop technique and (B) captive bubble technique.

This technique is one of the most sensitive of all surface analytical techniques because only the top nanometer of a surface influences wettability. Therefore, it can be used to detect surface modification, namely detection of AMP immobilization [12, 26-28].

A different technique, proposed by Taggart *et al.* is the captive bubble method (Figure 7B). In this case, the sample is immersed in the testing liquid and an air bubble is formed underneath the sample. As in the sessile drop method, the contact angle formed by the air bubble surrounded by liquid can also be directly measured. In this context, higher contact angles correspond to hydrophobic surfaces, as the air bubble tends to exclude water and spread across the surface, thus creating a larger contact angle, whereas smaller contact angles are associated with more hydrophilic surfaces. Briefly, a small amount of air is injected, through a J-shaped needle, into the liquid forming an air bubble below the surface. Applying this method ensures that the surface is in contact with a saturated atmosphere and reduces contamination of surface [31]. This method has the further advantage of maintaining the sample fully hydrated and, consequently, the surface energy unaltered. This effect on the surface energy can be explained due to conformation alterations of the hydrophilic macromolecular chains. In the case of the work described in this thesis, this is an interesting phenomenon as in the sessile drop measurement, the hydrophobic domains of the biomolecules tend to aggregate on the surface in order to reduce the interfacial energy. Whereas, in the captive bubble method, at the interface surface material and testing liquid, the molecular structure of the hydrophilic segments reorganizes throughout the surface, originating in lower contact angles [32].

8. Ellipsometry

Ellipsometry is a non-destructive optical method that measures the polarization state of light incident upon a material surface as a function of wavelength. This technique is very useful for the determination of the thickness of a thin film deposited onto a reflective substrate, since the state of reflected polarized light depends on the thickness and the refractive index of the coating [33-35]. This technique is schematically demonstrated in Figure 8.

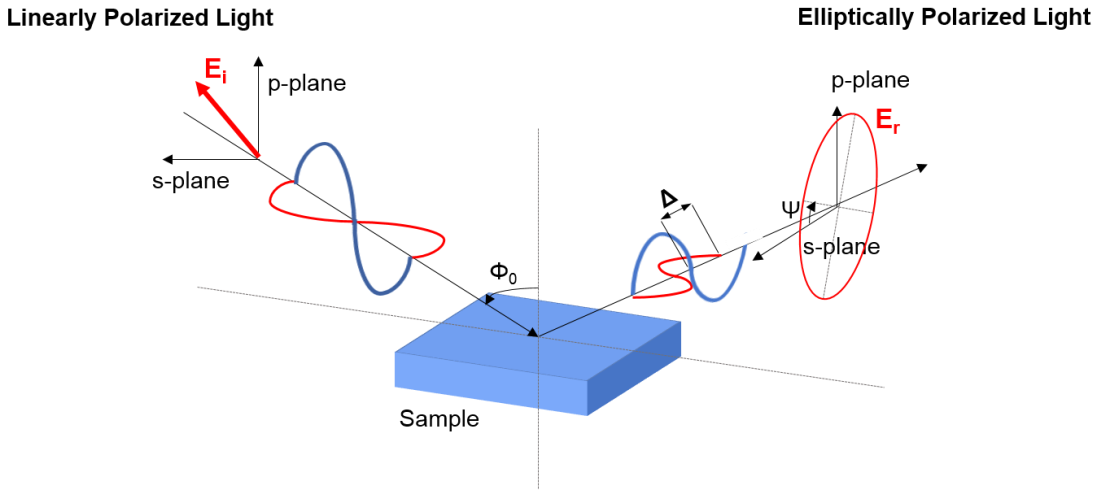

Figure 8 Schematic representation of light's polarization due to optical components and it is elliptical polarized upon reflection with asymmetric intensity difference (tan Ψ) and phase difference (Δ).

When light reflects from a surface both p- and s- components of the incident polarized light (p-parallel and s-perpendicular to the plan of incidence) will be changed from linear to elliptical. The change of polarization is characterized by the amplitude ratio (E_p/E_s), and the phase difference (δ_p-δ_s) of the two components (p- and s-) of the electric vector E. The change of polarization due to reflection at an interface is defined by two ellipsometric parameters, namely, Ψ (Equation 3) and Δ (Equation 4) [35, 36]:

$$Tan\ \Psi = \frac{(E_p/E_s)_{reflected}}{(E_p/E_s)_{incident}} \qquad \text{(Equation 3)}$$

and

$$\Delta = \left(\delta_p^r - \delta_s^r\right) - \left(\delta_p^i - \delta_s^i\right) \qquad \text{(Equation 4)}$$

where Ψ is the amplitude ratio due to reflection and Δ is the phase difference between the p- and s- components of the polarized light before (i) and after its reflection from a surface (r). These two angles are applied to evaluate the optical characteristics, namely, refractive index (n) and extinction coefficient (k), and thickness of a thin film deposited onto a reflective surface [33-36].

This technique can be very effective to detect surface modifications of thin films (<100 nm), especially when a thickness change is anticipated, such in the case of AMP immobilization.

9. Infrared Reflection-Absorption Spectroscopy (IRRAS)

Infrared Reflection-Absorption Spectroscopy (IRRAS) spectroscopy provides information about chemical bonds and chemical functional groups present in a sample deposited on a reflective surface (Figure 9). In fact, IRRAS is an adaptation of infrared spectroscopy for characterization of thin films deposited on reflective surfaces. The emitted beam stimulates molecular vibrations at specific frequencies corresponding to the fundamental vibrations modes of a given molecule. It is only when a vibration induces oscillating dipoles perpendicular to the surface that absorption occurs. IRRAS directly probes the vibrational modes associated with the various chemical bonds and chemical functional groups present in a sample by measuring absorption in the mid-infrared spectral region (3,000–600 cm^{-1}) [12, 37].

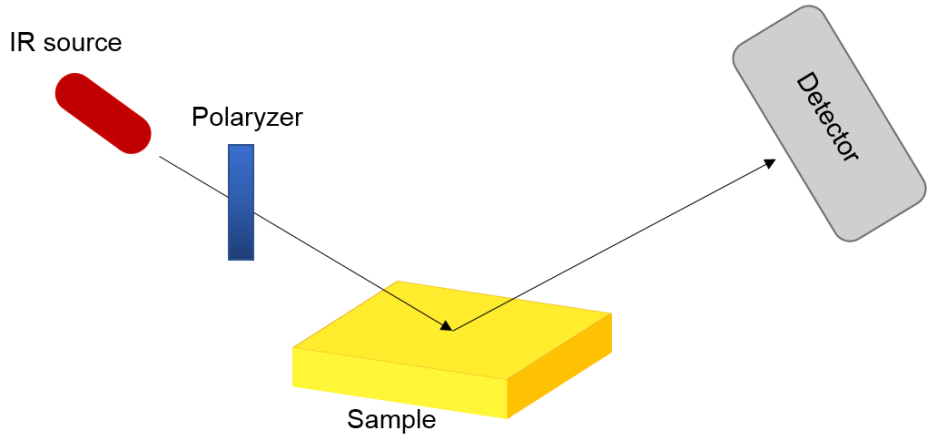

Figure 9 Scheme of IRRAS. Polarized Infrared is incident in to sample at 80° grazing angle and reflected to the detector.

The infrared beam emitted passes through a polarizer, after which the polarized light converges into the sample surface at a well-defined and controlled angle of incidence, increasing the sensitivity of superior layers of the surface. Subsequently, the reflected beam is detected at an angle equal to the angle of incidence. The frequencies absorbed by the film on the surface are a result of the difference between incident frequencies and reflected frequencies. The resulting spectra displays the absorption bands corresponding to the frequencies at which radiation was absorbed [38].

This method is extremely useful for characterization of thin films, as it is possible to detect alterations in functional groups, such as, functionalization of chitosan, and

increase/decrease of specific functional groups implicated in the immobilization of other compounds (e.g., AMP immobilization). As in FT-IR, the three reacting groups directly involved in the CuAAC reaction used throughout this work, namely, azido, alkyne and 1,2,3-triazole, are all IR-responsive and can be straightforwardly traced by FT-IRRAS.

References

[1] I. van den Broek, R.W. Sparidans, J.H.M. Schellens, J.H. Beijnen, Quantitative bioanalysis of peptides by liquid chromatography coupled to (tandem) mass spectrometry, Journal of Chromatography B 872(1) (2008) 1-22.

[2] M. Rauh, LC–MS/MS for protein and peptide quantification in clinical chemistry, Journal of Chromatography B 883-884(Supplement C) (2012) 59-67.

[3] M.J. Gouveia, P.J. Brindley, L.L. Santos, J.M. Correia da Costa, P. Gomes, N. Vale, Mass spectrometry techniques in the survey of steroid metabolites as potential disease biomarkers: A review, Metabolism 62(9) (2013) 1206-1217.

[4] X. Zhang, M. Cresswell, Chapter 3 - Materials Characterization of Inorganic Controlled Release, Inorganic Controlled Release Technology, Butterworth-Heinemann, Boston, 2016, pp. 57-91.

[5] C.T. Mant, Y. Chen, Z. Yan, T.V. Popa, J.M. Kovacs, J.B. Mills, B.P. Tripet, R.S. Hodges, HPLC Analysis and Purification of Peptides, in: G.B. Fields (Ed.), Peptide Characterization and Application Protocols, Humana Press, Totowa, NJ, 2007, 3-55.

[6] M.-I. Aguilar, HPLC of Peptides and Proteins: Methods and Protocols, Springer Science & Business Media2004.

[7] C.-P.S. Hsu, Infrared spectroscopy, Handbook of instrumental techniques for analytical chemistry 249 (1997).

[8] A.E. Hills, Spectroscopy in Biotechnology Research and Development A2 - Lindon, John C, in: G.E. Tranter, D.W. Koppenaal (Eds.), Encyclopedia of Spectroscopy and Spectrometry (Third Edition), Academic Press, Oxford, 2017, 198-202.

[9] M.J. Baker, J. Trevisan, P. Bassan, R. Bhargava, H.J. Butler, K.M. Dorling, P.R. Fielden, S.W. Fogarty, N.J. Fullwood, K.A. Heys, C. Hughes, P. Lasch, P.L. Martin-Hirsch, B. Obinaju, G.D. Sockalingum, J. Sulé-Suso, R.J. Strong, M.J. Walsh, B.R. Wood, P. Gardner, F.L. Martin, Using Fourier transform IR spectroscopy to analyze biological materials, Nature protocols 9(8) (2014) 1771-1791.

[10] V. Craige Trenerry, S.J. Rochfort, 9.16 - Natural Products Research and Metabolomics, Comprehensive Natural Products II, Elsevier, Oxford, 2010, 595-628.

[11] S. Sun, P. Wu, Mechanistic Insights into Cu(I)-Catalyzed Azide−Alkyne “Click” Cycloaddition Monitored by Real Time Infrared Spectroscopy, The Journal of Physical Chemistry A 114(32) (2010) 8331-8336.

[12] A.L. Hook, D.G. Anderson, R. Langer, P. Williams, M.C. Davies, M.R. Alexander, High throughput methods applied in biomaterial development and discovery, Biomaterials 31(2) (2010) 187-198.

[13] P. Kingshott, G. Andersson, S.L. McArthur, H.J. Griesser, Surface modification and chemical surface analysis of biomaterials, Current Opinion in Chemical Biology 15(5) (2011) 667-676.

[14] A.V. Lubenchenko, A.A. Batrakov, A.B. Pavolotsky, O.I. Lubenchenko, D.A. Ivanov, XPS study of multilayer multicomponent films, Applied Surface Science 427(Part A) (2018) 711-721.

[15] Appendix B XPS X-ray photoelectron spectroscopy, in: E.F. Vansant, P. Van Der Voort, K.C. Vrancken (Eds.), Studies in Surface Science and Catalysis, Elsevier1995, 501-504.

[16] G. Zorn, L.-H. Liu, L. Árnadóttir, H. Wang, L.J. Gamble, D.G. Castner, M. Yan, X-ray Photoelectron Spectroscopy Investigation of the Nitrogen Species in Photoactive Perfluorophenylazide-Modified Surfaces, The Journal of Physical Chemistry C 118(1) (2014) 376-383.

[17] M. Barbosa, N. Vale, F.M.T.A. Costa, M.C.L. Martins, P. Gomes, Tethering antimicrobial peptides onto chitosan: Optimization of azide-alkyne "click" reaction conditions, Carbohydrate Polymers 165 (2017) 384-393.

[18] M.P. Bartolomeo, F. Maisano, Validation of a Reversed-Phase HPLC Method for Quantitative Amino Acid Analysis, Journal of Biomolecular Techniques : JBT 17(2) (2006) 131-137.

[19] T. Masuko, N. Iwasaki, S. Yamane, T. Funakoshi, T. Majima, A. Minami, N. Ohsuga, T. Ohta, S.-I. Nishimura, Chitosan–RGDSGGC conjugate as a scaffold material for musculoskeletal tissue engineering, Biomaterials 26(26) (2005) 5339-5347.

[20] M. Fountoulakis, H.-W. Lahm, Hydrolysis and amino acid composition analysis of proteins, Journal of Chromatography A 826(2) (1998) 109-134.

[21] H. Kaspar, K. Dettmer, W. Gronwald, P.J. Oefner, Advances in amino acid analysis, Analytical and Bioanalytical Chemistry 393(2) (2009) 445-452.

[22] F.D. Macchi, F.J. Shen, R.G. Keck, R.J. Harris, Amino acid analysis, using postcolumn ninhydrin detection, in a biotechnology laboratory, Methods in molecular biology (Clifton, N.J.) 159 (2000) 9-30.

[23] K.K. Stenerson, The derivatization and analysis of amino acids by GC-MS, Sigma-Aldrich. Reporter US 25 (2011).

[24] M. Carter, J. Shieh, Chapter 5 - Microscopy, Guide to Research Techniques in Neuroscience (Second Edition), Academic Press, San Diego, 2015, pp. 117-144.

[25] J. Pérez-Arantegui, A. Larrea, Electron backscattering diffraction as a complementary analytical approach to the microstructural characterization of ancient materials by electron microscopy, TrAC Trends in Analytical Chemistry 72 (2015) 193-201.

[26] F. Costa, S. Maia, J. Gomes, P. Gomes, M.C.L. Martins, Characterization of hLF1–11 immobilization onto chitosan ultrathin films, and its effects on antimicrobial activity, Acta Biomaterialia 10(8) (2014) 3513-3521.

[27] X. Chen, H. Hirt, Y. Li, S.-U. Gorr, C. Aparicio, Antimicrobial GL13K Peptide Coatings Killed and Ruptured the Wall of Streptococcus gordonii and Prevented Formation and Growth of Biofilms, PLoS ONE 9(11) (2014) e111579.

[28] X. Li, P. Li, R. Saravanan, A. Basu, B. Mishra, S.H. Lim, X. Su, P.A. Tambyah, S.S.J. Leong, Antimicrobial functionalization of silicone surfaces with engineered short peptides having broad spectrum antimicrobial and salt-resistant properties, Acta Biomaterialia 10(1) (2014) 258-266.

[29] B.D. Ratner, A.S. Hoffman, F.J. Schoen, J.E. Lemons, Biomaterials science: an introduction to materials in medicine, Academic press2004.

[30] K.C. Dee, D.A. Puleo, R. Bizios, An introduction to tissue-biomaterial interactions, John Wiley & Sons2003.

[31] Y. Yuan, T.R. Lee, Contact angle and wetting properties, Surface science techniques, Springer2013, 3-34.

[32] Y. Zhu, C. Gao, T. He, J. Shen, Endothelium regeneration on luminal surface of polyurethane vascular scaffold modified with diamine and covalently grafted with gelatin, Biomaterials 25(3) (2004) 423-430.

[33] H. Tompkins, E.A. Irene, Handbook of ellipsometry, William Andrew 2005.

[34] H. Fujiwara, Spectroscopic ellipsometry: principles and applications, John Wiley & Sons 2007.

[35] T. Minamikawa, Y.-D. Hsieh, K. Shibuya, E. Hase, Y. Kaneoka, S. Okubo, H. Inaba, Y. Mizutani, H. Yamamoto, T. Iwata, T. Yasui, Dual-comb spectroscopic ellipsometry, Nature Communications 8(1) (2017) 610.

[36] A. Datta, S. Mukherjee, Structural and morphological evolution in metal-organic films and multilayers, CRC Press 2015.

[37] R. Adato, H. Altug, In-situ ultra-sensitive infrared absorption spectroscopy of biomolecule interactions in real time with plasmonic nanoantennas, Nature Communications 4 (2013) 2154.

[38] R. Mendelsohn, G. Mao, C.R. Flach, Infrared Reflection-Absorption Spectroscopy: Principles and Applications to Lipid-Protein Interaction in Langmuir Films, Biochimica et biophysica acta 1798(4) (2010) 788-800.

Chapter III

Grafting Techniques towards Production of Peptide-Tethered Hydrogels, a Novel Class of Materials with Biomedical Interest

This chapter corresponds to the following review article:

Mariana Barbosa[1,2,3,4], M. Cristina L. Martins[2,3,5] and Paula Gomes[1]

Gels **2015**, 1(2), 194-218

[1]UCIBIO-REQUIMTE, Departamento de Química e Bioquímica, Faculdade de Ciências, Universidade do Porto, Porto, Portugal
[2]Instituto de Investigação e Inovação em Saúde, Universidade do Porto, Porto, Portugal
[3]INEB-Instituto de Engenharia Biomédica, Universidade do Porto, Porto, Portugal
[4]FEUP - Faculdade de Engenharia da Universidade do Porto, Porto, Portugal
[5]Instituto de Ciências Biomédicas Abel Salazar, Universidade do Porto, Porto, Portugal

Abstract

In recent years, new highly functional polymeric biomaterials are being developed to increase the therapeutic efficacy in tissue regeneration approaches. Peptides regulate most physiological processes and display several other biological activities. Therefore, their importance in the field of biomedical research and drug development is rapidly increasing. However, the use of peptides as therapeutic agents is restricted by some of their physicochemical properties. The development of improved routes of delivery of peptide-based therapeutics is crucial and its biomedical value is expected to increase in the near future. The unique properties of hydrogels triggered their spreading as localized drug depots. Several strategies, such as the carbodiimide chemistry, have been used to successfully immobilize bioactive peptide sequences into the hydrogels backbone. Peptide tethering through the so-called "click" chemistry reactions is also a highly promising, yet underexplored, approach to the synthesis of hydrogels with varying dimensions and patterns. The present review focus on the approaches that are being used for the establishment of chemical bonds between peptides and non-peptidic hydrogels throughout the last decade.

Keywords: hydrogels; functionalization; peptides; tissue engineering

1. Introduction

In recent years, there has been significant progress in the development of polymers for biomedical applications. New highly functional biomaterials are being designed to increase the therapeutic efficacy in tissue regeneration approaches. In natural tissues, cells are surrounded by a three-dimensional (3D) extracellular matrix (ECM) composed of several biochemical and mechanical signals responsible for modulating their behavior, namely cell attachment, proliferation and differentiation. Fibrous proteins, such as fibronectin, collagen, and laminin, are found in the ECM constitution and are responsible for providing mechanical support. Moreover, ECM acts as a reservoir of cell signaling molecules, such as adhesion molecules and growth factors. Therefore, new generations of biomimetic and bioinstructive materials should act as 3D templates for cell culture, mimicking the ECM environment and promoting cell-matrix interactions responsible for modulating cellular activity and tissue organization [1–3].

Understanding the composition and functions of the ECM is of chief importance for developing new 3D cell culture platforms. The incorporation of specific cell signaling molecules, such as growth factors and ECM proteins, into these scaffolds is still a major challenge. These signals are usually adsorbed or covalently attached to a scaffold material, however, prolonged biological activity is thwarted by stability problems after administered into the body [2,3]. An effective functionalization is also dependent on the biomaterial propensity for functionalization and how those modifications will affect its properties. For these reasons, the development of new biomimetic polymers with tunable physicochemical characteristics, according to the desired application, and also capable of being easily functionalized with bioactive building blocks is highly needed. Hydrogels, due to their unique physicochemical properties and unique swelling behavior, are being widely used for tissue engineering applications. Peptides and polypeptides domains have been used to functionalize polymer-based materials in order to obtain new materials with controllable structure, degradability and stimuli-sensitive properties. Therefore, this approach is currently being used for the synthesis of highly multifunctional polymeric scaffolds with controllable assembly and characteristics. Peptide-based materials are now attractive candidates for biomedical used due to the progresses observed in synthesis methods and characterization techniques [1,4–6].

The aim of this review is to identify the recent approaches used to covalently bind peptides to hydrogels, describing advantages and limitations of each strategy [7], with particular emphasis on "click" chemistry techniques. These approaches are reviewed herein and refer to the last decade, i.e., reports from 2005 to the present date.

2. Peptides Underlying a Paradigm Shift in Traditional Therapies

The use of peptides, comprising the functional subunits of proteins, as drug candidates has been fostered over the last decades [8,9]. Peptides regulate most physiological processes, regulating cellular function and coordinating intercellular communication. In fact, specificity of molecular recognition and consequent ligand-binding interactions are determined by specific amino acid sequences of peptides and proteins [10,11]. Moreover, they may have several biological activities such as antimicrobial, antithrombotic, opioid, antioxidant, among others. Consequently, peptides are nowadays an important issue in biomedical research and drug development in various therapeutic classes, ranging from thrombolytics, immunomodulators and growth factors to antimicrobials [8,12–17].

Peptides have significant advantages over other small molecules in terms of specificity/affinity for targets and toxicity profiles, and over antibodies in terms of tissue penetration and immunogenicity owing to their smaller size [18–21]. Moreover, peptides are generally biocompatible and do not cause severe immune responses, particularly those with smaller sequences, as they are composed of naturally occurring or metabolically degradable amino acids. In general, the compositional homology between peptide drug candidates and its bioactive parent molecules significantly diminishes the risk of unpredicted side-reactions and the production complexity, thus lowering the production costs [11,22]. Furthermore, peptides are also very amenable to site-specific modifications that might be used to tailor specific properties [21].

Consequently, a large number of peptide-based drugs are now being marketed and the number of candidates entering clinical evaluation in recent years is steadily increasing [12,22]. Bioactive peptides and peptidomimetics compose several marketed drugs used against most diverse diseases, such as, just to name a few: the anti-HIV-1 agent Enfuvirtide, the natridiuretic peptide Nesiritide (used to treat acute congestive heart failure), antimicrobial peptides such as Gramicidin D (component of the topical antibiotic drug line Neosporin®), peptide hormones like Oxytocin (labor induction agent) or Leuprolide (gonadotropin-releasing hormone analogue), or even the bone density conservation agent salmotonin (salmon calcitonin), which is the active ingredient of antiosteporotic drugs like Miacalcin® from Novartis [8,22]. Therefore, the synthesis of such structures has been a major focus of organic chemistry for over a century in order to improve the prospects for synthetic therapeutic peptides [18,23].

The use of peptide therapeutics is expected to increase in the near future. More will go into clinical trials, some will be produced with increased potency and/or specificity, and new conjugated forms (for example with polysaccharides or synthetic polymers) will be designed expanding the range of targets [22,24]. Moreover, peptides are expected to find increased biomedical applications not only as the active ingredient of drugs, but also as "add-ons" to other therapeutic compounds or biomaterials.

In this context, peptides can be used as targeting moieties, as carriers to provide transport across cellular membranes, and to modify the bioactivity of the original compound/material. In the field of biomaterials, peptides have been extensively used as cell-instructive motifs with different roles, namely, to promote cell-adhesion to otherwise non-adhesive polymers [25,26]. Besides its active role in ligand-receptor interactions, peptides can also promote protein-protein interactions and antibody detection [27]. One

of the most interesting applications is the development of drug delivery carriers, since peptides can be used as stimuli-sensitive linkers that can be used for controlled drug release in the presence of certain enzymes, which allows the delivery of pharmaceuticals in very specific locations and conditions. In this context, enzyme-sensitive hybrid materials composed of synthetic or natural polymers and peptide/protein domains, which respond to specific proteases, have been prepared using genetic engineering and/or chemical approaches [26,28].

Finally, peptides alone are being successfully used as innovative biomaterials. One important example is the novel group of materials named self-assembling peptides (SAPs), which self-assemble into hydrogel-like nanostructures. Stupp's group has developed peptide amphiphiles (PA) by combining a hydrophobic block, usually an alkyl chain, a β-sheet forming peptide responsible for the self-assembling and a third section with the bioactivity molecules, such as peptides. These PA are capable of self-assemble and form highly ordered gels under physiological concentrations of salt solutions [29–32]. For instance, the RADA16-I (AcN-RADARADARADARADA-$CONH_2$) peptide can undergo spontaneous assembly into an organized network of nanofibers under physiological conditions, forming an ECM-like hydrogel for the encapsulation and delivery of growth factors and cells [33,34]. Consequently, these peptide-based hydrogels have been finding numerous applications in the biomedical field due to its functional supramolecular structure capable of forming 3D matrices [25,29,30,35].

3. Peptide Delivery Systems

The use of peptides as therapeutic agents is restricted by some of their physicochemical properties. The large molecular weight of peptides influences their diffusion through the epithelial layer, which leads to low bioavailability. Moreover, peptides are mostly hydrophilic so the transfer across biological membranes by passive diffusion is limited. Peptides can also undergo aggregation, adsorption and denaturation and are also vulnerable to proteolytic cleavage so their stability in the blood stream and concentration *in vivo* is limited [36,37]. Hence, progression of peptide-based compounds into clinical therapy is thwarted by stability problems and short circulating plasma half-life [11,38]. In fact, peptides are based on amino acid building blocks and thus can be rapidly inactivated or eliminated after administered into the body. Even when administered

parenterally, they can be rapidly metabolized by peptidases or cleared from circulation by the kidney, spleen, or liver [37,39].

The development of improved routes of delivery for peptide-based therapeutics is crucial and its biomedical value is expected to increase in the near future [11,38]. Research is focusing on improved routes of delivery that are expected to open up the potential of peptide drugs. In order to overcome the aforementioned drawbacks and extend the bioactivity of therapeutic peptides *in vivo*, it is possible to use a delivery matrix that protects peptides from neutralization and degradation. Cell-signaling peptides can act as tethered ligands and be cross-linked with matrix scaffolds by a plethora of chemical bonding strategies. The matrix can provide controlled peptide delivery at a specific site or systemically in a continuous manner, preventing repeated administrations of the drug. The use of tunable peptide delivery system is of major importance to achieve controllable dosage for higher effectiveness or to provide a sustained release during the course of the treatment [38,40]. Finally, by limiting the delivery to specific target sites and avoiding healthy tissues and cells the efficacy of the drug is improved and eventual toxic effects at non-target sites can be prevented [41–43].

Polymers are an ideal class of materials to prepare drug delivery systems, since they are quite versatile and their physicochemical properties, such as biocompatibility, biodegradability, network structure and mechanical strength, are easily adapted and tuned for a particular application. It is possible to customize the material by, for example, altering its molecular components, adjusting the polymerization conditions, or modifying the original polymer with new bioactive compounds [40,41,44]. When developing a drug-releasing polymer scaffold, several criteria should be addressed, namely the drug release profiles, the drug-loading capacity and binding affinity of the polymer and the spatial distribution of the bioactive compound within the matrix backbone. It is also important to consider how the incorporation of the drug into the polymer will affect its bioactive properties [45].

4. Hydrogels Hydrogels as Drug-Delivery Vehicles and Scaffolds for Tissue Regeneration

Current tissue engineering strategies comprises both cells and a matrix-scaffold. Therefore, it is essential to select a suitable biomaterial taking into account the envisioned application and the characteristics of the tissue (e.g., stiffness, chemical composition,

biological signals) [29]. The aforementioned scaffolds can be fabricated from either biological materials or from synthetic polymers. Biological scaffolds interact with resident cells providing biofunctional cues that modulate cellular behavior. However, they are structurally complex and present a high variability of cell-signaling cues making it difficult to precisely control cellular activity. On the other hand, synthetic scaffolds are usually not bioactive, providing inadequate biological information for cell culture. Nevertheless, they found many applications in the field of tissue engineering because they allow for precise control of their mechanical properties. In this regard, the ideal scaffold for biomedical applications should be developed combining the physicochemical properties of both synthetic and natural polymers [46,47].

Hydrogels have been broadly investigated as biomaterials for tissue engineering strategies, in which they are used as scaffolds, drug delivery systems, as well as 3D cell culture platforms [3,48,49]. Hydrogels are hydrophilic polymeric networks with 3D configuration that can retain a significant amount of water or biological fluids. Hydrogels generally possess excellent biocompatibility due to the tissue-like physicochemical properties and their ability to swell under biological conditions [48,50–54]. Hydrogels recreate the hydrated microenvironments and the structure of the ECM where cells are embedded in real 3D conditions, therefore they have been widely used as scaffolds [55]. When used as artificial ECM, hydrogels may act as a substitute of natural tissues by rearranging cells into an ordered scaffold to support the newly-forming tissues, and a hydrated space for diffusion of nutrients, oxygen and metabolites [56–58].

The presence of hydrophilic groups such as –OH, –CONH–, $–CONH_2$, $–SO_3H$ in polymer chains is responsible for their ability to absorb water. The water content depends on the nature of the aqueous environment and polymer composition and is the key factor which determines the physicochemical characteristics of the hydrogel [51,59–61]. The elastic nature of completely swollen hydrogels has been found to diminish the risk of irritation to the adjacent tissues after implantation. Non-specific protein adsorption and cellular adhesion, followed by increased risk of an immunological reaction, are prevented by the low interfacial tension between the hydrogel surface and the surrounding biological components [62]. Hydrogels are also used for cell encapsulation due to their high permeability which allows diffusion of nutrients, oxygen and cell metabolites [49,52,63]. Hydrogels are usually prepared under mild reaction conditions without need for organic solvents, at ambient temperatures [51]. Cells can be uniformly seeded within the interstitial pores created in the hydrogel network [49,64]. The density of those pores can

be adjusted during the polymerization reactions, namely the affinity of hydrogels for the swelling solvent and the cross-linking density within the matrix. In addition, it is possible to load bioactive drugs and biomolecules into the gel matrix, protecting them from degradation, and subsequently release them at a diffusion-dependent rate. Actually, controlling the hydrogel structure is the key factor to customize the release schedule allowing them to be either used for systemic delivery or to preserve the appropriated bioactive concentration around target site [49,53,65].

Hydrogels are extremely stable in the presence of high amounts of water, however, when desired, they can be designed to be sensitive to external stimuli such as the presence of enzymes or certain environmental conditions (e.g., pH, temperature, or electric field). The physical structure and bio-adhesive properties of hydrogels allows them to adapt and adhere to the surface to which they are applied, and depending on their bio-adhesive properties, they can be immobilized in [53,66]. However, hydrogels are also associated to several limitations. Nature-derived hydrogels are usually associated with low tensile forces which can promote their degradation or moving away from the desired application site, making them inappropriate for load-bearing applications. This restriction may not be critical in the traditional parental drug administration. Problems related to drug delivery properties of hydrogels are still a major concern. The drug-loading capacity and distribution of the bioactive compound, especially non-soluble drugs, within the hydrogel network may be limited. Promoting a faster drug delivery rate can be achieved by increasing pore sizes and water content of the hydrogel. Most hydrogels present deformable features and can be easily administrated by injection, otherwise they require surgical implantation. These limitations can restrict the application of hydrogels in the development of drug delivery systems [53].

There are different types of hydrogel-forming polymers generally divided in two categories according to their source, natural or synthetic, each presenting advantages and limitations. Natural hydrogels have been widely used for tissue engineering approaches and are synthesized from proteins and ECM components like collagen, fibrin, hyaluronic acid or Matrigel, or from biological sources such as agarose, alginate, chitosan, silk fibrils. Natural polysaccharides display endogenous factors responsible for modulating several cellular functions, such as adhesion, viability and proliferation. Furthermore, being biodegradable, they can be replaced by *bona fide* ECM over time. Therefore, natural hydrogels can act as scaffolds for cellular guidance and wound healing [3,5,48,63,67]. Still, natural polymeric hydrogels are complex and exhibit a plethora of

cell-signaling molecules and exhibit large batch to batch variability, making it difficult to correctly define the cell-modulating signals, to tune the material physicochemical properties and to attain highly reproducible results using such scaffolds. On the other hand, synthetic polymers, such as poly(ethylene glycol) (PEG), poly(acrylic acid) (PAA), poly(2-hydroxyethyl methacrylate) (PHEMA), poly(vinyl alcohol), (PVA) and polyacrylamide (PAAm), have emerged as an important alternative due to their reproducible properties and controllable physical properties. Synthetic hydrogels can act as a blank (i.e., without cell-binding ligands) scaffold for cell culture, as they maintain the viability of encapsulated cells and allow ECM deposition as they degrade. However, most synthetic hydrogels alone lack bioactivity and cell signaling motifs and only function as passive scaffolds for cells [3,63,68].

Limitations of both natural and synthetic hydrogels have motivated the development of new synthetic approaches and crosslinking strategies to modify these polymers with the essential biophysical and biochemical signals to match the physiological cellular environment [3,5,48,49,51,67]. In addition, these materials may be decorated with biochemical signals that bind to specific cell receptors and modulate cell behavior [57,69]. *In situ*-forming hydrogels present the added benefit of injectability and can be used to fill tissue defects with irregular patterns in a minimally invasive manner [58]. Overall, the unique properties of hydrogels triggered their spreading as localized drug depots. They form highly hydrated 3D networks, with a selective permeability that affords some control over drug release rates, which in addition may be triggered intelligently by interactions with biomolecular stimuli. Hydrogels are typically biocompatible since they possess native tissue-like properties [41,55]. Moreover, hydrophilic biomolecules, namely peptides, are compatible with hydrogels [56,70,71].

Polymers can be physically or chemically cross-linked to originate hydrogel-based scaffolds with distinct composition, networks and water solubility. Those characteristics affect other relevant properties such as the swelling degree and the degradation behavior. By controlling the physicochemical properties of hydrogels, the delivery kinetics of a drug can be adjusted to the desired rate. They can be prepared from soluble precursor solutions that crosslink in situ under mild conditions. Specific bioactive agents can be loaded into hydrogels, using different strategies involving physical or chemical interactions. Drug entrapment can be achieved either through drug trapping during hydrogel formation, or drug absorption by pre-fabricated hydrogels. If the drug of interest is added to the polymer solution before crosslinking, it becomes entrapped within the

network, generally retaining full bioactivity [41]. However, when a drug is physically loaded into a hydrogel matrix, assuring a long-term continuous delivery is difficult since the drug is essentially released by diffusion. Therefore, in order to achieve a sustained drug release, it is necessary to improve the chemical interactions of hydrogels and bioactive compounds. Another aspect to consider, is the degradation rate of hydrogels which greatly influence their drug delivery behavior [41,57]. Moreover, drug-containing biomaterials can also be programmed to release the drug at a specific site in response to a particular biological milieu [72].

The emergence of stimuli-sensitive hydrogels has gained special interest in the field of tissue regeneration and biomedical engineering due to their ability to undergo structural modifications and act as controllable drug-release systems in response to environmental changes. Also known as smart hydrogels, they are developed to recognize both physical (temperature, light, mechanical tension) and chemical (pH, biomolecules, biochemical environment) stimuli [41]. For local release and higher therapeutic efficacy in tissue-regeneration approaches, the hydrogel carriers may simultaneously act as a tissue-engineering scaffold, as is the case of delivery systems for pro-regeneration drugs, like growth factors. They consist in large polypeptides that bind to specific cell-surface ligands and modulate cellular activity and gene expression [37,73]. Stimuli-responsive polymers have been attractive materials for the drug delivery field. These polymers have the ability to change its properties according to the surrounding environment. As said previously, both physical and chemical stimuli can induce responses in these "smart" systems [26,74]. Jeong *et al.* developed an injectable drug delivery system from an enzymatically degradable polypeptide block copolymer capable of undergo sol-gel transition as the temperature increases [75,76]. These peptide-based biomaterials are not within the scope of this review however, the reader is referred to a variety of research and review papers that describe the fundamental aspects and application areas of peptide carriers with stimuli-sensitive properties [66,74,77–81].

The covalent coupling of a drug to a polymer, although generally irreversible in nature, may be used for delivery purposes if the carrier is biodegradable or if a labile drug–polymer linker is used. However, the first strategy is often inadequate since the degradation rate in the human body is usually slow and unpredictable. The second approach generally provides a higher degree of versatility and efficacy, as very selective triggering mechanisms can be chosen to enable drug release upon response to specific stimuli. The released drug acts locally to modulate the response of cells, within and/or

near the material, activating pro-regenerative functions [73]. If peptide-grafted polymers are subsequently used to prepare hydrogels the rate of peptide release will depend on the cleavage kinetics of the peptide-network linkage, and the rate of peptide diffusion from the matrix, once free from the polymer backbone [82]. At the same time, the hydrogel scaffold acts as an artificial 3D matrix that mimic the natural ECM, promoting an efficient exchange of nutrients, oxygen and cellular metabolites thus providing an adequate cellular microenvironment inducing the repair of injured tissues, and the restoration of natural functions in situ [58,83,84].

The immobilization of bioactive peptides onto the backbone of hydrogels derived from synthetic polymers improves cell-matrix interactions. Current approaches allow the use of synthetic PEG hydrogels as scaffolds for cell culture due to its hydrophilic nature and ability to incorporate adhesion-peptides which promotes cell-polymer interactions. For example, functionalized PEG hydrogels with cell-adhesion peptides offers biological matrix functionality and allows cells to interact with the scaffold. The amount of peptide loaded onto the hydrogel and distribution throughout the hydrogel network greatly influences cell adhesion and dispersion. Studies demonstrated that incorporation of peptide-based binding motifs on PEG-based hydrogels promoted binding and proliferation of osteoblasts, fibroblasts and smooth muscle cells. The hydrogel matrix provided an artificial ECM environment to the cells since the incorporated adhesion sequences recognize specific ligands displayed on the cell-surface [85,86]. The tripeptide RGD, found initially in fibronectin, is considered the minimal integrin-binding sequence. This adhesion motif was later identified within collagen, vitronectin, laminin, fibrinogen, among others ECM proteins. Peptide sequences derived from laminin, including GFOGER, IKLLI, LRE, IKVAV, YIGSR, DGEA, and PDSGR, have also been demonstrated to enable cell adhesion, proliferation, and differentiation [85,87]. Reactive acryloyl-PEG-*N*-hydroxysuccinimide was conjugated with RGD peptide by reaction of its amine terminus with the succinimide group. The resulting macromere reacted with an *in situ* photocrosslinkable chitosan by free radical photoinitiated polymerization after UV irradiation [86,88].

The use of a combinatorial library of different cell-binding and other matrix analogue peptides is mandatory to induce cellular activity and cell-matrix interactions, in order to promote tissue regeneration [89,90]. Such is the case of peptide domains sensitive to the action of proteases which were loaded into both synthetic hydrogels, such as PEG-polymer chains [91], and natural hydrogels, like alginate [92]. Their cleavage allows to

expand the interstitial space of the hydrogel network to promote cell growth and migration, and ECM deposition [86]. For example, covalently immobilized growth factors, like the basic fibroblast growth factor (bFGF), to PEG hydrogels promoted cellular functions involved in the process of tissue formation, namely cellular migration and proliferation [89].

The synthesis of novel cell-culture scaffolds with ECM-like properties in crucial for developing, *in vitro*, environments capable of promoting cellular activity [93,94]. There are several peptide motifs that exhibit biological activity, like cell-adhesion and proteolyzable peptides, or influence mechanical properties, such as elastin-like peptides. Using these bioactive cues allow the precise tuning of the material physicochemical characteristics. Therefore, a plethora of new bioactive peptides, for example structural and cell-signaling sequences, are being studied to improve the field of peptide-based materials [93].

5. Peptide Tethering onto Hydrogels through "Click" Chemistry

When small molecular-weight drugs, such as oligopeptides, are loaded into alginate hydrogels simply by physical entrapment, the diffusion-controlled release kinetics is generally too fast. If a more sustained release is to be attained, it might be necessary to conjugate both components via stronger interactions such as covalent bonds [57,95]. In this connection, the water-soluble 1-ethyl-3-(3-dimethylaminopropyl) carbodiimide (EDC), is the carbodiimide of choice for the covalent attachment of proteins and peptides to hydrogels such as alginate, by forming amide linkages between the amine containing biomolecules and the polymer's carboxylic groups [96]. In this crosslinking reaction, typically, performed between pH 4.5 and 7.5, EDC catalyzes the formation of amide bonds, usually in the presence of an auxiliary nucleophile such as *N*-hydroxysuccinimide (NHS) or *N*-hydroxysulfosuccinimide (sulfo-NHS). When used, the auxiliary nucleophile reacts with the intermediate *O*-acylisourea formed upon carboxyl activation with EDC, leading to a more stable, but still reactive, ester intermediate that ultimately reacts with the amine group. Consequently, coupling reactions mediated by EDC/[sulfo-]NHS (Figure 1) are more effective and high-yielding than with the use of EDC by itself [97,98].

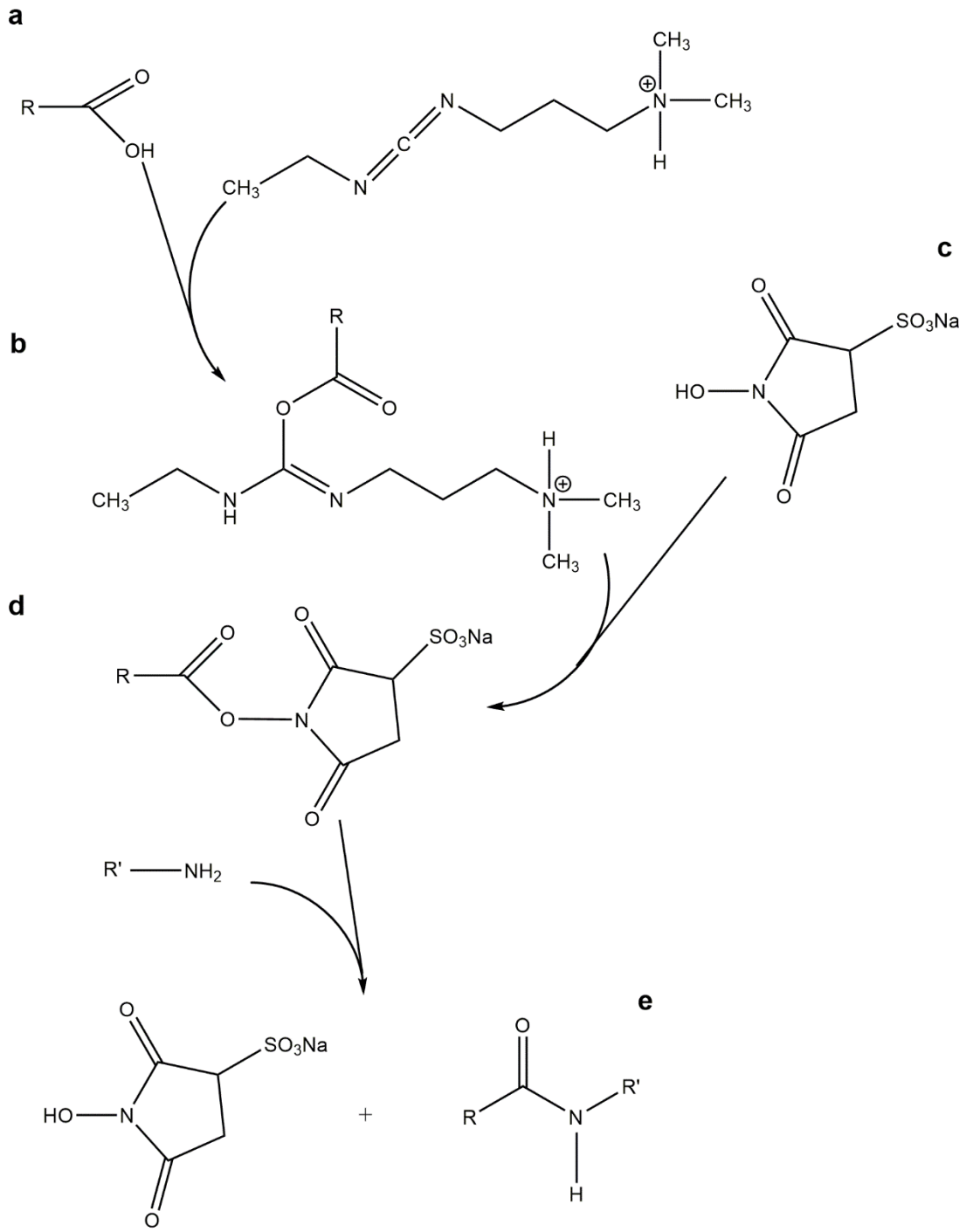

Figure 1 1-Ethyl-3-(3-dimethylaminopropyl) carbodiimide (EDC)-mediated amide formation in the presence of sulfo-*N*-hydroxysuccinimide (NHS): upon carboxyl activation with (a) EDC, the resultant intermediate (b) *O*-acylisourea reacts with the auxiliary nucleophile (c) sulfo-NHS leading to an (d) ester intermediate that ultimately reacts with the amine group, yielding the desired (e) amide bond.

Despite carbodiimide chemistry has been used to successfully immobilize bioactive peptide sequences in alginate [92,99], PEG-heparin hydrogels [100,101] and hyaluronic acid [102], peptide tethering through the so-called "click" chemistry reactions [103] is a highly promising, yet underexplored, approach to the synthesis of hydrogels with varying

dimensions and patterns. Sharpless and co-workers formulated in 2001 the concept of "click" chemistry [104] and defined it as a group of highly chemoselective reactions where two functional groups exclusively react with each other, even in the presence of other reactive functionalities, with minimal byproducts. Such reactions are thermodynamically favored (driving force superior to 20 kcal·mol^{-1}) and are quite appealing for *in vivo* applications where a diverse range of functionalities is present in aqueous media. Hence, "click" chemistry has been used as a high yield tool towards the immobilization, through covalent interactions, of peptides, bioactive drugs, or fluorescent markers onto biopolymers, following simple reaction routes under mild chemical conditions [105–110]. Remarkably, a selection of "click" reactions has been shown to occur efficiently in complex biological media and in the presence of living cells due to their high chemoselectivity. Currently, the fields of application of this type of chemistry are diverse and range from materials engineering and bioconjugation to pharmaceutical sciences and medical imaging and the number is expected to raise in the future [105–110]. One of the most studied reaction that fulfills all the criteria for "click" chemistry is the copper(I)-catalyzed azide-alkyne cycloaddition (CuAAC) to produce a stable 1,2,3-triazole linkage between the two "clicked" building blocks. However, during the years several equally effective metal-free strategies have emerged, such as copperless azide–alkyne cycloadditons and Diels-Alder reactions, just to name a few [110,111]. These "click" chemistry approaches are next revised in more detail.

5.1 Copper-Catalyzed Azide–Alkyne Cycloaddition (CuAAC)

The Huisgen's 1,3-dipolar cycloaddition between azides and alkynes yielding triazoles is gaining interest as an appealing chemoselective approach amongst the "click" reactions family (Figure 2). This reaction is widely used since several molecules can be easily functionalized with both alkyne and azide components which react selectively with each other [112–115].

The catalyst-free azide–alkyne cycloaddition (Figure 2a), pioneered by Huisgen in 1963, required high temperatures and pressures, since azides and alkynes have low reactivity, at atmospheric pressure and room temperature, towards each other and other functional groups present in the biological milieu. Consequently, this reaction is known to be extremely slow and inactive *in vivo*, due to the aqueous mild conditions. Furthermore,

this cycloaddition has low regioselectivity since it gives two different regioisomers, namely the 1,4- and 1,5-triazole, which are extremely difficult to separate. These issues were later overcome by Tornøe and Meldal, who introduced Cu(I) catalysis (Figure 2b) in alkyne-azide coupling reactions, rendering a faster and regioselective reaction; addition of copper as a catalyst favors formation of only the 1,4-regioisomer [105,107,112–114]. The CuAAC reaction, i.e., the copper-catalyzed cycloaddition reaction between alkynes and azides yielding triazoles, occurs effectively under an extensive range of environments and with many Cu(I) sources. Usually, copper(II) salts are used, such as copper sulfate pentahydrate or copper acetate, in combination with metallic copper or sodium ascorbate which act as reducing agents of copper(II) to copper(I) [114,116].

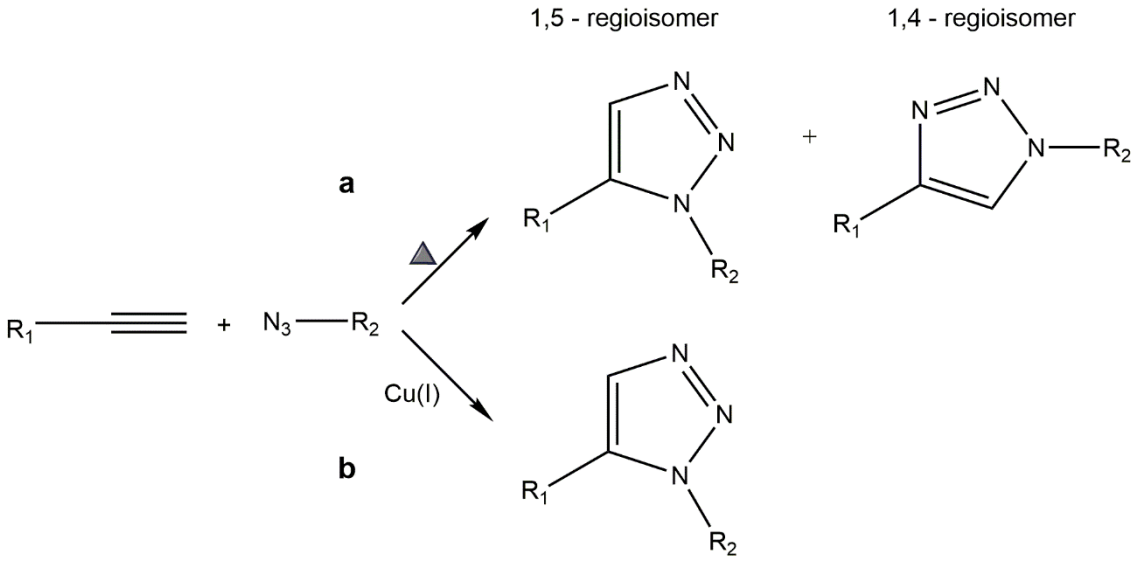

Figure 2 Huisgen's 1,3-dipolar cycloaddition of azides and alkynes to give triazoles: (a) unactivated azide–alkyne cycloaddition yielding a mixture of the 1,4- and 1,5-triazole regioisomers; (b) CuAAC leading to regioselective formation of the 1,4-triazole isomer.

This reaction has attracted much attention for the synthesis and post-polymerization modification of polymers. Both unprotected reactive groups are stable to the synthesis conditions used in the course of solid phase peptide synthesis (SPPS), so they can be easily introduced into the peptide sequences. Several studies confirmed this statement by successfully grafting and immobilizing biomolecules to polymers and synthesizing copolymers [115,117]. The triazole link created between the two building blocks that are coupled is very stable and chemically inert to most reactive conditions. In contrast to amides, and due to their high aromatic stabilization, triazoles are extremely stable to hydrolysis, and are resistant to the activity of both reducing and oxidizing agents,

diverging from other aromatic heterocycles, and to metabolic degradation [113,114]. The dipole moment (around 5D) of these heterocycles favors the formation of hydrogen bonds as well as helps them to participate in π stacking and dipole-dipole interactions [112]. Interestingly, triazoles have been found to display diverse biological activities, including anti-HIV and antibacterial activity [118].

It stems from the above that CuAAC are extremely relevant for tissue engineering applications, given not only the simple experimental conditions but also the chemoselectivity, since both reactive groups only react with each other even in the presence of additional functional groups. Such cycloadditions are effective strategies to develop hydrogels for cell-culture due to its mild aqueous reaction conditions, and also as drug release materials since it is relatively easy to load bioactive drugs and other biomacromolecules within the hydrogel network throughout its formation [119]. In addition, CuAAC can also be used in the crosslinking of PEG hydrogels with peptide sequences susceptible to degradation [91]. A chitosan derivative bearing an alkyne moiety was successfully modified with a PEG-like azide through this "click" reaction, proving the facile chitosan conjugation with drugs and other bioactive molecules, such as peptides [120]. The CuAAC reaction was also used to covalently attach a PEGylated peptide with poly(lactide-co-ethylene oxide fumarate) (PLEOF) hydrogel [121].

Overall, CuAAC is an extremely valuable tool towards peptide tethering onto hydrogels and other biomaterials. Still, use of the copper catalyst can be problematic in some cases and, especially, towards *in vivo* applications, which underlies recent interest in copper-free azide-alkyne click reactions [91].

5.2 Strain-Promoted Azide–Alkyne Cycloaddition (SPAAC)

CuAAC has been used successfully in the *in vitro* modification of biomacromolecules and also in the labeling of bacterial and mammalian cells, however, the negative effects associated with the required copper catalyst is a major limitation for its *in vivo* application. This has promoted not only the optimization of CuAAC bioconjugation strategies suitable for *in vivo* applications, but also the development of azide-alkyne cycloaddition protocols, without the need for copper or other cytotoxic catalysts [122,123].

The Bertozzi group developed a strain-promoted azide-alkyne cycloaddition (SPAAC) reaction (Figure 3a) for the bioorthogonal chemoselective modification of biomolecules and living cells. As proven by Bertozzi and colleagues, cyclooctynes ring strain is

responsible for lowering the aforementioned activation barrier of azide-alkyne cycloadditons, surpassing the need of the copper catalyst. Furthermore, they performed successful cycloaddition reactions between several low molecular weight compounds and novel substituted cyclooctynes (Figure 3b). SPAAC is characterized by its simplicity and great orthogonality which promoted the spread of this approach from biomedical and polymers science to materials engineering [122–124].

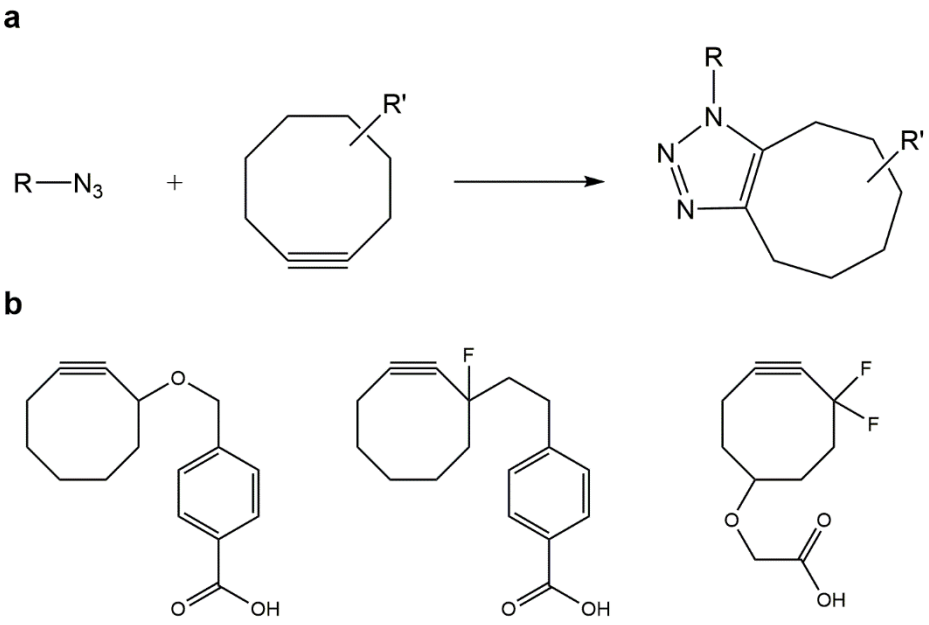

Figure 3 (a) Strain-promoted azide–alkyne cycloaddition (SPAAC); (b) substituted cyclooctynes currently employed to lower the activation barrier of azide–alkyne cycloadditions, thus avoiding use of copper catalysts.

In the past years, the Cu-free reaction between several cyclooctyne derivatives and azides was found to be extremely fast due to the previously mentioned ring strain and also to electron-withdrawing effects from fluorine substituents. However, the synthesis of cyclooctyne is comprised of over ten steps with a low overall yield, which makes this strategy unsuitable for large-scale synthesis [108]. Moreover, insertion of cyclooctyne-based building blocks in peptides is incompatible with current procedures in SPPS, since cyclooctynes are highly reactive, especially with the acidic compounds used in the final cleavage/deprotection steps in SPPS. This may be circumvented by alternative synthesis of azido-peptides to be subsequently reacted with cyclooctyne-modified scaffolds; in this connection, DeForest and Anseth developed a SPAAC "click" reaction between a terminal difluorinated cyclooctyne (DIFO)-PEG hydrogel and a bis(azide) di-functionalized polypeptide [125].

5.3 Thiol-ene "Click" Chemistry

The thiol-ene chemistry occurs between thiols and carbon–carbon double bonds, also known as "enes". This highly reactive reaction involves either a radical mediated addition or an anionic chain process, the so-called thiol Michael addition [126].

Radical mediated thiol-ene chemistry occurs under light irradiation (Figure 4) towards incorporation of any biomolecule containing a thiol group and is efficient, high yielding and highly flexible [108,126–128]. In addition, it allows to obtain a homogeneous network through a step-growth mechanism controllable by standard lithographic processes. The cytocompatible polymerization conditions used make this technique suitable to develop 3D culture platforms. A multi-armed thiolated PEG was modified with alkene- and acrylate-functionalized small molecules via UV-initiated thiol-ene coupling chemistry. This technique was used to form peptide-functionalized PEG hydrogels [127–129]. The incorporation of an enzyme-sensitive linker into a norbornene-functionalized PEG rendered hydrogels with controllable rates of degradation [91] and with both enzymatically degradable peptide and adhesive peptide, CRGDS, originated cell- and enzyme-responsive hydrogels [127,130]. Other example is the introduction of biochemical cues by thiol-ene photoconjugation in a PEG-based hydrogel previously formed by SPAAC, which was proved to be cytocompatible allowing cells to be readily encapsulated and cultured in these gels [131].

A PEG-based hydrogel with tunable mechanical properties was developed by combination of both photoinitiated thiol-ene chemistry, for the surface functionalization of a PEG-hydrogel, and oxime ligation, for the synthesis of the hydrogel [132].

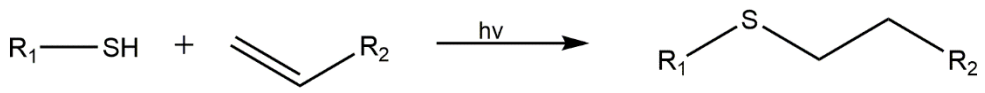

Figure 4 Radical-mediated thiol-ene chemistry: the tiol-ene "click" reaction involves the addition of a thiol to a double bond under light irradiation (hν).

The radical mediated thiol-ene chemistry was also applied to natural hydrogels. Desai and co-workers developed a "click" alginate system using photoinitated thiol-ene based modification of norbornene groups to present thiol-bearing peptides. The carboxyl group of alginate was previously modified with norbornene methanamine by carbodiimide

chemistry [133]. This type of reaction is an attractive approach for hydrogel formation, in spite of this, thiols, in the presence of oxygen tend to form disulfides, as the major product of thiol oxidation; moreover, the presence of cysteine and amine residues can threaten the process of hydrogel formation [91].

Michael addition reactions have been widely used as functionalization tools since they are fast and applicable at low concentrations of reagents. Furthermore, they provide a high selectivity in the presence of common functional groups, ensuring oriented and homogeneous peptide immobilization without affecting materials properties such as stiffness or swelling. Michael additions can selectively link a thiol group from any peptide (e.g., from a cysteine residue) with an electronically deficient double bond of, e.g., maleimide, vinyl sulfone groups or acrylic, in a polymer backbone by creating a stable thioether bond (Figure 5). The nature of the electron-withdrawing group (EWG) on the carbon-carbon double bond influences the overall rate and yield of such reactions. The order of reactivity among types of double bonds in thiol-Michael addition is as follows: maleimide, vinyl sulfone, acrylates/acrylamides, acrylonitrile and methacrylates/methacrylamides [9,134]. Michael additions have been seen as a crosslinking strategy to functionalize polymer matrices with proteins, integrin binding peptides and enzymatically degradable linkers under aqueous-buffered conditions [87,91].

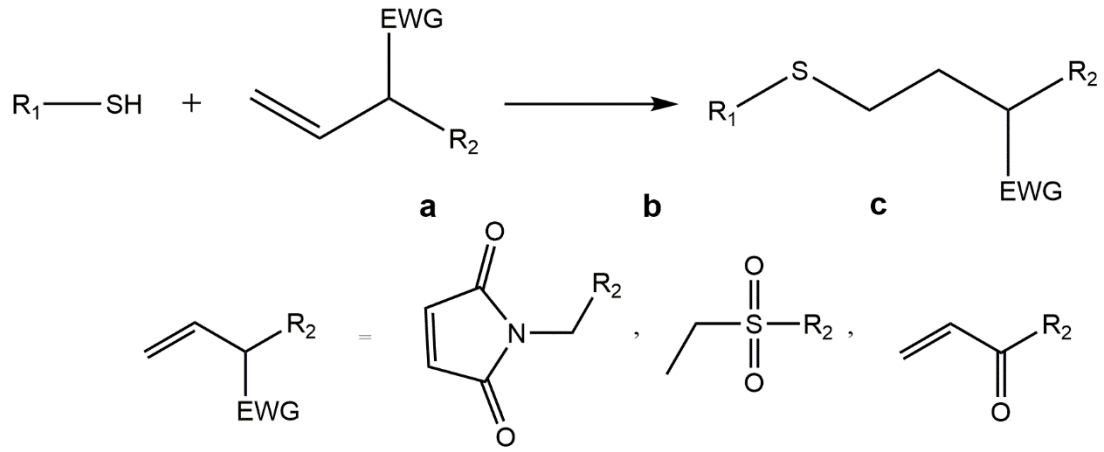

Figure 5 Michael additions can selectively link a thiol group from any peptide (e.g., from a cysteine residue) with an electronically-deficient double bond of, e.g., (a) maleimide; (b) vinyl sulfone or (c) acrylic groups, in a polymer backbone through a stable thioether bond.

Michael addition reactions have been used, for instance, by Tsurkan and colleagues for the functionalization of PEG-heparin hydrogels with various biofunctional peptides

preserving the hydrogel network. The reaction proved to be a highly effective and fast strategy to covalently graft peptides onto the surface of hydrogels in a controllable manner [87]. Hubbel and co-workers used thiol-acrylate Michael addition reactions to form drug-delivery hydrogels using; the materials thus produced showed controllable polymerization reactivity and degradability [126,135,136]. The same type of chemoselective reaction was equally used by Anseth and colleagues to develop cell adhesion scaffolds by incorporating thiol-functionalized peptide sequences within the PEG-based hydrogel network, previously modified with methacrylate groups [137].

Michael additions were also used by Su and co-workers to functionalize a cysteine-terminated PEG-based hydrogel with maleimide-terminated peptides. Interestingly, this study used native chemical ligation (NCL, Figure 6), another type of "click" reaction, to previously crosslink the hydrogel. This chemistry proceeds through transesterification of the *C*-terminal thioester and the N-terminal cysteine to form a new thioester, under mild conditions. This thioester then spontaneously rearranges by an *S* to *N* acyl shift, in aqueous environment, leading to the desired amid bond. Current biological applications have been using NCL for cross-linking hydrogel-based scaffolds. Furthermore, this reaction is exceptionally chemo and regioselective, avoiding unwanted side reactions [31,138,139].

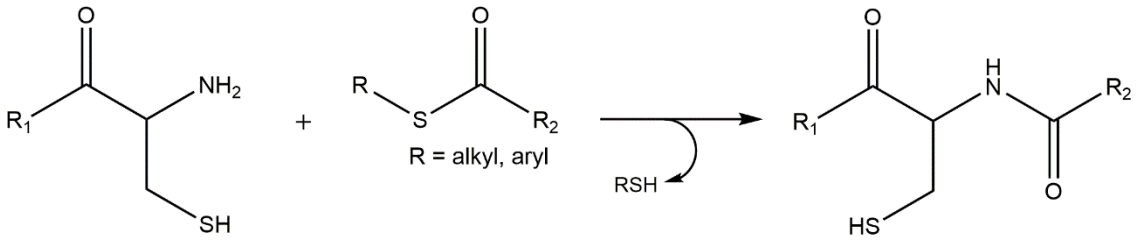

Figure 6 Native chemical ligation (NCL): this reaction proceeds through transesterification of the *C*-terminal thioester and the *N*-terminal cysteine to form a new intermediate thioester, in aqueous solution, under mild conditions. This thioester spontaneously rearranges by an *S* to *N* acyl shift leading to the desired amid bond.

5.4 Diels-Alder Cycloadditions

The Diels–Alder (DA) [4+2] cycloaddition combines a diene and a substituted alkene, commonly referred to as the dienophile. This is a highly selective reaction that gives a substituted cyclohexene without any catalyst or byproduct, and which is greatly accelerated in water due to increased hydrophobic effects. DA cycloadditions are

eventually reversed at high temperature through the retro-DA reaction, which opens a way to controlled drug release [108,140,141].

Amongst DA reactions, the inverse electron demand DA cycloaddition of tetrazine and a dienophile (for example norborene or *trans*-cyclooctene), is known to be a powerful biorthogonal chemistry tool suitable for cell-labelling and occurs. This type of "click" chemistry was also used for covalently cross-link polymer networks, even in the absence of a catalyst or other additives. For example, Alge *et al.* developed a cell-laden hydrogel using a functionalized PEG-based hydrogel with a biologically active ECM-mimetic peptide. Results demonstrated the potential of the tetrazine-norbornene cycloaddition (Figure 7) as an interesting strategy to develop novel hydrogel-scaffolds for cell-culture [142].

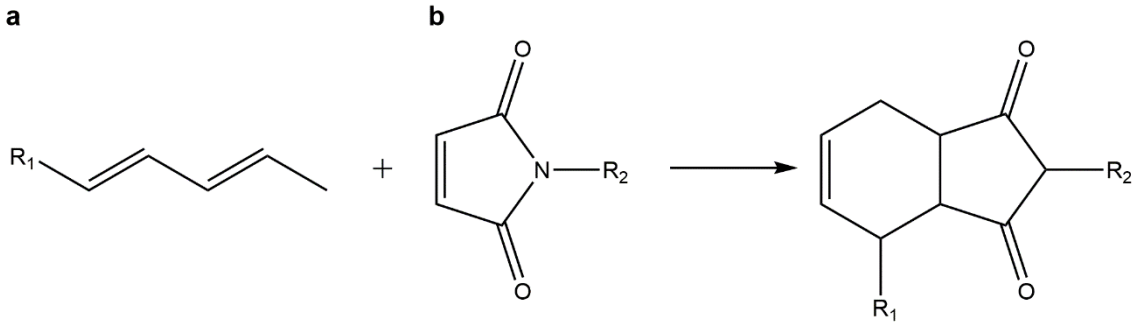

Figure 7 Diels–Alder reaction: in this cycloaddition reaction a (a) diene reacts with a (b) dienophile yielding a substituted cyclohexene without any catalyst or byproduct.

5.5 Oxime "Click" Chemistry

Oxime "click" reactions occur between an aminooxy group and carbonyl groups of aldehydes or ketones, which are stable when compared to thiols (Figure 8). These are ideal reactions for formation of protein-polymer conjugates, since those reactive groups can be easily incorporated into proteins and peptides. In fact, this biorthogonal reaction has already been used in cell surface modification, and to label biological molecules [91]. The oxime bond formation is fast producing only water as a by-product. Interestingly, the reaction kinetics is pH-sensitive, and also depends on catalyst concentration. These features allow to create hydrogels with tunable properties and varying degrees of reversibility [91,132]. In a recent study by Grover and co-workers, a ketone-modified RGD peptide was used to successfully functionalize an aminooxy PEG hydrogel through oxime chemistry [91].

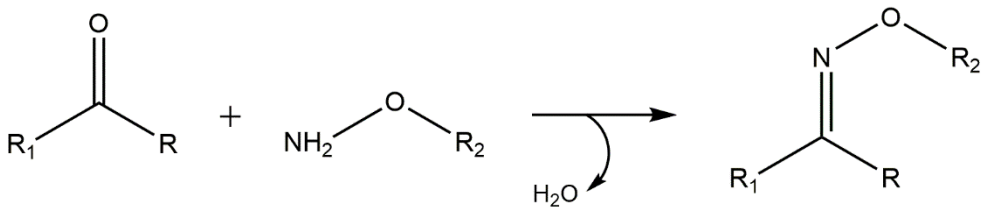

Figure 8 Oxime "click" reaction between an aminooxy group and carbonyl groups.

6. Concluding Remarks

Bioactive peptides are highly specific, effective and safe, thus representing an interesting alternative to other bioactive drugs. Given the relevance of peptides, many methods and strategies have been studied and developed for the chemical synthesis of novel peptides with improved physicochemical properties. Therefore, new classes of peptides, such as cell penetrating peptides and peptide-conjugates, are emerging, broadening the number of possible biomedical applications. The progression of peptide compounds into clinical therapy requires alternatives to their traditional parenteral administration and also the development of peptide-conjugates, namely to polymer scaffolds [11]. In order to create more effective polymeric peptide carriers, studies are now exploring the potential of combining multiple tethering strategies [132,143]. For example, De Forest *et al.* reported the formation of hydrogels merging two "click" chemistry schemes, from PEG-azides and strained alkyne-flanked peptides followed by a second thiol-ene "click" reaction to incorporate biological functionalities within the gel network [125,129,143]. Polizzotti and colleagues developed a PEG functionalized hydrogel using multiple "click" chemistries, CuAAC for gelation and thiol-ene photocoupling for complex patterning [144]. Consequently, "click" chemistry is showing great promise towards the development of polymer-drug/peptide conjugates of biomedical interest.

Acknowledgments

Thanks are due to Fundação para a Ciência e Tecnologia (FCT), Portugal, for funding through project UID/Multi/04378/2013.

Author Contributions

Mariana Barbosa (Mariana Moreira da Silva Alves Barbosa) compiled, analyzed and selected literature resources to be cited within scope of this review, and wrote the manuscript; M. Cristina L. Martins (Maria Cristina Teixeira Lopes da Costa Pinto Lopes Martins) contributed with scientific reasoning, and revision of all versions of the manuscript; Paula Gomes (Paula Alexandra de Carvalho Gomes) planned the manuscript's scope and organization, and revised all of its versions.

Conflicts of Interests

The authors declare no conflict of interest.

References

1. Zhang, L.; Li, K.; Xiao, W.; Zheng, L.; Xiao, Y.; Fan, H.; Zhang, X. Preparation of collagen–chondroitin sulfate–hyaluronic acid hybrid hydrogel scaffolds and cell compatibility *in vitro*. Carbohydr. Polym. 2011, 84, 118–125.

2. Orsi, S.; de Capua, A.; Guarnieri, D.; Marasco, D.; Netti, P.A. Cell recruitment and transfection in gene activated collagen matrix. Biomaterials 2010, 31, 570–576.

3. Tibbitt, M.W.; Anseth, K.S. Hydrogels as extracellular matrix mimics for 3D cell culture. Biotechnol. Bioeng. 2009, 103, 655–663.

4. Cameron, N.; Deming, T. Peptide-based materials for nanomedicine. Macromol. Biosci. 2015, 15, 7–8.

5. Jing, J.; Fournier, A.; Szarpak-Jankowska, A.; Block, M.R.; Auzély-Velty, R. Type, density, and presentation of grafted adhesion peptides on polysaccharide-based hydrogels control preosteoblast behavior and differentiation. Biomacromolecules 2015, 16, 715–722.

6. Guarnieri, D.; de Capua, A.; Ventre, M.; Borzacchiello, A.; Pedone, C.; Marasco, D.; Ruvo, M.; Netti, P.A. Covalently immobilized RGD gradient on PEG hydrogel scaffold influences cell migration parameters. Acta Biomater. 2010, 6, 2532–2539.

7. Ito, Y. Covalently immobilized biosignal molecule materials for tissue engineering. Soft Matter 2008, 4, 46–56.

8. Albericio, F.; Kruger, H.G. Therapeutic peptides. Future Med. Chem. 2012, 4, 1527–1531.

9. Tang, W.; Becker, M.L. "Click" reactions: A versatile toolbox for the synthesis of peptide-conjugates. Chem. Soc. Rev. 2014, 43, 7013–7039.

10. Montalbetti, C.A.G.N.; Falque, V. Amide bond formation and peptide coupling. Tetrahedron 2005, 61, 10827–10852.

11. Fosgerau, K.; Hoffmann, T. Peptide therapeutics: Current status and future directions. Drug Discov. Today 2015, 20, 122–128.

12. Góngora-Benítez, M.; Tulla-Puche, J.; Albericio, F. Handles for Fmoc solid-phase synthesis of protected peptides. ACS Comb. Sci. 2013, 15, 217–228.

13. Loffet, A. Peptides as drugs: Is there a market? J. Pept. Sci. 2002, 8, 1–7.

14. Edwards, C.M.B.; Cohen, M.A.; Bloom, S.R. Peptides as drugs. QJM 1999, 92, 1–4.

15. Pires, D.; Bemquerer, M.; Nascimento, C. Some mechanistic aspects on Fmoc solid phase peptide synthesis. Int. J. Pept. Res. Ther. 2014, 20, 53–69.

16. Chow, D.; Nunalee, M.L.; Lim, D.W.; Simnick, A.J.; Chilkoti, A. Peptide-based biopolymers in biomedicine and biotechnology. Mater. Sci. Eng. R Rep. 2008, 62, 125–155.

17. Lu, Y.; Yang, J.; Sega, E. Issues related to targeted delivery of proteins and peptides. AAPS J. 2006, 8, E466–E478.

18. McGregor, D.P. Discovering and improving novel peptide therapeutics. Curr. Opin. Pharmacol. 2008, 8, 616–619.

19. Sato, A.K.; Viswanathan, M.; Kent, R.B.; Wood, C.R. Therapeutic peptides: Technological advances driving peptides into development. Curr. Opin. Biotechnol. 2006, 17, 638–642.

20. Chandrudu, S.; Simerska, P.; Toth, I. Chemical methods for peptide and protein production. Molecules 2013, 18, 4373–4388.

21. Craik, D.J.; Fairlie, D.P.; Liras, S.; Price, D. The future of peptide-based drugs. Chem. Biol. Drug Des. 2013, 81, 136–147.

22. Vlieghe, P.; Lisowski, V.; Martinez, J.; Khrestchatisky, M. Synthetic therapeutic peptides: Science and market. Drug Discov. Today 2010, 15, 40–56.

23. Coin, I.; Beyermann, M.; Bienert, M. Solid-phase peptide synthesis: From standard procedures to the synthesis of difficult sequences. Nat. Protoc. 2007, 2, 3247–3256.

24. Kaspar, A.A.; Reichert, J.M. Future directions for peptide therapeutics development. Drug Discov. Today 2013, 18, 807–817.

25. Collier, J.H.; Segura, T. Evolving the use of peptides as components of biomaterials. Biomaterials 2011, 32, 4198–4204.

26. Du, A.W.; Stenzel, M.H. Drug carriers for the delivery of therapeutic peptides. Biomacromolecules 2014, 15, 1097–1114.

27. Kogan, M.J.; Olmedo, I.; Hosta, L.; Guerrero, A.R.; Cruz, L.J.; Albericio, F. Peptides and metallic nanoparticles for biomedical applications. Nanomedicine 2007, 2, 287–306.

28. Lin, C.-C.; Anseth, K. PEG hydrogels for the controlled release of biomolecules in regenerative medicine. Pharm. Res. 2009, 26, 631–643.

29. Stephanopoulos, N.; Ortony, J.H.; Stupp, S.I. Self-assembly for the synthesis of functional biomaterials. Acta Mater. 2013, 61, 912–930.

30. Matson, J.B.; Zha, R.H.; Stupp, S.I. Peptide self-assembly for crafting functional biological materials. Curr. Opin. Solid State Mater. Sci. 2011, 15, 225–235.

31. Khan, S.; Sur, S.; Dankers, P.Y.W.; da Silva, R.M.P.; Boekhoven, J.; Poor, T.A.; Stupp, S.I. Post-assembly functionalization of supramolecular nanostructures with bioactive peptides and fluorescent proteins by native chemical ligation. Bioconjugate Chem. 2014, 25, 707–717.

32. Webber, M.J.; Tongers, J.; Renault, M.-A.; Roncalli, J.G.; Losordo, D.W.; Stupp, S.I. Reprint of: Development of bioactive peptide amphiphiles for therapeutic cell delivery. Acta Biomater. 2015, 23, S42–S51.

33. Tao, H.; Zhang, Y.; Wang, C.-F.; Zhang, C.; Wang, X.-M.; Wang, D.-L.; Bai, X.-D.; Wen, T.-Y.; Xin, H.-K.; Wu, J.-H.; *et al.* Biological evaluation of human degenerated nucleus pulposus cells in functionalized self-assembling peptide nanofiber hydrogel scaffold. Tissue Eng. A 2014, 20, 1621–1631.

34. Branco, M.C.; Schneider, J.P. Self-assembling materials for therapeutic delivery. Acta Biomater. 2009, 5, 817–831.

35. Kopeček, J.; Yang, J. Peptide-directed self-assembly of hydrogels. Acta Biomater. 2009, 5, 805–816.

36. Antosova, Z.; Mackova, M.; Kral, V.; Macek, T. Therapeutic application of peptides and proteins: Parenteral forever? Trends Biotechnol. 2009, 27, 628–635.

37. Censi, R.; di Martino, P.; Vermonden, T.; Hennink, W.E. Hydrogels for protein delivery in tissue engineering. J. Control. Release 2012, 161, 680–692.

38. Casault, S.; Kenward, M.; Slater, G.W. Combinatorial design of passive drug delivery platforms. Int. J. Pharm. 2007, 339, 91–102.

39. Vandermeulen, G.W.M.; Klok, H.-A. Peptide/protein hybrid materials: Enhanced control of structure and improved performance through conjugation of biological and synthetic polymers. Macromol. Biosci. 2004, 4, 383–398.

40. Furth, M.E.; Atala, A.; van Dyke, M.E. Smart biomaterials design for tissue engineering and regenerative medicine. Biomaterials 2007, 28, 5068–5073.

41. Lee, K.Y.; Yuk, S.H. Polymeric protein delivery systems. Prog. Polym. Sci. 2007, 32, 669–697. 42. Tessmar, J.K.; Göpferich, A.M. Matrices and scaffolds for protein delivery in tissue engineering. Adv. Drug Deliv. Rev. 2007, 59, 274–291.

43. Lalatsa, A.; Schätzlein, A.G.; Mazza, M.; Le, T.B.H.; Uchegbu, I.F. Amphiphilic poly(L-amino acids)—New materials for drug delivery. J. Control. Release 2012, 161, 523–536.

44. Park, J.H.; Saravanakumar, G.; Kim, K.; Kwon, I.C. Targeted delivery of low molecular drugs using chitosan and its derivatives. Adv. Drug Deliv. Rev. 2010, 62, 28–41.

45. Sokolsky-Papkov, M.; Agashi, K.; Olaye, A.; Shakesheff, K.; Domb, A.J. Polymer carriers for drug delivery in tissue engineering. Adv. Drug Deliv. Rev. 2007, 59, 187–206.

46. Almany, L.; Seliktar, D. Biosynthetic hydrogel scaffolds made from fibrinogen and polyethylene glycol for 3D cell cultures. Biomaterials 2005, 26, 2467–2477.

47. Strehin, I.; Nahas, Z.; Arora, K.; Nguyen, T.; Elisseeff, J. A versatile pH sensitive chondroitin sulfate-PEG tissue adhesive and hydrogel. Biomaterials 2010, 31, 2788–2797.

48. Lee, K.Y.; Mooney, D.J. Hydrogels for tissue engineering. Chem. Rev. 2001, 101, 1869–1880.

49. Zhu, J.; Marchant, R.E. Design properties of hydrogel tissue-engineering scaffolds. Expert Rev. Med. Devices 2011, 8, 607–626.

50. Kopeček, J. Hydrogel biomaterials: A smart future? Biomaterials 2007, 28, 5185–5192.

51. Hamidi, M.; Azadi, A.; Rafiei, P. Hydrogel nanoparticles in drug delivery. Adv. Drug Deliv. Rev. 2008, 60, 1638–1649.

52. Slaughter, B.V.; Khurshid, S.S.; Fisher, O.Z.; Khademhosseini, A.; Peppas, N.A. Hydrogels in regenerative medicine. Adv. Mater. 2009, 21, 3307–3329.

53. Hoare, T.R.; Kohane, D.S. Hydrogels in drug delivery: Progress and challenges. Polymer 2008, 49, 1993–2007.

54. Deligkaris, K.; Tadele, T.S.; Olthuis, W.; van den Berg, A. Hydrogel-based devices for biomedical applications. Sens. Actuators B Chem. 2010, 147, 765–774.

55. Hu, X.; Li, D.; Zhou, F.; Gao, C. Biological hydrogel synthesized from hyaluronic acid, gelatin and chondroitin sulfate by click chemistry. Acta Biomater. 2011, 7, 1618–1626.

56. Bidarra, S.J.; Barrias, C.C.; Fonseca, K.B.; Barbosa, M.A.; Soares, R.A.; Granja, P.L. Injectable in situ crosslinkable RGD-modified alginate matrix for endothelial cells delivery. Biomaterials 2011, 32, 7897–7904.

57. Augst, A.D.; Kong, H.J.; Mooney, D.J. Alginate hydrogels as biomaterials. Macromol. Biosci. 2006, 6, 623–633.

58. Bae, K.H.; Wang, L.-S.; Kurisawa, M. Injectable biodegradable hydrogels: Progress and challenges. J. Mater. Chem. B 2013, 1, 5371–5388.

59. Buwalda, S.J.; Boere, K.W.M.; Dijkstra, P.J.; Feijen, J.; Vermonden, T.; Hennink, W.E. Hydrogels in a historical perspective: From simple networks to smart materials. J. Control. Release 2014, 190, 254–273.

60. Samchenko, Y.; Ulberg, Z.; Korotych, O. Multipurpose smart hydrogel systems. Adv. Colloid Interface Sci. 2011, 168, 247–262.

61. Hennink, W.E.; van Nostrum, C.F. Novel crosslinking methods to design hydrogels. Adv. Drug Deliv. Rev. 2012, 64, S223–S236.

62. Bhattarai, N.; Gunn, J.; Zhang, M. Chitosan-based hydrogels for controlled, localized drug delivery. Adv. Drug Deliv. Rev. 2010, 62, 83–99.

63. Zhu, J. Bioactive modification of poly(ethylene glycol) hydrogels for tissue engineering. Biomaterials 2010, 31, 4639–4656.

64. Hoffman, A.S. Hydrogels for biomedical applications. Adv. Drug Deliv. Rev. 2012, 64, S18–S23. 65. Branco, M.C.; Pochan, D.J.; Wagner, N.J.; Schneider, J.P. The effect of protein structure on their controlled release from an injectable peptide hydrogel. Biomaterials 2010, 31, 9527–9534.

66. Ko, D.Y.; Shinde, U.P.; Yeon, B.; Jeong, B. Recent progress of in situ formed gels for biomedical applications. Prog. Polym. Sci. 2013, 38, 672–701.

67. Drury, J.L.; Mooney, D.J. Hydrogels for tissue engineering: Scaffold design variables and applications. Biomaterials 2003, 24, 4337–4351.

68. Appelman, T.P.; Mizrahi, J.; Elisseeff, J.H.; Seliktar, D. The influence of biological motifs and dynamic mechanical stimulation in hydrogel scaffold systems on the phenotype of chondrocytes. Biomaterials 2011, 32, 1508–1516.

69. Lee, K.Y.; Mooney, D.J. Alginate: Properties and biomedical applications. Prog. Polym. Sci. 2012, 37, 106–126.

70. Boontheekul, T.; Kong, H.-J.; Mooney, D.J. Controlling alginate gel degradation utilizing partial oxidation and bimodal molecular weight distribution. Biomaterials 2005, 26, 2455–2465.

71. Jeon, O.; Powell, C.; Ahmed, S.M.; Alsberg, E. Biodegradable, photocrosslinked alginate hydrogels with independently tailorable physical properties and cell adhesivity. Tissue Eng. A 2010, 16, 2915–2925.

72. Kim, S.; Kim, J.-H.; Jeon, O.; Kwon, I.C.; Park, K. Engineered polymers for advanced drug delivery. Eur. J. Pharm. Biopharm. 2009, 71, 420–430.

73. Lee, K.; Silva, E.A.; Mooney, D.J. Growth factor delivery-based tissue engineering: General approaches and a review of recent developments. J. R. Soc. Interface 2011, 8, 153–170.

74. Qiu, Y.; Park, K. Environment-sensitive hydrogels for drug delivery. Adv. Drug Deliv. Rev. 2012, 64, S49–S60.

75. Jeong, B.; Bae, Y.H.; Kim, S.W. Drug release from biodegradable injectable thermosensitive hydrogel of PEG–PLGA–PEG triblock copolymers. J. Control. Release 2000, 63, 155–163.

76. Cha, M.-H.; Choi, J.; Choi, B.G.; Park, K.; Kim, I.H.; Jeong, B.; Han, D.K. Synthesis and characterization of novel thermo-responsive f68 block copolymers with cell-adhesive RGD peptide. J. Colloid Interface Sci. 2011, 360, 78–85.

77. Jeong, Y.; Joo, M.K.; Bahk, K.H.; Choi, Y.Y.; Kim, H.-T.; Kim, W.-K.; Jeong Lee, H.; Sohn, Y.S.; Jeong, B. Enzymatically degradable temperature-sensitive polypeptide as a new in situ gelling biomaterial. J. Control. Release 2009, 137, 25–30.

78. Choi, B.G.; Park, M.H.; Cho, S.-H.; Joo, M.K.; Oh, H.J.; Kim, E.H.; Park, K.; Han, D.K.; Jeong, B. In situ thermal gelling polypeptide for chondrocytes 3D culture. Biomaterials 2010, 31, 9266–9272.

79. Lee, J.; Joo, M.K.; Oh, H.; Sohn, Y.S.; Jeong, B. Injectable gel: Poly(ethylene glycol)-sebacic acid polyester. Polymer 2006, 47, 3760–3766.

80. Jeong, B.; Kim, S.W.; Bae, Y.H. Thermosensitive sol-gel reversible hydrogels. Adv. Drug Deliv. Rev. 2012, 64, 154–162.

81. Huang, J.; Heise, A. Stimuli responsive synthetic polypeptides derived from N-carboxyanhydride (NCA) polymerisation. Chem. Soc. Rev. 2013, 42, 7373–7390.

82. DuBose, J.W.; Cutshall, C.; Metters, A.T. Controlled release of tethered molecules via engineered hydrogel degradation: Model development and validation. J. Biomed. Mater. Res. Part A 2005, 74A, 104–116.

83. Lutolf, M.P.; Hubbell, J.A. Synthetic biomaterials as instructive extracellular microenvironments for morphogenesis in tissue engineering. Nat. Biotechnol. 2005, 23, 47–55.

84. Fonseca, K.B.; Granja, P.L.; Barrias, C.C. Engineering proteolytically-degradable artificial extracellular matrices. Prog. Polym. Sci. 2014, 39, 2010–2029.

85. Weber, L.M.; Hayda, K.N.; Haskins, K.; Anseth, K.S. The effects of cell-matrix interactions on encapsulated β-cell function within hydrogels functionalized with matrix-derived adhesive peptides. Biomaterials 2007, 28, 3004–3011.

86. DeLong, S.A.; Gobin, A.S.; West, J.L. Covalent immobilization of RGDs on hydrogel surfaces to direct cell alignment and migration. J. Control. Release 2005, 109, 139–148.

87. Tsurkan, M.V.; Chwalek, K.; Schoder, M.; Freudenberg, U.; Werner, C. Chemoselective peptide functionalization of starPEG-GAG hydrogels. Bioconjugate Chem. 2014, 25, 1942–1950.

88. Yeo, Y.; Geng, W.; Ito, T.; Kohane, D.S.; Burdick, J.A.; Radisic, M. Photocrosslinkable hydrogel for myocyte cell culture and injection. J. Biomed. Mater. Res. Part B Appl. Biomater. 2007, 81, 312–322.

89. DeLong, S.A.; Moon, J.J.; West, J.L. Covalently immobilized gradients of BFGF on hydrogel scaffolds for directed cell migration. Biomaterials 2005, 26, 3227–3234.

90. Bryant, S.; Nicodemus, G.; Villanueva, I. Designing 3D photopolymer hydrogels to regulate biomechanical cues and tissue growth for cartilage tissue engineering. Pharm. Res. 2008, 25, 2379–2386.

91. Grover, G.N.; Lam, J.; Nguyen, T.H.; Segura, T.; Maynard, H.D. Biocompatible hydrogels by oxime click chemistry. Biomacromolecules 2012, 13, 3013–3017.

92. Maia, F.R.; Barbosa, M.; Gomes, D.B.; Vale, N.; Gomes, P.; Granja, P.L.; Barrias, C.C. Hydrogel depots for local co-delivery of osteoinductive peptides and mesenchymal stem cells. J. Control. Release 2014, 189, 158–168.

93. Romano, N.H.; Sengupta, D.; Chung, C.; Heilshorn, S.C. Protein-engineered biomaterials: Nanoscale mimics of the extracellular matrix. Biochim. Biophys. Acta Gen. Subj. 2011, 1810, 339–349.

94. Yang, J.-A.; Yeom, J.; Hwang, B.W.; Hoffman, A.S.; Hahn, S.K. In situ-forming injectable hydrogels for regenerative medicine. Prog. Polym. Sci. 2014, 39, 1973–1986.

95. Nicodemus, G.D.; Bryant, S.J. Cell encapsulation in biodegradable hydrogels for tissue engineering applications. Tissue Eng. Part B Rev. 2008, 14, 149–165.

96. Rowley, J.A.; Madlambayan, G.; Mooney, D.J. Alginate hydrogels as synthetic extracellular matrix materials. Biomaterials 1999, 20, 45–53.

97. Bartczak, D.; Kanaras, A.G. Preparation of peptide-functionalized gold nanoparticles using one pot EDC/sulfo-NHS coupling. Langmuir 2011, 27, 10119–10123.

98. Sinz, A. Chemical cross-linking and mass spectrometry for mapping three-dimensional structures of proteins and protein complexes. J. Mass Spectrom. 2003, 38, 1225–1237.

99. Connelly, J.T.; García, A.J.; Levenston, M.E. Inhibition of *in vitro* chondrogenesis in RGD-modified three-dimensional alginate gels. Biomaterials 2007, 28, 1071–1083.

100. Freudenberg, U.; Hermann, A.; Welzel, P.B.; Stirl, K.; Schwarz, S.C.; Grimmer, M.; Zieris, A.; Panyanuwat, W.; Zschoche, S.; Meinhold, D.; *et al.* A star-PEG-heparin hydrogel platform to aid cell replacement therapies for neurodegenerative diseases. Biomaterials 2009, 30, 5049–5060. 101. Tsurkan, M.V.; Chwalek, K.; Levental, K.R.; Freudenberg, U.; Werner, C. Modular starPEG-heparin gels with bifunctional peptide linkers. Macromol. Rapid Commun. 2010, 31, 1529–1533.

102. Cui, F.Z.; Tian, W.M.; Hou, S.P.; Xu, Q.Y.; Lee, I.S. Hyaluronic acid hydrogel immobilized with RGD peptides for brain tissue engineering. J. Mater. Sci. Mater. Med. 2006, 17, 1393–1401.

103. Iha, R.K.; Wooley, K.L.; Nyström, A.M.; Burke, D.J.; Kade, M.J.; Hawker, C.J. Applications of orthogonal "click" chemistries in the synthesis of functional soft materials. Chem. Rev. 2009, 109, 5620–5686.

104. Kolb, H.C.; Finn, M.G.; Sharpless, K.B. Click chemistry: Diverse chemical function from a few good reactions. Angew. Chem. Int. Ed. 2001, 40, 2004–2021.

105. Nwe, K.; Brechbiel, M.W. Growing applications of "click chemistry" for bioconjugation in contemporary biomedical research. Cancer Biother. Radiopharm. 2009, 24, 289–302.

106. Zeng, D.; Zeglis, B.M.; Lewis, J.S.; Anderson, C.J. The growing impact of bioorthogonal click chemistry on the development of radiopharmaceuticals. J. Nucl. Med. 2013, 54, 829–832.

107. Amblard, F.; Cho, J.H.; Schinazi, R.F. Cu(I)-catalyzed huisgen azide–alkyne 1, 3-dipolar cycloaddition reaction in nucleoside, nucleotide, and oligonucleotide chemistry. Chem. Rev. 2009, 109, 4207–4220.

108. Jiang, Y.; Chen, J.; Deng, C.; Suuronen, E.J.; Zhong, Z. Click hydrogels, microgels and nanogels: Emerging platforms for drug delivery and tissue engineering. Biomaterials 2014, 35, 4969–4985.

109. Truong, V.X.; Ablett, M.P.; Gilbert, H.T.J.; Bowen, J.; Richardson, S.M.; Hoyland, J.A.; Dove, A.P. In situ-forming robust chitosan-poly(ethylene glycol) hydrogels prepared by copper-free

azide–alkyne click reaction for tissue engineering. Biomater. Sci. 2014, 2, 167–175.

110. Such, G.K.; Johnston, A.P.R.; Liang, K.; Caruso, F. Synthesis and functionalization of nanoengineered materials using click chemistry. Prog. Polym. Sci. 2012, 37, 985–1003.

111. Becer, C.R.; Hoogenboom, R.; Schubert, U.S. Click chemistry beyond metal-catalyzed cycloaddition. Angew. Chem. Int. Ed. 2009, 48, 4900–4908.

112. Meldal, M.; Tornøe, C.W. Cu-catalyzed azide–alkyne cycloaddition. Chem. Rev. 2008, 108, 2952–3015.

113. Kolb, H.C.; Sharpless, K.B. The growing impact of click chemistry on drug discovery. Drug Discov. Today 2003, 8, 1128–1137.

114. Tron, G.C.; Pirali, T.; Billington, R.A.; Canonico, P.L.; Sorba, G.; Genazzani, A.A. Click chemistry reactions in medicinal chemistry: Applications of the 1,3-dipolar cycloaddition between azides and alkynes. Med. Res. Rev. 2008, 28, 278–308.

115. Jagasia, R.; Holub, J.M.; Bollinger, M.; Kirshenbaum, K.; Finn, M.G. Peptide cyclization and cyclodimerization by CuI-mediated azide–alkyne cycloaddition. J. Org. Chem. 2009, 74, 2964–2974.

116. Castro, V.; Rodriguez, H.; Albericio, F. Wang linker free of side reactions. Org. Lett. 2012, 15, 246–249.

117. Zampano, G.; Bertoldo, M.; Ciardelli, F. Defined chitosan-based networks by C-6-azide–alkyne “click” reaction. React. Funct. Polym. 2010, 70, 272–281.

118. Tornøe, C.W.; Christensen, C.; Meldal, M. Peptidotriazoles on solid phase:[1,2,3]-triazoles by regiospecific copper(I)-catalyzed 1,3-dipolar cycloadditions of terminal alkynes to azides. J. Org. Chem. 2002, 67, 3057–3064.

119. Crescenzi, V.; Cornelio, L.; di Meo, C.; Nardecchia, S.; Lamanna, R. Novel hydrogels via click chemistry: Synthesis and potential biomedical applications. Biomacromolecules 2007, 8, 1844–1850.

120. Oliveira, J.R.; Martins, M.C.L.; Mafra, L.; Gomes, P. Synthesis of an O-alkynyl-chitosan and its chemoselective conjugation with a PEG-like amino-azide through click chemistry. Carbohydr. Polym. 2012, 87, 240–249.

121. He, X.; Ma, J.; Jabbari, E. Effect of grafting RGD and BMP-2 protein-derived peptides to a hydrogel substrate on osteogenic differentiation of marrow stromal cells. Langmuir 2008, 24, 12508–12516.

122. Lallana, E.; Riguera, R.; Fernandez-Megia, E. Reliable and efficient procedures for the conjugation of biomolecules through huisgen azide–alkyne cycloadditions. Angew. Chem. Int. Ed. 2011, 50, 8794–8804.

123. Sachin, K.; Jadhav, V.H.; Kim, E.-M.; Kim, H.L.; Lee, S.B.; Jeong, H.-J.; Lim, S.T.; Sohn, M.-H.; Kim, D.W. F-18 labeling protocol of peptides based on chemically orthogonal strain-promoted cycloaddition under physiologically friendly reaction conditions. Bioconjugate Chem. 2012, 23, 1680–1686.

124. Lutz, J.-F. Copper-free azide–alkyne cycloadditions: New insights and perspectives. Angew. Chem. Int. Ed. 2008, 47, 2182–2184.

125. DeForest, C.A.; Anseth, K.S. Cytocompatible click-based hydrogels with dynamically tunable properties through orthogonal photoconjugation and photocleavage reactions. Nat. Chem. 2011, 3, 925–931.

126. Hoyle, C.E.; Bowman, C.N. Thiol-ene click chemistry. Angew. Chem. Int. Ed. 2010, 49, 1540–1573.

127. Singh, S.P.; Schwartz, M.P.; Lee, J.Y.; Fairbanks, B.D.; Anseth, K.S. A peptide functionalized poly(ethylene glycol) (PEG) hydrogel for investigating the influence of biochemical and biophysical matrix properties on tumor cell migration. Biomater. Sci. 2014, 2, 1024–1034.

128. Lowe, A.B. Thiol-ene “click” reactions and recent applications in polymer and materials synthesis. Polym. Chem. 2010, 1, 17–36.

129. DeForest, C.A.; Sims, E.A.; Anseth, K.S. Peptide-functionalized click hydrogels with independently tunable mechanics and chemical functionality for 3D cell culture. Chem. Mater. 2010, 22, 4783–4790.

130. Fairbanks, B.D.; Schwartz, M.P.; Halevi, A.E.; Nuttelman, C.R.; Bowman, C.N.; Anseth, K.S. A versatile synthetic extracellular matrix mimic via thiol-norbornene photopolymerization. Adv. Mater. (Deerfield Beach, FL) 2009, 21, 5005–5010.

131. DeForest, C.A.; Anseth, K.S. Photoreversible patterning of biomolecules within click-based hydrogels. Angew. Chem. Int. Ed. 2012, 51, 1816–1819.

132. Lin, F.; Yu, J.; Tang, W.; Zheng, J.; Defante, A.; Guo, K.; Wesdemiotis, C.; Becker, M.L. Peptide-functionalized oxime hydrogels with tunable mechanical properties and gelation behavior. Biomacromolecules 2013, 14, 3749–3758.

133. Desai, R.M.; Koshy, S.T.; Hilderbrand, S.A.; Mooney, D.J.; Joshi, N.S. Versatile click alginate hydrogels crosslinked via tetrazine–norbornene chemistry. Biomaterials 2015, 50, 30–37.

134. El-Sagheer, A.H.; Brown, T. Click chemistry with DNA. Chem. Soc. Rev. 2010, 39, 1388–1405.

135. Lutolf, M.P.; Tirelli, N.; Cerritelli, S.; Cavalli, L.; Hubbell, J.A. Systematic modulation of michael-type reactivity of thiols through the use of charged amino acids. Bioconjugate Chem. 2001, 12, 1051–1056.

136. Lutolf, M.P.; Hubbell, J.A. Synthesis and physicochemical characterization of end-linked poly(ethylene glycol)-co-peptide hydrogels formed by michael-type addition. Biomacromolecules 2003, 4, 713–722.

137. Salinas, C.N.; Cole, B.B.; Kasko, A.M.; Anseth, K.S. Chondrogenic differentiation potential of human mesenchymal stem cells photoencapsulated within poly(ethylene glycol)-arginine-glycine-aspartic acid-serine thiol-methacrylate mixed-mode networks. Tissue Eng. 2007, 13, 1025–1034.

138. Jung, J.P.; Sprangers, A.J.; Byce, J.R.; Su, J.; Squirrell, J.M.; Messersmith, P.B.; Eliceiri, K.W.; Ogle, B.M. ECM-incorporated hydrogels cross-linked via native chemical ligation to engineer stem cell microenvironments. Biomacromolecules 2013, 14, 3102–3111.

139. Hu, B.-H.; Su, J.; Messersmith, P.B. Hydrogels cross-linked by native chemical ligation. Biomacromolecules 2009, 10, 2194–2200.

140. Nimmo, C.M.; Owen, S.C.; Shoichet, M.S. Diels–Alder click cross-linked hyaluronic acid hydrogels for tissue engineering. Biomacromolecules 2011, 12, 824–830.

141. Montiel-Herrera, M.; Gandini, A.; Goycoolea, F.; Jacobsen, N.; Lizardi-Mendoza, J.; Recillas-Mota, M.; Argüelles-Monal, W. Furan–chitosan hydrogels based on click chemistry. Iran. Polym. J. 2015, 24, 349–357.

142. Alge, D.L.; Azagarsamy, M.A.; Donohue, D.F.; Anseth, K.S. Synthetically tractable click hydrogels for three-dimensional cell culture formed using tetrazine–norbornene chemistry. Biomacromolecules 2013, 14, 949–953.

143. DeForest, C.A.; Polizzotti, B.D.; Anseth, K.S. Sequential click reactions for synthesizing and patterning three-dimensional cell microenvironments. Nat. Mater. 2009, 8, 659–664.

144. Polizzotti, B.D.; Fairbanks, B.D.; Anseth, K.S. Three-dimensional biochemical patterning of click-based composite hydrogels via thiolene photopolymerization. Biomacromolecules 2008, 9, 1084–1087.

Chapter IV

Tethering antimicrobial peptides onto chitosan: Optimization of azide-alkyne "click" reaction conditions

Mariana Barbosa[1,2,3,4], Nuno Vale[1], Fabíola M.T.A. Costa[2,3], M. Cristina L. Martins[2,3,5], Paula Gomes[1]

Carbohydrate Polymers **2017**, 165, 384-393

[1]UCIBIO-REQUIMTE, Departamento de Química e Bioquímica, Faculdade de Ciências, Universidade do Porto, Porto, Portugal
[2]i3S, Instituto de Investigação e Inovação em Saúde, Universidade do Porto, Porto, Portugal
[3]INEB – Instituto de Engenharia Biomédica, Universidade do Porto, Porto, Portugal
[4]Faculdade de Engenharia, Universidade do Porto, Porto, Portugal
[5]Instituto de Ciências Biomédicas Abel Salazar, Universidade do Porto, Porto, Portugal

Abstract

Antimicrobial peptides (AMP) are promising alternatives to classical antibiotics, due to their high specificity and potency at low concentrations, and low propensity to elicit pathogen resistance. Immobilization of AMP onto biomaterials is an emergent field of research, towards creation of novel antimicrobial materials able to avoid formation of biofilms on the surfaces of medical devices. Herein, we report the chemical route towards one such material, where chitosan was used as biocompatible carrier for the covalent grafting of Dhvar-5, a well-known potent AMP, via the chemoselective ("click") Cu(I)-catalyzed azide-alkyne cycloaddition (CuAAC). The material's structure, as well as peptide loading, were confirmed by Fourier-transformed infra-red (FT-IR) and X-ray photoelectron (XPS) spectroscopies, and by Amino Acid Analysis (AAA), respectively. Results herein reported demonstrate that, with proper optimization, the "click" CuAAC is an attractive approach for the tethering of AMP onto chitosan, in order to create novel antimicrobial materials potentially valuable for biomedical applications.

Keywords: antibiotics; antimicrobial peptides; azide-alkyne coupling; biofilms; chitosan; click chemistry; CuAAC

1. Introduction

The relevance of AMP, active components of the innate immune response, as alternatives to currently available antibiotics is increasing. AMP have valuable features, including broad spectrum of activity, even at low concentrations, target specificity, synergistic effect with conventional antibiotics, and low tendency to induce pathogen resistance (Costa, Carvalho, Montelaro, Gomes, & Martins, 2011; Hancock & Patrzykat, 2002; Jenssen, Hamill, & Hancock, 2006; Oliveira, Martins, Mafra, & Gomes, 2012; van der Weerden, Bleackley, & Anderson, 2013). However, AMP can be easily degraded in *in vivo* environments and are potentially toxic in high concentrations (Costa *et al.*, 2011; Sahariah *et al.*, 2015; Seo, Won, Kim, Mishig-Ochir, & Lee, 2012). Hence, at the present status of their development as therapeutic agents, AMP are more appealing for topical/local antibiotherapies rather than for systemic approaches, as demonstrated by the use of, e.g., AMPs of the polymyxins and gramicidins families in ophthalmic antibiotics (https://www.drugs.com/pro/neomycin-polymyxin-b-gramicidin.html), or by the recent

submission for approval, by the European Medicines Agency, of Locilex®, an antimicrobial ointment based on the AMP known as Pexiganan or MSI-78 (Ge *et al.*, 1999; Gottler & Ramamoorthy, 2009; Monteiro *et al.*, 2015), for the topical treatment of skin infections such as diabetic foot ulcers (http://www.dipexiumpharmaceuticals.com /locilex/overview).

AMP immobilization onto material surfaces is an alternative effective strategy to circumvent obstacles associated to systemic administration of AMP, while taking advantage of the potential of AMP to fight bacterial biofilms associated to medical devices (Donlan, 2001). Actually, covalent immobilization of AMP onto surfaces through different coupling strategies has already been reported, and the overall results suggest that covalent immobilization of AMP onto surfaces may be responsible for inhibiting bacterial adhesion and bacterial death upon contact with peptide-functionalized surfaces (Costa *et al.*, 2011; Onaizi & Leong, 2011). Moreover, improving tethering parameters and procedures, may enhance peptide stability profiles while overcoming AMP's cytotoxicity associated with high concentrations, suggesting a promising potential for immobilized AMP in clinical applications (Chen, Hirt, Li, Gorr, & Aparicio, 2014).

In connection with the above, we have been working on AMP covalent tethering onto chitosan, towards the development of a novel efficient antimicrobial implant coating (Costa, Maia, Gomes, & Martins, 2015). Chitosan is a biocompatible natural polymer with bioadhesive properties, intrinsic antimicrobial activity, and ability to enhance cell proliferation and induce wound-healing (Berger *et al.*, 2004; Bernkop-Schnürch & Dünnhaupt, 2012; Dash, Chiellini, Ottenbrite, & Chiellini, 2011).

Our group has previously succeeded in the chemoselective tethering of a PEG-like amine onto chitosan's primary (C-6) hydroxyl groups by means of the copper(I)-catalyzed azide-alkyne coupling (CuAAC), a well-known "click" reaction (Oliveira *et al.*, 2012). Moreover, we have recently demonstrated that bacterial adhesion to chitosan surfaces is significantly reduced upon covalent tethering of a potent wide-spectrum AMP, Dhvar-5, through formation of a persulfate bond (i.e., disulfide bridge) between the side chain thiol of a Cys residue incorporated in the AMP, and *N*-acetylcysteine-chitosan (NAC) (Costa *et al.*, 2015). In view of this, and given that disulfide bridges are chemo- and bio-reversible, we now set out for development of an alternative approach for stable covalent grafting of the same AMP, by means of the chemoselective CuAAC (Liang & Astruc, 2011; Meldal & Tornøe, 2008). CuAAC is one of the most interesting "click" reactions, given the stability of the triazole link created between the building blocks that are coupled

together, and selective reactivity between azides and alkynes (Hong, Presolski, Ma, & Finn, 2009; Meldal & Tornøe, 2008; Tang & Becker, 2014). Moreover, peptide sequences can be easily modified with either azide or alkyne moieties by standard solid phase peptide synthesis (SPPS), since both functional groups are stable even through the harsher steps of conventional SPPS (Meldal & Tornøe, 2008). CuAAC has already been applied in the synthesis of block and graft copolymers, surface and polymers functionalization, and bioconjugation for *in vivo* labeling (Barbosa, Martins, & Gomes, 2015; Jagasia, Holub, Bollinger, Kirshenbaum, & Finn, 2009; Meldal & Tornøe, 2008; Zampano, Bertoldo, & Ciardelli, 2010). CuAAC has also been successfully employed for the tethering of peptides onto hydrogels and other biomaterials (Ahmad-Fuaad, Azmi, Skwarczynski, & Toth, 2013; Barbosa *et al.*, 2015). However, careful tuning of experimental conditions is often required, especially when dealing with Arg-containing peptides (the majority of AMP). The guanidine side chain of Arg reacts with ascorbic acid and ascorbate salts (Pischetsrieder, 1996), which are usually employed in CuAAC approaches for *in situ* generation of the catalytic Cu(I) from Cu(II) salts (Barbosa *et al.*, 2015). The present report demonstrates that, with careful control of experimental parameters, the Arg-containing AMP, Dhvar-5, can be successfully tethered onto chitosan, *via* CuAAC promoted by the standard copper(II) sulfate/sodium ascorbate system in aqueous medium.

2. Materials and Methods

2.1 Synthesis and characterization of the designed peptide sequence

2.1.1 Materials

Rink amide MBHA resin (0.38 mmol/g), N^{α}-Fmoc-protected acids amino acids and 2-(1*H*-Benzotriazole-1-yl)-1,1,3,3-tetramethyluronium hexafluorophosphate (HBTU) were obtained from NovaBiochem-EMD4Biosciences. Piperidine, *N*,*N*-dimethylformamide (DMF), *N*-methylpyrrolidone (NMP), N-ethyl-N,N-diisopropylamine (DIPEA), 1-hydroxybenzotriazole (HOBt), trifluoroacetic acid (TFA), triisopropylsilane (TIS), and all solvents for SPPS were from Sigma-Aldrich.

2.1.2 Peptide Synthesis

The 14-amino acid antimicrobial peptide Dhvar-5 sequence, LLLFLLKKRKKRKY (from N to C: leucine-leucine-leucine-phenylalanine-leucine-leucine-lysine-lysine-arginine-lysine-lysine-arginine-lysine-tyrosine), with an additional 6-aminohexanoic acid (Ahx) spacer and an *N*-terminal propargylglycine (Pra) as the alkyne moiety, was synthesized (Figure 1). The full oligopeptide sequence will be hereafter designated Pra-Ahx-Dhvar-5 (MW = 2056 Da). The peptide (*C*-terminal amide) was assembled by standard Fmoc/^{t}Bu SPPS methodologies assisted with microwave (MW) energy, using a Liberty1 Microwave Peptide Synthesizer (CEM Corporation, Mathews, NC, USA). The resin (Rink amide MBHA) was preconditioned for 15 min in DMF and then transferred into the MW-reaction vessel. The initial Fmoc deprotection step was carried out using 20% piperidine in DMF containing 0.1 M of HOBt in two MW irradiation pulses: 30 s at 24 W plus 3 min at 28 W, in both cases temperature being no higher than 75 °C. The C-terminal amino acid was then coupled to the deprotected Rink amide resin, using 5 molar equivalents (eq) of the Fmoc-protected amino acid in DMF (0.2 M), 5 eq of 0.5 M HBTU/HOBt in DMF, and 10 eq of 2 M DIPEA in NMP; the coupling step was carried out for 5 min at 35 W MW irradiation, with maximum temperature reaching 75 °C. The remaining amino acids were sequentially coupled in the C → N direction by means of similar deprotection and coupling cycles. Following completion of the sequence assembly, the peptide was released from the resin with concomitant removal of side-chain protecting groups, by a 1.5 h acidolysis at room temperature using a TFA-based cocktail containing TIS and water (95:2.5:2.5 v/v/v) as scavengers.

2.1.3 Characterization and purification of the synthetic peptide

The crude peptide was purified by preparative HPLC to a purity of at least 95%. Samples were injected in a preparative HPLC system (LaPrep Sigma VWR with UV detector LP 3104 and LP 1200 pump) with a reverse-phase Merck C18 column (250 × 25 mm ID and 5 μm pore size) at a flow rate of 10 mL/min using as solvents 0.05% aqueous TFA (eluent A) and acetonitrile (eluent B) for 60 min. Subsequently, pure peptide fractions isolated were pooled, freeze-dried, and stored at -20 °C until use. Peptide purity degree was determined by analytical HPLC, using a Hitachi-Merck LaChrom Elite system equipped with a quaternary pump, a thermostatted automated sampler, and a diode-array detector (DAD). MS analyses were performed on an LTQ Orbitrap TM XL hybrid mass

spectrometer (Thermo Fischer Scientific, Bremen, Germany) controlled by LTQ Tune Plus 2.5.5 and Xcalibur 2.1.0. The electrospray ionization source settings (ESI) were as follows: source voltage, 3.1 kV; the capillary temperature was 275 °C with a sheath gas flow rate at 40 and auxiliary gas flow rate at 10 (arbitrary unit as provided by the software settings). The capillary voltage was 36 V and the tube lens voltage 110 V. MS data handling software (Xcalibur QualBrowser software, Thermo Fischer Scientific) was used to obtain the confirmation of the synthetic peptide by their exact *m/z* value.

2.2 Synthesis of AMP-Chitosan conjugates

2.2.1 Materials

High molecular weight chitosan, with a 94% degree of deacetylation (DD), was obtained from France-Chitine. Dialysis membrane (MW cut-off 3.5 kDa) was from Spectrum Lab. Sodium ascorbate, copper(II) sulfate pentahydrate (CuSO4·H2O), *N*-ethyl-*N*,*N*-diispropylamine (DIEA), 2,6-lutidine,tris(3-hydroxypropyltriazolylmethyl)amine (THPTA), copper(I) bromide, propargylamine, ethylenediaminetetraacetic acid (EDTA) and potassium carbonate were all purchased from Sigma-Aldrich. Aminoguanidine hydrochloride was from TCI Chemicals. Imidazole-1-sulfonyl azide hydrochloride (ISA·HCl) was a kind gift from Professor Fernando Albericio, from the Institute of Biomedical Research of Barcelona (IRB-Barcelona). Except for chitosan, all reagents were of analytical grade and used directly without any further purification

2.2.2 Purification of commercial chitosan

High-molecular weight chitosan (CHIT) was purified by the reprecipitation method. Briefly, 1 g of chitosan powder was pre-hydrated in 197.92 mL of distilled and deionized water, for 24 h at 4 °C under slow magnetic stirring. Then, 2.28 mL of acetic acid was added, and the slurry left stirring overnight at room temperature. After complete solubilization, the resulting gel was filtered through a 20 μm pore size filter to remove undissolved or gelatinous particles. Chitosan was then precipitated through dropwise addition of 1 M aqueous NaOH, while stirring. Finally, the regenerated chitosan was washed with distilled and deionized water by centrifugation until neutrality, freeze-dried and grounded in a laboratory mill (IKA mill) to yield a fine powder.

2.2.3 Preparation of azido-chitosan

Chitosan was functionalized by direct conversion of the polymer's amines into azides, following a recent report (Castro, Blanco-Canosa, Rodriguez, & Albericio, 2013). Briefly, the reaction was carried out using potassium carbonate and ISA·HCl in aqueous medium, under magnetic stirring, for 24 h at room temperature (Figure 1A). The final product, azido-chitosan (N_3-CHIT) was dried in vacuum.

2.2.4 Synthesis of peptide-CHIT conjugate

The conjugation between modified AMP, Pra-Ahx-Dhvar-5, and N_3-CHIT was obtained under standard CuAAC reaction conditions, i.e., in the presence of Cu(II) sulfate and sodium ascorbate, for *in situ* generation of the Cu(I) catalyst, in aqueous medium. Briefly, 100 mg of N_3-CHIT reacted with 250 mg of Pra-Ahx-Dhvar-5 in the presence of 17.2 mg of $CuSO_4 \cdot H_2O$ and 711.4 mg of sodium ascorbate. THPTA ligand (295.5 mg) and aminoguanidine hydrochloride (375.9 mg) were also added. The reaction was performed in water, at room temperature, for 48 h (Figure 1B). The solid fraction was collected by centrifugation, thoroughly washed with 0.1 M aqueous EDTA, 5% aqueous sodium bicarbonate, and finally water. Modified chitosan was dialyzed against 1 hydrochloric acid for three days and deionized water for two days. After dialysis, the final chitosan conjugate (peptide-N_3-CHIT) was centrifuged and dried in vacuum.

2.2.5 Capping of unreacted azide groups

The conjugate peptide-N_3-CHIT was reacted with propargylamine, under CuAAC conditions similar to those described above, in Section 2.2.4. Briefly, 100 mg of peptide-CHIT was reacted with 3.30 mL of propargylamine in the presence of 17.2 mg of $CuSO_4 \cdot H_2O$ and 711.4 mg of sodium ascorbate. The reaction was performed in water, at room temperature, for 48 h (Figure 1C). The resulting solid (peptide-CHIT) was washed, as described previously, and then centrifuged and dried in vacuum.

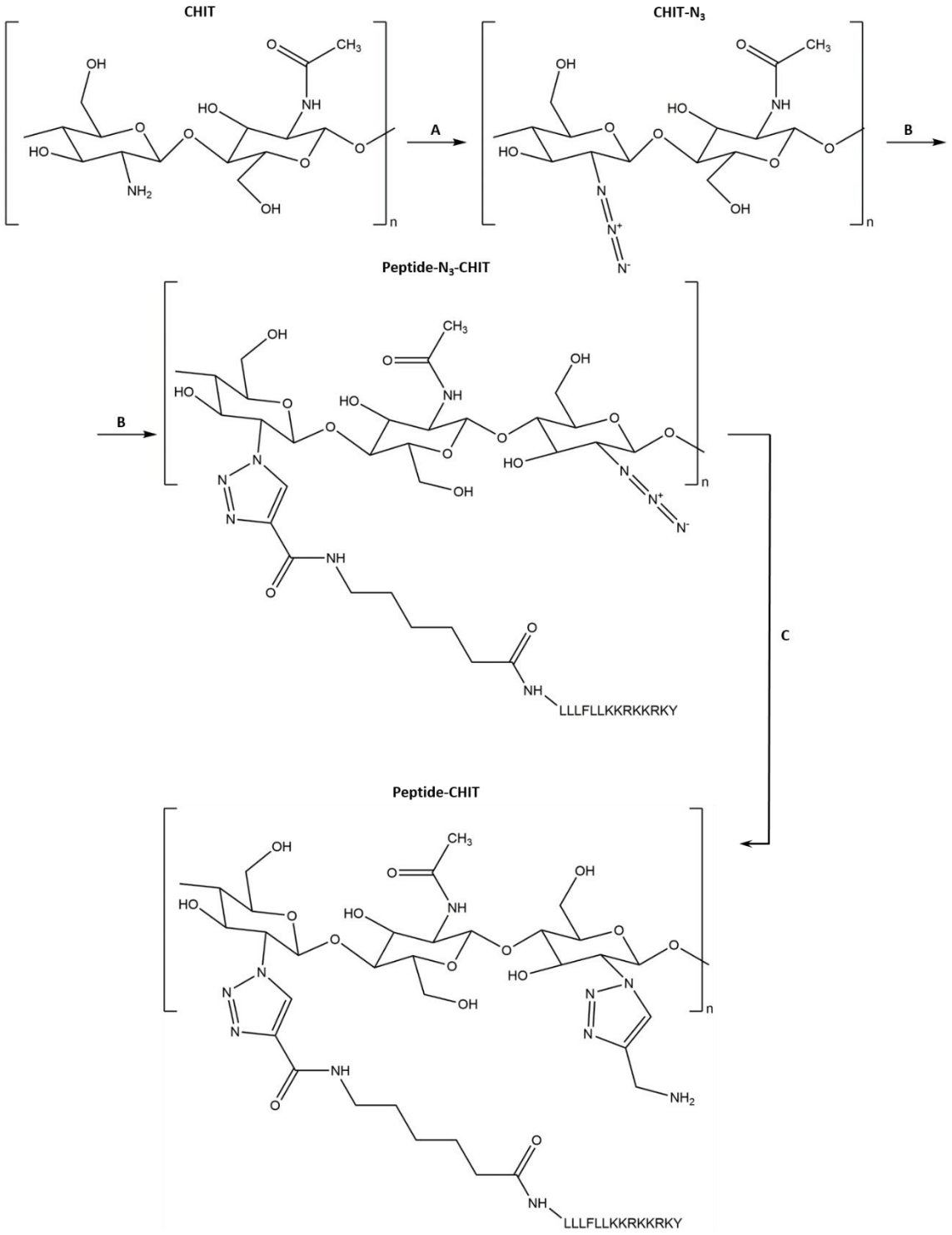

Figure 1 Chemical route towards peptide-CHIT conjugate, obtained after an azide-alkyne conjugation reaction involving the N_3-CHIT derivative: A) ISA·HCl, K_2CO_3, water, room temperature (rt), 24 h; B) $CuSO_4 \cdot H_2O$, sodium ascorbate, THPTA, aminoguanidine hydrochloride, Pra-Ahx-Dhvar-5, water, rt, 48 h; C) $CuSO_4 \cdot H_2O$, sodium ascorbate, propargylamine, water, rt, 48 h.

2.3 Scanning electron microscopy with energy-dispersive X-ray analysis (SEM/EDS)

The SEM/EDS exam was performed using a high-resolution Scanning Electron Microscope with X-Ray Microanalysis JEOL JSM 6301F/Oxford INCA Energy 350. Samples were coated with an Au/Pd thin film, by sputtering, using the SPI Module Sputter Coater equipment.

2.4 FT-IR analysis

FT-IR spectra of chitosan and its derivatives were acquired using a Perkin-Elmer Spectrum BX FTIR spectrophotometer. FT-IR spectra in transmission mode were acquired in a Bruker Tensor 27 coupled to HTS-XT. All the samples were recorded as KBr pellets prepared by blending 2 mg of the powdered polymer, previously dried overnight under reduced pressure, with 200 mg KBr, previously dried at 110 °C for 24 h. The spectra resulted of the average of 32 consecutive interferograms at 4 cm^{-1} resolution, between 4000 and 400 cm^{-1}. Spectra were fitted using the Spectrum GX FT-IR (version 5.3) software.

2.5 XPS analysis

Chitosan and its derivatives were analyzed by XPS. Samples were prepared by compressing the powdered polymers into thin pellets. Measurements were carried out on a Kratos Axis Ultra HAS spectrometer (from CEMUP – Centro de Materiais da Universidade do Porto) using aluminum (15 kV) as a radiation source. Photoelectrons were analyzed at a 90° take-off angle between the horizontal surface plane and the electron analyzer optics. Survey spectra were collected over the 0-1350 eV range with analyzer pass energy of 80 eV. High-resolution of C1 and N1s spectra were collected with analyzer pass energy of 40 eV. The binding energy scales were referenced by setting the C1s binding energy to 285.0 eV. Spectra were fitted using the CasaXPS (version 2.3.17PR 1.1) software.

2.6 Amino Acid analysis

The content and ratio of amino acids present in the peptide-CHIT conjugate was determined by ion exchange chromatographic analysis after hydrolysis. The hydrolysis was performed with 6 M aqueous HCl at 110 °C for 24 h. After that time, the sample was evaporated to dryness at reduced pressure. The residue was dissolved in ultrapure water with aminobutyric acid as an internal standard, and then derivatized using the AccQ-Tag protocol from Waters, which uses 6-aminoquinoyl-*N*-hydroxysuccinimidyl carbamate as derivatization reagent. Finally, the sample was analyzed by HPLC (Waters 600) with a UV-detector Waters 2487 (λ = 254 nm).

3. Results and Discussion

3.1 Peptide design, synthesis and characterization

The rationale behind Pra-Ahx-Dhvar-5, an alkyne derivative of the known AMP Dhvar-5, was based on previous findings in our group; similar Dhvar-5 derivatives, bearing an additional cysteine linked through different spacers to either the *N*- or *C*-terminus of the peptide, had been prepared and grafted onto *N*-acetyl cysteine-chitosan surfaces through a disulfide bridge. Surfaces thus produced were tested for their ability to repel bacterial adhesion (Costa *et al.*, 2015). This study allowed us to conclude that when the peptide is grafted through its N-terminus, thus exposing the cationic *C*-terminus of Dhvar-5, through a 6-aminohexanoic acid (Ahx) spacer, a significantly more pronounced decrease in bacterial adhesion is observed. In opposite, when the peptide is grafted through the C-terminus, no further antimicrobial activity is obtained regarding control chitosan film (Costa *et al.*, 2015). As such, for the present study, the non-natural alkynylated amino acid, propargylglycine (Pra) was linked to the *N*-terminus of the bioactive Dhvar-5 sequence also through an Ahx spacer, resulting in the target Pra-Ahx-Dhvar-5 peptide. This was successfully synthesized by standard SPPS procedures according to the orthogonal Fmoc/^{t}Bu protection scheme (Benoiton, 2016). The molecular weight and purity were assessed by LC–MS and analytical HPLC, respectively. The mass spectrum (MS) was acquired in the positive mode, using an electrospray ionization source coupled to an ion trap detector (ESI-IT), and the observed peaks at *m/z* 1028.20, 685.80, 514.60 and 411.88 atomic mass units (a.m.u.), were consistent with the peptide at different

protonation degrees, i.e., respectively due to species $[M + 2H]^{2+}$, $[M + 3H]^{3+}$, $[M + 4H]^{4+}$, $[M + 5H]^{5+}$, and $[M + 6H]^{6+}$. The HPLC chromatogram of the purified peptide, which presented a retention time of 12.6 min under the analysis conditions described in 2.1.3., showed a peptide purity degree of 95%.

3.2 Synthesis of the target peptide-CHIT conjugate

The final conjugate was prepared in three reaction steps, as depicted in Figure 1. After purification, chitosan was first functionalized by direct conversion of the polymer's amines into azides, by means of the diazo-transfer reagent ISA·HCl (Figure 1A). The choice of this reagent was based not only on its reported efficacy, but also and especially, because it is a green chemistry approach for the conversion of amines into azides, as the reaction can be carried out in water, only requiring the presence of a mild base like K_2CO_3 (Castro *et al.*, 2013). Since chitosan does not dissolve in alkaline medium, the reaction was carried out under heterogeneous conditions, and produced the desired azido-chitosan (N_3-CHIT), as confirmed by structural analyses (see following sections). For comparison, the reaction was also performed in methanol, but conversion yields were significantly lower, as observed by FT-IR (data not shown).

To prepare the target peptide-CHIT conjugate, different conditions were tested in order to optimize coupling of Pra-Ahx-Dhvar-5 with N_3-CHIT in aqueous medium containing the Cu^{2+}/ascorbate pair, for *in situ* formation of the Cu^{+} catalyst required in CuAAC. As shown by data on Table 1, the target conjugate could only be obtained when both THPTA, a ligand that stabilizes Cu^{+} in solution (Kim, Harker, De Leon, Advincula, & Pokorski, 2015), and excess aminoguanidine hydrochloride, which avoids modification of Arg side chains by ascorbate (Presolski, Hong, & Finn, 2011), were employed (entry 4). Confirmation of peptide tethering onto chitosan, *via* the desired triazole link, was provided by structural and amino acid analyses, as described in the following sections.

Table 1 Optimization of CuAAC reaction conditions.

Entry	Reaction conditions				Results	Method adapted from
	Activator	**Base**	**Ligand**	**Additives**		
1	$CuSO_4 \cdot H_2O$	–	–	Sodium ascorbate	Only minor conversion could be detected by FT-IR	(Oliveira *et al.*, 2012)
2	CuBr	DIEA	2,6-lutidine	Sodium ascorbate	No conversion could be detected by FT-IR	(Castro *et al.*, 2013; Castro, Rodriguez, & Albericio, 2012)
3	$CuSO_4 \cdot H_2O$	–	THPTA	Sodium ascorbate	Reasonable conversion confirmed by FT-IR; AAA of the final conjugate showed levels of arginine lower than expected	(Kim, Harker, De Leon, Advincula, & Pokorski, 2015)
4	$CuSO_4 \cdot H_2O$	–	THPTA	Sodium ascorbate, aminoguanidine hydrochloride	FT-IR showed the success of the reaction; AAA compatible with expected peptide structure	(Hong *et al.*, 2009; Presolski, Hong, & Finn, 2011)

Finally, given that FT-IR analysis of the conjugate (see next section) showed that some azide groups remained unreacted, these were capped through a second "click" step using excess propargylamine (Figure 1C), in order to avoid the potential toxic effects of free azide groups (Crownover, Duvall, Convertine, Hoffman, & Stayton, 2011). Moreover, this final capping step also allows the polymer's backbone to regain primary amine groups similar to those in unmodified chitosan, and to which chitosan owes some of its appealing features, such as its bio-adhesive and bacteriostatic properties (Croisier & Jérôme, 2013). The surfaces of both unmodified chitosan and final peptide-CHIT conjugate were characterized by SEM (Figure 2). The images were recorded at two magnifications.

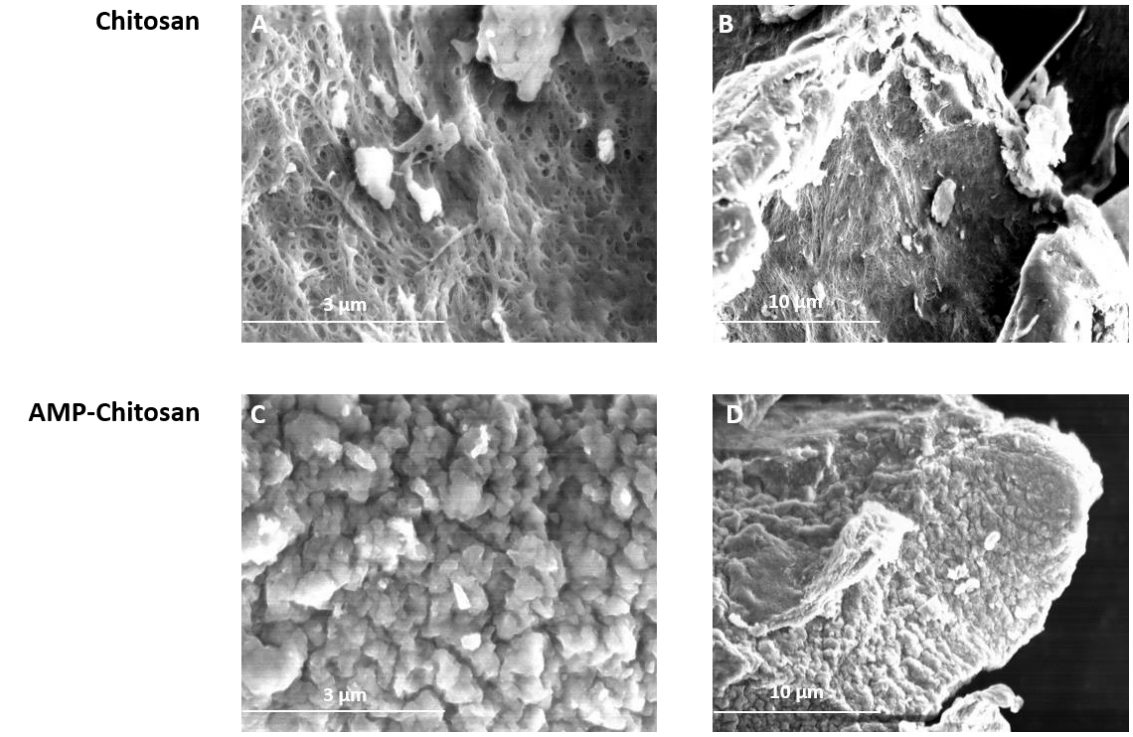

Figure 2 SEM images of unmodified chitosan (A, B) and peptide-CHIT conjugate (C, D). Magnification at 20000 × (A, C) and at 5000 × (B, D).

As shown in Figure 2A and B, the unmodified chitosan exhibited a slightly porous and smooth surface, whereas peptide-CHIT conjugate (Figure 2C and D) presents a nonporous rough surface. These images show significant differences in the morphology of the chitosan surface after peptide tethering.

3.2.1 FT-IR analysis of chitosan and derivatives

After purification, unmodified chitosan was analyzed by FT-IR, and, as expected, displayed the previously described characteristic bands (Amaral, Granja, & Barbosa, 2005; Gomes, Gomes, Batista, Pinto, & Silva, 2008; Oliveira *et al.*, 2012). The spectrum (Figure 3A) presented a broad and intense band at 3450-3200 cm^{-1} characteristic of hydrogen-bonded X–H stretching vibrations; bands due to GlcNHAc units at 1643 cm^{-1}, 1592 cm^{-1}, and 1417 cm^{-1} typical of amide I (C=O stretching), amide II (N–H bending), amide III (C–N stretching coupled with NH in plane deformation), respectively, and at 1374 cm^{-1} for $–CH_3$ symmetrical angular deformation; C–N stretching of the amino groups at 1321 cm^{-1}; O–H plane deformation at 1253 cm^{-1}; C–O–C stretching vibration in the glucopyranose ring at 1076 cm^{-1}; and the specific bands of the β(1–4) glycoside bridge at 1153 and 895 cm^{-1} (Figure 3A).

For production of N_3-CHIT, ISA·HCl-mediated conversion of amines into azides was carried out both in water, as preferred solvent, and methanol, for comparison. Both reactions were monitored by FT-IR, which allowed to conclude that, in methanol, only low conversion rates were detected (data not shown). This finding could be attributed to only partial dissociation of the base, K_2CO_3, under these non-aqueous conditions, which would result in incomplete neutralization of the diazo-transfer reagent (used as a hydrochloride salt) and protonation of the more basic amine, with the consequent reduction of efficiency. On the other hand, when the reaction was carried out in water, extensive conversions were obtained, as demonstrated through the appearance of two characteristic azide peaks at 2115 cm^{-1}, which was actually the most intense of the FT-IR spectrum of N_3-CHIT (Figure 3B), and at 1319 cm^{-1} assigned to the asymmetric and symmetric $N^-=N^+=N^-$ stretches, respectively (Castro *et al.*, 2013; Sahariah *et al.*, 2015). Upon reaction of N_3-CHIT with Pra-Ahx-Dhvar-5, under best CuAAC reaction conditions found in this study (Table 1, entry 4), the product obtained presented the FT-IR spectrum displayed in Figure 3C (peptide-N_3-CHIT). This spectrum demonstrated that the desired "click" reaction had occurred, as three relevant changes could be noted, when comparing to N_3-CHIT,: (i) a weak band at 836 cm^{-1}, typical of N–C=N in plane bending (Krishnakumar & Xavier, 2004; Oliveira *et al.*, 2012), arising from formation of the triazole ring produced via the CuAAC, (ii) the significant intensity decrease of both azide bands (at 2115 and 1319 cm^{-1}), supporting partial consumption of available azides upon reaction with the alkynylated peptide, and (iii) intensity increase of the amide I and amide II bands (1640–1560 cm^{-1}) (Andreas Barth, 2007), strongly supporting successful peptide grafting onto N_3-CHIT. Noteworthy, the characteristic bands of chitosan remained throughout the procedure, indicating that "click" reaction provides a mild chemical environment for chemoselective functionalization of chitosan (Hu *et al.*, 2014).

Capping of unreacted azides *via* CuAAC, using excess propargylamine instead of peptide, produced the final material (peptide-CHIT), whose FT-IR spectrum is shown on Figure 3D, where the characteristic azide peaks have completely disappeared. This, on the one hand, confirms total consumption of unreacted azides and, on the other hand, provides a final proof that CuAAC reaction conditions employed are efficient, allowing quantitative conversions when using the alkyne partner in excess.

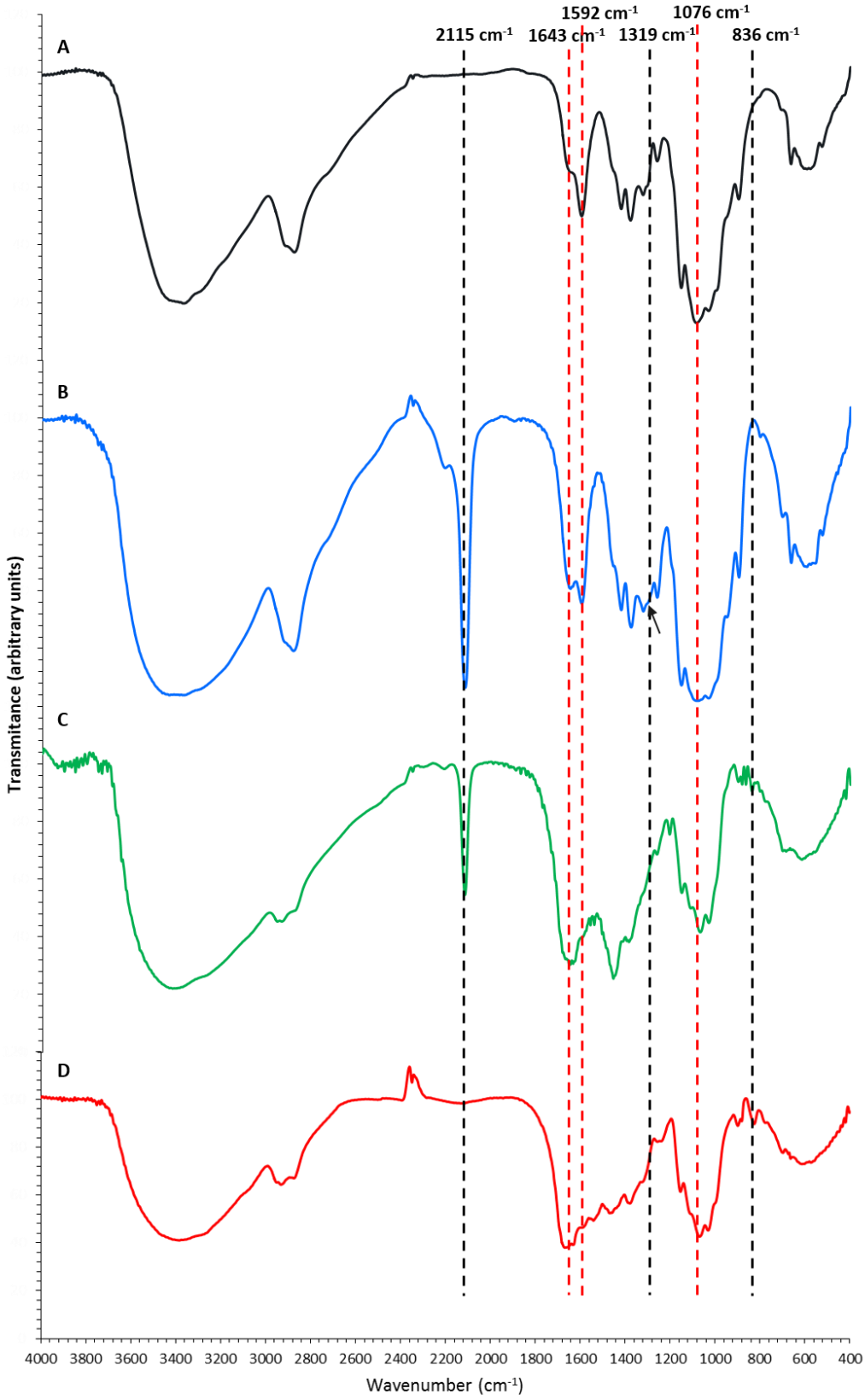

Figure 3 FT-IR spectra (KBr pellets) of A) unmodified chitosan, B) N_3-CHIT, C) peptide-N_3-CHIT and D) peptide-CHIT powders. Lines in red correspond to bands present in unmodified chitosan and remain visible throughout the procedures, while the ones in black are consequence of further chitosan functionalization.

3.2.2 XPS analysis of chitosan and derivatives

Chitosan, N_3-CHIT and both peptide-CHIT conjugates were further analyzed by XPS. Table 2 shows the relative atomic percentages of carbon, oxygen and nitrogen of unmodified chitosan and respective derivatives.

Table 2 Elemental analysis data (% C, N, O) as determined by XPS analysis of unmodified chitosan and derivatives.

Polymer	**Atomic compositon (%)**		
	C1s	**N1s**	**O1s**
Chitosan	62.8	7.3	29.9
N_3-Chit	59.6	9.6	30.8
Peptide-N_3-CHIT	63.6	11.1	25.3
Peptide-CHIT	62.7	13.1	24.2

The XPS survey revealed the presence of residual sulfur, probably due to a surface contaminant. As anticipated, the N_3-CHIT derivative presented a small decrease in the atomic percentage of carbon with concomitant increase in the percentage of nitrogen, as a consequence of the introduction of the azide group onto the chitosan backbone. After CuAAC reaction, the percentage of oxygen of the peptide-N_3-CHIT derivative decreased while both carbon and nitrogen atomic composition increased, suggesting that the peptide was successfully coupled to N_3-CHIT through a triazole ring. The XPS analysis of the final peptide-CHIT conjugate showed an increase in the percentage of nitrogen and concomitant decrease in the percentages of carbon and oxygen, compatible with insertion of propargylamine by an additional azide-alkyne coupling procedure. High resolution XPS spectra of C1s and N1s were also analyzed and are displayed on Figure 4.

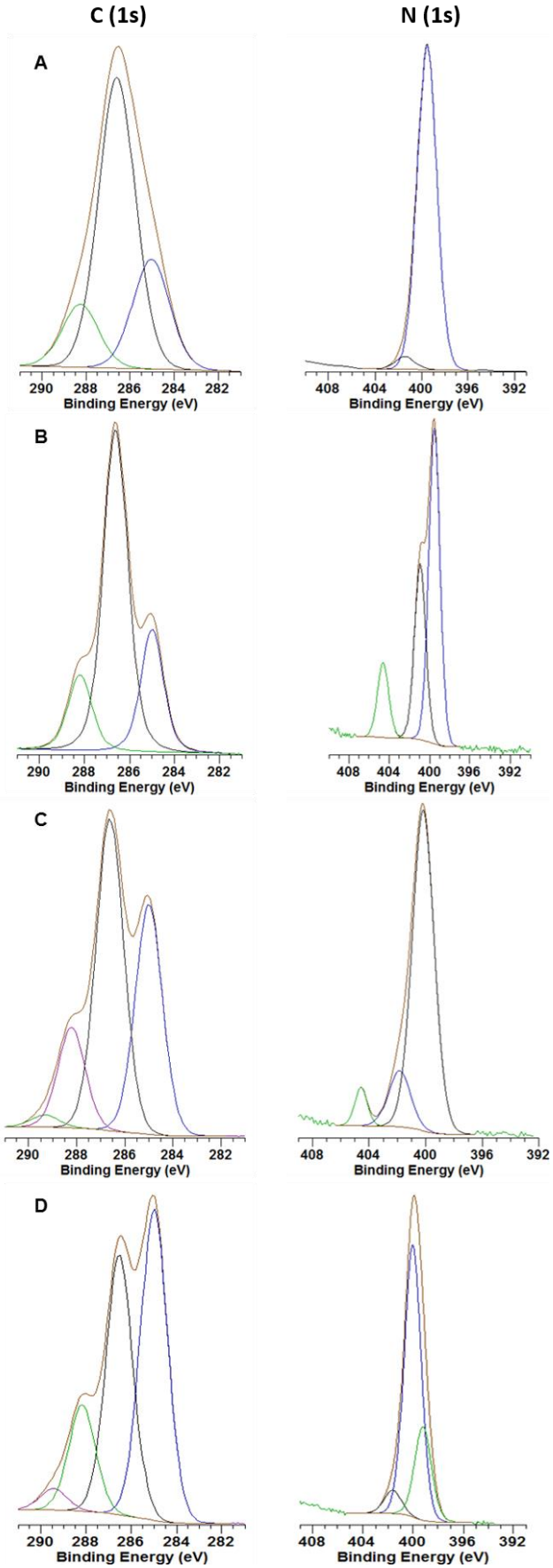

Figure 4 XPS high resolution spectra of A) unmodified chitosan, B) N_3-CHIT, C) peptide-N_3-CHIT, and D) final peptide-CHIT conjugate after capping reaction, for C1s and N1s regions.

The C1s spectrum of unmodified chitosan (Figure 4A) was resolved into three peaks as previously described by (Amaral *et al.*, 2005). The peak at 285.0 eV was assigned to C–C and C–H type carbons that are typically related with a surface contaminant (Amaral *et al.*, 2005), the peak at 286.6 eV was assigned to C–NH_2, C–OH and C–O–C carbons, whereas the peak at 288.3 eV was assigned to carbons from the O–C–O and N–C=O groups. Regarding N1s, the resolved spectrum displayed two peaks: at 399.5 eV, assigned to nitrogens in C–N and CO–N bonds, and at 401.8 eV, assigned to protonated amines, i.e., ammonium groups (NH_3^+).

N_3-CHIT (Figure 4B) did not shown significant changes in C1s high-resolution XPS spectra as compared to its unmodified chitosan precursor. The high-resolution XPS N1s spectrum of the N_3-CHIT derivative, which exhibited two peaks at 399.5 and 401.4 eV, for NH_2 and NH_3^+, respectively, and another at 404.5 eV associated with nitrogen in the azide group, clearly demonstrated the success of conversion of the chitosan's amines into azides (Hu *et al.*, 2014; Shakiba, Jamison, & Lee, 2015).

Regarding the XPS results of peptide-N_3-chitosan (Figure 4C), the C1s high-resolution spectrum showed an increase in the 285.0 eV peak (C–C and C–H) suggesting the insertion of C–C and C–H type carbons present in the peptide chain. In addition, the peak at 400.0 eV assigned to nitrogen atoms on the triazole ring, is in agreement with reported spectra for the triazole ring (Hu *et al.*, 2014; Shakiba *et al.*, 2015). However, the peak corresponding to nitrogen in the azide group (404.5 eV) is still visible, corroborating data from FT-IR analysis which revealed that some azide groups remained unreacted after peptide tethering *via* CuAAC.

After capping the unreacted azides with propargylamine (peptide-CHIT), the C1s spectrum (Figure 4D) displays an intensity increase of the peak at 285.0 eV due to C–C and C–H bond after coupling propargylamine onto chitosan through a triazole linkage. Additionally, the band at 404.5 eV in the XPS N1s spectra, associated with the azide moiety, disappeared, while the peaks characteristic of nitrogens in C–N and CO–N bonds and amine groups (399.5 eV and 401.4 eV, respectively) and the triazole moiety (400.0 eV) are present. Hence, results obtained for the N1s region of the XPS spectrum demonstrates total consumption of unreacted azides and confirms the success of the CuAAC reaction.

The data for relative atomic percentages of different types of nitrogen, obtained from the N1s XPS high-resolution spectra is shown in Table 3.

Table 3 Chemical surface high-resolution analysis of N(1s) region for chitosan and respective derivatives.

Polymer	**Atomic% N(1s)**			
	C–N/CO–N	CO–N–CO/N–CO–O	NH_3^+	$N^-=N^+=N^-$
	399.5 eV	**400.0 eV**	**401.4 eV**	**404.5 eV**
Chitosan	96	-	4	-
N_3-Chit	56	-	31	13
Peptide-N_3-CHIT	–	81	14	5
Peptide-CHIT	24	70	6	-

The success of amine-azide conversion in chitosan was clearly demonstrated by the appearance of a peak at 404.5 eV assigned to nitrogen in azide groups. Additionally, the success of the subsequent CuAAC reaction was confirmed by the substitution of the previous band by a peak at 400.0 eV, which corroborates the formation of the triazole ring.

Therefore, these results provided further evidences of the success of all reactional steps towards the synthesis of target peptide-CHIT conjugate.

3.2.3 Amino Acid Analysis of the peptide-CHIT conjugate

Amino Acid Analysis (AAA) was used to determine the relative amino acid composition and peptide content of the peptide-CHIT conjugate, and to confirm the integrity of arginine residues (whose retention time is changed if modified upon reaction with ascorbate).

As described in the Experimental Section, the conjugate was first hydrolyzed under harsh acidic conditions, to yield a mixture of free amino acids and the products of hydrolysis of the polysaccharide backbone, which do not interfere in the AAA. Data obtained are displayed on Table 4 and reveal that the relative proportions of each amino acid residue that composes the sequence of Dhvar-5 were as expected.

Table 4 Amino acid composition and peptide load of the final peptide-CHIT conjugate.

Amino Acid	nmol (hydrolyzed residue)	Expected proportion	Result
Arg	192.2	2	1.98
Tyr	26.6	1	0.27
Lys	465.6	5	4.81
Leu	501.6	5	5.18
Phe	100.0	1	1.03
μmol peptide per g of chitosan 48.6			

Exception is made to tyrosine, whose levels were considerably lower than expected, but this is a typical observation in AAA of peptide hydrolysates produced upon acidic hydrolysis in the absence of phenol or mercaptoethanol (Fountoulakis & Lahm, 1998). Still, though addition of an excess of any of these reagents to the hydrolysis medium allows for a more accurate quantitation of Tyr, we considered that the cost (additive toxicity)/benefit of such procedure was not justified in our particular case, as the other four different amino acid residues of Dhvar-5 would be enough to quantitate the amount of grafted peptide and to confirm its sequence.

According to AAA results, the CuAAC carried out allowed us to graft around 50 μmol of peptide per g of chitosan, i.e., nearly 2 mg of Dhvar-5 per g of polymer. Given the promising antimicrobial activity of Dhvar-5 peptide at low concentrations against biofilm-forming organisms such as methicillin-resistant *Staphylococcus aureus* (MRSA) and *Staphylococcus epidermidis* (Costa *et al.*, 2015; Stallmann *et al.*, 2005) the synthesized peptide-CHIT conjugate, by means of the CuAAC reaction previously described, has the potential to be used as an AMP-based antimicrobial material.

4. Concluding Remarks

A chitosan derivative was successfully synthesized following a facile and mild diazo-transfer reaction with ISA·HCl, in a near quan titative amine to azide conversion. The resulting N_3-CHIT polymer was afterwards coupled to alkyne-AMP, by means of CuAAC reaction, and yielded a polymer whose XPS and FT-IR data were in agreement with the formation of the expected triazole ring and insertion of the peptide chain, indicating that the target Peptide-CHIT conjugate was effectively produced. Interestingly, we could observe that the final peptide-grafted material was more soluble than both the starting chitosan and the azido-chitosan intermediate in aqueous media at pH $\leq$ 4, possibly due to solvent exposure of the hydrophilic cationic (Lys/Arg rich) *C*-terminal part of Dhvar-5.

The CuAAC approach is one of the most attractive reactions amongst the so-called "click" chemistry concept, given not only the selectivity between azide and alkyne moieties, but also the diversity of adequately functionalized building blocks that can be synthesized, bearing either an azide or an alkyne functionality. Moreover, the triazole linkage formed between the two building blocks is extremely stable under physiological conditions (Meldal & Tornøe, 2008; Tang & Becker, 2014).

Other reports have already addressed the potential of AMP-chitosan conjugates in the development of thin films (Costa, Maia, Gomes, Gomes, & Martins, 2014). In this connection, CuAAC can be easily applied towards the development of new and effective AMP-based biomaterials, provided immobilization parameters are optimized, when using a plethora of peptide sequences with controlled orientation, conformation and surface exposure (Costa *et al.*, 2011). Our work demonstrates that the fine tuning of reaction conditions may be instrumental towards success of peptide tethering *via* CuAAC; in fact, reasonable levels of azide to triazole conversion could only be observed when adding THTPA to stabilize Cu(I) in solution (Table 1, entries 3 and 4), whereas use of excess aminoguanidine hydrochloride was required to protect the peptide's arginines from being modified by ascorbate. Noteworthy, we could not find any report in the literature regarding peptide grafting onto bulk chitosan powder *via* CuAAC; while this reinforces the novelty of our work, it also prevents us from judging whether the peptide grafting yield achieved in this work is or not within expected values.

The importance of future research work in the area of AMP immobilization for biomedical applications is arising, considering the impact of increasing bacterial resistance to conventional antibiotics (Brooks & Brooks, 2014), and the emergence of

specific cases as chronic wound infections, like diabetic foot ulcers (Moura, Dias, Carvalho, & de Sousa, 2013) or acute osteomyelitis associated with bone implant surgery (Goodman, Yao, Keeney, & Yang, 2013).

Acknowledgments

The authors thank Fundação para a Ciência e Tecnologia (FCT), Portugal, for funding through project UID/Multi/04378/2013 and PhD Grant SFRH/BD/108966/2015 to MB. Thanks are also due to "Comissão de Coordenação e Desenvolvimento Regional do Norte (CCDR-N)/NORTE2020/Portugal2020" for funding through project DESignBIOtechHealth (ref. Norte-01-0145-FEDER-000024).

References

Ahmad-Fuaad, A. A., Azmi, F., Skwarczynski, M., & Toth, I. (2013). Peptide conjugation via CuAAC 'click'chemistry. Molecules, 18(11), 13148–13174.

Amaral, I., Granja, P., & Barbosa, M. (2005). Chemical modification of chitosan by phosphorylation: An XPS, FT-IR and SEM study. Journal of Biomaterials Science, Polymer Edition, 16(12), 1575–1593.

Barbosa, M., Martins, M. C. L., & Gomes, P. (2015). Grafting techniques towards production of peptide-tethered hydrogels, a novel class of materials with biomedical interest. Gels, 1(2), 194–218.

Barth, A. (2007). Infrared spectroscopy of proteins. Biochimica et Biophysica Acta, 1767, 1073–1101.

Benoiton, N. L. (2016). Chemistry of peptide synthesis. CRC Press.

Berger, J., Reist, M., Mayer, J. M., Felt, O., Peppas, N. A., & Gurny, R. (2004). Structure and interactions in covalently and ionically crosslinked chitosan hydrogels for biomedical applications. European Journal of Pharmaceutics and Biopharmaceutics, 57(1), 19–34.

Bernkop-Schnürch, A., & Dünnhaupt, S. (2012). Chitosan-based drug delivery systems. European Journal of Pharmaceutics and Biopharmaceutics, 81(3), 463–469.

Brooks, B. D., & Brooks, A. E. (2014). Therapeutic strategies to combat antibiotic resistance. Advanced Drug Delivery Reviews, 78, 14–27.

Castro, V., Rodriguez, H., & Albericio, F. (2012). Wang Linker free of side reactions. Organic Letters, 15(2), 246–249.

Castro, V., Blanco-Canosa, J. B., Rodriguez, H., & Albericio, F. (2013). Imidazole-1-sulfonyl azide-based diazo-transfer reaction for the preparation of azido solid supports for solid-phase synthesis. ACS Combinatorial Science, 15(7), 331–334.

Chen, X., Hirt, H., Li, Y., Gorr, S.-U., & Aparicio, C. (2014). Antimicrobial GL13K peptide coatings killed and ruptured the wall of streptococcus gordonii and prevented formation and growth of biofilms. PLoS One, 9(11), e111579.

Costa, F., Carvalho, I. F., Montelaro, R. C., Gomes, P., & Martins, M. C. L. (2011). Covalent immobilization of antimicrobial peptides (AMPs) onto biomaterial surfaces. Acta Biomaterialia, 7(4), 1431–1440.

Costa, F., Maia, S., Gomes, J., Gomes, P., & Martins, M. C. L. (2014). Characterization of hLF1-11 immobilization onto chitosan ultrathin films, and its effects on antimicrobial activity. Acta Biomaterialia, 10(8), 3513–3521.

Costa, F. M. T. A., Maia, S. R., Gomes, P. A. C., & Martins, M. C. L. (2015). Dhvar-5 antimicrobial peptide (AMP) chemoselective covalent immobilization results on

higher antiadherence effect than simple physical adsorption. Biomaterials, 52(0), 531–538.

Croisier, F., & Jérôme, C. (2013). Chitosan-based biomaterials for tissue engineering. European Polymer Journal, 49(4), 780–792.

Crownover, E., Duvall, C. L., Convertine, A., Hoffman, A. S., & Stayton, P. S. (2011). RAFT-synthesized graft copolymers that enhance pH-dependent membrane destabilization and protein circulation times. Journal of Controlled Release, 155(2), 167–174.

Dash, M., Chiellini, F., Ottenbrite, R. M., & Chiellini, E. (2011). Chitosan—A versatile semi-synthetic polymer in biomedical applications. Progress in Polymer Science, 36(8), 981–1014.

Donlan, R. M. (2001). Biofilms and device-associated infections. Emerging Infectious Diseases, 7(2), 277.

Fountoulakis, M., & Lahm, H.-W. (1998). Hydrolysis and amino acid composition analysis of proteins. Journal of Chromatography A, 826(2), 109–134.

Ge, Y., MacDonald, D. L., Holroyd, K. J., Thornsberry, C., Wexler, H., & Zasloff, M. (1999). *In vitro* antibacterial properties of pexiganan, an analog of magainin. Antimicrobial Agents and Chemotherapy, 43(4), 782–788.

Gomes, P., Gomes, C. A. R., Batista, M. K. S., Pinto, L. F., & Silva, P. A. P. (2008). Synthesis, structural characterization and properties of water-soluble N-(γ-propanoyl-amino acid)-chitosans. Carbohydrate Polymers, 71(1), 54–65.

Goodman, S. B., Yao, Z., Keeney, M., & Yang, F. (2013). The future of biologic coatings for orthopaedic implants. Biomaterials, 34(13), 3174–3183.

Gottler, L. M., & Ramamoorthy, A. (2009). Structure, membrane orientation, mechanism, and function of pexiganan—A highly potent antimicrobial peptide designed from magainin. Biochimica et Biophysica Acta (BBA)—Biomembranes, 1788(8), 1680–1686.

Hancock, R., & Patrzykat, A. (2002). Clinical development of cationic antimicrobial peptides: From natural to novel antibiotics. Current Drug Targets—Infectious Disorders, 2(1), 79–83.

Hong, V., Presolski, S. I., Ma, C., & Finn, M. (2009). Analysis and optimization of copper-catalyzed azide-alkyne cycloaddition for bioconjugation. Angewandte Chemie International Edition, 48(52), 9879–9883.

Hu, L., Zhao, P., Deng, H., Xiao, L., Qin, C., Du, Y., *et al.* (2014). Electrical signal guided click coating of chitosan hydrogel on conductive surface. RSC Advances, 4(26), 13477–13480.

Jagasia, R., Holub, J. M., Bollinger, M., Kirshenbaum, K., & Finn, M. G. (2009). Peptide cyclization and cyclodimerization by CuI-mediated azide-alkyne cycloaddition. The Journal of Organic Chemistry, 74(8), 2964–2974.

Jenssen, H., Hamill, P., & Hancock, R. E. (2006). Peptide antimicrobial agents. Clinical Microbiology Reviews, 19(3), 491–511.

Kim, S. E., Harker, E. C., De Leon, A. C., Advincula, R. C., & Pokorski, J. K. (2015). Coextruded, aligned, and gradient-modified poly(epsilon-caprolactone) fibers as platforms for neural growth. Biomacromolecules, 16(3), 860–867.

Krishnakumar, V., & Xavier, R. J. (2004). FT Raman and FT-IR spectral studies of 3-mercapto-1, 2, 4-triazole. Spectrochimica Acta Part A: Molecular and Biomolecular Spectroscopy, 60(3), 709–714.

Liang, L., & Astruc, D. (2011). The copper(I)-catalyzed alkyne-azide cycloaddition (CuAAC) click reaction and its applications. An overview. Coordination Chemistry Reviews, 255(23–24), 2933–2945.

Meldal, M., & Tornøe, C. W. (2008). Cu-catalyzed azide-alkyne cycloaddition. Chemical Reviews, 108(8), 2952–3015.

Monteiro, C., Pinheiro, M., Fernandes, M., Maia, S., Seabra, C. L., Ferreira-da-Silva, F., *et al.* (2015). A 17-mer membrane-active MSI-78 derivative with improved selectivity toward bacterial cells. Molecular Pharmaceutics, 12(8), 2904–2911.

Moura, L. I. F., Dias, A. M. A., Carvalho, E., & de Sousa, H. C. (2013). Recent advances on the development of wound dressings for diabetic foot ulcer treatment—A review. Acta Biomaterialia, 9(7), 7093–7114.

Oliveira, J. R., Martins, M. C. L., Mafra, L., & Gomes, P. (2012). Synthesis of an O-alkynyl-chitosan and its chemoselective conjugation with a PEG-like amino-azide through click chemistry. Carbohydrate Polymers, 87(1), 240–249.

Onaizi, S. A., & Leong, S. S. J. (2011). Tethering antimicrobial peptides: Current status and potential challenges. Biotechnology Advances, 29(1), 67–74. Pischetsrieder, M. (1996). Reaction of L-ascorbic acid with L-arginine derivatives. Journal of Agricultural and Food Chemistry, 44(8), 2081–2085.

Presolski, S. I., Hong, V. P., & Finn, M. G. (2011). Copper-catalyzed azide-alkyne click chemistry for bioconjugation. Current Protocols in Chemical Biology, 3(4), 153–162.

Sahariah, P., Sorensen, K. K., Hjalmarsdottir, M. A., Sigurjonsson, O. E., Jensen, K. J., Masson, M., *et al.* (2015). Antimicrobial peptide shows enhanced activity and reduced toxicity upon grafting to chitosan polymers. Chemical Communications, 51(58), 11611–11614.

Seo, M.-D., Won, H.-S., Kim, J.-H., Mishig-Ochir, T., & Lee, B.-J. (2012). Antimicrobial peptides for therapeutic applications: A review. Molecules, 17(10), 12276–12286.

Shakiba, A., Jamison, A. C., & Lee, T. R. (2015). Poly(l-lysine) interfaces via dual click reactions on surface-bound custom-designed dithiol adsorbates. Langmuir, 31(22), 6154–6163.

Stallmann, H. P., Faber, C., Bronckers, A. L. J. J., de Blieck-Hogervorst, J. M. A., Brouwer, C. P. J. M., Amerongen, A. V. N., *et al.* (2005). Histatin and lactoferrin derived peptides: Antimicrobial properties and effects on mammalian cells. Peptides, 26(12), 2355–2359.

Tang, W., & Becker, M. L. (2014). Click reactions: A versatile toolbox for the synthesis of peptide-conjugates. Chemical Society Reviews, 43(20), 7013–7039.

Van der Weerden, N., M., Bleackley, M., & Anderson, M. (2013). Properties and mechanisms of action of naturally occurring antifungal peptides. Cellular and Molecular Life Sciences, 70(19), 3545–3570.

Zampano, G., Bertoldo, M., Ciardelli, F. (2010). Defined Chitosan-based networks by C-6-Azide-alkyne click reaction. Reactive and Functional Polymers, 70(5), 272–281.

Web References

Dipexium Pharmaceuticals, Inc. (2016) Locilex® Available: [Online]. http://www.dipexiumpharmaceuticals.com/locilex/overview [Accessed 22 July 2016].

Drugs.com (2016) Neomycin, Polymyxin B, Gramicidin [Online]. Available: https://www.drugs.com/pro/neomycin-polymyxin-b-gramicidin.html [Accessed 22 July 2016].

Chapter V

Only a “click” away: development of novel antibacterial coatings

Mariana Barbosa[1,2,3,4], Cláudia Monteiro[2,3], Fabíola Costa[2,3], Filipa Duarte[1], M. Cristina L. Martins[2,3,5], Paula Gomes[1]

Submitted, **2018**

[1]LAQV-REQUIMTE, Departamento de Química e Bioquímica, Faculdade de Ciências, Universidade do Porto, Porto, Portugal
[2]i3S, Instituto de Investigação e Inovação em Saúde, Universidade do Porto, Porto, Portugal
[3]INEB – Instituto de Engenharia Biomédica, Universidade do Porto, Porto, Portugal
[4]Faculdade de Engenharia, Universidade do Porto, Porto, Portugal

Abstract

Antimicrobial peptides (AMP) are powerful components of the innate immune system, as they display wide activity spectrum and low tendency to induce pathogen resistance. Hence, the development of AMP-based coatings is a very promising strategy to prevent biomaterials-associated infections. This work aims to investigate if Dhvar-5-chitosan conjugates, previously synthesized by us *via* azide-alkyne "click" reaction (Barbosa *et al.*), can be applied as antimicrobial coatings. Ultrathin coatings were prepared by spin coater after dissolving Dhvar-5-chitosan conjugate powder in acetic acid. Peptide orientation and exposure from the surface was confirmed by ellipsometry and contact angle measurements. Bactericidal activity was evaluated against *Staphylococcus epidermidis* (*S. epidermidis*), *Staphylococcus aureus* (*S. aureus*), *Escherichia coli* (*E. coli*) and *Pseudomonas aeruginosa* (*P. aeruginosa*), the most prevalent pathogens associated with infected biomaterials. Results showed that Dhvar-5-chitosan coatings displayed bactericidal effect. Moreover, since Dhvar-5 has head-to-tail amphipathicity, it was clear that the bactericidal potency was dependent on which domain of the peptide (cationic or hydrophobic) was exposed. In this context, Dhvar-5 immobilized through its *C*-terminus (exposing its hydrophobic end) presented a higher antimicrobial activity against Gram-positive bacteria (*S. epidermidis* and *S. aureus*) and reduced adhesion of Gram-negative bacteria (*E. coli* and *P. aeruginosa*).

Keywords: antimicrobial peptides, antimicrobial surfaces, bacterial adhesion, biomaterials, chitosan functionalization

1. Introduction

Implant-associated infections (IAI) represent a major problem in medical care with significant societal and economic impact.[1] The decline in the effectiveness of current antibiotherapies is accompanied by the decrease of the period of time between the discovery of a new therapeutic drug and the appearance of a corresponding resistant bacterial strain.[2] The incapacity to fight infection on its onset and consequent bacterial colonization leads to the establishment of biofilms. Fundamentally, biofilms consist of a structured aggregate of bacteria enclosed in a self-produced extracellular matrix capable to adhere and grow on surfaces (either living or non-living).[3] Bacterial cells within the

biofilm matrix assume a dormant state,[3a, 4] which can significantly compromise the efficacy of currently available antibiotics, since their mechanisms of action interfere with bacterial metabolism or proliferation.[3a, 3b, 5] Moreover, biofilms can be resistant to the host's innate and adaptive immune and inflammatory defense systems.[3b, 6] Therefore, it is imperative to develop new therapeutic alternatives that could prevent the onset of biofilm in its first steps of bacterial colonization.

Global interest on antimicrobial peptides (AMP) and their potential applications is regaining momentum, as worldwide healthcare initiatives and facilities are getting out of options to tackle with widespread growth of antibiotic resistance. AMP are natural antibiotics found in every kingdom of life, most of which are easily addressable by chemical synthesis, which in turn enables production of designed analogues with improved therapeutic properties at shorter more cost-effective length.[7] AMP are powerful components of the innate immune system as they display wide spectrum of activity, even at low concentrations, and low tendency to induce pathogen resistance.[2] While originally thought to owe their antimicrobial properties exclusively to interference with pathogen cell membrane permeability, AMP are now known to have other modes of action, such as inhibition of protein and cell wall synthesis or of bacterial enzymes, stimulation of host defense mechanisms, among others.[7a, 7b] Moreover, it has been reported that a given AMP may display different antimicrobial potency and modes of action, depending on diverse factors, such as, concentration (which influences peptide-to-membrane lipid ratio, and peptide aggregation state) or conformation (which affects exposure of charged *versus* hydrophobic regions, and consequent efficiency of the AMP to disturb or even internalize pathogen cells).[8] Therefore, there is still a long way to go in order to completely understand AMP and the influence of different structural and chemical parameters on their overall antimicrobial properties. This is the case of Dhvar-5, a synthetic AMP whose sequence is inspired in salivary histatins, with *N*-terminal hydrophobic and *C*-terminal cationic domains.[9] Originally known to possess antifungal activity against *Candida albicans*, subsequent studies demonstrated both *in vitro* and *in vivo* efficacy against methicillin resistant *S. aureus* (MRSA).[10] The work of Amerongen and colleagues provided some mechanistic insights into the antimicrobial activity of Dhvar-5 associating its "head-to-tail" amphipathicity to the formation of temporary pores on the phospholipid bilayer of bacterial cells with concomitant leakage of cell content.[11] In view of the above, development of AMP-based materials is a highly promising field of research. According to previous studies, AMP were successfully immobilized onto

biomaterial surfaces through different covalent coupling strategies.[12] The overall results demonstrated that, after optimization of immobilization parameters, AMP-coated surfaces can have antiadhesive and antibacterial activity, thus effectively preventing bacterial colonization and consequent biofilm formation, while overcoming AMP's limitations such as low bioavailability, susceptibility to metabolic degradation and cytotoxicity at high concentrations.[2, 12b, 13]

A wide variety of peptide tethering strategies have already been described.[12a] Ranging from a simple amide coupling chemistry, between the pre-synthesized peptide and the material, to the sulfur chemistry in which a thiol-bearing material reacts with a cysteine-containing peptide.[12b, 14] However, some of these strategies end up to be non-selective or originating an unstable bond under bio-reducing conditions.[12b] To tackle with such limitations, chemoselective approaches, the so-called "click" reactions, can be explored; among these, the copper-catalyzed azide-alkyne cycloaddition (CuAAC) is one of the most attractive, given the (i) stability of the triazole link created between the building blocks that are joint together, and (ii) diversity of adequately functionalized building blocks that are commercially available.[15] In this connection, the main goal of the work herein reported was the evaluation of the antimicrobial properties of Dhvar-5-chitosan conjugates whose synthesis *via* CuAAC has been previously optimized by us, [16] and to explore the adaptability of these conjugates in the production of ultrathin films as AMP-based antimicrobial coatings of clinical interest. Overall, the development of highly versatile bulk AMP-chitosan conjugates can be a valuable solution to scale-up production of peptide-based polymer materials and customized manufacturing of multiple more complex scaffolds.

2. Results and Discussion

2.1 Synthesis and Characterization of Dhvar-5 and derivatives

2.1.1. Design and synthesis of Dhvar-5 and derivatives

The selected 14-mer AMP Dhvar-5 (M_w = 1847 Da), LLLFLLKKRKKRKY (from *N* to *C*: leucine-leucine-leucine-phenylalanine-leucine-leucine-lysine-lysine-arginine-lysine-lysine-arginine-lysine-tyrosine), was synthesized as a *C*-terminal carboxamide by means of standard Solid Phase Peptide Synthesis (SPPS), as reported elsewhere.[13]

To evaluate the effect of peptide orientation, two derivatives of Dhvar-5 were designed and synthesized incorporating a spacer and an alkyne functionality (alkyne-AMP), at either the peptide's *N*- or *C*- terminus. The selected flexible spacer, 6-aminohexanoic acid (Ahx), was located between the terminal alkyne moiety provided by the non-natural amino acid propargylglycine (Pra), and the bioactive sequence. The full oligopeptide sequences (M_w = 2056 Da), which will be hereafter designated as Ahx-C_t-Dhvar-5 (Figure 1a) and Ahx-N_t-Dhvar-5 (Figure 1b), were equally assembled by SPPS, as previously described.[13]

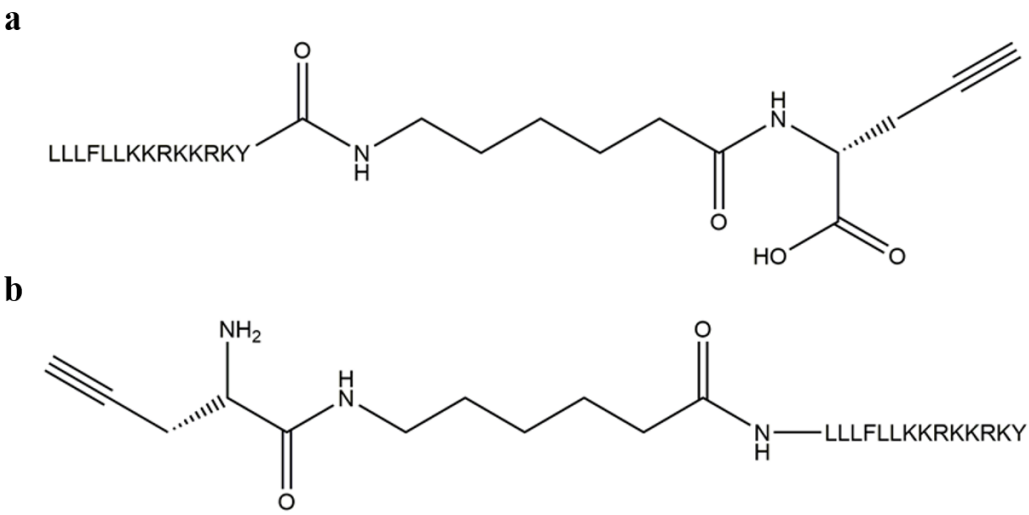

Figure 1 Synthetic derivatives of the antimicrobial peptide Dhvar-5, modified with a flexible spacer and an alkyne moiety at either the peptide's (**a**) N-terminus, or (**b**) C-terminus.

2.1.2. Purification and Analysis of Dhvar-5 and derivatives

The crude peptides were purified by means of preparative high-performance liquid chromatography (HPLC), to an acceptable minimal purity degree of 95%. The final purity was assessed by analytical HPLC. The purified peptides presented the HPLC chromatograms displayed in Figure 1S. The mass spectra (MS) were acquired in the positive mode, using an electrospray ionization source coupled to an ion trap detector. Liquid Chromatography-Electrospray Ionization/Ion Trap Mass Spectrometry (LC-ESI/IT MS) were performed to confirm that the target peptides had been successfully obtained. The LC-ESI/IT MS spectra (Figure 2S) revealed several peaks consistent with the peptides at different protonation degrees.

2.2 Synthesis of AMP-chitosan conjugates

Chitosan was selected as the biocompatible polymer carrier for covalent grafting of AMP by means of "click" chemistry. Chitosan is the result of chitin deacetylation in the presence of alkaline agents. The amine groups present in chitosan are responsible for its charge, reactivity and a soluble-insoluble transition depending on pH. This pH-dependent transition makes chitosan extremely versatile, allowing its application in different biomaterials processing techniques.[17] Importantly, chitosan structure is also responsible for a number of clinically interesting features, such as antimicrobial properties[18], mucoadhesivity[19], anti-inflammatory[20], antioxidant[21], osteogenic[22] and biodegradability[23], making this polymer a very interesting candidate for biomedical application. Taking the above in consideration we carried out modification of chitosan amines and subsequent AMP tethering *via* CuAAC as previously optimized by us.[16] Briefly, chitosan was first functionalized by direct conversion of the polymer's amines into azides, using imidazole-1-sulfonyl azide hydrochloride (ISA·HCl) as the diazo-transfer reagent, yielding azido-chitosan (N_3-chitosan).[16, 24] Then, both alkyne-AMP, previously assembled by SPPS, were reacted with N_3-chitosan via CuAAC. Both N_3-chitosan and chitosan-Ahx-Nt-Dhvar-5 conjugate were synthesized as previously reported by us, evidencing the expected structural characteristics.[16] To evaluate the effect of peptide orientation, a novel conjugate was synthesized following a similar procedure, but where the peptide Ahx-Ct-Dhvar-5 was immobilized onto chitosan *via* its *C*-terminus. The successful synthesis of the new chitosan-Ahx-Ct-Dhvar-5 conjugate was confirmed by X-ray photoelectron spectroscopy (XPS) and Fourier transform infrared spectroscopy (FT-IR), as follows.

XPS N (1s) high-resolution spectroscopy was useful to detect chemical modifications, since both functionalization and immobilization reactions translate into different chemical states of nitrogen. Table 1A shows the percentage of N (1S) involved in the different chemical bonds. The success of CuAAC reaction, was corroborated by the substitution of a peak at 404.5 eV, assigned to nitrogen in azide groups, by a peak at 400.0 eV, which validates the formation of the triazole ring.[16]

Regarding FT-IR results (Table 1B), chitosan-Ahx-C_t-Dhvar-5 conjugate displayed the expected characteristic peaks, similar to those previously described for the analogous chitosan-Ahx-N_t-Dhvar-5 conjugate.[14b, 16] As such, success of CuAAC reaction was confirmed by (i) the disappearance of characteristic azide peaks (2115 and 1319 cm^{-1}),

(ii) intensity increase of both amide I and II bands (1640–1560 cm^{-1}), corroborating effective peptide immobilization onto N_3-chitosan and (iii) appearance of a weak band at 836 cm^{-1}, typical of N–C=N in plane bending, arising from formation of the expected triazole ring.[14b, 16]

Table 1 The synthesis of chitosan-Ahx-C_t-Dhvar-5 conjugate was confirmed by FT-IR and XPS analysis: (A) N (1s) relative surface atomic composition of chitosan and its derivatives; (B) FT-IR main characteristic bands of the conjugate.

(A)	**Atomic% N (1s)**			
	C–N/CO–N	CO–N–CO/N–CO–O	NH_3^+	$N=N^+=N^-$
	399.5 eV	**400.0 eV**	**401.4 eV**	**404.5 eV**
	33	50	17	-
(B)	**Wavelength (cm^{-1})**			
	$N^- =N^+= N^-$ Asymmetric stretching	C=O stretching/N–H bending	C–O–C Stretching vibration	N–C=N in plane bending
	2115/1319	**1640-1560**	**1076**	**836**
	Disappearance of characteristic azide peaks	Intense amide I/II bands (supporting peptide grafting)	Glucopyranose ring (characteristic of chitosan)	Formation of triazole ring

The application of CuAAC click chemistry for AMP immobilization was previously performed by Li *et al.*,[25] Santos *et al.*[26], Lin *et al.*[27] and Sahariah *et al.*[14b]. First attempts (Li *et al.*,[25] Santos *et al.*[26] and Lin *et al.*[27]) had important differences regarding the work herein described, namely, (i) the immobilization was performed upon pre-prepared surfaces (such as Ti or silicon(111)) and (ii) the click-chemistry building blocks were applied the other way around, i.e., with the azide moiety being linked to the AMP. In the work of Sahariah *et al.*[14b] work, CuAAC click chemistry was similarly applied for the development of AMP-chitosan conjugates, however, in this case organic solvents were applied instead of our aqueous conditions, and no further report on the application of such conjugates on biomaterial/device fabrication seems to have been published. The major advantage of developing ground conjugates is that they are amenable to direct fabrication in customized biomaterial forms (e.g, scaffolds, coatings, particles) without further optimization of the AMP immobilization procedures.

Amino Acid Analysis (AAA) of the chitosan-Ahx-C_t-Dhvar-5 conjugate was used to quantify the amount of Dhvar-5 grafted onto chitosan backbone. Result (~50 μmol of peptide per g of chitosan) was in accordance with that previously obtained for the chitosan-Ahx-N_t-Dhvar-5 conjugate.[16] This peptide density suggests that both bulk AMP-chitosan conjugates, chitosan-Ahx-N_t-Dhvar-5 and chitosan-Ahx-C_t-Dhvar-5, have potential to be used in the preparation of tailored antimicrobial materials, given the promising antimicrobial activity of Dhvar-5 peptide at low concentrations against biofilm-forming organisms such as MRSA and *Staphylococcus epidermidis* (*S. epidermidis*).[9, 13b]

2.3 Antimicrobial activity of Dhvar-5 and its chitosan conjugates

The antimicrobial activity of Dhvar-5 and Dhvar-5-based conjugates was evaluated against four of the most prevalent pathogens found within the setting of biomaterials-associated infections: two Gram-positive bacteria, *S. aureus* (ATCC 49230) and *S. epidermidis* (ATCC 35984), and two Gram-negative bacteria, *Escherichia coli* (*E. coli*, ATCC 25922) and *Pseudomonas aeruginosa* (*P. aeruginosa*, ATCC 27853).[28] Dhvar-5 antimicrobial activity was firstly assessed in solution, by an adaptation of the microtiter broth dilution method proposed by Wiegand and co-workers.[29] Minimum inhibitory concentration (MIC) and minimum bactericidal concentration (MBC) values for Dhvar-5 are given in Table 2.

Table 2 MIC and MBC values for soluble Dhvar-5 against the four selected microorganisms.

Microorganisms	**MIC (μg/mL)**	**MBC (μg/mL)**
S. aureus (ATCC 49230)	4	32
S. epidermidis (ATCC 35984)	2	16
E. coli (ATCC 25922)	16	64
P. aeruginosa (ATCC 27853)	4	64

Both MIC and MBC values were lower for *S. epidermidis* (2 μg/mL and 16 μg/mL, respectively), meaning that this bacterium was the most susceptible to Dhvar-5. The MIC value observed for *E. coli* (16 μg/mL), although being the highest amongst the assayed bacteria, was still a relatively low concentration, as opposed to a previous study where this peptide was reported not show any activity against *E. coli*.[30]

Regarding MBC values, both Gram-negative species, *E. coli* and *P. aeruginosa*, required higher AMP concentrations to achieve a bactericidal effect. Cationic AMP have been shown to permeabilize the bacterial cell wall of Gram-negative bacteria by binding to existing lipopolysaccharides (LPS).[31] Schneider's group highlighted the importance of arginine residues to the activity of AMP against Gram-negative bacteria, as the guanidinium groups of arginine side chains can establish strong bidentate hydrogen bonds and salt bridges with the phospho-rich membrane surface of such bacteria.[32] Thus, high arginine content often equates to strong lytic behavior for AMP. However, peptides with up to two arginine residues, as in Dhvar-5, were found to display lower affinity for LPS, thus being less active against Gram-negative bacteria. In this connection, the same research group further demonstrated that a minimum of four arginine residues was needed for an improved activity against *E. coli*.[31-32] Recent work by Cutrona and colleagues reported the relevance of cationic residues content, namely arginine and lysine, on the overall antibacterial activity against an *E. coli* strain, using AMP with distinct mechanisms of action. This study highlighted the importance of increasing the arginine to lysine ratio. Previous studies had also implied that the corresponding arginine and lysine amino acid side chains (guanidinium and amine group, respectively) interact differently with the lipidic portion of bacterial cell walls.[33] Moreover, a previous study by Strom *et al.* evaluated the effect of peptide hydrophobicity and net charge on the AMP's bactericidal effect on different bacteria.[34] They observed that a peptide with a net charge of +2 and the presence of at least two bulky/lipophilic moieties was active against Gram-positive *S. aureus* but demonstrated limited activity against Gram-negative *E. coli*.[34] Although having a much higher positive net charge, Dhvar-5 is also very rich in hydrophobic residues like leucine and phenylalanine, which may contribute to its lower activity against *E. coli*.

Overall, Dhvar-5 presented promising MIC values against the bacterial species tested, which were lower than those reported elsewhere.[9, 30, 35] However, a direct comparison between the MIC values herein reported and those found in the literature, is very challenging. On one hand, distinct bacterial strains were employed in the different studies, and on the other hand, there is a lack of conventional standardized procedures to determine AMP efficacy. Consequently, assessment of our data at the light of previously reported MIC will hardly be meaningful.

Noteworthy, the antimicrobial activity of chitosan and AMP-conjugates in solution was evaluated following a similar procedure. In solution, unmodified chitosan displayed

antimicrobial activity at significantly higher concentrations (MIC values ranged from 0.16 to 1.25 mg/mL, depending on the bacteria). Results (not shown) demonstrated that, in solution, azide-modified and peptide immobilized-chitosan seemed to lose their intrinsic antimicrobial effect against all bacterial species tested, independently of peptide orientation and concentration. This result contrasts those obtained by Sahariah *et al*., where anoplin-chitosan conjugates were effective against both Gram-positive and Gram-negative bacteria. Anoplin is a naturally occurring short AMP (10 amino acid residues) exhibiting a heptad repeat sequence. The differences may be connected with the much lower molecular weight of the chitosan used (~94 kDa) by those autors, and/or with the conformation adopted by anoplin after the immobilization procedure (which was reported to have a similar conformation to soluble anoplin upon contact with membranes). Literature suggests that chitosan owes its antimicrobial activity to the presence of free amino groups found in the polymer's backbone.[36] Therefore, functionalization of chitosan at the polymer's primary amino groups might have influence in its amine-dependent properties in solution and, consequently, in its ability to exert bactericidal effects when in its soluble form.[37However, modification of chitosan's primary amines does not seem a fair justification for the lack of antimicrobial activity of our AMP-chitosan conjugates in solution, as Dhvar-5 is an AMP rich in lysine residues, which exhibit primary amine groups in their side-chain. Actually, the observed loss of bactericidal effect may be due to a substantial change in the structure and packaging of the polymer, which is not only supported by the morphological changes previously observed in the amorphous powder of the chitosan-Ahx-Nt-Dhvar-5 conjugate [16], but also by the significant decrease in the viscosity of the aqueous solutions of the conjugates, when compared with those of the original chitosan; eventually, the antibacterial activity of chitosan in solution depends not only on the amines, but also on the very structure that the polymeric mesh adopts in that medium, which is clearly altered after conjugation with the peptides *via* CuAAC.

2.4 Synthesis and characterization of AMP-chitosan ultrathin films

The synthetic AMP-chitosan conjugates were used to produce thin films by spin-coating (Figure 2). Surfaces thus obtained were characterized using ellipsometry and contact angle measurements, as next described.

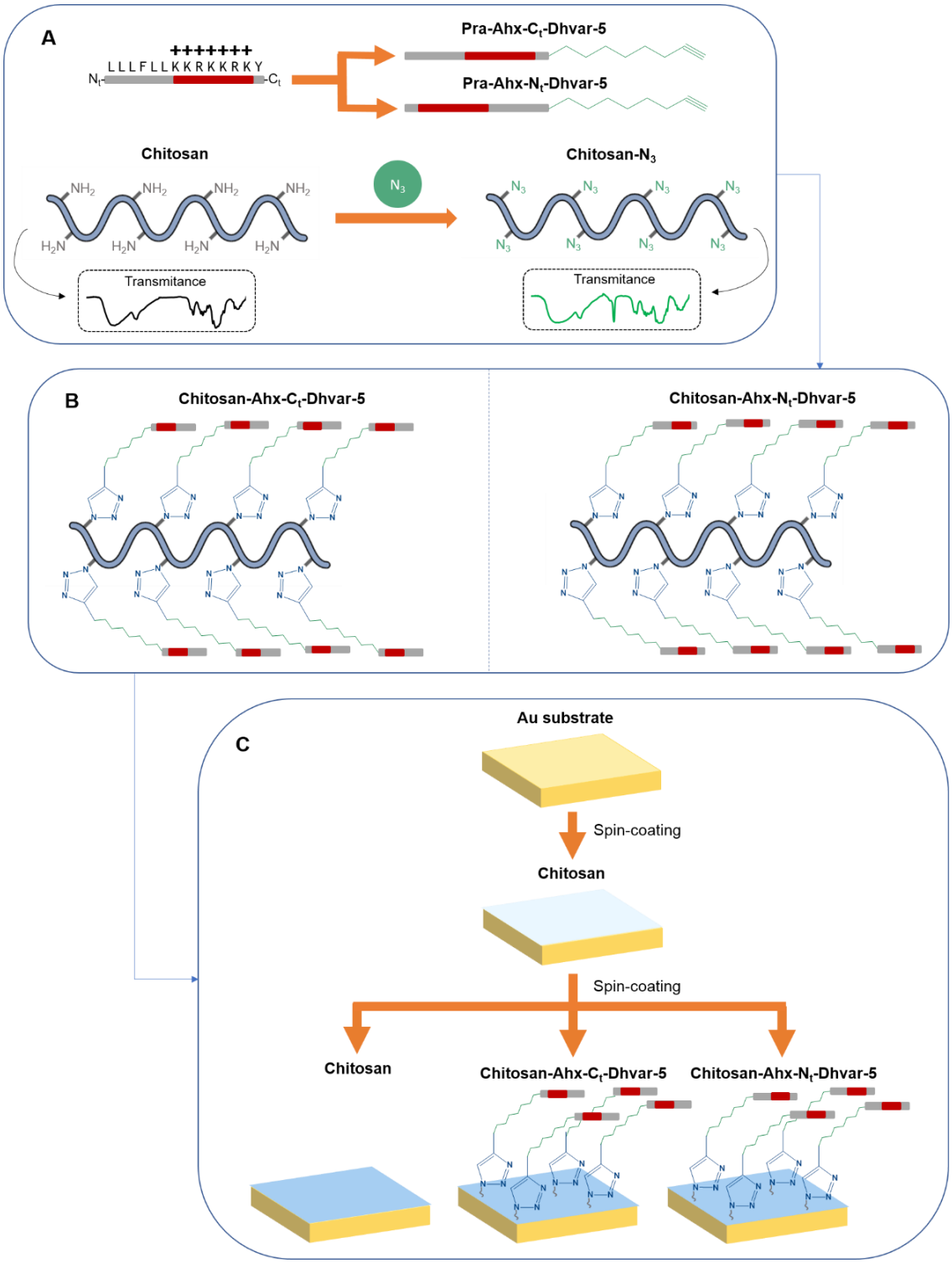

Figure 2 Schematic synthetic route towards AMP-chitosan conjugates[13] and respective ultrathin films: (**a**) two derivatives of the selected AMP incorporating an alkyne functionality (alkyne-AMP) at either the *N*- and *C*-terminus were prepared to assess the effect of peptide orientation; in parallel, N_3-chitosan was produced by conversion of chitosan's amines into azides, which could be confirmed by the appearance of a band in the infra-red (IR) transmittance spectrum at ca. 2115 cm^{-1}, typical of azide groups; (**b**) synthesis of bulk Peptide-chitosan powders, by means of CuAAC between each of the two alkyne-AMP and N_3-chitosan; progress of this reaction could be monitored by disappearance of the aforementioned azide-associated IR band; (**c**) thin film production by spin-coating, using chitosan as control.

2.4.1 Ellipsometry

The thickness of chitosan and AMP-chitosan ultrathin films is depicted in Figure 3. Noteworthy, the thickness of each film was determined at several regions of interest of the samples, to access their homogeneity.

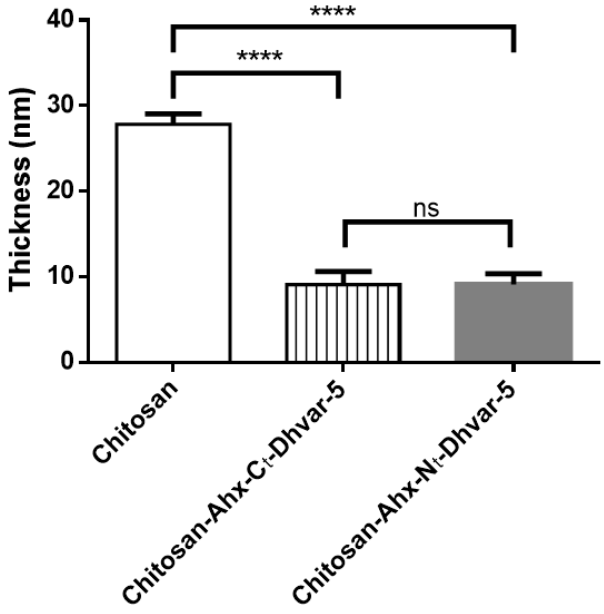

Figure 3 Ellipsometry analysis of chitosan and AMP-chitosan thin films (One-Way ANOVA analysis, $p < 0.05$).

The spin-coating process resulted in chitosan ultrathin films of 28 ± 1.2 nm and AMP-chitosan ultrathin films of 9.1 ± 1.5 nm and 9.1 ± 1.3 nm for chitosan-Ahx-C_t-Dhvar-5 and chitosan-Ahx-N_t-Dhvar-5, respectively. Results showed a significant thickness decrease ($p < 0.05$; One-way ANOVA) in AMP-chitosan thin films when compared to control chitosan films. This was likely due to observable differences in viscosity between the AMP-chitosan conjugates and chitosan solutions used to prepare the films, since immobilization of Dhvar-5 onto chitosan improved the solubility of the final polymer, as compared to the original one. Moreover, no significant difference was observed between the two AMP-chitosan films.

2.4.2 Water contact angle measurements

Water optical contact angles (WCA) of the control and AMP-chitosan films were evaluated following two methodologies: (i) sessile drop method (Figure 4a) and (ii) captive bubble method (Figure 4b).

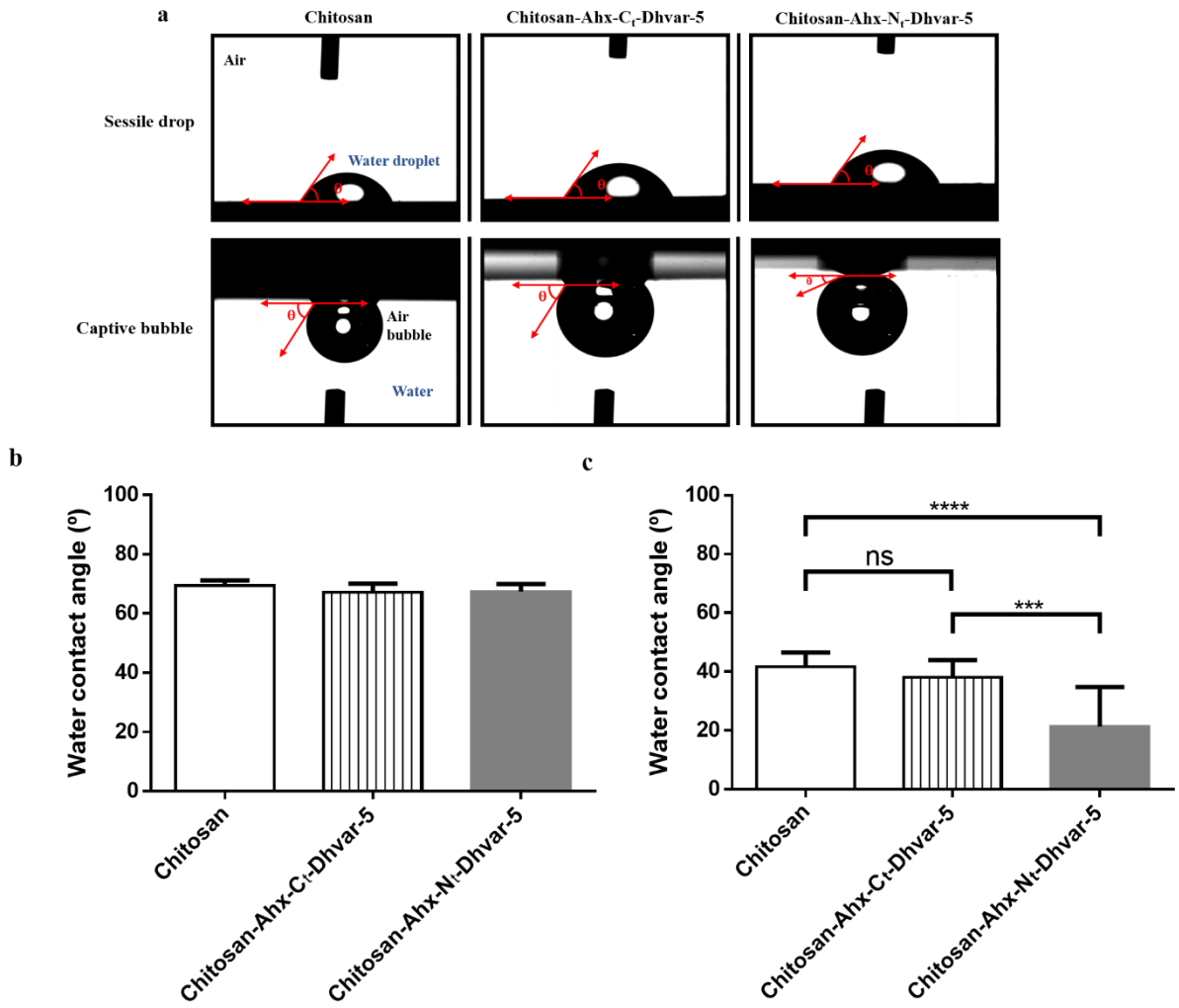

Figure 4 Water optical contact angles for chitosan and AMP-chitosan thin films: (**a**) schematic view of the sessile drop and the captive bubble methods (θ: contact angle); and contact angle measurements by (**b**) sessile drop, and (**c**) captive bubble methods (One-Way ANOVA analysis, $p < 0.05$).

The sessile drop method was our first choice, whereby the control chitosan thin film presented a contact angle of $\theta_w = 69^o$. However, no significant difference was observed between the samples with immobilized peptide (Figure 4a), independently of peptide's orientation, which was puzzling. Differences arising from the two distinct peptide orientations had been anticipated, with the surface exposing the peptide's *N*-terminus being predictably more hydrophobic than the other that exposes the cationic *C*-terminus of Dhvar-5. We postulated that such unexpected result might arise from the fact that the sessile drop method requires the use of a dry surface, which could have driven the peptide chains to aggregate and/or "fold inwards", resulting in a surface whose behavior would resemble that of chitosan itself. As such, we opted to reassess WCA values by means of the captive bubble method, which maintains the surface of the sample completely

hydrated and, consequently, the surface energy unaltered throughout the measurements.[38] This effect on the surface energy can be explained as a consequence of the conformation alteration of the hydrophilic macromolecular chains. In brief, at the interface of AMP-chitosan films and air, in the sessile drop measurement, the hydrophobic domain of the peptide tends to aggregate on the surface in order to reduce the interfacial energy. On the other hand, in the captive bubble method, at the interface of thin films and water, the molecular structure of the hydrophilic moieties reorganize occupying the surface, resulting in the expected lower contact angles.[39] Moreover, in this method, the hydration of the films closely reproduces the conditions to which the films will be exposed during antimicrobial activity assays.

As depicted in Figure 4b, the captive bubble method revealed significant differences in the contact angles of the conjugates. The AMP-chitosan films with Dhvar-5 immobilized through its *C*-terminus (exposure of the hydrophobic region of the peptide) presented a relatively high WCA value of $\theta_w = 38^o$, since the air bubble tends to exclude water and to spread across the surface, thus creating a larger contact angle. On the other hand, in the case of chitosan-Ahx-N_t-Dhvar-5, the samples showed a more hydrophilic behavior associated with a smaller WCA ($\theta_w = 21^o$), which is consistent with exposure of the positively charged region of the peptide ($p<0.05$, One-Way ANOVA). No significant difference was observed between samples with peptide immobilized through its *C*-terminus and unmodified chitosan.

2.4.3 Surface adhesion and viability assays of AMP-chitosan ultrathin films

Antimicrobial activity assays were carried out through surface adhesion and viability measurements using the aforementioned Gram-positive (*S. aureus* and *S. epidermidis*) and Gram-negative (*E. coli* and *P. aeruginosa*) bacteria.

Bacterial adhesion and viability studies on *S. aureus* and *S. epidermidis* demonstrated that AMP-chitosan thin films had a bactericidal effect on both species (Figure 5, Figures 6a,b).

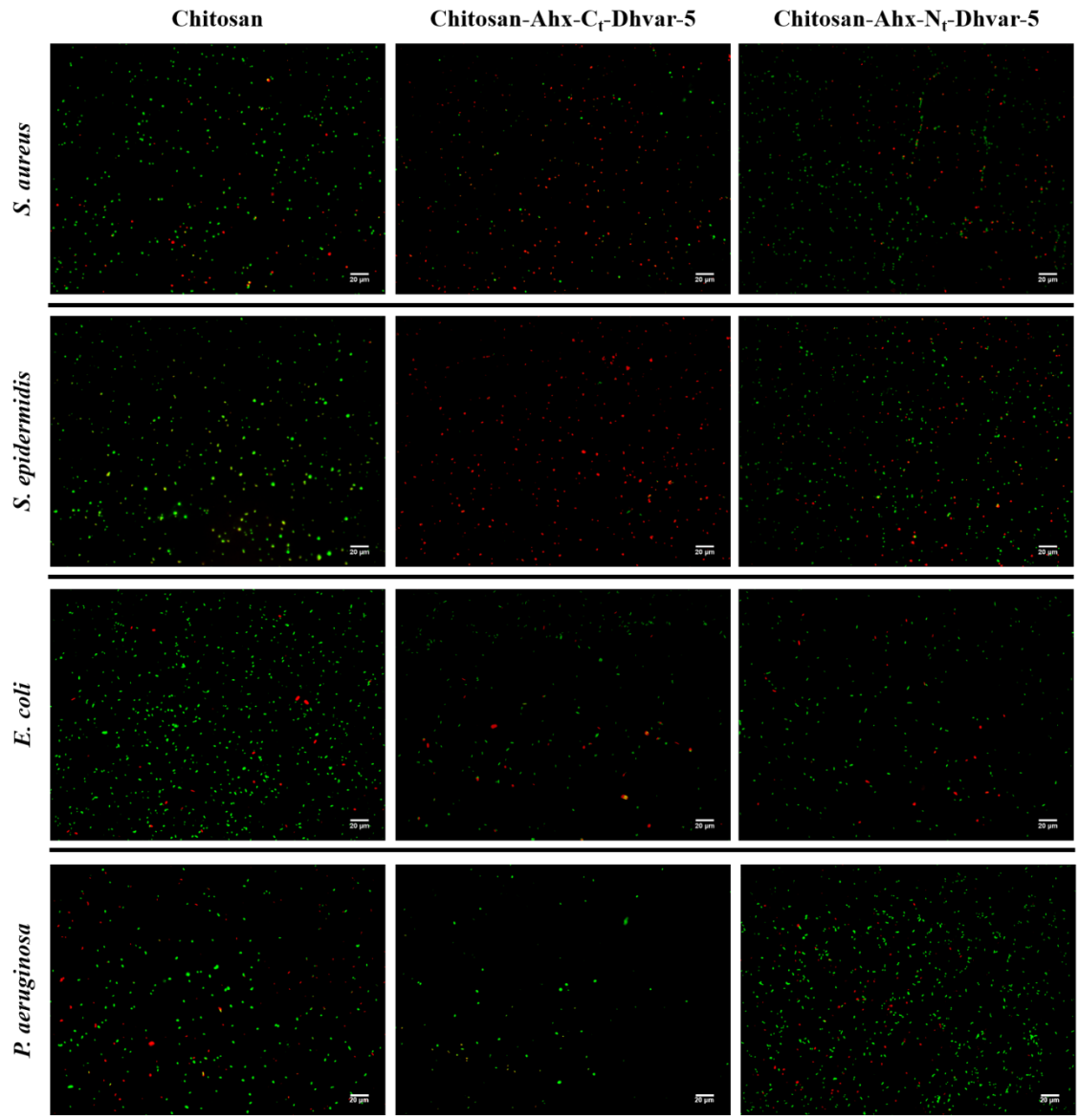

Figure 5 Representative images of the LIVE/DEAD® Bacterial Viability Kit (Baclight™) staining of the total adhered bacteria in the different thin film surfaces prepared. An inverted fluorescence microscope was used with a magnification of 400×. Scale bar corresponds to 20 μm.

Covalently immobilized Dhvar-5 resulted in different antimicrobial activity depending on the peptide terminus/domain that was exposed. This is in agreement with Sahariah *et al.*[14b] work, where the orientation of the AMP relative to the chitosan backbone was also found to influence the activity profile of the anoplin-chitosan conjugates, as anoplin tends to adopt an amphipathic α-helical structure. In their case, AMP N-linkage was more effective against *Enterococcus faecalis* and *P. aeruginosa*, while AMP C-linkage was more effective against *E. coli*. In our work, the AMP-chitosan surface with higher antimicrobial activity, for both Gram-positive species, was chitosan-Ahx-C_t-Dhvar-5, where Dhvar-5 was covalently bound through its *C*-terminus, thus exposing the *N*-

terminal hydrophobic domain. In fact, samples of chitosan-Ahx-C_t-Dhvar-5 coatings exhibited an improved antibacterial effect, thus an increase in dead adhered bacteria, when compared to chitosan control sample (~60% and ~50% increase for *S. aureus* and *S. epidermidis*, respectively) (Figures 6a,b).

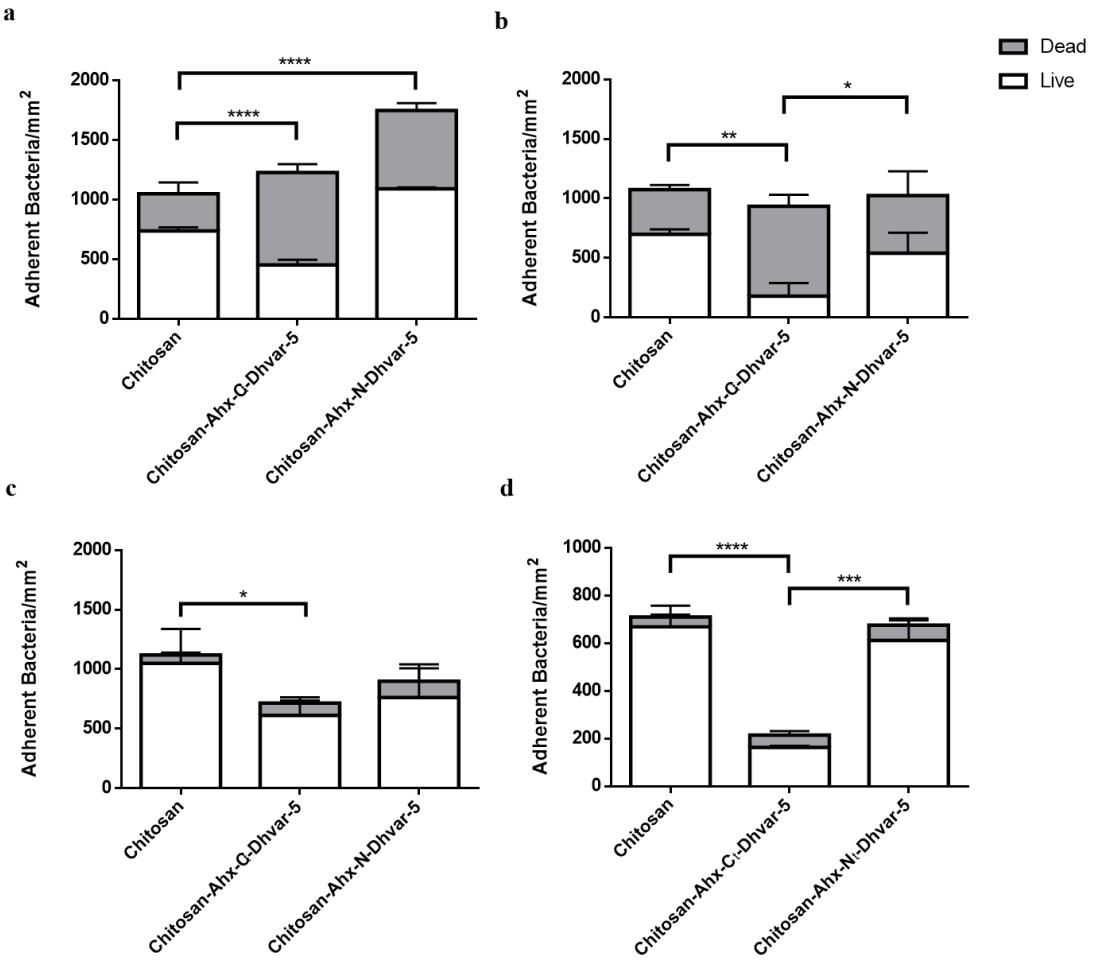

Figure 6 Viability of adhered (**a**) S. aureus, (**b**) S. epidermidis, (**c**) E. coli, and (**d**) P. aeruginosa, incubated at 37 °C for 5 h (Two-Way ANOVA analysis for total adherent bacteria, $p < 0.05$).

With regard to Gram-negative bacteria used, *C*-terminal immobilization of Dhvar-5 equally led to stronger antibacterial effects, by decreasing bacterial colonization, than when immobilized through its *N*-terminus, further supporting that exposure of the hydrophobic domain seems to be a key feature to optimize antimicrobial effects of peptides with head-to-tail amphipathicity,[40] like Dhvar-5. Indeed, Hilpert *et al.* [41] rearranged the sequence of a known active peptide, *C*-terminally immobilizing the different variants, and concluded that the placement of cationic residues close to the linker site correlated with increased antimicrobial activity in opposition to peptides with cationic residues localized at the exposed *N*-terminus or within the middle portion of the peptide.

The positioning of hydrophobic residues proximal to the *N*-terminus was critical to the activity of their immobilized AMPs, supporting the conclusion that the exposure of the hydrophobic domain might maximize insertion into the bacterial lipid bilayer.
Regarding Gram-negative bacteria, antimicrobial activity was associated to a significant decrease in bacterial adhesion rather than to the killing of adhered cells (Figure 5, Figure 6c,d). The lack of a strong bactericidal effect in this case was not surprising, based on our own observations (*cf.* **2.3**) and previous reports[30] for this AMP in solution. Still, it is quite remarkable that chitosan-grafted Ahx-C_t-Dhvar-5 has nonetheless a considerable anti-fouling effect, equally holding great promise for development of anti-fouling coatings against Gram-negative bacteria. Noteworthy, this effect was also more evident for samples with peptide covalently immobilized through its *C*-terminus displaying an evident antiadhesive effect (~31% and ~70% reduction for *E. coli* and *P. aeruginosa*, respectively, when compared to control chitosan).

The above observations are not in agreement with the reported anti-fouling effect of *N*-terminally immobilized Dhvar-5 against *S. aureus*, formerly described by Costa *et al.*[11c] Also, Chen *et al.* [42], Lim *et al.*, [43] and Lin *et al.*, [27] studied head-to-tail amphipathic AMPs, and found promising results with cationic domain exposure. Instead, our results suggest that immobilization of Dhvar-5 by its *N*-terminus may actually promote bacterial adhesion to the coating, as compared to control chitosan (Figures 5, 6a,b), an apparent discrepancy which may be due to the different immobilization chemistries used in the two works, eventually leading to different peptide density/conformations/exposures in the final material. The different methods used to evaluate antibacterial activity (*cf.* **4: Experimental Section** - *Surface antimicrobial activity evaluation*) can also account for the aforementioned disparities. The mode of action and efficacy of a given AMP is highly influenced by several structural and chemical parameters.[12b] Indeed, Lozeau *et al.*,[44] covalently tethered cysteine-modified chrysophsin-1 (C-CHY1) *via* polyethylene glycol (PEG) linkers of three different molecular weights, 866, 2000, and 7500, and suggested different AMP mode of action to each immobilization: the PEG 866 tether was associated to the displacement of positive cations from bacterial membranes, the PEG 7500 tether was associated to the C-CHY1's ability to effectively form membrane pores, promoting the highest activity, while the PEG 2000 tether had limited antimicrobial activity apparently because neither mechanism of AMP activity was able to occur. This may explain the apparently contradictory results found by us regarding the activity of (i)

soluble *versus* immobilized Dhvar-5 conjugates, or (ii) the stronger antibacterial activity herein reported for *C*-terminally immobilized Dhvar-5 *via* "click" chemistry, in contrast with the higher anti-fouling effects previously reported for an *N*-terminally immobilized Dhvar-5 *via* surface-peptide disulfide bond formation.[11c] While conformational and local concentration differences are to be expected when going from soluble to surface-grafted AMP,[45] it is also reasonable to assume that similar differences may occur between peptide-grafted surfaces *via* a bio-reducible, polarizable, and bulky (due to sulfur atoms) disulfide linker, as compared with a stable, more rigid and planar triazole one, which is also more prone to establish hydrogen bonds, favoring stronger solvation in aqueous environments as under physiological conditions. Indeed, changes in peptide conformational and bioactivity properties in consequence of replacement of disulfide bonds by triazole linkers have been reported.[46] Moreover, in Raspch *et al.*[47] work, different immobilization chemistries were applied (pre-activated reactive surfaces with epoxy, aldehyde, NHS, and *p*-phenylene diisothiocyanate (PDITC) functionalities were used to conjugate with AMPs free amines), using AMPs with different putative mechanisms of action. They reported that different immobilization moieties could strongly influence the antimicrobial surface performance. They also suggested that the inclusion of a spacer and peptide surface density are more important than peptide orientation. However, they did not actually test specific immobilization orientation, as the peptide's free amines were unspecifically used for immobilization.[47] Also, Yu *et al.*,[48] reported that at similar graft and AMP density, the variation of the brushes chemistry applied, influenced the immobilized AMP antimicrobial activity. They stated that conformation changes of tethered AMP are dependent on brush chemistry. Moreover, in the work of Santos *et al.*,[26] the CuAAC click chemistry was applied to immobilize N_3-OEG-IG-25 to the alkynyl group on the surface of fluorous slides and compared with IG-25 randomly bound *via* carbodiimide chemistry. The surfaces presenting IG-25 tethering to the surface at the *N*-terminus *via* click chemistry displayed higher antibacterial activities against *P. aeruginosa* (strain PA-O1), although presenting a lower surface concentration regarding the carbodiimide immobilization. The lower activity of the carbodiimide linked surfaces is probably due to the lack of control on the number and location of sites at which the molecule is attached onto the surface, since the molecule has multiple amino groups that can react with the carboxylated surface; this highlights the usefulness of the chemo-selective approaches as CuAAC click chemistry.[25-26] The CuAAC-produced triazole linkage is known for its stability, and bioactivity, which

explains why "click" chemistry is becoming increasingly popular in the development of peptide-based drugs and materials.[49]

Finally, it seems relevant to highlight the fact that we have applied CuAAC "click" chemistry to graft the AMP onto ground chitosan and using next the bulk powder produced to prepare thin films. To the best of our knowledge, all previous reports on covalent peptide immobilization have addressed peptide grafting onto pre-assembled surfaces or scaffolds, meaning that immobilization procedures have to be repeated and optimized each time a different type of material is targeted. In turn, powdered peptide-tethered biopolymers, as those herein reported and used to prepare the films, are (i) fitter for large-scale production, and (ii) easier to handle for fabrication of different materials.

3. Concluding Remarks

Dhvar-5 grafting onto chitosan by CuAAC was produced in both possible orientations, i.e., the peptide was covalently immobilized via either its *N*- or its *C*-terminus. Antimicrobial activity assays demonstrated that the AMP-chitosan thin films had bactericidal effects whose potency depended on which region of the peptide was exposed; as such, higher antimicrobial activity was observed when Dhvar-5 was immobilized through its cationic *C*-terminus, i.e., exposing its hydrophobic domain.

Altogether, the work herein reported contributes to demonstrate the use of CuAAC "click" chemistry as an efficient and highly selective method to graft AMP onto chitosan, yielding conjugate powders that are suitable for the production of thin films with excellent prospects for application as antimicrobial coatings.

4. Experimental Section

Synthesis, purification and characterization of Dhvar-5 and derivatives: Peptide syntheses, purification and analyses were carried out as previously described by us.[16] Briefly, peptides were produced as *C*-terminal carboxamides by means of standard Fmoc/^{t}Bu SPPS methodologies assisted with microwave (MW) energy, on a Liberty1 equipment from CEM (Mathews, NC, USA). Crude peptides were purified by preparative HPLC to a purity of at least 95%, as determined by analytical HPLC. Peptides were injected into a preparative HPLC system (LaPrep Sigma VWR with UV detector LP 3104

and LP 1200 pump) with a reverse-phase Merck C18 column (250 × 25 mm ID and 5 μm pore size) at a flow rate of 15 mL/min using as solvents 0.05% aqueous TFA (eluent A) and acetonitrile (eluent B) for 60 min. Purity degree was then determined by analytical HPLC, using a Hitachi-Merck LaChrom Elite system equipped with a quaternary pump, a thermostatted automated sampler, and a diode-array detector (DAD).
LC-MS analysis was used to obtain a clear-cut confirmation that target peptides had been correctly synthesized. MS analyses were performed on an LTQ Orbitrap TM XL hybrid mass spectrometer (Thermo Fischer Scientific, Bremen, Germany). MS data handling software (Xcalibur QualBrowser software, Thermo Fischer Scientific) was used to obtain the confirmation of the synthetic peptide by their exact *m/z* value.

Chitosan purification: Commercial squid pen chitosan with high-molecular weight (M_w > 500 kDa) and a 94% degree of deacetylation (DD), was obtained from France-Chitine. Chitosan was purified by the reprecipitation method, as reported elsewhere.[50] Briefly, chitosan was hydrated in type I water, completely solubilized in acetic acid (0.2 M), filtered through a 20 μm pore size filter and then precipitated upon addition of 1M NaOH. Finally, the recovered chitosan was rinsed with type 2 water by centrifugation until neutrality, freeze-dried and grounded in a laboratory mill (IKA mill) to yield a fine powder.

Preparation of N_3-chitosan: Chitosan was functionalized by direct conversion of the polymer's amines into azides, following a recent report.[16] Briefly, the reaction was carried out using potassium carbonate (Sigma-Aldrich) and ISA·HCl (kind gift from Professor Fernando Albericio, from the Institute of Biomedical Research of Barcelona (IRB-Barcelona)) in aqueous medium, under magnetic stirring, for 24 h at room temperature. The product, N_3-chitosan (N_3-chitosan), was then dried in vacuum.

AMP-immobilization onto N_3-chitosan: The conjugation between both alkyne-modified AMP and N_3-chitosan was carried out as previously described by Barbosa *et al.*[16] Briefly, N_3-Chitosan reacted with the peptide in the presence of $CuSO_4$•H_2O (Sigma-Aldrich) and sodium ascorbate (Sigma-Aldrich). Tris(3-hydroxypropyltriazolylmethyl) amine (THPTA) (Sigma-Aldrich) and aminoguanidine hydrochloride (TCI Chemicals) were also added. The reaction was performed in type 2 water, at room temperature, for

48 h. The solid fraction was collected by centrifugation, thoroughly washed with 0.1 M aqueous EDTA (Sigma-Aldrich), 5% aqueous sodium bicarbonate (Sigma-Aldrich), and finally type 2 water. Modified chitosan was dialyzed (M_w cut-off 3.5 kDa from Spectrum Lab) against 1% hydrochloric acid (Sigma-Aldrich) for three days, against type 2 water for two days. After dialysis, the final AMP-chitosan conjugates were centrifuged and dried in vacuum.

XPS analysis: Samples were prepared by compressing the powdered polymers into thin pellets. Analysis were performed on a Kratos Axis Ultra HAS spectrometer (from CEMUP – Centro de Materiais da Universidade do Porto) with aluminum (15 kV) as the radiation source. Photoelectrons were analyzed at a 90° take-off angle between the horizontal surface plane and the electron analyzer optics. High-resolution of N1s spectrum was collected with analyzer pass energy of 40 eV. Spectra were fitted using the CasaXPS software (version 2.3.17PR 1.1).

FT-IR analysis: FT-IR spectra of chitosan and its derivatives were acquired using a Perkin-Elmer Perkin Elmer FT-IR spectrophotometer, model Frontier. FTIR spectra in transmission mode were acquired in a DTGS (deuterated triglycine sulfate) detector. All the samples were recorded as KBr pellets prepared by combining 2 mg of the powdered polymer, previously dried overnight under reduced pressure, with 200 mg of KBr, previously dried at 110 °C for 24 h. The spectra resulted of the average of 100 consecutive interferograms at 4 cm^{-1} resolution, between 4000 and 400 cm^{-1}.

AAA: The content and ratio of amino acids present in the AMP-chitosan conjugates were determined by AAA. The first step of AAA involves acid hydrolysis of the samples. The hydrolysis was performed with 6 M aqueous HCl at 110 °C for 24 h. After that time, the sample was evaporated to dryness at reduced pressure. The dry residue was dissolved in type 1 water with aminobutyric acid as an internal standard, and then derivatized using 6-aminoquinoyl-*N*-hydroxysuccinimidyl carbamate following the AccQ-Tag protocol from Waters. Finally, the sample was analyzed by HPLC (Waters 600) with a UV-detector Waters 2487 (λ = 254 nm).

Preparation of chitosan and AMP-chitosan thin films: Gold (Au) substrates were used due to their higher suitability for ellipsometry, one of the surface characterization techniques employed. Au substrates (1×1 cm^2) were prepared and characterized as

previously described by others.[51] Briefly, the substrates were cleaned with "piranha" solution (7 parts of H_2SO_4 and 3 parts of 30% H_2O_2) for 5 min (**warning**: this solution strongly react with many organic materials and should be handled with extreme caution) and successively rinsed with ethanol, type 1 water, ethanol, and dried with a gentle stream of argon.

Chitosan ultrathin films were produced according to the work of Amaral and colleagues.[50] In brief, a chitosan solution (0.4% in acetic acid w/v) was deposited by spin coating (at 9000 rpm during 1 min; Laurell Technologies Corporation, NorthWales, UK)[52] on the center of the Au substrates, followed by a second spin coating of the same solution, forming double-layered chitosan ultrathin films. AMP-chitosan ultrathin films were obtained following a similar procedure. Peptide-chitosan conjugates (0.4% w/v) were dissolved in 0.1 M acetic acid and then deposited by spin-coating on the center of Au substrates previously coated with unmodified chitosan.

The ultrathin films produced were then neutralized with 0.1 M NaOH and rinsed with type 1 water. Each sample was dried with a gentle stream of argon and stored in plastic Petri dishes saturated with argon.

Surface characterization: Ellipsometry measurements were performed using an imaging ellipsometer, model EP3, from Nanofilm Surface Analysis (Goettingen, Germany). This ellipsometer was operated in a polarizer-compensator-sample-analyzer (PCSA) mode (null ellipsometry). The light source was a solid-state laser with a wavelength of 532 nm. The Au substrate refractive index (n = 0.7078) and extinction coefficient (k = 2.6564) were determined by using a delta and psi spectrum with an angle variation between 66.5° and 76.5°. These measurements were made in four zones of the substrate to correct for any instrument misalignment. The thickness of the chitosan films was determined considering n = 1.54 and k = 0, for the chitosan film.[53] Results are presented as the average of two measurements on each of the three samples.

Water contact angle measurements were performed using the sessile drop and the captive bubble methods. In both methods the contact angles were determined with a contact angle measuring system from Data Physics (San Jose, CA, USA), model OCA 15, equipped with a video CCD-camera and SCA 20 software. Regarding the sessile drop method, the contact angle was measured as previously described.[51b] Briefly, after deposition of 4μL drops of type 1 water, images were taken every 2 s over 180 s. Droplet profiles were fitted using Young-Laplace formula, to calculate the contact angle. The water contact angle of

each substrate was calculated by extrapolating the time-dependent curve to zero. Results are the average of two measurements on three independent samples.

Regarding the captive bubble method, chitosan and AMP-chitosan films were tape glued to a microscope slide and placed in a quartz chamber filled with type 1 water for 30 min, at room temperature, to keep the samples hydrated prior to contact angle measurements. Subsequently, 20 μL bubbles of room air were introduced to the wet ultrathin films using a J-shaped syringe. The bubble images were stored, and respective contact angles were calculated from the shape of the drop as described for the sessile drop method.[38b, 54] The contact angles for each film were the average of a total of four bubble measurements made on three different samples.

Determination of MIC and MBC: MIC were established with a modified broth microdilution method in Mueller-Hinton Broth (MHB). Bacteria were inoculated (1×10^5 CFU/mL) into MHB in the presence of different concentrations of Dhvar-5, previously dissolved in an 0.02% (v/v) acetic acid with 0.4% (w/v) bovine serum albumin (BSA) solution. Growth is assessed after incubation at 37 ºC for 18 h and the MIC value is read.[29] The MIC of chitosan and AMP-chitosan conjugates was determined following a similar procedure. Briefly, stock solutions of chitosan and AMP-chitosan conjugates were prepared in 1% (v/v) solution of glacial acetic acid to promote complete dissolution. This solution was diluted (with type 1 water) to obtain a 0.25% (v/v) polymer-based solution. As previously, bacteria were inoculated into MHB in the presence of different concentrations of the previous solution, at 37 °C for 18 h.

MBC values were assessed by plating in Tryptic Soy Agar (TSA)(Merck) the content of the first three wells where visible growth was not observed.

Surface antimicrobial activity evaluation: All substrates were washed successively in 70% ethanol and sterile type 1 water, and then dried in sterile environment.

Bacterial suspension in phosphate buffered saline (PBS) (5 μL, 10^8 CFU/mL) was deposited onto the surface of each sample, covered with a glass coverslip (∅=13mm), to force contact between bacteria and surface, and incubated at 37 °C for 5 h. Surrounding wells were filled with sterile type 2 water, in order to avoid medium evaporation. Substrates were rinsed with 0.9% sterile aqueous NaCl solution and then stained with a combination dye of the LIVE/DEAD® Bacterial Viability Kit (Baclight™) for 15 min in the dark. This kit is a combination of two nucleic acid dyes: (i) green-fluorescent Syto9,

capable to penetrate all bacteria, and (ii) red-fluorescent propidium iodide (PI), which only stains bacteria with damage membranes. As PI reduces the fluorescence of Syto9, it is assumed that live cells are green while red fluorescent cells are dead. Images were obtained with an inverted fluorescence microscope (Axiovert 200M, Zeiss, Germany). For quantifying the viability of adherent bacteria, eight fields on each of triplicate replicates were obtained with a 400× magnification, corresponding to a net area of about 0.0946 mm^2 per sample. The bacteria count was performed using the manual counting software included in ImageJ software.

Statistical analysis: Statistical analysis was performed using One-way ANOVA with post-hoc Tukey's multiple comparison test and Two-way ANOVA with post-hoc Tukey's multiple comparison test and. All statistical analyses were calculated usingGraphPad Prism program. Data is expressed as the mean ± standard deviation (SD) and p values of <0.05 were considered significant.

Acknowledgments

The authors thank Fundação para a Ciência e Tecnologia, Portugal, for funding through project UID/QUI/50006/2013, PhD Grant SFRH/BD/108966/2015 to MB and Post-doc Grant SFRH/BPD/79439/2011 to CM. Thanks are also due to Comissão de Coordenação e Desenvolvimento Regional do Norte (CCDR-N)/NORTE2020/Portugal2020 for funding through projects DESignBIOtechHealth (ref. Norte-01-0 145-FEDER-000024) and BIOENGINEERED THERAPIES FOR INFECTIOUS DISEASES AND TISSUE REGENERATION (ref. NORTE-01-0145-FEDER-000012).

References

[1] a) A. Y. Hwang, J. G. Gums, *Bioorganic & Medicinal Chemistry* **2016**, *24*, 6440; b) C. J. Sanchez, Jr., K. Mende, M. L. Beckius, K. S. Akers, D. R. Romano, J. C. Wenke, C. K. Murray, *BMC Infect Dis* **2013**, *13*, 47.

[2] B. D. Brooks, A. E. Brooks, *Adv. Drug Deliv. Rev* **2014**, *78*, 14.

[3] a) J. A. Inzana, E. M. Schwarz, S. L. Kates, H. A. Awad, *Biomaterials* **2016**, *81*, 58; b) C. R. Arciola, D. Campoccia, P. Speziale, L. Montanaro, J. W. Costerton, *Biomaterials* **2012**, *33*, 5967; c) R. M. Donlan, *Clin Infect Dis* **2001**, *33*, 1387.

[4] J. W. Costerton, *Int J Antimicrob Agents* **1999**, *11*, 217.

[5] C. de la Fuente-Núñez, F. Reffuveille, L. Fernández, R. E. W. Hancock, *Curr Opin Microbiol* **2013**, *16*, 580.

[6] R. Serra, R. Grande, L. Butrico, A. Rossi, U. F. Settimio, B. Caroleo, B. Amato, L. Gallelli, S. de Franciscis, *Expert Rev Anti Infect Ther* **2015**, *13*, 605.

[7] a) R. E. W. Hancock, E. F. Haney, E. E. Gill, *Nat Rev Immunol* **2016**, *16*, 321; b) C.-F. Le, C.-M. Fang, S. D. Sekaran, *Antimicrob Agents Chemother* **2017**, *61*; c) C. Monteiro, M. Fernandes, M. Pinheiro, S. Maia, C. L. Seabra, F. Ferreira-da-Silva, F. Costa, S. Reis, P. Gomes, M. C. L. Martins, *Biochim. Biophys. Acta, Rev. Biomembr.* **2015**, *1848*, 1139; d) C. Monteiro, M. Pinheiro, M. Fernandes, S. Maia, C. L. Seabra, F. Ferreira-da-Silva, S. Reis, P. Gomes, M. C. L. Martins, *Mol. Pharm* **2015**, *12*, 2904.

[8] a) E. C. Spindler, J. D. F. Hale, T. H. Giddings, R. E. W. Hancock, R. T. Gill, *Antimicrob Agents Chemother* **2011**, *55*, 1706; b) M. N. Melo, R. Ferre, M. A. R. B. Castanho, *Nat. Rev. Microbiol* **2009**, *7*, 245; c) M. N. Melo, M. A. R. B. Castanho, *Front Immunol* **2012**, *3*, 236.

[9] H. P. Stallmann, C. Faber, A. L. J. J. Bronckers, J. M. A. de Blieck-Hogervorst, C. P. J. M. Brouwer, A. V. N. Amerongen, P. I. J. M. Wuisman, *Peptides* **2005**, *26*, 2355.

[10] a) C. Faber, R. J. W. Hoogendoorn, D. M. Lyaruu, H. P. Stallmann, J. van Marle, A. van Nieuw Amerongen, T. H. Smit, P. I. J. M. Wuisman, *Biomaterials* **2005**, *26*, 5717; b) A. L. Ruissen, J. Groenink, E. J. Helmerhorst, E. Walgreen-Weterings, W. Van't Hof, E. C. Veerman, A. V. Nieuw Amerongen, *Biochem J* **2001**, *356*, 361; c) C. Faber, R. J. W. Hoogendoorn, H. P. Stallmann, D. M. Lyaruu, A. van Nieuw Amerongen, P. I. J. M. Wuisman, *J Antimicrob Chemother* **2004**, *54*, 1078.

[11] A. L. den Hertog, H. W. W. F. Sang, R. Kraayenhof, J. G. M. Bolscher, W. V. T. Hof, E. C. I. Veerman, A. V. N. Amerongen, *Biochem J* **2004**, *379*, 665.

[12] a) R. R. Silva, K. Y. Avelino, K. L. Ribeiro, O. L. Franco, M. D. Oliveira, C. A. Andrade, *Front Biosci (Schol Ed)* **2016**, *8*, 129; b) F. Costa, I. F. Carvalho, R. C. Montelaro, P. Gomes, M. C. L. Martins, *Acta Biomater* **2011**, *7*, 1431.

[13] a) S. S. Usmani, G. Bedi, J. S. Samuel, S. Singh, S. Kalra, P. Kumar, A. A. Ahuja, M. Sharma, A. Gautam, G. P. S. Raghava, *PLoS ONE* **2017**, *12*, e0181748; b) F.

M. T. A. Costa, S. R. Maia, P. A. C. Gomes, M. C. L. Martins, *Biomaterials* **2015**, *52*, 531; c) X. Chen, H. Hirt, Y. Li, S.-U. Gorr, C. Aparicio, *PLoS ONE* **2014**, *9*, e111579; d) S. A. Onaizi, S. S. J. Leong, *Biotechnol. Adv* **2011**, *29*, 67.

[14] a) M. K. S. Batista, M. Gallemí, A. Adeva, C. A. R. Gomes, P. Gomes, *Synth. Commun* **2009**, *39*, 1228; b) P. Sahariah, K. K. Sorensen, M. A. Hjalmarsdottir, O. E. Sigurjonsson, K. J. Jensen, M. Masson, M. B. Thygesen, *Chem Comm* **2015**, *51*, 11611; c) P. Li, C. Zhou, S. Rayatpisheh, K. Ye, Y. F. Poon, P. T. Hammond, H. Duan, M. B. Chan-Park, *Adv. Mater* **2012**, *24*, 4130; d) C. Zhou, M. Wang, K. Zou, J. Chen, Y. Zhu, J. Du, *ACS Macro Letters* **2013**, *2*, 1021.

[15] a) M. Meldal, C. W. Tornøe, *Chem. Rev* **2008**, *108*, 2952; b) L. Liang, D. Astruc, *Coord. Chem. Rev.* **2011**, *255*, 2933.

[16] M. Barbosa, N. Vale, F. M. T. A. Costa, M. C. L. Martins, P. Gomes, *Carbohydr Polym.* **2017**, *165*, 384.

[17] a) J. Kumirska, M. Czerwicka, Z. Kaczyński, A. Bychowska, K. Brzozowski, J. Thöming, P. Stepnowski, *Mar Drugs* **2010**, *8*, 1567; b) T. K. Giri, A. Thakur, A. Alexander, Ajazuddin, H. Badwaik, D. K. Tripathi, *Acta Pharm Sin B.* **2012**, *2*, 439.

[18] a) F. Nogueira, I. C. Goncalves, M. C. Martins, *Acta Biomater* **2013**, *9*, 5208; b) R. P. Carlson, R. Taffs, W. M. Davison, P. S. Stewart, *J Biomater Sci Polym Ed* **2008**, *19*, 1035.

[19] a) M. Fernandes, I. C. Goncalves, S. Nardecchia, I. F. Amaral, M. A. Barbosa, M. C. Martins, *Int J Pharm* **2013**, *454*, 116; b) I. A. Sogias, A. C. Williams, V. V. Khutoryanskiy, *Biomacromolecules* **2008**, *9*, 1837; c) N. Shrestha, M. A. Shahbazi, F. Araujo, E. Makila, J. Raula, E. I. Kauppinen, J. Salonen, B. Sarmento, J. Hirvonen, H. A. Santos, *Biomaterials* **2015**, *68*, 9.

[20] D. P. Vasconcelos, A. C. Fonseca, M. Costa, I. F. Amaral, M. A. Barbosa, A. P. Aguas, J. N. Barbosa, *Biomaterials* **2013**, *34*, 9952.

[21] W. Xie, P. Xu, Q. Liu, *Bioorg Med Chem Lett* **2001**, *11*, 1699.

[22] a) I. F. Amaral, A. L. Cordeiro, P. Sampaio, M. A. Barbosa, *J Biomater Sci Polym Ed* **2007**, *18*, 469; b) I. F. Amaral, M. Lamghari, S. R. Sousa, P. Sampaio, M. A. Barbosa, *J Biomed Mater Res A* **2005**, *75*, 387; c) A. G. Moutzouri, G. M. Athanassiou, *Ann Biomed Eng* **2011**, *39*, 730; d) T. Kawai, T. Yamada, A. Yasukawa, Y. Koyama, T. Muneta, K. Takakuda, *J Biomed Mater Res B Appl Biomater* **2009**, *88*, 264.

[23] a) A. L. Torres, S. G. Santos, M. I. Oliveira, M. A. Barbosa, *Acta Biomater* **2013**, *9*, 6553; b) K. Tomihata, Y. Ikada, *Biomaterials* **1997**, *18*, 567; c) H. Onishi, Y. Machida, *Biomaterials* **1999**, *20*, 175.

[24] V. Castro, J. B. Blanco-Canosa, H. Rodriguez, F. Albericio, *ACS Comb. Sci* **2013**, *15*, 331.

[25] Y. Li, C. M. Santos, A. Kumar, M. Zhao, A. I. Lopez, G. Qin, A. M. McDermott, C. Cai, *Chemistry* **2011**, *17*, 2656.

[26] C. M. Santos, A. Kumar, S. S. Kolar, R. Contreras-Caceres, A. McDermott, C. Cai, *ACS ACS Appl. Mater. Interfaces* **2013**, *5*, 12789.

[27] W. Lin, Junjian, C., Chenzhi, C., Lin, S., Sa, L., Li, R., Yingjun, W., *J Mater Chem B* **2015**, 30.

[28] B. Gottenbos, H. C. van der Mei, F. Klatter, P. Nieuwenhuis, H. J. Busscher, *Biomaterials* **2002**, *23*, 1417.

[29] I. Wiegand, K. Hilpert, R. E. W. Hancock, *Nat. Protocols* **2008**, *3*, 163.

[30] G. J. Elving, H. C. Van der Mei, H. J. Busscher, A. van Nieuw Amerongen, E. C. I. Veerman, R. van Weissenbruch, F. W. J. Albers, *Laryngoscope* **2000**, *110*, 321.

[31] R. E. W. Hancock, D. S. Chapple, *Antimicrob Agents Chemother* **1999**, *43*, 1317.

[32] A. S. Veiga, C. Sinthuvanich, D. Gaspar, H. G. Franquelim, M. A. R. B. Castanho, J. P. Schneider, *Biomaterials* **2012**, *33*, 8907.

[33] a) K. J. Cutrona, B. A. Kaufman, D. M. Figueroa, D. E. Elmore, *FEBS Letters* **2015**, *589*, 3915; b) L. Li, I. Vorobyov, T. W. Allen, *J Phys Chem B* **2013**, *117*, 11906.

[34] M. B. Strøm, B. E. Haug, M. L. Skar, W. Stensen, T. Stiberg, J. S. Svendsen, *J. Med. Chem* **2003**, *46*, 1567.

[35] M. M. Welling, C. P. J. M. Brouwer, W. van ′t Hof, E. C. I. Veerman, A. V. N. Amerongen, *Antimicrob Agents Chemother* **2007**, *51*, 3416.

[36] R. C. Goy, D. De Britto, O. B. G. Assis, *Polimeros* **2009**, *19*, 241.

[37] a) Y. Andres, L. Giraud, C. Gerente, P. Le Cloirec, *Environ. Technol.* **2007**, *28*, 1357; b) M. Kong, X. G. Chen, K. Xing, H. J. Park, *Int J Food Microbiol* **2010**, *144*, 51; c) J. R. Oliveira, M. C. L. Martins, L. Mafra, P. Gomes, *Carbohydr Polym.* **2012**, *87*, 240.

[38] a) A. R. Roudman, F. A. DiGiano, *J Memb Sci.* **2000**, *175*, 61; b) Y. Baek, J. Kang, P. Theato, J. Yoon, *Desalination* **2012**, *303*, 23.

[39] Y. Zhu, C. Gao, T. He, J. Shen, *Biomaterials* **2004**, *25*, 423.

[40] A. L. A. Ruissen, J. Groenink, W. Van ’t Hof, E. Walgreen-Weterings, J. van Marle, H. A. van Veen, W. F. Voorhout, E. C. I. Veerman, A. V. Nieuw Amerongen, *Peptides* **2002**, *23*, 1391.

[41] K. Hilpert, M. Elliott, H. Jenssen, J. Kindrachuk, C. D. Fjell, J. Korner, D. F. H. Winkler, L. L. Weaver, P. Henklein, A. S. Ulrich, S. H. Y. Chiang, S. W. Farmer, N. Pante, R. Volkmer, R. E. W. Hancock, *Chem. Biol.* **2009**, *16*, 58.

[42] R. Chen, M. D. Willcox, N. Cole, K. K. Ho, R. Rasul, J. A. Denman, N. Kumar, *Acta Biomater* **2012**, *8*, 4371.

[43] K. Lim, R. R. Chua, R. Saravanan, A. Basu, B. Mishra, P. A. Tambyah, B. Ho, S. S. Leong, *ACS Appl Mater Interfaces* **2013**, *5*, 6412.

[44] L. D. Lozeau, T. E. Alexander, T. A. Camesano, *J Phys Chem B* **2015**, *119*, 13142.

[45] G. Gao, John T. J. Cheng, J. Kindrachuk, Robert E. W. Hancock, Suzana K. Straus, Jayachandran N. Kizhakkedathu, *Chem. Biol.* **2012**, *19*, 199.

[46] a) G. M. Williams, K. Lee, X. Li, G. J. S. Cooper, M. A. Brimble, *Org. Biomol. Chem* **2015**, *13*, 4059; b) K. Holland-Nell, M. Meldal, *Angew. Chem. e Angew. Chem. Int. Ed.* **2011**, *50*, 5204.

[47] K. Rapsch, F. F. Bier, M. Tadros, M. von Nickisch-Rosenegk, *Bioconjug Chem* **2014**, *25*, 308.

[48] K. Yu, J. C. Y. Lo, Y. Mei, E. F. Haney, E. Siren, M. T. Kalathottukaren, R. E. W. Hancock, D. Lange, J. N. Kizhakkedathu, *ACS Appl. Mater. Interfaces* **2015**, *7*, 28591.

[49] a) H. Li, R. Aneja, I. Chaiken, *Molecules (Basel, Switzerland)* **2013**, *18*, 9797; b) M. Barbosa, M. Martins, P. Gomes, *Gels* **2015**, *1*, 194.

[50] I. Amaral, P. Granja, M. Barbosa, *J Biomater Sci Polym Ed* **2005**, *16*, 1575.

[51] a) S. R. Sousa, P. Moradas-Ferreira, B. Saramago, L. Viseu Melo, M. A. Barbosa, *Langmuir* **2004**, *20*, 9745; b) M. C. L. Martins, B. D. Ratner, M. A. Barbosa, *J Biomed Mater Res A* **2003**, *67A*, 158.

[52] F. Nogueira, I. C. Gonçalves, M. C. L. Martins, *Acta Biomater* **2013**, *9*, 5208.

[53] M. Lundin, L. Macakova, A. Dedinaite, P. Claesson, *Langmuir* **2008**, *24*, 3814.

[54] M. Hashizume, M. Ohashi, H. Kobayashi, Y. Tsuji, K. Iijima, *Colloids Surf A Physicochem Eng Asp.* **2015**, *483*, 18.

Supporting Information

Only a “click” away: development of novel antibacterial coatings

Mariana Barbosa, Claudia Monteiro, Fabíola Costa, Filipa Duarte, M. Cristina L. Martins, Paula Gomes**

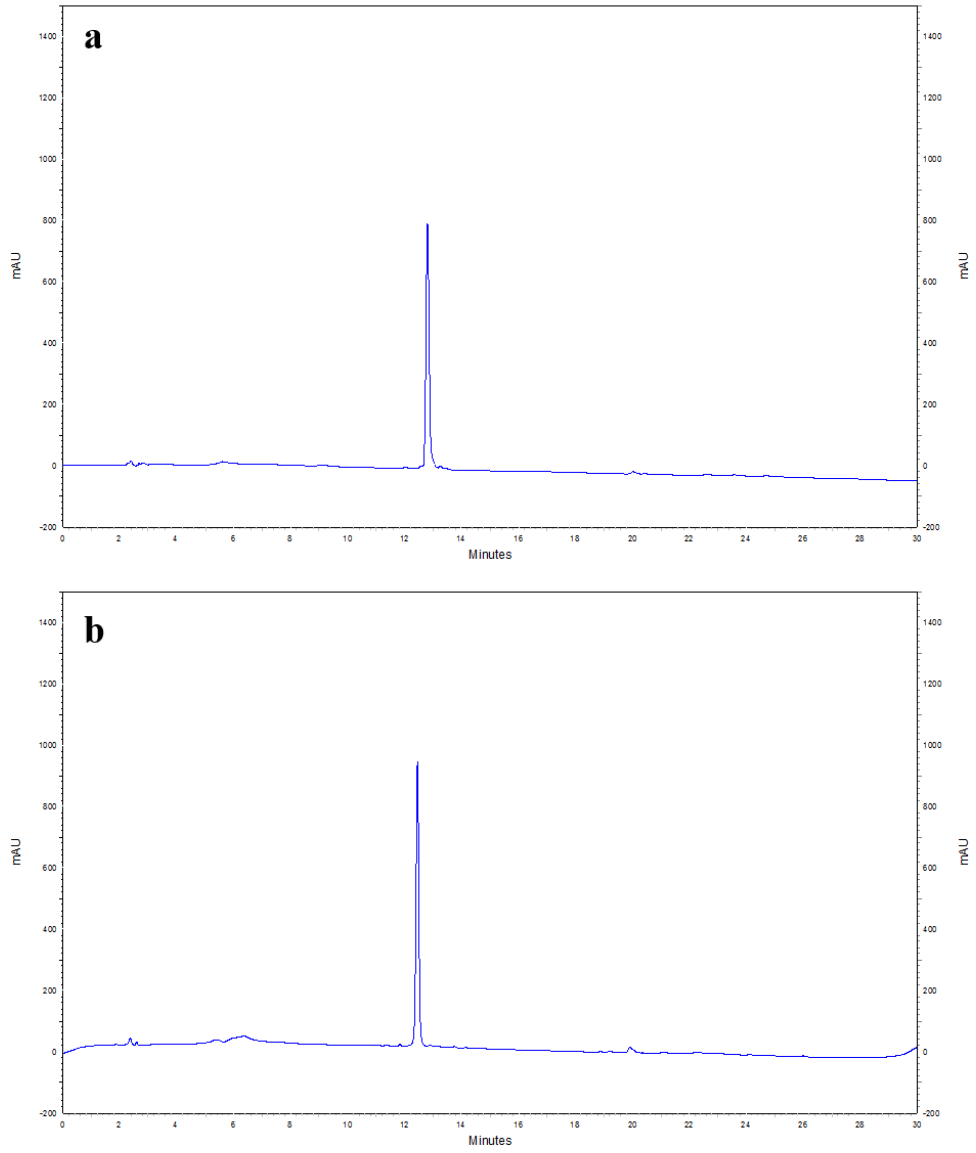

Figure 1S HPLC chromatograms of (a) Ahx-C_t-Dhvar-5 and (b) Ahx-N_t-Dhvar-5 peptides (major peak in each chromatogram corresponds to the target peptide). Under the analysis conditions employed the Ahx-Ct-Dhvar-5 peptide presented a retention time (RT) of 12.8 minutes, while the Ahx-Nt-Dhvar-5 peptide presented an RT of 12.5 minutes.

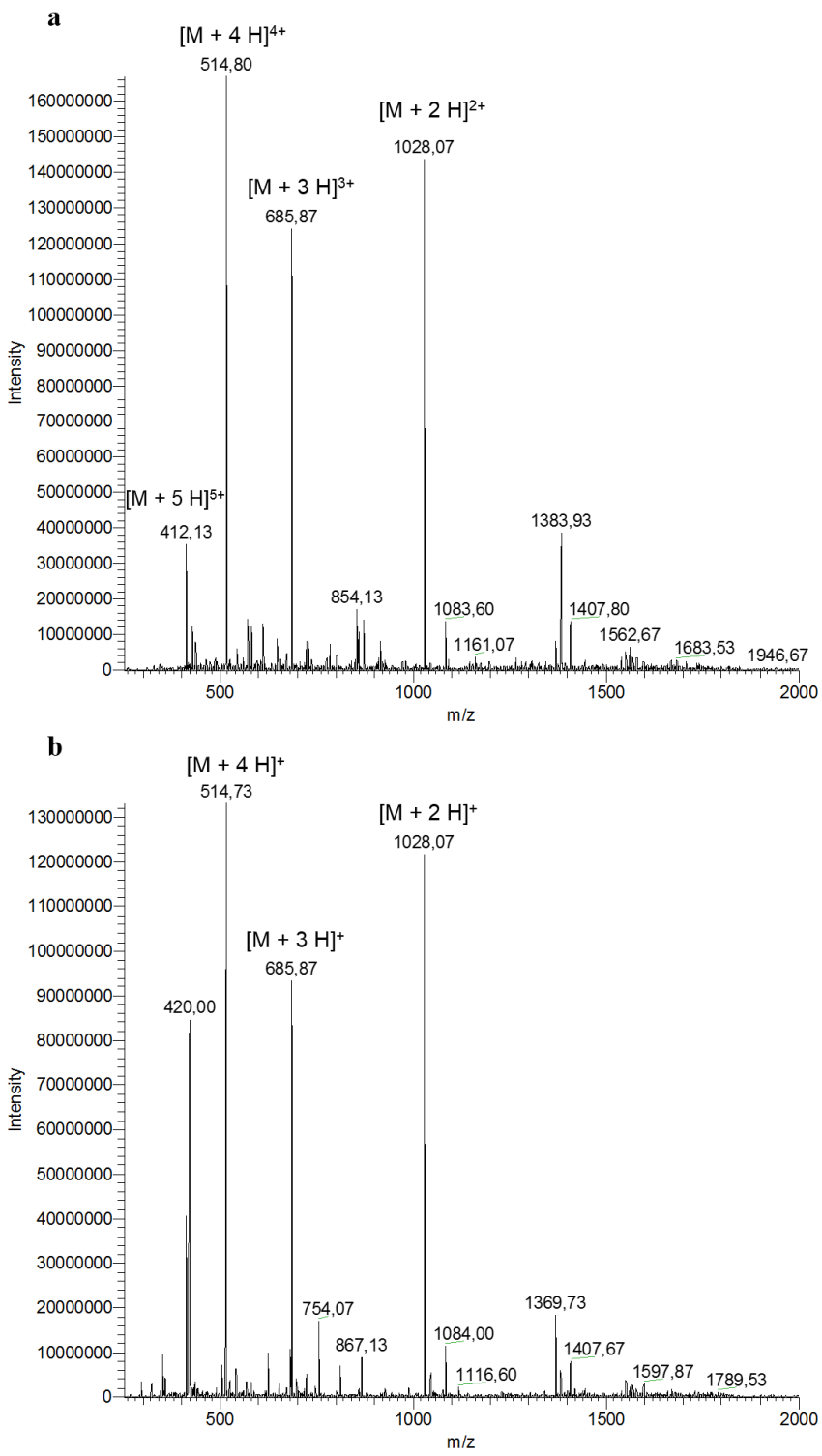

Figure 2S LC-MS spectra of (a) Ahx-C_t-Dhvar-5 and (b) Ahx-N_t-Dhvar-5 peptides.

Chapter VI

Influence of chemical immobilization parameters on the antibacterial properties of antimicrobial peptide-based coatings

Mariana Barbosa[1,2,3,4], Cláudia Monteiro[2,3], Fabíola Costa[2,3], M. Cristina L. Martins[2,3,5], Paula Gomes[1]

(manuscript in preparation)

[1]LAQV-REQUIMTE, Departamento de Química e Bioquímica, Faculdade de Ciências, Universidade do Porto, Porto, Portugal
[2]i3S, Instituto de Investigação e Inovação em Saúde, Universidade do Porto, Porto, Portugal
[3]INEB – Instituto de Engenharia Biomédica, Universidade do Porto, Porto, Portugal
[4]Faculdade de Engenharia, Universidade do Porto, Porto, Portugal

Abstract

Fighting bacterial adhesion and colonization is a crucial step in the prevention of subsequent biofilm establishment. Surface immobilization of antimicrobial peptides (AMP) onto biomaterials is a promising strategy to avoid bacterial colonization. This work aims at evaluating the effect of immobilization parameters on antibacterial activity of Dhvar-5, an AMP with a head-to-tail amphipathicity. In this connection, Dhvar-5-based coatings were developed to compare the influence of different chemical procedures, namely peptide tethering before or after fabrication of chitosan ultrathin films, on the overall antibacterial properties of the produced materials. Dhvar-5 was linked to thin chitosan coatings in controlled orientation, *via* either its *N*- or its *C*-terminus. Surface characterization demonstrated the chemoselective immobilization of the peptide for both orientations. Efficacy assays demonstrated that covalent immobilization of Dhvar-5, exposing either its hydrophobic or cationic ends, improves the chitosan coating antimicrobial effect by decreasing *Staphylococcus aureus* (*S. aureus*) colonization. Relevantly, surface antimicrobial performance depends on peptide tethering procedure, as thin films produced using previously prepared AMP-chitosan conjugates displayed bactericidal effects, whereas anti-adhesive properties were exhibited by thin films fabricated from unmodified chitosan on which the peptide was subsequently grafted.

Keywords: antimicrobial peptides, bacterial adhesion, characterization, chitosan, surface immobilization

---

1. Introduction

Targeting early stages of infection, i.e. bacterial adhesion and colonization, is a key factor in the fight against biofilm establishment [1, 2]. Thus, it comes as no surprise that a number of strategies aimed at developing antimicrobial surfaces, by preventing protein adsorption and cell adhesion (anti-fouling surfaces), or by inactivating bacteria, triggering cell death (bactericidal surfaces), have been emerging [3, 4]. The physicochemical properties of the surface, such as surface roughness energy and potential, are fundamental issues in the initial adhesion and subsequent growth of bacteria. Unfortunately, some of the reported anti-fouling approaches face serial difficulties, such as cytotoxicity, low

efficiency and ineffective long-term stability profiles [3-5]. The development of covalent immobilization has emerged as a promising strategy to overcome the aforementioned problems [3, 6]. Several reports already describe covalent coupling of well-known antibiotics, such as vancomycin [7] or penicillin [8]. However, the success of this class of coatings is conditioned not only by the spectrum of activity of the chosen antibiotic, but also by the possibility of development of antibiotic-resistant bacteria in a relatively short period of time. Therefore, there is an urgent need for an effective and non-cytotoxic broad-spectrum antimicrobial coating [3].

Antimicrobial peptides (AMP) emerge as promising alternative compounds to state-of-the-art antibiotherapies, since they display broad spectrum of activity, high efficiency even at low concentrations, fast killing, good cytotoxic profile, without promoting significant rise of bacterial resistance [3, 9, 10]. For the majority of these peptides, the mode of action suggested is peptide insertion into bacterial membranes with subsequent cell death induction by, in some cases, cell lysis [3].

Dhvar-5, a synthetic peptide derived from the histatins family, is an AMP with *N*- to *C*-terminal amphipathicity. It was originally described as strongly active against *Candida albicans*, but has also a potent and broad antibacterial activity, including against methicillin-resistant *Staphylococcus aureus* (MRSA). The precise mechanism of action of soluble Dhvar-5 is still not fully elucidated. Previous studies demonstrated that Dhvar-5 binds to the membrane of yeast cells and induces leakage of intracellular content, but without permanent pore formation [11-13]. However, *in vivo*, results showed that this AMP did not reveal the same efficacy pattern than gentamicin [14]. This situation may be associated with the inherent AMP-associated limitations, namely proteolytic degradation, self-aggregation and binding to plasma proteins. As previously revised by Costa *et al.* [3], covalent immobilization of AMP may offer the answer to such problems. Covalent tethering of AMP has the further advantage of preventing the formation of peptide concentration gradients, associated with peptide-releasing therapies, minimizing the cytotoxicity and improving the long-term stability [1]. Another advantage of covalent immobilization of AMP is efficient prevention of biofilm formation by reduction of microorganism viability after contact with the coated material, which holds promise for clinical applications [3]. Still, peptide immobilization is not a straightforward issue, several parameters should be considered, such as proper orientation (*N- versus C*-terminal immobilization) and selection of adequate immobilizations strategies.

In this context, peptide tethering through the so-called "click chemistry" reaction is a highly promising approach. Amongst the chemoselective reactions that fit the "click" chemistry concept, the copper-catalyzed azide-alkyne cycloaddition (CuAAC) is one of the most attractive, given the (i) stability of the triazole link created between the building blocks that are joint together, and (ii) diversity of adequately functionalized (i.e., bearing either an azide or an alkyne functionality) building blocks that are available [15, 16].
According to our previous findings, "click" chemistry, namely, CuAAC, is an effective chemoselective approach to synthesize AMP-chitosan conjugates suitable for use as antimicrobial coatings. Moreover, the bacterial adhesion studies demonstrated that the AMP-chitosan thin films had bactericidal effects whose potency depended on which region of the peptide was exposed; as such, higher antimicrobial activity was observed when Dhvar-5 was immobilized through its cationic *C*-terminus, i.e., exposing its hydrophobic domain [17, 18]. In this study, we developed novel coatings to infer about the influence of immobilization procedure (e.g., peptide grafting before or after formation of the thin films) on the overall antibacterial properties of the produced materials. Therefore, we immobilized Dhvar-5 *via* CuAAC chemistry by both its *C*- and *N*-terminal end (exposing the cationic and hydrophobic regions, respectively) directly to pre-fabricated chitosan thin films and compared their antimicrobial activity with those previously observed for thin films fabricated using previously prepared peptide-chitosan conjugates.

2. Materials and Methods

2.1 Dhvar-5 synthesis and characterization

Peptide Dhvar5 (LLLFLLKKRKKRKY C-terminal amide, M_w = 1847 Da) and its derivatives were produced by standard Fmoc/^{t}Bu solid-phase peptide synthesis (SPPS) methodologies as previously reported [17]. Dhvar5-derived peptides exhibited a spacer and an alkyne functionality (alkyne-AMP), at either the peptide's *N*- or *C*- terminus, so it would be possible to evaluate the effect of peptide orientation. The selected flexible spacer, 6-aminohexanoic acid (Ahx), was placed between the bioactive sequence and the terminal alkyne moiety, in this case the non-natural amino acid propargylglycine (Pra). The full oligopeptide sequences (M_w = 2056 Da) will be hereafter designated as Ahx-C_t-Dhvar-5 (Figure 1A) and Ahx-N_t-Dhvar-5 (Figure 1B).

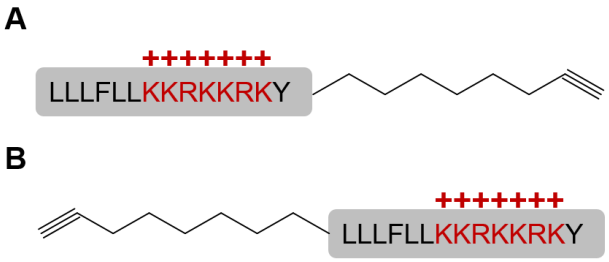

Figure 1 Synthetic derivatives of the antimicrobial peptide Dhvar-5, modified with a flexible spacer and an alkyne moiety at either the peptide's (a) *C*-terminus, or (b) *N*-terminus.

Finally, the crude peptides were purified by reverse-phase liquid chromatography and confirmed by High Performance Liquid Chromatography (HPLC) (Hitachi-Merck LaChrom Elite) and Liquid Chromatography-Electrospray Ionization/Ion Trap Mass Spectrometry (LC-ESI/IT MS) (LCQ-DecaXP LC-MS system, ThermoFinnigan). Purified peptides used presented a purity level higher than 95%.

2.2 Preparation of chitosan ultrathin films

Commercial squid pen chitosan was obtained from France Chitine with high molecular weight (M_w > 500 kDa) and a 94% degree of deacetylation (DD). Prior to its handling, chitosan was purified by the re-precipitation method, as previously described by others [19]. Afterwards, chitosan ultrathin films were produced accordingly to the work of Barbosa *et al.* [17]. Briefly, a 50 µL drop of chitosan (0.4% w/v solution) was deposited by spin-coating (at 9000 rpm during 1 min; Laurell Technologies Corporation, NorthWales, UK) on top of gold substrates (1 × 1 cm^2).

Double-layered chitosan ultrathin films were produced by performing twice the spin-coating process. Once synthesized, chitosan films were neutralized with 0.1 M NaOH, rinsed with type 1 water, dried with a gentle stream of argon and stored in sealed plastic Petri dishes saturated with argon.

2.3 Conversion of chitosan ultra-thin films amines into azides

Conversion of chitosan thin films with amines into azides was previously optimized by Barbosa *et al.* [17]. Briefly, chitosan thin films were treated with a solution of 2 mM of imidazole-1-sulfonyl azide hydrochloride (ISA·HCl; kind gift from Professor Fernando Albericio, from the Institute of Biomedical Research of Barcelona, IRB-Barcelona) and

1.5 mM of potassium carbonate, in type 1 water, for 24 h, at room temperature and 100 rpm. The modified films were then rinsed with type 1 water and immersed 1 min on an ultrasound bath (Bandelin Sonorex Digitec Bath 35 kHz) and rinsed again with type 1 water.

2.4 Dhvar-5 tethering onto functionalized films

Immobilization of Dhvar-5 derivatives onto N_3-chitosan thin films was obtained under standard CuAAC reaction conditions between the alkyne group of the terminal propargylglycine of both peptides and the azide group on the modified chitosan films, by an adaptation of a previously described method [17]. Briefly, N_3-chitosan substrates were incubated with excess peptide solutions (10 mg/mL) in the presence of Cu(II) sulfate (2 mM of $CuSO_4 \cdot H_2O$) and 0.1 M of sodium ascorbate, for *in situ* generation of the Cu(I) catalyst, in aqueous medium. THPTA ligand (0.01 M) and aminoguanidinium hydrochloride (0.1 M) were also added. The reaction was performed in type 2 water for 24 h at 37 ºC and 100 rpm (Figure 2B). The modified films were then rinsed with type 1 water, 0.1 M aqueous EDTA, 5% aqueous sodium bicarbonate, and rinsed again with type 1 water. Each sample was dried with a gentle stream of argon and stored in plastic Petri dishes saturated with argon.

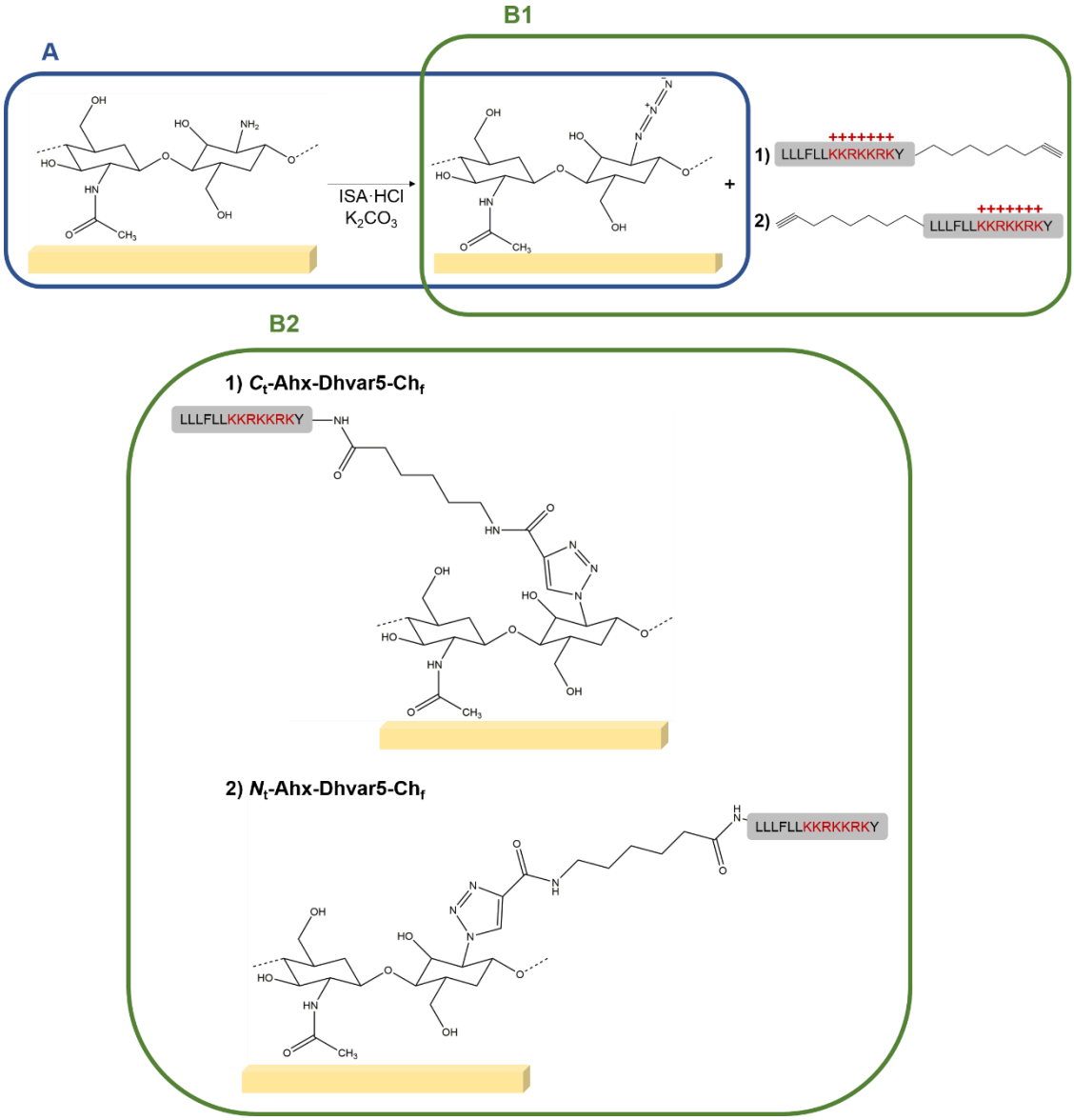

Figure 2 **A)** Functionalization of chitosan by direct conversion of the polymer's amines into azides; **B1)** CuACC reaction between the alkyne group of the terminal propargylamine of both peptides and the azide group on pre-functionalized chitosan originating **B2)** two AMP-chitosan conjugates: **1)** C_t-Ahx-Dhvar5-Ch_f and **2)** N_t-Ahx-Dhvar5-Ch_f.

2.5 Surface characterization

2.5.1 Infrared Reflection-Absorption Spectroscopy Analysis (FT-IRRAS)

Measurements were carried out on a Perkin Elmer FTIR spectrophotometer, model 2000, equipped with a VeeMax II Accessory (PIKE) and a liquid-nitrogen cooled MCT detector. The sample chamber was purged with dry nitrogen for 2 min prior to and during measurement of each sample in order to ensure that there was no water vapor adsorption. For each substrate, a similar gold surface was used as a background. Incident light was p-

polarized and spectra were collected using the 80º grazing angle reflection mode. For each sample, 100 scans were collected with 4 cm^{-1} resolution.

2.5.2 X-ray photoelectron spectroscopy (XPS)

XPS measurements were carried out on a Kratos Axis Ultra HAS spectrometer using aluminum (15 kV) as the radiation source (from CEMUP – Centro de Materiais da Universidade do Porto). The photoelectrons were analyzed at a take-off angle of 90º between the horizontal surface plane and the electron analyzer optics. Survey spectra were collected over a range of 0–1350 eV with an analyzer pass energy of 80 eV. High-resolution C1s, O1s and N1s spectra were collected with an analyzer pass energy of 40 eV. The binding energy (BE) scales were referenced by setting the C1s BE to 285.0 eV. All spectra were fitted using the CasaXPS (version 2.3.17PR 1.1) software. Element atomic percentages were calculated from the integrated intensities of the XPS peaks, taking into account the atomic sensitivity factors of the instrument data system.

2.5.3 Ellipsometry

Ellipsometry measurements were performed using an imaging ellipsometer, model EP3, from Nanofilm Surface Analysis. This ellipsometer was operated in a polarizer-compensator-sample-analyzer (PCSA) mode (null ellipsometry). The light source was a solid-state laser with a wavelength of 532 nm. The gold substrate refractive index (n = 0. 0.7078) and extinction coefficient (k = 2.6564) were determined by using a delta and psi spectrum with an angle variation between 66.5º and 76.5º. These measurements were made in four zones to correct for any instrument misalignment. The thickness of the chitosan films was determined considering n = 1.54 and k = 0, for the chitosan film [20]. Results are presented as the average of three measurements on each of two samples.

2.5.4 Water contact angle measurements

Water contact angle measurements were performed using the sessile drop method with a contact angle measuring system from Data Physics, model OCA 15, equipped with a video CCD-camera and SCA 20 software, as described at [21]. After deposition of 4 ml drops of type 1 water, images were taken every 2 s over 300 s. Droplet profiles were fitted using Young-Laplace formula, to calculate the contact angle. The water contact angle of each substrate was calculated by extrapolating the time dependent curve to zero. Results are the average of two measurements on three independent samples.

2.6 Bacterial assays

2.6.1 Bacterial strains, media and growth conditions

These assays were carried out using *Staphylococcus aureus* (*S. aureus*, ATCC 49230). Bacteria were firstly grown on Tryptic Soya Agar (TSA) (Merck) and then overnight on Tryptic Soya Broth (TSB) (Merck) at 37 ºC, 150 rpm. Bacterial suspensions were adjusted by measuring Optical Density (600 nm). Bacterial numbers were confirmed by a retrospective viable count.

2.6.2 Surface antimicrobial activity evaluation

All samples were washed successively in 70% ethanol and sterile type 2 water, and then dried in sterile environment. Samples were then placed onto flat-bottom 24-well cell suspension culture plates.

Bacterial suspension (5 µL, 10^8 CFU/mL) in phosphate buffered saline (PBS) was deposited onto the surface of each sample and then covered with a glass coverslip, to force contact between bacteria and surface, and incubated at 37 ºC for 5 h. Surrounding wells were filled with sterile type 2 water, in order to avoid medium evaporation. Substrates were rinsed with 0.9 sterile aqueous NaCl solution and then stained with a combination dye of the LIVE/DEAD® Bacterial Viability Kit (Baclight™) for 15 min in the dark. Briefly, the kit contains two fluorescent dyes, Syto9 which stains all bacteria in green, and propidium iodide (PI) which can only crossover damaged cells membranes, originating red stained cells. As PI quenches the fluorescent emission of Syto9, it is assumed that green cells are alive whereas red cells are dead. Images were obtained with an inverted fluorescence microscope (Axiovert 200M, Zeiss, Germany).

For quantifying the viability of adherent bacteria, eight fields on each of triplicate replicates were obtained with a 400× magnification, corresponding to a net area of about 0.0946 mm^2 per sample. The bacteria count was performed using the manual counting software included in ImageJ software.

3. Results

3.1 Surface characterization

Control chitosan and Dhvar-5-modified surfaces were analyzed by FT-IRRAS, XPS, ellipsometry and water contact angle (WCA) measurements.

3.1.1 FT-IRRAS

FT-IRRAS spectra of chitosan, N_3-chitosan and Dhvar5-chitosan thin films are depicted in Figure 3. Unmodified chitosan spectrum (Figure 3A) allowed the identification of characteristic absorption bands of chitosan, as previously described [17, 19, 22-24]. Briefly, a broad intense band at 3600–3000 cm^{-1} due to the contributions of different hydrogen-bonded stretching vibrations (O–H stretching, NH_2 asymmetric stretching and N–H stretching). The characteristic vibration modes from the *N*-acetyl-glucosamine units of chitosan as the amide I at 1650 cm^{-1} (C=O stretching from secondary amides), and N–H bending of a primary amine at 1530 cm^{-1} and the amide III at 1328 cm^{-1} (C–N stretching vibrations) were also detected. Finally, the absorption band at 1081 cm^{-1} can be associated to the stretching vibration C–O–C in the glucopyranose ring characteristic of glucose monomers of the chitosan. This band was slightly shifted from that observed when powder chitosan was analyzed by IR using transmission on KBr pellet (1076 cm^{-1}) [17]. The small differences in chitosan IR spectra obtained using different acquisition modes have also been described by Brugnerotto and co-workers [25].

After ISA·HCl-mediated conversion of chitosan amines into azides, the characteristic azide peak, assigned to the asymmetric $N^-= N^+=N^-$ stretching mode, appeared at 2120 cm^{-1}, which was actually one of the most intense of the FT-IR spectrum of N_3-chitosan (Figure 3B) [26, 27].

Subsequent covalent tethering of Ahx-C_t-Dhvar-5 and Ahx-N_t-Dhvar-5 onto N_3-chitosan films yielded Dhvar-5-chitosan ultrathin films whose FT-IR spectra are displayed in Figures 3C and 3D, respectively. Both spectra demonstrated that the desired "click" reaction had occurred, as two relevant changes could be noted, when comparing to N_3-chitosan: (i) disappearance of the azide band (at 2120 cm^{-1}), supporting total consumption of available azides upon reaction with the alkynyl-peptides, and (ii) intensity increase of the amide I and amide II bands (1650–1530 cm^{-1}) [28], strongly corroborating peptide grafting onto N_3-chitosan. Noteworthy, the characteristic bands of chitosan remained

throughout the procedure, indicating that "click" reaction provides a mild chemical environment for chemoselective functionalization of chitosan [29]. This further delivers a conclusive proof that CuAAC reaction conditions employed are efficient, allowing quantitative conversions. Altogether, FT-IRRAS results clearly support the success of the covalent immobilization chemistry applied.

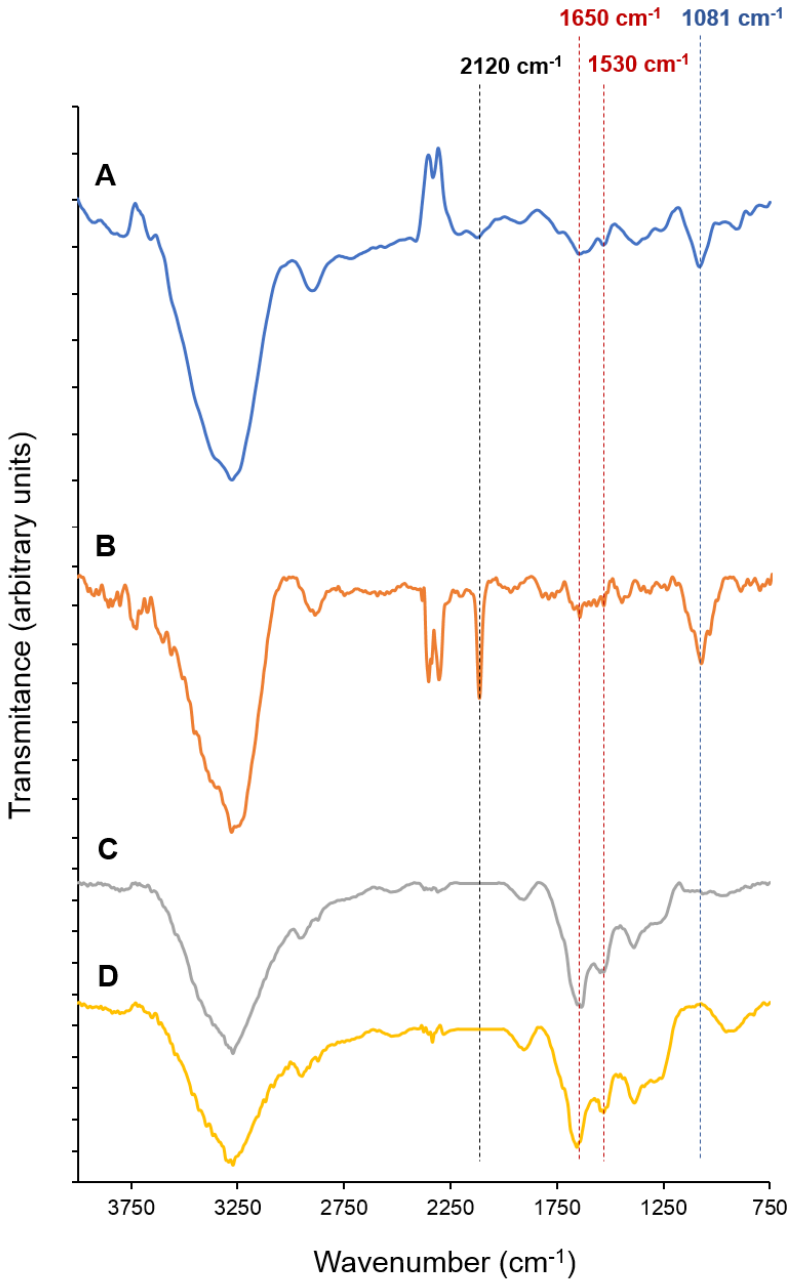

Figure 3 FT-IRRAS spectra of A) unmodified chitosan, B) N_3-chitosan, C) C_t-Ahx-Dhvar-5-Ch_f and D) N_t-Ahx-Dhvar-5-Ch_f ultrathin films. Lines in red correspond to I (C=O stretching), amide II (N–H bending), while the one in blue is associated with stretching vibration C–O–C in the glucopyranose ring. The relative intensity of these (amide versus C-O-C bands) undergoes the expected evolution as a consequence of the entry of the peptide chains. The one in black denotes change in the azide band in consequence of film modifications.

3.1.2 XPS analysis of chitosan and derivatives

Chitosan, N_3-chitosan and both AMP-chitosan conjugates thin films were further analyzed by XPS. Table 1 shows the relative atomic percentages of carbon, oxygen and nitrogen of unmodified chitosan and respective derivatives.

Table 1 Elemental analysis data (% C, N, O) as determined by XPS analysis of unmodified chitosan thin film and respective derivatives.

Polymer	Atomic composition (%)		
	C 1s	**N 1s**	**O 1s**
Chitosan	56.9	8.3	34.8
N_3-chitosan	56.5	10.4	33.1
C_t-Ahx-Dhvar-5-Ch_f	64.7	16.4	18.9
N_t-Ahx-Dhvar-5-Ch_f	65.3	16.4	18.3

The XPS survey of unmodified chitosan and N_3-chitosan revealed the presence of residual gold, probably due to some heterogeneity of the surface' thickness (< 10 nm) which leads to the detection of the gold substrate beneath the polymer. As anticipated, the N_3-chitosan derivative presented a small decrease in the atomic percentage of carbon with concomitant increase in the percentage of nitrogen, as a consequence of the introduction of the azide group onto the chitosan backbone. After the CuAAC reaction, the percentage of oxygen of both AMP-chitosan derivatives decreased, while both carbon and nitrogen atomic compositions increased, suggesting that the peptides were successfully coupled to N_3-chitosan through a triazole ring.

High-resolution XPS spectra of C1s and N1s were also analyzed and are displayed on Figure 4. The C1s spectrum of unmodified chitosan (Figure 4A) was resolved into three peaks as previously described by us [19]. The peak at 285.0 eV was assigned to C–C and C–H type carbons that are typically related with a surface contaminant [19], the peak at 286.6 eV was assigned to C–NH_2, C–OH and C–O–C carbons, whereas the peak at 288.3 eV was assigned to carbons from the O–C–O and N–C=O groups. Regarding N1s, the resolved spectrum displayed a peak at 399.5 eV, assigned to nitrogen in C–N and CO–N bonds. N_3-chitosan (Figure 4B) did not show any significant changes in C1s high-resolution XPS spectra as compared to its unmodified chitosan precursor. The high-resolution XPS N1s spectrum of the N_3-chitosan derivative, which exhibited two peaks at 399.5 and 401.4 eV, for NH_2 and NH_3^+, respectively, and another at 404.5 eV

associated with nitrogen in the azide group, clearly demonstrated the success of conversion of the chitosan's amines into azides [29, 30].

The high-resolution spectra of C1s and N1s for both AMP-chitosan conjugates (Figures 4C and D) were similar suggesting that CuAAC occurred, independently of peptide orientation. The C1s high-resolution spectrum showed an increase in the 285.0 eV peak (C–C and C–H) suggesting the insertion of C–C and C–H type carbons present in the peptide chain. In addition, the peak at 400.2 eV in the XPS N1s spectra, assigned to nitrogen atoms on the triazole ring, is in agreement with reported spectra for the triazole ring [29, 30]. Moreover, the peak corresponding to nitrogen in the azide group (404.3 eV) disappeared, while the peaks characteristic of nitrogens in C–N and CO–N bonds and amine groups (399.5 eV and 401.3 eV, respectively) and the triazole moiety (400.2 eV) are present. Hence, results obtained for the N1s region of the XPS spectrum demonstrates total consumption of unreacted azides and confirms the success of the CuAAC reaction.

The data for relative atomic percentages of distinct types of nitrogen, obtained from the N1s XPS high-resolution spectra is shown in Table 2. The success of amine-azide conversion in chitosan was clearly demonstrated by the appearance of a peak at 404.5 eV assigned to nitrogen in azide groups. Therefore, the success of the subsequent CuAAC reaction was confirmed by the substitution of the previous band by a peak at 400.0 eV, which corroborates the formation of the triazole ring. Therefore, these results provided further evidences of the success of all reactional steps towards the synthesis of target peptide-chitosan conjugates.

Table 2 Chemical surface high-resolution analysis of N (1s) region for chitosan and respective derivatives.

Polymer	Atomic% N (1s)			
	C–N/CO–N	CO–N–CO/N–CO–O	NH_3^+	$N^-=N^+=N^-$
	399.5 eV	**400.2 eV**	**401.3 eV**	**404.3 eV**
Chitosan	100	-	-	-
N_3-chitosan	61.7	-	26.2	12.1
C_t-Ahx-Dhvar-5-Ch_f	32.9	50.1	17.0	-
N_t-Ahx-Dhvar-5-Ch_f	6.70	79.8	13.5	-

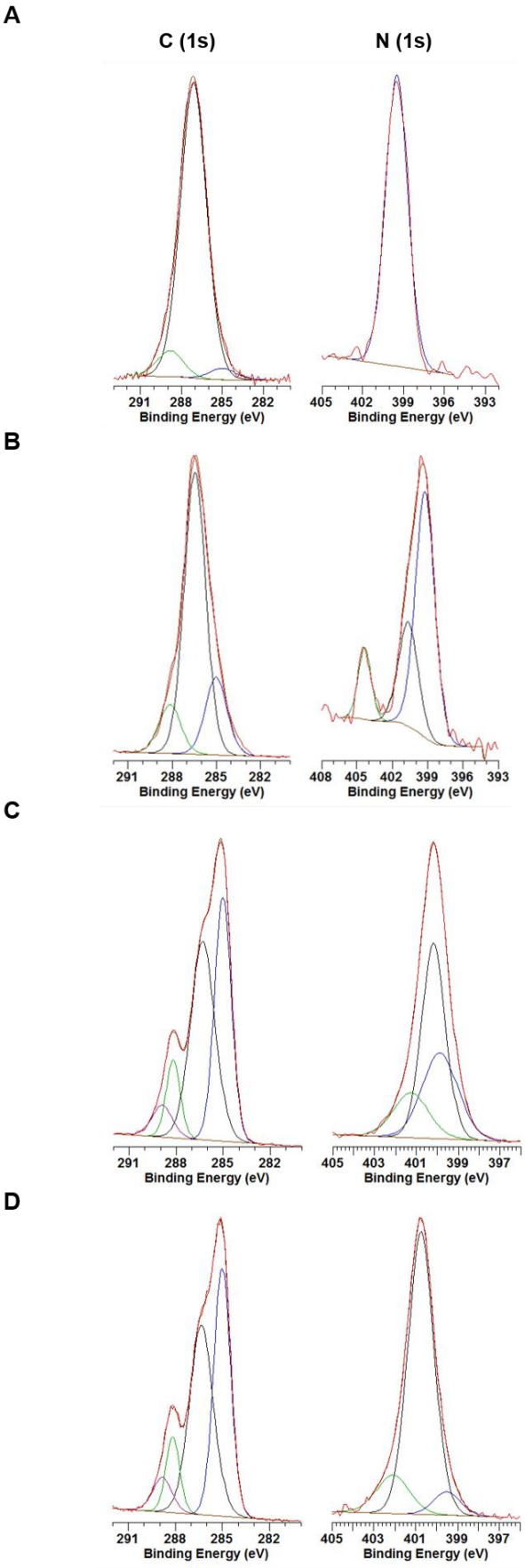

Figure 4 XPS high resolution spectra of A) unmodified chitosan, B) N_3-chitosan, C) C_t-Ahx-Dhvar-5-Ch_f, and D) N_t-Ahx-Dhvar-5-Ch_f, for C1s and N1s regions.

3.1.3 Ellipsometry

The spin-coating process resulted on chitosan ultrathin films of 20 ± 0.5 nm. Figure 5 presents chitosan films thickness before and after surface modification. The significant increase of the chitosan film thickness after incubation with Dhvar-5, supports the success of peptide attachment. No significant difference was observed between the distinct peptide immobilization orientations.

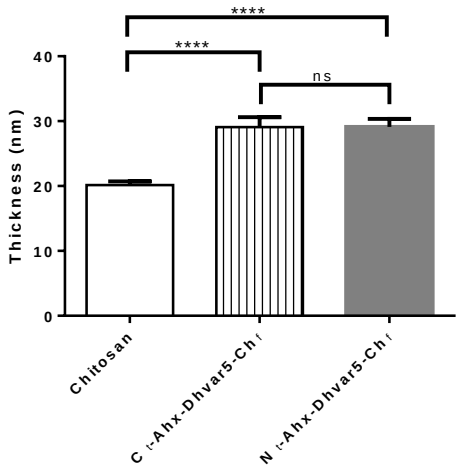

Figure 5 Ellipsometry analysis of the chitosan and chitosan-functionalized films (One-Way ANOVA analysis, $p < 0.05$).

3.1.4 Water optical contact angle (OCA) analysis

Water contact angles (WCA) of the control and modified chitosan films are presented on Figure 6. After Dhvar-5 binding through its *C*-terminus (exposing its hydrophobic region) the WCA increased (θ_w = 64°). On the other hand, when the peptide was immobilized through its *N*-terminus, samples showed a more hydrophilic behavior (θ_w = 53°) than unmodified chitosan (θ_w = 59°), consistent with the immobilization of the peptide exposing its hydrophilic domain, rich in positively-charged amino acids.

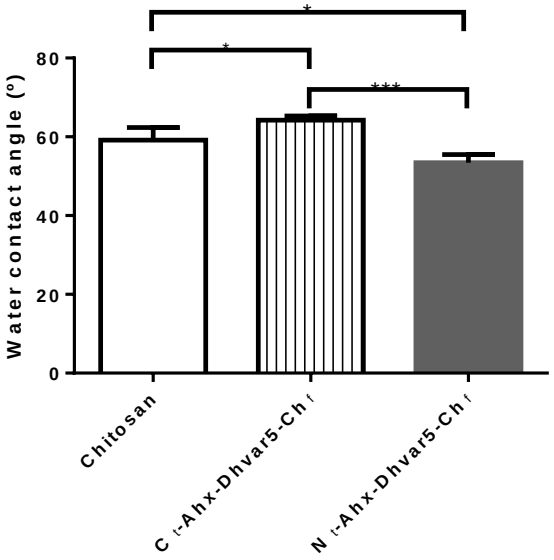

Figure 6 Water optical contact angles of chitosan and chitosan-functionalized film (One-Way ANOVA analysis, $p < 0.05$).

3.2 Bacterial assays

3.2.1 Surface antimicrobial activity evaluation

Viability of bacteria attached to the surfaces was evaluated using LIVE/DEAD® Bacterial Viability Kit (Baclight™). Figure 5 presents the average number of bacteria per mm^2 of each surface sample, after 5 h incubation at 37 ºC.

Regarding total adhered bacteria, control sample, Au (data not shown), exhibited high values, whereas chitosan coating promoted a reduction of bacterial adhesion by around 40%. This result was expected, since we previously demonstrated the antimicrobial properties of these chitosan ultrathin films [18]. Samples with peptide covalently immobilized exhibited a marked decrease of bacterial adhesion as compared to chitosan, reaching an ~60% reduction when peptide was immobilized through its *C*-terminus (C_t-Ahx-Dhvar-5-Ch_f) ($p < 0.05$). Only slightly lower (~52%) reduction of bacterial adhesion was achieved when the peptide was tethered through its *N*-terminus (N_t-Ahx-Dhvar-5-Ch_f) ($p < 0.05$). Hence, amongst all chitosan surfaces analyzed, those coated with Dhvar-5 were the best suited to avoid bacterial colonization. It was also observed that, for all surfaces analyzed, most of the adhered bacteria were not dead. Still, surfaces with *C*-terminally immobilized Dhvar-5 were the most bactericidal ones, with a total number of live adhered bacteria two-fold lower than those observed in unmodified chitosan.

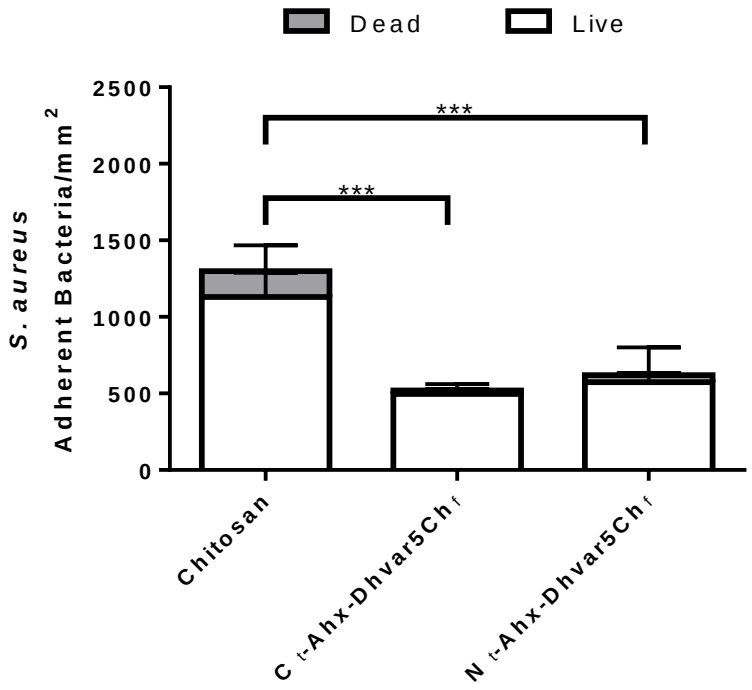

Figure 7 Viability of adhered *S. aureus* incubated at 37 °C for 5 h.

4. Discussion

In this study, Dhvar-5 was covalently immobilized onto chitosan thin films in order to evaluate if this strategy is able to prevent bacterial adhesion in a sustainable way, as well as to compare the antimicrobial performance of peptide-tethered chitosan surfaces prepared upon grafting of the peptide before or after fabrication of the films.

Different surface characterization techniques (FT-IRRAS, XPS, ellipsometry and WCA) confirmed that the target peptide-grafted films were successfully obtained, *via* chemoselective covalent immobilization of the peptide in both possible orientations. Ellipsometry measurements demonstrated a clear thickness increase of Dhvar-5-modified chitosan films comparing to control chitosan. However, such analysis alone did not prove the covalent immobilization of the peptide, nor its proper orientation. Demonstration of the covalent immobilization of the peptide was provided by FT-IRRAS analysis, namely through comparison of the amide I peak intensity (1654 cm^{-1})/C–O–C glucopiranose peak intensity (1083 cm^{-1}) ratio, which was clearly increased when Dhvar-5 was covalently bound to chitosan. The covalent immobilization of Dhvar-5 was also confirmed by XPS analysis, as (i) the success of amine-azide conversion in chitosan was clearly demonstrated by the appearance of a peak assigned to nitrogen in azide groups (404.5

eV), and (ii) subsequent CuAAC reaction was also confirmed by the substitution of the previous band by a peak at 400.0 eV, corroborating the formation of the triazole ring. Both FT-IRRAS and XPS results were in accordance to what was expected, based on chemical transformations carried out and on previous work in our group [17, 18].

Regarding the specificity of the immobilization orientation, useful information was brought by WCA measurements. Chitosan films became significantly more hydrophobic upon immobilization of Dhvar-5 through its *C*-terminus, which agrees with exposure of the peptide's hydrophobic portion, and only slightly more hydrophilic when immobilization was made through the *N*-terminus, thus exposing the peptide's cationic residues.

Antimicrobial activity of control and peptide-grafted surfaces was assessed through evaluation of adhesion and viability after 5 h of incubation. Both Dhvar-5 modified surfaces presented a significant reduction of bacterial adhesion when compared to chitosan, whereas most adhered bacteria remained alive. This puts in evidence that strong anti-adherence rather than bactericidal effects take place upon peptide tethering onto chitosan. Still, when Dhvar-5 was immobilized through its *C*-terminus, exposing its hydrophobic region, a higher degree of bacterial death could be observed. This comes into agreement with previous reports on viability of adhered bacteria as highly dependent of the terminus used for peptide immobilization. Hilpert *et al.* [31] found that immobilized AMP exposing their hydrophobic termini exhibited higher bactericidal activity, which was regarded as indicative that AMP should have their hydrophobic domain free to be able to interact with the lipophilic portion of the bacterial membrane. As such, peptides with sequence-based amphipathicity should be covalently immobilized through the position farthest away from the hydrophobic domain in order to insert into the bacterial lipid bilayer [31]. Previous studies by Ruissen *et al.* [13] are also in accordance with our findings; according to these authors, Dhvar-5 is a membrane-active AMP which can cause cytoplasmic membrane depolarization, but without forming permanent pores. This mechanism of action, in addition to the sequence-based amphipathicity of Dhvar-5, would suggest that its optimal immobilization position should be through the *C*-terminus, as this would result on greater exposition of the hydrophobic domain [13]. In contrast to these results, Chen *et al.* [32], reported higher antimicrobial activity with a clear anti-adherence effect when melimine, a 28-amino acid AMP with hydrophobic *N*-terminus and *C*-terminal cationic domain, was immobilized through its *N*-terminus, exposing the cationic domain away from the substrate [32].

With regard to effect of immobilization parameters on the antimicrobial properties of Dhvar-5-tethered surfaces, this works confirms, and provides final demonstration, that the former strongly influence the later. In other words, an integrated analysis of all the findings we have made thus far regarding Dhvar-5-grafted chitosan surfaces, allow us to conclude that antimicrobial behavior of such surfaces depends, among other unaccounted factors, on:

(i) peptide orientation: the influence of peptide orientation (i.e., which of its ends is used for covalent grafting onto the material surface, leaving the opposite end more exposed) has been widely reported both by others [1, 13, 31, 32], and by us, both in this and previous works [18], as above discussed;

(ii) immobilization chemistry: CuAAC grafting used in this work *versus* chitosan-Dhvar-5 binding *via* disulfide bridge previously reported by Costa *et al.* [1] lead to different anti-fouling behaviors, as, in opposition to the findings herein reported, the earlier work showed lowest bacterial adhesion on the surface exposing the hydrophilic cationic end of Dhvar-5 (i.e., peptide immobilized by its *N*-terminus);

(iii) immobilization procedure: CuAAC was used both in this and our previous work, recently reported [18], differing in the moment at which Dhvar-5 is grafted onto chitosan - before (previous report) or after (this work) fabrication of thin films; this change had impact not only in the properties of the surfaces (thickness and wettability), but also in the fact that, when grafting the peptide through its *C*-terminus prior to fabrication of the thin film, the latter is able to display bactericidal activity in addition to anti-adhesive effects.

Overall, the present and earlier works show that different immobilization parameters likely lead to distinct peptide conformations (thus, different exposure degrees and regions) and surface peptide densities, underlying diverse antimicrobial performances. Accordingly, previous reports highlight the effect of peptide concentration on AMP's antimicrobial activity. For instance, Chen *et al.* [32] found that higher peptide concentration was associated with stronger antibacterial activity. Humblot *et al.* [33] connected low peptide concentrations with bacteriostatic rather than bactericidal effect as low peptide concentration prevents multiple peptides to access the cell membrane. Moreover, Hilpert and co-workers [34] described a concentration-dependent antimicrobial activity of the immobilized peptide. Altogether, all these apparently

discrepant findings highlight how little is known about the mechanisms of action of immobilized AMP [35]. Therefore, each individual AMP must be carefully studied regarding immobilization parameters, towards creation of effective anti-fouling coatings.

5. Conclusions

This work demonstrates that covalent immobilization of AMP Dhvar-5 onto a chitosan thin coating, by means of chemoselective CuAAC, improves the anti-fouling properties of the coating by decreasing *S. aureus* colonization. Moreover, findings herein described corroborate previous reports highlighting the fact that antimicrobial performance of AMP-tethered surfaces is highly dependent on peptide immobilization parameters, such as peptide concentration and orientation, chemistry used for tethering, and specific experimental procedures adopted. In conclusion, provided careful optimization of immobilization parameters is carried out, AMP-tethered biomaterials hold great promise towards development of effective antimicrobial coatings for biomedical applications.

Acknowledgments

The authors thank Fundação para a Ciência e Tecnologia, Portugal, for funding through project UID/QUI/50006/2013, PhD Grant SFRH/BD/108966/2015 to MB and Post-doc Grant SFRH/BPD/79439/2011 to CM. Thanks are also due to Comissão de Coordenação e Desenvolvimento Regional do Norte (CCDR-N)/NORTE2020/Portugal2020 for funding through projects DESignBIOtechHealth (ref. Norte-01-0 145-FEDER-000024) and BIOENGINEERED THERAPIES FOR INFECTIOUS DISEASES AND TISSUE REGENERATION (ref. NORTE-01-0145-FEDER-000012).

References

[1] F.M.T.A. Costa, S.R. Maia, P.A.C. Gomes, M.C.L. Martins, Dhvar-5 antimicrobial peptide (AMP) chemoselective covalent immobilization results on higher antiadherence effect than simple physical adsorption, Biomaterials 52(0) (2015) 531-538.

[2] K.A. Floyd, A.R. Eberly, M. Hadjifrangiskou, 3 - Adhesion of bacteria to surfaces and biofilm formation on medical devices, in: Y. Deng, W. Lv (Eds.), Biofilms and Implantable Medical Devices, Woodhead Publishing (2017) 47-95.

[3] F. Costa, I.F. Carvalho, R.C. Montelaro, P. Gomes, M.C.L. Martins, Covalent immobilization of antimicrobial peptides (AMPs) onto biomaterial surfaces, Acta Biomaterialia 7(4) (2011) 1431-1440.

[4] J. Hasan, R.J. Crawford, E.P. Ivanova, Antibacterial surfaces: the quest for a new generation of biomaterials, Trends in Biotechnology 31(5) (2013) 295-304.

[5] M. Cloutier, D. Mantovani, F. Rosei, Antibacterial Coatings: Challenges, Perspectives, and Opportunities, Trends in Biotechnology 33(11) (2015) 637-652.

[6] R.R. Silva, K.Y. Avelino, K.L. Ribeiro, O.L. Franco, M.D. Oliveira, C.A. Andrade, Chemical immobilization of antimicrobial peptides on biomaterial surfaces, Frontiers in bioscience (Scholar edition) 8 (2016) 129-42.

[7] M. Varisco, N. Khanna, P.S. Brunetto, K.M. Fromm, New Antimicrobial and Biocompatible Implant Coating with Synergic Silver–Vancomycin Conjugate Action, ChemMedChem 9(6) (2014) 1221-1230.

[8] N. Aumsuwan, S. Heinhorst, M.W. Urban, The effectiveness of antibiotic activity of penicillin attached to expanded poly (tetrafluoroethylene)(ePTFE) surfaces: a quantitative assessment, Biomacromolecules 8(11) (2007) 3525-3530.

[9] H. Jenssen, P. Hamill, R.E. Hancock, Peptide antimicrobial agents, Clinical microbiology reviews 19(3) (2006) 491-511.

[10] N. van der Weerden, M. Bleackley, M. Anderson, Properties and mechanisms of action of naturally occurring antifungal peptides, Cellular and Molecular Life Sciences 70(19) (2013) 3545-3570.

[11] A.L. den HERTOG, H.W.W.F. SANG, R. KRAAYENHOF, J.G.M. BOLSCHER, W.V.T. HOF, E.C.I. VEERMAN, A.V.N. AMERONGEN, Interactions of histatin 5 and histatin 5-derived peptides with liposome membranes: surface effects, translocation and permeabilization, Biochemical Journal 379(3) (2004) 665-672.

[12] A.L. Ruissen, J. Groenink, E.J. Helmerhorst, E. Walgreen-Weterings, W. Van't Hof, E.C. Veerman, A.V. Nieuw Amerongen, Effects of histatin 5 and derived peptides on Candida albicans, Biochemical Journal 356(Pt 2) (2001) 361-368.

[13] A.L.A. Ruissen, J. Groenink, W. Van ’t Hof, E. Walgreen-Weterings, J. van Marle, H.A. van Veen, W.F. Voorhout, E.C.I. Veerman, A.V. Nieuw Amerongen, Histatin 5 and derivatives: Their localization and effects on the ultra-structural level, Peptides 23(8) (2002) 1391-1399.

[14] C. Faber, R.J.W. Hoogendoorn, H.P. Stallmann, D.M. Lyaruu, A. van Nieuw Amerongen, P.I.J.M. Wuisman, o.b.o. STEGA, *In vivo* comparison of Dhvar-5 and

gentamicin in an MRSA osteomyelitis prevention model, Journal of Antimicrobial Chemotherapy 54(6) (2004) 1078-1084.

[15] M. Meldal, C.W. Tornøe, Cu-catalyzed azide− alkyne cycloaddition, Chemical reviews 108(8) (2008) 2952-3015.

[16] R.K. Iha, K.L. Wooley, A.M. Nyström, D.J. Burke, M.J. Kade, C.J. Hawker, Applications of Orthogonal "Click" Chemistries in the Synthesis of Functional Soft Materials, Chemical Reviews 109(11) (2009) 5620-5686.

[17] M. Barbosa, N. Vale, F.M.T.A. Costa, M.C.L. Martins, P. Gomes, Tethering antimicrobial peptides onto chitosan: Optimization of azide-alkyne "click" reaction conditions, Carbohydrate Polymers 165 (2017) 384-393.

[18] M. Barbosa, C. Monteiro, F.M.T.A. Costa, M.C.L. Martins, P. Gomes, Only a "click" away: development of novel antibacterial coatings Advanced Functional Materials Manuscript submited (2018).

[19] I. Amaral, P. Granja, M. Barbosa, Chemical modification of chitosan by phosphorylation: an XPS, FT-IR and SEM study, Journal of Biomaterials Science, Polymer Edition 16(12) (2005) 1575-1593.

[20] M. Lundin, L. Macakova, A. Dedinaite, P. Claesson, Interactions between Chitosan and SDS at a Low-Charged Silica Substrate Compared to Interactions in the BulkThe Effect of Ionic Strength, Langmuir 24(8) (2008) 3814-3827.

[21] M.C.L. Martins, B.D. Ratner, M.A. Barbosa, Protein adsorption on mixtures of hydroxyl- and methyl-terminated alkanethiols self-assembled monolayers, Journal of Biomedical Materials Research Part A 67A(1) (2003) 158-171.

[22] P. Gomes, C.A.R. Gomes, M.K.S. Batista, L.F. Pinto, P.A.P. Silva, Synthesis, structural characterization and properties of water-soluble N-(γ-propanoyl-amino acid)-chitosans, Carbohydrate Polymers 71(1) (2008) 54-65.

[23] J.R. Oliveira, M.C.L. Martins, L. Mafra, P. Gomes, Synthesis of an O-alkynyl-chitosan and its chemoselective conjugation with a PEG-like amino-azide through click chemistry, Carbohydrate Polymers 87(1) (2012) 240-249.

[24] F. Nogueira, I.C. Goncalves, M.C. Martins, Effect of gastric environment on Helicobacter pylori adhesion to a mucoadhesive polymer, Acta Biomaterialia 9(2) (2013) 5208-15.

[25] J. Brugnerotto, J. Lizardi, F.M. Goycoolea, W. Argüelles-Monal, J. Desbrières, M. Rinaudo, An infrared investigation in relation with chitin and chitosan characterization, Polymer 42(8) (2001) 3569-3580.

[26] V. Castro, J.B. Blanco-Canosa, H. Rodriguez, F. Albericio, Imidazole-1-sulfonyl Azide-Based Diazo-Transfer Reaction for the Preparation of Azido Solid Supports for Solid-Phase Synthesis, ACS Combinatorial Science 15(7) (2013) 331-334.

[27] P. Sahariah, K.K. Sorensen, M.A. Hjalmarsdottir, O.E. Sigurjonsson, K.J. Jensen, M. Masson, M.B. Thygesen, Antimicrobial peptide shows enhanced activity and reduced toxicity upon grafting to chitosan polymers, Chemical Communications 51(58) (2015) 11611-11614.

[28] A. Barth, Infrared spectroscopy of proteins, Biochimica et Biophysica Acta (BBA) - Bioenergetics 1767(9) (2007) 1073-1101.

[29] L. Hu, P. Zhao, H. Deng, L. Xiao, C. Qin, Y. Du, X. Shi, Electrical signal guided click coating of chitosan hydrogel on conductive surface, RSC Advances 4(26) (2014) 13477-13480.

[30] A. Shakiba, A.C. Jamison, T.R. Lee, Poly(l-lysine) Interfaces via Dual Click Reactions on Surface-Bound Custom-Designed Dithiol Adsorbates, Langmuir 31(22) (2015) 6154-6163.

[31] K. Hilpert, M. Elliott, H. Jenssen, J. Kindrachuk, C.D. Fjell, J. Korner, D.F.H. Winkler, L.L. Weaver, P. Henklein, A.S. Ulrich, S.H.Y. Chiang, S.W. Farmer, N. Pante, R. Volkmer, R.E.W. Hancock, Screening and Characterization of Surface-Tethered Cationic Peptides for Antimicrobial Activity, Chemistry & Biology 16(1) (2009) 58-69.

[32] R. Chen, M.D. Willcox, N. Cole, K.K. Ho, R. Rasul, J.A. Denman, N. Kumar, Characterization of chemoselective surface attachment of the cationic peptide melimine and its effects on antimicrobial activity, Acta Biomaterialia 8(12) (2012) 4371-9.

[33] V. Humblot, J.-F. Yala, P. Thebault, K. Boukerma, A. Héquet, J.-M. Berjeaud, C.-M. Pradier, The antibacterial activity of Magainin I immobilized onto mixed thiols Self-Assembled Monolayers, Biomaterials 30(21) (2009) 3503-3512.

[34] K. Hilpert, M. Elliott, H. Jenssen, J. Kindrachuk, C.D. Fjell, J. Körner, D.F. Winkler, L.L. Weaver, P. Henklein, A.S. Ulrich, Screening and characterization of surface-tethered cationic peptides for antimicrobial activity, Chemistry & biology 16(1) (2009) 58-69.

[35] G. Gao, John T.J. Cheng, J. Kindrachuk, Robert E.W. Hancock, Suzana K. Straus, Jayachandran N. Kizhakkedathu, Biomembrane Interactions Reveal the Mechanism of Action of Surface-Immobilized Host Defense IDR-1010 Peptide, Chemistry & Biology 19(2) (2012) 199-209.

Chapter VII

Recapitulation and Perspectives

Chronic wound infections (CWI) and implant-associated infections (IAI) represent a major health care problem with significant economic implications and a growing impact on public health worldwide. The ineffectiveness to control early stages of infection and subsequent bacterial colonization leads to formation of mixed-strains biofilms [1, 2].

The decline in the effectiveness of current antibiotherapies is accompanied by the decrease in the period of time between the discovery of a new therapeutic drug and the appearance of a corresponding resistant bacterial strain. Therefore, it is crucial to develop new and more effective antimicrobials in the prevention or treatment of severe CWI and IAI at their onset [3-5].

As the search for the next antibacterial gold-standard capable of tackling the widespread growth of antibiotic-resistant bacteria continues, AMP are gaining prominence as interesting alternatives [6, 7]. AMP are natural antibiotics found in virtually every living being, most of which are addressable by straightforward chemical synthesis, which in turn allows the improvement of their therapeutic properties by designing custom-made synthetic derivatives. AMP therefore, as promising components of the innate immune system, display a wide spectrum of activity, even at low concentrations, and are not prone to eliciting bacterial resistance [6-8]. Originally it was thought that their antimicrobial activity was exclusively associated with their intrinsic pore-forming activity which lead to membrane permeation and disruption of bacterial membranes integrity. Nowadays, AMP are known to have other modes of action, such as the inhibition of protein and cell wall synthesis or of bacterial enzymes, stimulation of host defense mechanisms, among others [6, 7].

However, AMP are associated with some disadvantages such as poor stability in the presence of proteolytic enzymes, associated to short half-life *in vivo*, and cytotoxicity, when administered in higher concentrations [9]. Covalent immobilization of AMP onto surfaces through different tethering strategies has already been reported and the overall results suggest that immobilized AMP can have anti-adhesive and antibacterial activity, thus effectively preventing biofilm formation while overcoming AMP's referred limitations [8-13]. In view of the above, development of AMP-based materials is a highly promising field of research.

The selection of adequate coupling strategies and the optimization of the immobilization parameters are crucial to obtain more effective prospective candidates within peptide-based materials for applications in medicine, e.g., to be used either as scaffolds, namely orthopedic implants or as bioactive wound dressings, boasting such features [9, 14].

A wide variety of peptide tethering strategies has already been described before. Ranging from the popular amide coupling chemistry, between the pre-synthesized peptide and the surface, to the straightforward sulfur chemistry whereby a thiolated surface reacts with a cysteine-containing peptide [9]. However, some of these strategies are either not chemoselective or produce a chemo- and/or bio-reversible peptide-surface grafting [9]. To tackle with such limitations, research is focused on chemoselective routes, the so-called "click" reactions, which have been widely explored as described in Chapter II [15]. Despite the prior uses of carbodiimide chemistry, which has been successfully applied to immobilize bioactive peptide sequences in a plethora of biopolymers, peptide tethering through the so-called "click" chemistry reactions [16] is a highly promising, yet underexplored, approach to the synthesis of hydrogels with varying dimensions and patterns. Among these, the copper-catalyzed azide-alkyne cycloaddition (CuAAC) is one of the most attractive, given the (i) selectivity between azide and alkyne moieties, (ii) stability of the triazole link created between the building blocks that are joint together, even under physiological conditions, and (iii) diversity of adequately functionalized building blocks that can be synthesized, bearing either an azide or an alkyne functionality [17, 18]. These unprotected reactive groups are stable to the synthesis conditions used throughout SPPS, so they can be easily introduced into the peptide sequences. Therefore, this reaction has attracted much attention for its valences of synthesis and post-polymerization modification of polymers [15].

While taking advantage of its appealing features, CuAAC can be easily directed towards the development of new and effective AMP-based biomaterials, provided immobilization parameters are optimized, such as controlled peptide orientation, conformation and surface exposure [9]. In fact, our work demonstrates that the fine tuning of reaction conditions may be instrumental towards success of AMP tethering via CuAAC; thus, as described in Chapter III, reasonable levels of azide to triazole conversion were only observed when using THTPA to stabilize Cu(I) in solution, while use of excess aminoguanidine hydrochloride was crucial to avoid Arg modification by ascorbate [19].

Moreover, it has been reported that a given AMP may display different antimicrobial powers and modes of action, depending on diverse factors, such as, e.g., concentration (influencing, among other factors, peptide-to-membrane lipid ratio, and peptide aggregation state) or conformation (affecting, e.g., exposure of charged *versus* hydrophobic regions, and consequent efficiency of the AMP to disturb or even internalize pathogen cells) [20-22]. Therefore, there is still a long way to go in order to completely

understand AMP and the influence of different structural and chemical parameters on their overall antimicrobial properties [16, 23].

The strong dependence of antimicrobial activity on peptide immobilization parameters explains why apparently contradictory findings have been made, both by others and by us, regarding the antibacterial performance of AMP-tethered surfaces. For instance, the apparently contradictory results on antimicrobial activity of soluble *versus* surface-cast AMP-chitosan conjugates, described in Chapter III, may arise from differences in peptide conformation and polymer chains packing. For instance, in solution, Dhvar-5-chitosan conjugates lost antimicrobial activity as compared to unmodified chitosan, which seems unlikely to correlate with modification of the polymer's primary amines, considered a key asset for chitosan's antimicrobial properties [24-26]; in fact, in the present work, modification of the original polymer's amines was largely compensated by identical groups from both the (i) Lys side chains of the tethered peptide, and (ii) propargylamine used to cap unreacted azides in the polymer matrix. Possibly, insertion of peptide chains changed the polymer's packing, eventually caused by peptide-peptide electrostatic repulsions due to the highly cationic character of Dhvar-5. This assumption may further explain why conjugates solutions had significantly lower viscosity than chitosan ones.

Another important aspect to consider is influence of tethered peptide orientation on antimicrobial performance. At the light of recent reports on tethered AMP, it is not possible to establish a rule-of-thumb regarding preferred orientations for grafting AMP; for instance, Costa *et al.* [11] reported a stronger anti-fouling effect when Dhvar-5 was immobilized through its *N*-terminus, exposing its cationic region, while Ruissen *et al.* [27] found that membrane-active AMP should have their hydrophobic domain exposed in order to maximize insertion into bacterial lipid bilayers. Although the present work reinforces that peptide orientation is indeed relevant for the overall antimicrobial performance of AMP-tethered surfaces, as shown in Chapters IV and V, and globally agrees with Ruissen's observations in the sense that exposure of Dhvar-5's hydrophobic region generally led to stronger antibacterial effects, it also highlights how puzzling findings in this specific field may be; on the one hand, our results contradict previous ones from Costa *et al.*, equally on Dhvar-5-grafted chitosan surfaces [11], which can be attributed to different peptide conformation, surface density, and/or peptide-chitosan bond (chemo-/bio-reducible disulfide bridge) lability in consequence of a different immobilization chemistry [28,29]; on the other hand, this work demonstrates that, even when the same immobilization chemistry is used, surface antimicrobial performance

depends on the specific way how Dhvar-5-chitosan thin films were fabricated (Chapter IV *versus* Chapter V), as thin films produced using previously prepared peptide-chitosan conjugates (Chapter IV) displayed bactericidal effects, whereas anti-adhesive (but not bactericidal) properties were exhibited by thin films prepared from unmodified chitosan and only after modified with peptide (Chapter V).

Hence, this work proves that the mode of action and efficacy of a given AMP can be highly influenced by peptide orientation, coupling chemistry, and specific procedures for surface fabrication. More relevantly, this work reports an unprecedented approach where CuAAC "click" chemistry was applied to graft an AMP onto ground chitosan, yielding a bulk powder next used to fabricate thin films. Such a powdered biopolymer is expectedly easier to handle for ensuing synthesis scale-up, and production of different materials. Such approach yielded an anti-fouling bactericidal coating (Dhvar-5-C_t-chitosan).

Altogether, information and work herein reported contribute to reinforce the importance of chemoselective covalent coupling, as we were able to demonstrate that use of CuAAC "click" chemistry is an efficient and highly selective method to graft AMP onto chitosan, yielding bulk materials that are suitable for the production of tailored biomaterials with excellent prospects for application as antimicrobial coatings. Future work comprises further development of the most promising conjugate, namely, Dhvar-5-C_t-chitosan. To this end, a number of additional studies need to be performed: (i) stability assays in simulated physiologic medium harsh processing assays, (ii) *in vitro* cytocompatibility assays, using fibroblast and pre-osteoblast cell lines through metabolic and differentiation assays, and, finally (iii) *in vivo* assays on rodent model bone (osteomyelitis) and skin (chronic diabetic foot ulcers) infections.

References

[1] A.Y. Hwang, J.G. Gums, The emergence and evolution of antimicrobial resistance: Impact on a global scale, Bioorganic & Medicinal Chemistry 24(24) (2016) 6440-6445.

[2] C.J. Sanchez, Jr., K. Mende, M.L. Beckius, K.S. Akers, D.R. Romano, J.C. Wenke, C.K. Murray, Biofilm formation by clinical isolates and the implications in chronic infections, BMC Infect Dis 13 (2013) 47.

[3] J.A. Inzana, E.M. Schwarz, S.L. Kates, H.A. Awad, Biomaterials approaches to treating implant-associated osteomyelitis, Biomaterials 81 (2016) 58-71.

[4] C.R. Arciola, D. Campoccia, P. Speziale, L. Montanaro, J.W. Costerton, Biofilm formation in Staphylococcus implant infections. A review of molecular mechanisms and implications for biofilm-resistant materials, Biomaterials 33(26) (2012) 5967-5982.

[5] R.M. Donlan, Biofilm formation: a clinically relevant microbiological process, Clinical infectious diseases: an official publication of the Infectious Diseases Society of America 33(8) (2001) 1387-92.

[6] R.E.W. Hancock, E.F. Haney, E.E. Gill, The immunology of host defence peptides: beyond antimicrobial activity, Nature Reviews Immunology 16 (2016) 321.

[7] C.-F. Le, C.-M. Fang, S.D. Sekaran, Intracellular Targeting Mechanisms by Antimicrobial Peptides, Antimicrobial Agents and Chemotherapy 61(4) (2017).

[8] B.D. Brooks, A.E. Brooks, Therapeutic strategies to combat antibiotic resistance, Advanced Drug Delivery Reviews 78 (2014) 14-27.

[9] F. Costa, I.F. Carvalho, R.C. Montelaro, P. Gomes, M.C.L. Martins, Covalent immobilization of antimicrobial peptides (AMPs) onto biomaterial surfaces, Acta Biomaterialia 7(4) (2011) 1431-1440.

[10] S.S. Usmani, G. Bedi, J.S. Samuel, S. Singh, S. Kalra, P. Kumar, A.A. Ahuja, M. Sharma, A. Gautam, G.P.S. Raghava, THPdb: Database of FDA-approved peptide and protein therapeutics, PLoS ONE 12(7) (2017) e0181748.

[11] F.M.T.A. Costa, S.R. Maia, P.A.C. Gomes, M.C.L. Martins, Dhvar-5 antimicrobial peptide (AMP) chemoselective covalent immobilization results on higher antiadherence effect than simple physical adsorption, Biomaterials 52(0) (2015) 531-538.

[12] X. Chen, H. Hirt, Y. Li, S.-U. Gorr, C. Aparicio, Antimicrobial GL13K Peptide Coatings Killed and Ruptured the Wall of Streptococcus gordonii and Prevented Formation and Growth of Biofilms, PLoS ONE 9(11) (2014) e111579.

[13] S.A. Onaizi, S.S.J. Leong, Tethering antimicrobial peptides: Current status and potential challenges, Biotechnology Advances 29(1) (2011) 67-74.

[14] N. Cameron, T. Deming, Peptide-based Materials for Nanomedicine, Macromolecular Bioscience 15(1) (2015) 7-8.

[15] M. Barbosa, M.C.L. Martins, P. Gomes, Grafting Techniques towards Production of Peptide-Tethered Hydrogels, a Novel Class of Materials with Biomedical Interest, Gels 1(2) (2015) 194-218.

[16] H. Li, R. Aneja, I. Chaiken, Click Chemistry in Peptide-Based Drug Design, Molecules (Basel, Switzerland) 18(8) (2013) 9797-9817.

[17] M. Meldal, C.W. Tornøe, Cu-catalyzed azide− alkyne cycloaddition, Chemical reviews 108(8) (2008) 2952-3015.

[18] L. Liang, D. Astruc, The copper(I)-catalyzed alkyne-azide cycloaddition (CuAAC) "click" reaction and its applications. An overview, Coordination Chemistry Reviews 255(23–24) (2011) 2933-2945.

[19] M. Barbosa, N. Vale, F.M.T.A. Costa, M.C.L. Martins, P. Gomes, Tethering antimicrobial peptides onto chitosan: Optimization of azide-alkyne "click" reaction conditions, Carbohydrate Polymers 165 (2017) 384-393.

[20] E.C. Spindler, J.D.F. Hale, T.H. Giddings, R.E.W. Hancock, R.T. Gill, Deciphering the Mode of Action of the Synthetic Antimicrobial Peptide Bac8c, Antimicrobial Agents and Chemotherapy 55(4) (2011) 1706-1716.

[21] M.N. Melo, R. Ferre, M.A.R.B. Castanho, Antimicrobial peptides: linking partition, activity and high membrane-bound concentrations, Nature Reviews Microbiology 7 (2009) 245.

[22] M.N. Melo, M.A.R.B. Castanho, The Mechanism of Action of Antimicrobial Peptides: Lipid Vesicles vs. Bacteria, Frontiers in Immunology 3 (2012) 236.

[23] M. Barbosa, M. Martins, P. Gomes, Grafting Techniques towards Production of Peptide-Tethered Hydrogels, a Novel Class of Materials with Biomedical Interest, Gels 1(2) (2015) 194.

[24] Y. Andres, L. Giraud, C. Gerente, P. Le Cloirec, Antibacterial Effects of Chitosan Powder: Mechanisms of Action, Environmental Technology 28(12) (2007) 1357-1363.

[25] M. Kong, X.G. Chen, K. Xing, H.J. Park, Antimicrobial properties of chitosan and mode of action: A state of the art review, International Journal of Food Microbiology 144(1) (2010) 51-63.

[26] J.R. Oliveira, M.C.L. Martins, L. Mafra, P. Gomes, Synthesis of an O-alkynyl-chitosan and its chemoselective conjugation with a PEG-like amino-azide through click chemistry, Carbohydrate Polymers 87(1) (2012) 240-249.

[27] A.L.A. Ruissen, J. Groenink, W. Van 't Hof, E. Walgreen-Weterings, J. van Marle, H.A. van Veen, W.F. Voorhout, E.C.I. Veerman, A.V. Nieuw Amerongen, Histatin 5 and derivatives: Their localization and effects on the ultra-structural level, Peptides 23(8) (2002) 1391-1399.

[28] G.M. Williams, K. Lee, X. Li, G.J.S. Cooper, M.A. Brimble, Replacement of the CysA7-CysB7 disulfide bond with a 1,2,3-triazole linker causes unfolding in insulin glargine, Organic & Biomolecular Chemistry 13(13) (2015) 4059-4063.

[29] K. Holland-Nell, M. Meldal, Maintaining Biological Activity by Using Triazoles as Disufide Bond Mimetics, Angewandte Chemie International Edition 50(22) (2011) 5204-5206.